MODULES OF THE SAGA CHROMATIN-MODIFYING COMPLEX PLAY DISTINCT ROLES IN *DROSOPHILA* GENE EXPRESSION AND DEVELOPMENT

By

Xuanying Li

B.S., Tsinghua University, 2011

Submitted to the graduate degree program in Anatomy and Cell Biology and the Graduate Faculty of the University of Kansas in partial fulfillment of the requirements for the degree of Doctor of Philosophy.

_____

Co-Chair: Susan Abmayr, Ph.D.

_____

Co-Chair: Brenda Rongish, Ph.D.

_____

Jerry Workman, Ph.D.

_____

Ting Xie, Ph.D.

_____

Patrick Fields, Ph.D.

Date Defended: November 21, 2017

The dissertation committee for Xuanying Li

certifies that this is the approved version of the following dissertation:

MODULES OF THE SAGA CHROMATIN-MODIFYING COMPLEX PLAY DISTINCT ROLES IN *DROSOPHILA* GENE EXPRESSION AND DEVELOPMENT

_____

Co-Chair: Susan Abmayr, Ph.D.

_____

Co-Chair: Brenda Rongish, Ph.D.

Date Approved: December 8, 2017

ABSTRACT

Histone modifications are an important component of epigenetic control. Histone modifying enzymes are often integrated into large multi-subunit complexes. The Spt-Ada-Gcn5-acetyltransferase (SAGA) chromatin-modifying complex is a transcriptional coactivator that contains four different modules of subunits. The intact SAGA complex has been well characterized for its function in transcription regulation and development. However, little is known about the roles of individual modules within SAGA and if they have any SAGA independent functions. In this study, I took advantage of genetic approaches in *Drosophila* to remove the maternal contribution and investigated the requirement for the SAGA individual modules in early development. I found that perturbation of the HAT and the TAF module caused defects in oogenesis and a complete inability to form mature oocytes. By contrast, DUB activity was expendable during oogenesis, and at least some early zygotic genes were transcriptionally active. Nevertheless it was essential for normal cellularization in these early embryos, and their survival through embryogenesis. It was also essential for wild-type levels of transcription. I identified binding sites for several SAGA subunits genome wide in early embryos and found coincident binding at most sites. Notably, the DUB module bound to chromatin with other SAGA subunits even when it was not required for transcription of the associated genes. More interestingly, we identified sites in which DUB and TAF module subunits bound chromatin independent of the core SAGA modules, where it regulated transcription.

ACKNOWLEDGEMENTS

I would like to thank my mentors Dr. Susan Abmayr and Dr. Jerry Workman for all the support during all my years in the laboratory. I appreciate their patience and encouragement for me to overcome all the difficulties in my research. I am often impressed by their great ideas and learned the principles of how to be a good scientist. In addition to the great science, I also appreciate their help for me to pursuing my future career.

I also would like to thank my graduate committee: Dr. Brenda Rongish, Dr. Ting Xie and Dr. Patrick Fields for all the great suggestions to my project. I wish to thank Dr. Julie Christianson for keeping track of my graduate study progress and resolving all my concerns towards graduation.

I would like to thank all members in the Workman lab, past and present, for their advice and encouragement. I learned a lot from them and had many discussion with them. I also want to thank all the lab members for providing a good environment to do research. In particular, I want to thank Leanne Well (Szerszen) for her contribution of ovary staining data.

I would never be able to have gone this far without support from Stowers Core Facilities. A great thanks goes to Chris Seidel, who contributed a lot to the genome-wide data analysis. I would like to thank Anoja Perera, Michael Peterson, Rhonda Egidy, Kate Hall and Troy Green for the running of RNA-seq and ChIP-seq samples. I thank Cynthia Chen and Hua Li with the assistance for bioinformatics. I want to thank Jeff Lange for helping with live imaging and I also want to thank Steven Hoffman, Cindy Maddera, Jay Unruh and Brian Slaughter for assistance with confocal images and imaging process.

I would like to thank my parents for their support.

TABLE OF CONTENTS

LIST OF FIGURES AND TABLES

Chapter 1

Introduction

1.1 Chromatin

1.1.1 Nucleosomes and chromatin

In eukaryotic cells, an octamer of core histone proteins (H2A, H2B, H3, and H4) is wrapped around by 147 base pair (bp) of DNA with 1.65 turns to form the nucleosome core particle (Khorasanizadeh 2004). The histone octamer is made from four histone-fold heterodimers. The centrally located two H3-H4 dimers are flanked by two H2A-H2B dimers (Arents et al. 1991). H3 and H4 form a central tetramer through interaction of two H3, and each H3-H4 dimer interacts with one H2A-H2B dimer through a four-helix bundle between H4 and H2B (Luger et al. 1997). Each histone-fold pair is associated with 27–28 bp of DNA with 4 bp between these dimers. N-terminal tails of H3 and H2B provide additional interactions to DNA. In the absence of DNA, no stable octamer forms (Luger et al. 1997). In most eukaryotic cells, linker histones such as histone H1 associates with 15-20 bp of linker DNA, increasing the nuclease protection of nucleosome DNA to 167 bp (An et al. 1998a, An, van Holde and Zlatanova 1998b, Hayes and Wolffe 1993, Hayes, Pruss and Wolffe 1994, Noll and Kornberg 1977). The 167 bp DNA, the core histone octamer, and the linker histone make up the chromatosome (Simpson 1978). The remaining length of linker DNA and chromatosome form the nucleosome, which is the basic repeat unit of chromatin.

The nucleosome is a small compaction, further compaction gives rise to a higher-order chromatin structure, which can be broken into primary, secondary and tertiary structures. The primary structure of chromatin is the linear arrangement of nucleosomes on DNA, observed as a "beads on a string" with a width of 11nm (Thoma, Koller and Klug 1979). Local compaction of a nucleosomal array forms the secondary structure: a 30nm fiber (Marsden and Laemmli 1979). Tertiary structure of mitotic chromatin is achieved by interstrand contacts between secondary structural elements (Belmont, Sedat and Agard 1987).

1.2 Chromatin remodeling complexes

Although chromatin is highly condensed, it is quite dynamic, flexible and is regulated by histone modification and nucleosome remodeling. Chromatin remodeling complexes or remodelers use the energy of ATP hydrolysis to promote assembly of chromatin, access of factors to chromatin and restructuring of nucleosomes. ATP-dependent chromatin remodelers are classified into four distinct families SWI/SNF, ISWI, CHD and INO80. All the remodelers have a conserved ATPase domain that split into two RecA-like lobes. Functionally, the ISWI complexes are linked to nucleosome assembly and repression, CHD remodelers are involved in assembly, editing and access, INO80-family complexes are closely associated with editing, and SWI/SNF remodelers are associated with chromatin access.

SWI/SNF was the first identified ATP-dependent chromatin complex (Cairns et al. 1994). The purified SWI/SNF complex alters the structure of nucleosomes and promotes activator binding to nucleosomal DNA in an ATP-dependent manner (Cote et al. 1994, Kwon et al. 1994). The yeast SWI/SNF contains 11 subunits and has a molecular mass of ~1.1 MDa (Smith et al.

2003). Homologs of yeast SWI/SNF complex are identified in *Drosophila* (Dingwall et al. 1995) and human (Kwon et al. 1994, Wang et al. 1996a), indicating it is highly conserved. All the SWI/SNF complexes have core components, which are conserved with yeast counterparts, including Snf/Swi2, Snf5 and Swi3 (Kingston and Narlikar 1999). The rest of the subunits of the complex can regulate the ATPase activity, recognize histone modifications, and participate in targeting and retention. For example, mutations in most SWI/SNF subunits cause similar phenotypes (Winston and Carlson 1992, Kingston, Bunker and Imbalzano 1996), suggesting that non-core subunits are required for nucleosome remodeling. In addition, mammalian SWI/SNF complexes have heterogeneity from different tissues (Wang et al. 1996a, Wang et al. 1996b), indicating that some subunits contribute to the tissue specificity. Moreover, mutations of actin or actin-related subunits in SWI/SNF complexes give similar phenotypes as *swi/snf* mutants (Cairns et al. 1998). The actin subunit is required for ATPase activity of mammalian SWI/SNF (Zhao et al. 1998).

Genetic studies in yeast show that SWI/SNF complex genes are required for transcriptional activation (Winston and Carlson 1992). In flies, the SWI/SNF complex is present at many active genes and is required for Pol II to associate with chromatin (Armstrong et al. 2002). How are these complexes recruited to promoters? Some studies suggest that the SNF/SWI complex is recruited to DNA by activators (Yudkovsky et al. 1999, Kwon et al. 1994). Moreover, acetylation may facilitate the binding of the SWI/SNF complex. The ATPase subunits of SWI/SNF -family remodelers always have bromodomains at the C–terminus. Histone acetylation increases the retention of SWI/SNF on the promoter (Hassan, Neely and Workman 2001) and the bromodomains of the Swi2/Snf2 are required for the occupancy of SWI/SNF in the absence of

transcription activators (Hassan et al. 2002). Furthermore, the acetylated histones are preferentially displaced by SWI/SNF complex (Chandy et al. 2006).

1.3 Histone modification and histone modifying complexes

1.3.1 Histone modification

Histones are subject to a large number of different post-translational modifications (PTMs) (Bannister and Kouzarides 2011, Kouzarides 2007), which regulate transcription (Figure 1.1). There are at least nine distinct types of modifications found on histones: acetylation, methylation, phosphorylation, ubiquitination, sumoylation, ADP ribosylation, deamination, proline isomerization and proteolysis. While acetylation, methylation, phosphorylation and ubiquitination have been well characterized, current studies of other types of modifications are not completed. These modifications alter the interaction between histone-DNA and/or histone-histone, therefore controlling chromatin stability and DNA accessibility.

1.3.1a Histone acetylation

Acetylation is carried out by histone acetyltransferases (HATs) and can be removed by histone deacetylases (HDACs). According to their structures, HATs are classified into several families: the predominant GNAT family and MYST family, as well as p300/CBP family and SRC/p160 family (Roth, Denu and Allis 2001, Lee and Workman 2007). The GNAT family HATs share sequence or structure similarity with yeast Gcn5 (Neuwald and Landsman 1997). The MYST family members have an acetyltransferase homology region: MYST domain

(Avvakumov and Cote 2007). Despite the sequence diversity of different HATs, they nevertheless all have a conserved core region for acetyl-coA binding (Wang et al. 2008a). Similarly, HDACs are divided into four classes (I, II, III and IV) according to phylogenetic analysis and sequence homology. Class I, II, IV are classical family HDACs, which are Zinc-dependent deacetylases: Class I HDACs have a catalytic domain homologous to yeast Rpd, class II HDACs are homologs of yeast Hda1, and class IV HDACs are only found in higher eukaryotes. Class III is comprised of Sirtuin family members, which are dependent on NAD^+.

An acetyl group from acetyl-coA is transferred to an ε-amino group of a histone lysine residue, removing the positive charge of the lysine residue. Acetylation of H3 and H4 and the localization of HATs, show a positive correlation with transcription activation (Kurdistani, Tavazoie and Grunstein 2004, Bernstein et al. 2005, Liu et al. 2005, Pokholok et al. 2005, Robert et al. 2004, Roh, Cuddapah and Zhao 2005, Wang et al. 2008c). HATs recruitment and acetylation of histones are necessary for the activation of many genes. Most of HATs are found in multi-subunit complexes (see below) and are recruited to active genes via transcription activators. Also, many HAT complex subunits have histone marks reading domains.

There are two ways to activate transcription by histone acetylation. Firstly, charge neutralization weakens the interaction between the histone and negatively charged DNA, and opens the landscape of chromatin to support the entry of transcriptional machinery (Shahbazian and Grunstein 2007, Li and Reinberg 2011). The histone tails play an important role in stabilizing nucleosomes (Ausio, Dong and van Holde 1989). Many studies demonstrate that acetylation of lysine residues at the histone tails weakens the DNA-histone interaction and directly affects nucleosome stability (Allfrey 1966, Ausio et al. 1989, Garcia-Ramirez, Rocchini and Ausio 1995, Zheng and Hayes 2003). For example, acetylation of H2A by p300 facilitates

disassembly of H2A-H2B dimers (Ito et al. 2000). Moreover, acetylation also affects higher order structure of chromatin. For example, H4K16 inhibits the formation of compact 30-nanometer-like fibers (Shogren-Knaak et al. 2006). Secondly, acetylation is recognized by specific domains of proteins, such as bromodomain and double PHD finger domain proteins, which influence chromatin dynamics and function. For example, the bromodomain-containing acetyl-histone binding proteins Swi2 and Bdf1 facilitate the recruitment of ATP-dependent chromatin remodeler SWI/SNF and TFIID to promoters, which stimulates chromatin remodeling and transcription initiation (Durant and Pugh 2007, Hassan et al. 2002, Hassan, Awad and Prochasson 2006, Huisinga and Pugh 2004). Moreover, the acetylated histones are preferentially displaced by the SWI/SNF complex (Chandy et al. 2006). Another bromodomain-containing ATP-dependent remodeler, RSC, is also recruited to promoters through histone acetylation and facilitates Pol II elongation (Carey, Li and Workman 2006, Kasten et al. 2004). Thus, acetylation of histones potentiates nucleosome eviction and binding of transcription machinery.

1.3.1b Histone methylation

Methylation is the most diverse modification, occurring in numerous lysine and arginine residues. Lysine residues can have up to three methyl groups (mono-, di- and trimethylation). Arginine residues can be monomethylated or dimethylated (symmetrically and asymmetrically). The main lysine methylation sites are H3K4, H3K9, H3K27, H3K36, H3K79, and H4K20. The main arginine methylation sites are H3R2, H3R8, H3R17, H3R26, H4R3, and H2AR3. Lysine methylation is generated by lysine histone methyltransferases (HMTs), which transfer a methyl group from S-adenosylmethionine (SAM) to the amino group of the lysine residues. All the known lysine HMTs, except Dot1, contain a conserved catalytic region: SET domain. Unlike

HATs, methyltransferases are more specific for their targets. Methylation can be removed by demethylases (Mosammaparast and Shi 2010, Kooistra and Helin 2012).

Histone lysine methylation can be found in both active and repressive genes. In general, H3K4me, H3K36me and H3K79me are associated with active transcription within euchromatin, while H3K9me and H3K27me are often located in heterochromatin (Li, Carey and Workman 2007). Methylation creates a unique molecular architecture on histones recognized by specialized "reader" domains present within chromatin-regulatory proteins (Kouzarides 2007). For example, chromodomain-containing heterochromatin protein 1 (HP1) specifically recognizes H3K9me and H3K27me (Bannister et al. 2001, Jacobs and Khorasanizadeh 2002, Fischle et al. 2003b). When H3K36me is present in coding regions, it is recognized by the Rpd3S histone deacetylase complex subunit Eaf3, which contains a chromodomain. Deacetylation in the coding region during transcription prevents cryptic transcription (Carrozza et al. 2005, Joshi and Struhl 2005, Keogh et al. 2005)

1.3.1c Histone phosphorylation

Histone phosphorylation is mediated by many kinases and is removed by phosphatases (Nowak and Corces 2004). Phosphorylation can occur at serine, threonine and tyrosine residues. Phosphorylation of H3 serine 10 is associated with chromosome condensation during mitosis and gene activation in interphase (Nowak and Corces 2004, Sawicka and Seiser 2012). The association of H3S10 phosphorylation with contrary phenomena supports the idea that there are context-dependent outcomes of histone modifications (Fischle, Wang and Allis 2003a). Moreover, phosphorylation of H3 serine 10 enhances H3K14 acetylation but inhibits H3K9

methylation (Cheung et al. 2000, Lo et al. 2000, Rea et al. 2000), indicating that H3S10 phosphorylation, together with other modifications, forms a network to regulate transcription. In addition to H3 serine 10, Histone H1 and H2A can be phosphorylated (Happel and Doenecke 2009, Aihara et al. 2004). Phosphorylation of H1 plays a role in transcription by facilitating the binding of ATP-dependent remodeling complexes (Koop, Di Croce and Beato 2003, Horn et al. 2002). It has been shown that phosphorylation of H1 weakens the interaction between H1 and nucleosomes, increasing the disassociation rate of H1 from chromatin (Dou et al. 2002, Green, Lee and Poccia 1993). The well-studied reader proteins for phosphorylation are 14-3-3 proteins, which recognize H3S10 phosphorylation. It has been shown that 14-3-3 proteins associate with BRG1, the ATPase subunit of the SWI/SNF remodeler, at the promoters for transcription activation (Drobic et al. 2010).

1.3.1d Histone ubiquitination

The 76 amino acid protein, ubiquitin, can attach to the histones, and H2A and H2B are the predominant histones for mono-ubiquitination (Osley 2006). Ubiquitin is conjugated to histones by three enzymes (Osley 2006): a ubiquitin activating enzyme (E1), a ubiquitin-conjugating enzyme (E2) and a ubiquitin ligase (E3). E3 plays an important role in substrate selection (Weissman, Shabek and Ciechanover 2011, Clague and Urbe 2010). Ubiquitination is reversible by deubiquitinases (DUBs).

High levels of ubH2B are observed downstream of transcription start sites (TSS) into the coding region (Kim and Roeder 2009, Minsky et al. 2008, Jung et al. 2012, Shieh et al. 2011). At some genes, ubH2B is required for transcription activation and facilitates Pol II elongation

(Henry et al. 2003, Pavri et al. 2006). However, studies also show that ubH2B has a repressive function on a subset of genes (Batta et al. 2011, Lee et al. 2012). Specifically, ubH2B activates highly expressed genes but represses lowly expressed genes (Batta et al. 2011, Lee et al. 2012). The explanation for the difference is that ubH2B promotes nucleosome stability/occupancy and the increased stability/occupancy has different effects at promoters and transcribed regions (Batta et al. 2011, Chandrasekharan, Huang and Sun 2009, Davies and Lindsey 1994). UbH2B stabilizes nucleosomes at promoters of lowly expressed genes and prevents recruitment of Pol II, whereas it promotes reassembly of nucleosomes following the passage of Pol II to enable rounds of transcription at highly expressed genes.

Several studies demonstrate that ubH2B is a prerequisite for H3K4 and H3K79 methylation (Briggs et al. 2002, Dover et al. 2002, Ng et al. 2002, Sun and Allis 2002). This histone crosstalk is unidirectional: mutations that disrupt ubH2B reduce the level of these methylated H3, however, the absence of the H3 methylation sites does not affect ubH2B levels (Briggs et al. 2002, Sun and Allis 2002). Notably, ubH2B only affects di- and tri-methylation of H3K4 and H3K79 but not mono-methylation (Dehe et al. 2005, Schneider et al. 2005, Shahbazian, Zhang and Grunstein 2005). The mechanism for such histone crosstalk was revealed by the Shilatifard group. UbH2B controls the binding of Cps35, which is required for COMPASS (complex proteins associated with Set1) complex catalytic activity (Lee et al. 2007). Specifically, Cps35 regulates the recruitment of Spp1, a COMPASS subunit necessary for tri-methylation (Vitaliano-Prunier et al. 2008).

Deubiquitination of ubH2B is required for optimal transcription activation. For example, full transcription activation of GAL1 in yeast requires both ubiquitination and deubiquitination (Henry et al. 2003). The removal of ubiquitin is critical for the recruitment of Ctk1 kinase to the

paused Pol II for its second CTD phosphorylation at Ser2 (Wyce et al. 2007). This phosphorylation is important for Pol II to undergo the transition from initiation to elongation status (Fuda, Ardehali and Lis 2009). These data demonstrate that ubH2B may be a checkpoint when Pol II pauses during early elongation.

Mono-ubiquitination of H2A is generally associated with transcription repression. The enzymes that ubiquitinate H2A are often in transcription repressor complexes. RNF2, the first ubH2A specific E3 ligase, is a subunit of RPC1 (Polycomb Repressive Complex 1) complexes (Wang et al. 2004, Cao, Tsukada and Zhang 2005, Kerppola 2009). Moreover, ubH2A is localized on silenced regions like the inactive X chromosome (de Napoles et al. 2004, Fang et al. 2004). Some studies might explain the mechanism of ubH2A-mediated repression. For example, ubH2A inhibits recruitment of FACT subunit Spt16 and decreases transcription elongation (Zhou et al. 2008). Moreover, in contrast to ubH2B, ubH2A inhibits H3K4 methylation (Nakagawa et al. 2008, Vissers et al. 2008). Furthermore, ubH2A enhances binding of linker histone H1 to nucleosomes (Jason et al. 2005, Luger et al. 1997, Zhu et al. 2007), thus it might regulate higher order chromatin structure to repress transcription.

1.3.2 Histone modifying complexes

The histone modifying enzymes are often integrated into complexes. Integration of histone modifying enzymes into multiple complexes facilitates them to perform diverse tasks in creating an appropriate epigenetic environment for gene expression. In some cases, complex components are essential for catalytic subunit activity, specificity and gene-specific targeting. For example, lysine methyltransferase Set1 is present in the COMPASS (complex proteins

associated with Set1) complex and is active only when present within COMPASS (Krogan et al. 2002, Shilatifard 2012). The PRC2 (Polycomb Repressive Complex 2) is responsible for H3K27 methylation. The catalytic subunit EZH2 requires other non-catalytic subunits in the complex to methylate histones (Cao and Zhang 2004). H2A ubiquitin ligase RNF2 (Ring finger protein 2) is identified in RPC1 (Polycomb repressive complex 1), which may target it to repressive loci for ubH2A (Wang et al. 2004, Cao et al. 2005). Here I focus on MYST and GNAT complexes (Table 1.1) and will discuss details about the SAGA (Spt-Ada-Gcn5 acetyltransferase) complex in the next section.

1.3.2a MYST family HAT complexes

MYST (MOZ, Ybf2/Sas3, Sas2 and Tip60) family members have a particular acetyltransferase homolog region: MYST domain. The yeast HAT Esa1 is in the NuA4 (Nucleosome acetyltransferase of histone H4) complex (Allard et al. 1999) and its homolog Tip60 is in the TIP60 complex (Ikura et al. 2000). In yeast, NuA4 is a 1.3MD HAT complex that acetylates histone H4/H2A (Grant et al. 1997), and Esa1 is the catalytic subunit (Allard et al. 1999). NuA4 also contains Tra1 (subunit of SAGA), which recruits NuA4 to specific promoters by direct interaction with transcription activators (Allard et al. 1999, Brown et al. 2001). By affinity purification assay, NuA4 complex is found to have 13 subunits (Doyon and Cote 2004). Based on biochemical analyses of NuA4 subunits, there are four main functional modules in the complex: a scaffold for the assembly, a recruitment module including Tra1, a histone methylation/transcription elongation module and a DNA repair/telomere boundary module.

Human TIP60 is the homolog of yeast NuA4. Out of the 13 NuA4 subunits, 12 human homologs can be found in TIP60 (Doyon et al. 2004). However, there are several human TIP60 specific subunits: ruvB-like helicases RUVBL1/2 and a bromodomain-containing protein Brd8 (homolog of yeast Bdf1) (Doyon et al. 2004). Moreover, the subunit p400/Domino (human homolog of Eaf1) contains a SWI2-related domain, which is absent in the yeast counterpart. P400/Domino is also highly related to the subunit of yeast ATP-dependent remodeling complex SWR1. These data suggest that human TIP60 is the fusion of yeast NuA4 and yeast SWR1 (Doyon and Cote 2004).

NuA4/TIP60 functions as a transcription coactivator. It can be recruited by activators to chromatin to acetylate H4 and stimulate transcription (Utley et al. 1998, Vignali et al. 2000). For example, NuA4 can be recruited to promoters by activation domains and stimulate transcription on reconstituted chromatin templates (Ikeda et al. 1999). Loss of yeast Esa1 decreases transcription of specific genes such as ribosomal protein genes (Galarneau et al. 2000, Reid et al. 2000). Besides these, TIP60 is involved in DNA repair and TIP60 lacking histone acetyltransferase activity causes defects in double-strand break repair (Ikura et al. 2000).

1.3.2b Gcn5-containing HAT complexes

The GNAT (Gcn5-related acetyltransferase) family HATs share sequence similarity with yeast Gcn5. Gcn5 is in SAGA, ADA (yeast) and ATAC (metazoan) complexes. The yeast ADA (Transcriptional adaptor) complex is a 0.8MD complex containing the HAT module of SAGA (Gcn5, Ada2, Ada3, Sgf29) and ADA-specific subunits Ahc1 and Ahc2 (Grant et al. 1997,

Eberharter et al. 1999, Lee et al. 2011). Integration of Gcn5 into ADA expands the lysine acetylation specificity from H3K14 only to H3K9, H3K14 and H3K18 (Grant et al. 1999).

Ada Two A-containing (ATAC) complex is identified in flies as a multi-subunit complex containing two HAT proteins: Gcn5 and Atac2 (Suganuma et al. 2008). Gcn5 mainly acetylates H3, while Atac2 prefers H4 (Grant et al. 1999, Suganuma et al. 2008). Later, mammalian ATAC was identified (Wang et al. 2008b) and the mammalian YEAST2, ATAC2 and MBIP may function as a scaffold for the ATAC complex (Guelman et al. 2009, Wang et al. 2008b). ATAC shares the core HAT module subunits (Gcn5, Ada3 and Sgf29) with SAGA but has its own specific subunit Ada2a (Kusch et al. 2003, Muratoglu et al. 2003). ATAC has been shown to play important, but distinct, roles in development and transcription from SAGA. In *Drosophila*, *Ada2a* and *Atac2* mutants are larval lethal (Pankotai et al. 2005, Suganuma et al. 2008). Similarly, ATAC2 is essential for mouse embryogenesis (Guelman et al. 2009). Interestingly, ectopic expression of Ada2b could not rescue the *Ada2a* defects, nor the Ada2a in the *Ada2b* mutants, suggesting that ATAC and SAGA have distinct function during development (Pankotai et al. 2005). Moreover, in mammals, ATAC has been shown to bind to both promoters and enhancers at distinct genomic loci from SAGA (Krebs et al. 2011). How is ATAC recruited to chromatin? ATAC was first shown to bind to DNA in flies (Suganuma et al. 2008) and several subunits may contribute to its binding: the SWIRM domain of Ada2a can bind to DNA; Atac1 has a SANT domain and Yeast2 contains a YEAST2 domain (Spedale, Timmers and Pijnappel 2012). Furthermore, ATAC interplays with chromatin remodelers. hAda2a physically interacts with SWI/SNF complex subunit BRG1 (Barlev et al. 2003). dAda2a binding and H4K12 acetylation are reduced in NURF (nucleosome remodeling factor) mutants, suggesting that NURF remodeling complex is required for ATAC chromatin binding (Carre et al. 2008).

1.4 SAGA (Spt-Ada-Gcn5 acetyltransferase) complex

1.4.1 SAGA is a chromatin modifying complex

1.4.1a SAGA is modular, containing several submodules

SAGA was first identified by the Workman laboratory in yeast (Grant et al. 1997) and is highly conserved across many species (Table 1.2 & Figure 1.2). ySAGA contains a transcription activator interaction module (Tra1, Spt7, Spt20, Spt3, Spt8 and Ada1), a TATA-binding protein (TBP) interaction module (Taf5, Taf6, Taf9, TAF10 and Taf12) and two enzymatic modules: an acetyltransferase (HAT) module (Gcn5, Ada2, Ada3, Sgf29) and a deubiquitinase (DUB) module (Ubp8, Sgf73, Sgf11, Sus1) (Koutelou, Hirsch and Dent 2010, Rodriguez-Navarro 2009).

The association of Gcn5 with SAGA enables it to acetylate multiple lysine residues on nucleosomes. Recombinant Gcn5 alone cannot acetylate nucleosomes, whereas Gcn5 in SAGA can acetylate nucleosomes (Grant et al. 1997). Additionally, Gcn5 alone acetylates H3K14 on free histones, while SAGA acetylates H3K9, K14, K18 and K23 (Grant et al. 1999, Balasubramanian et al. 2002). Ada2 enhances the Gcn5 catalytic activity and Ada3 facilitates nucleosomal acetylation and expanded lysine specificity (Balasubramanian et al. 2002). Sgf29 is also important for SAGA HAT activity (Bian et al. 2011, Shukla et al. 2012).

The deubiquitinase activity of SAGA was first shown by Berger and Grant labs and Ubp8 is the deubiquitinase (Daniel et al. 2004, Henry et al. 2003). Later, Sgf11, a Zinc-Finger protein, was identified as another DUB module subunit (Ingvarsdottir et al. 2005, Lee et al. 2005, Powell et al. 2004), which is necessary for the DUB activity. Sus1 forms a stable submodule with Sgf11 and Ubp8 (Rodriguez-Navarro et al. 2004) and the association of the DUB module with the rest of SAGA is mediated by the fourth subunit Sgf73 (Kohler et al. 2008).

The third module of SAGA is the TATA-binding protein (TBP) interaction module, consisting of several TATA-binding protein associated factor (TAF) proteins which are shared with the general transcription factor TFIID (Lee et al. 2011, Wu et al. 2004). The TAF module serves important roles in maintaining the integrity of SAGA and certain TAF proteins are required for SAGA-dependent nucleosomal HAT activity (Grant et al. 1998).

Transcription activator-binding protein Tra1, together with several Spt proteins, forms the fourth module of SAGA. Tra1 recruits SAGA to chromatin by the interaction with specific transcription activators (Brown et al. 2001). Spt8, Spt3 and Ada1 can interact with TBP to facilitate PIC formation and transcription activation (Sterner et al. 1999, Mohibullah and Hahn 2008, Sermwittayawong and Tan 2006, Laprade, Rose and Winston 2007). Loss of Spt7, Spt20 or Ada1 causes complete loss of the SAGA complex (Sterner et al. 1999).

Although the general composition and function of SAGA is highly conserved through yeast to human, there are some differences in certain subunits. Metazoans have two homologs of yAda2: Ada2a and Ada2b (Kusch et al. 2003, Muratoglu et al. 2003, Gamper, Kim and Roeder 2009). Specifically, Ada2b is in SAGA and is required for the HAT activity (Qi, Larsson and Mannervik 2004). The TAF module subunits in ySAGA are shared with TFIID, however, *Drosophila* Taf6-like subunit Saf6 is SAGA specific (Weake et al. 2009). Similarly, WDA is another *Drosophila* SAGA specific subunit (Guelman et al. 2006b). Until now, no Spt8 homolog has been identified in either *Drosophila* or human.

1.4.1b Recruitment of SAGA is mediated by multiple interactions

As a transcription co-activator, SAGA is recruited to promoters prior to Pol II and PIC formation (Larschan and Winston 2001, Bhaumik and Green 2001, Bryant and Ptashne 2003). This raises a question of how SAGA is recruited. Multiple studies indicate that several SAGA subunits can interact with chromatin to recruit and retain SAGA in chromatin. In *S. cerevisiae*, Tra1 is crucial for recruiting SAGA to promoters (Brown et al. 2001, Bhaumik et al. 2004, Fishburn, Mohibullah and Hahn 2005, Reeves and Hahn 2005). However, in *S. pombe*, Tra1 is essential for SAGA recruitment to some genes but not for others, suggesting that there is a Tra1 independent mechanism for SAGA recruitment (Helmlinger et al. 2011). Although Tra1 seems to be the main target of transcription activators, other SAGA subunits might be involved in the interactions and contribute to SAGA recruitment. Taf12 is identified as a transcription activator target in crosslinking studies (Fishburn et al. 2005, Reeves and Hahn 2005), suggesting that it might mediate the interaction between transcription activators and SAGA. additionally, SAGA may also be recruited to promoters by interacting with TBP via Spt3 and Spt8 (Larschan and Winston 2001, Mohibullah and Hahn 2008, Laprade et al. 2007).

Furthermore, SAGA could be recruited and retained by distinct mechanisms. Many SAGA subunits have the ability to bind chromatin. Gcn5 has bromodomains which can interact with acetylated nucleosomes. Studies show that SAGA can anchor to acetylated histones after removal of activators by bromodomains of Gcn5 (Hassan et al. 2002). Sgf11 is a Zinc-Finger (Znf) protein and can bind to nucleosomal DNA (Koehler et al. 2014). Sgf73/ATXN7 can bind to nucleosomes via a SCA7 domain (Bonnet et al. 2010). Moreover, the Tudor domains of Sgf29 recognize H3K4me2/3 marks (Bian et al. 2011). Altogether, these studies suggest that SAGA recruitment/retention is regulated by a combination of multiple interactions.

1.4.1c Architecture of the SAGA complex

Several studies have investigated the structural features of SAGA and how SAGA subunits integrate into the whole complex. In yeast, loss of Spt7, Spt20 or Ada1 causes complete loss of the SAGA complex, while Gcn5, Spt3 and Spt8 have moderate effects on SAGA integrity (Sterner et al. 1999). Deletion of Sgf73 causes the disassociation of the DUB module from SAGA and the isolated DUB module could not deubiquitinate ubH2B, suggesting that Sgf73 is essential to anchor and activate the DUB module (Kohler et al. 2008, Lee et al. 2009). Combining deletions with affinity purification of tagged subunits and mass spectrometry revealed the organization of subunits into modules within yeast SAGA. Only the HAT module subunits are lost in *Ada2*Δ strain, whereas deletion of Gcn5 or Sgf29 only affects the subunit itself. Upon Ubp8 deletion, the DUB is lost from SAGA while Sgf73 is still bound to SAGA. Sgf73 interacts with Spt20 in order to bring DUB to SAGA. After loss of Spt20, small sub-modules like HAT and DUB still form, suggesting sub-complexes form first and then join together to form the SAGA complex (Lee et al. 2011).

Electron Microscopy (EM) and crosslinking analyses identified the interactions of subunits and the 3D structure of SAGA. Steven Hahn's group identified that the TFIID-like core is at the center of SAGA to nucleate assembly of other SAGA modules. Spt7 and Spt20 crosslink to different sets of subunits. The C-terminal end of Sgf73 crosslinks with TFIID-like core, Spt20, Ada2 and Ada3. The Ada3 C-terminus links HAT to SAGA. The HAT and DUB modules are close to each other (Han et al. 2014). Dheva and colleagues propose that the TAF module combines with Spt7, Spt20, and Tra1 to form a central core; while the remaining subunits attach to the core. Sgf73 anchors the DUB modules to SAGA, interacting with Spt20 and Taf5. They

generate a model of SAGA: the top layer is Tra1; the TAF, SPT and DUB modules are in the middle layer; the bottom layer contains the HAT module (Setiaputra et al. 2015).

Due to the large number of subunits and dynamic configuration, no structural picture of the entire SAGA complex has been shown yet. However, several studies give insights for the assembly and activation of the DUB module. Kohler et al determined the structure of a recombinant yeast DUB module at 2.7Å resolution (Kohler et al. 2010). In this study, they show that the DUB module forms two functional lobes: the N terminal Znf-UBP domain of Ubp8 and the other three subunits forms the assembly lobe, whereas the C terminal catalytic domain of Ubp8 and the C terminus of Sgf11 ZnF domain constitute the catalytic lobe. The N terminus of Sgf73 joins the two lobes so that they can work together as one module. Similar structures are observed at 2.45 Å resolution too (Samara et al. 2010). Additional crystal structure study reveals that the catalytic lobe contacts the H2A/H2B acidic patch and H2B of the nucleosome (Morgan et al. 2016, Workman 2016).

So far, the architecture and structure of SAGA and its submodules are mostly from yeast studies. Although SAGA is highly conserved, there are some difference in higher eukaryotes. For example, loss of *Drosophila* Ataxin-7 causes disassociation of the DUB module and the free DUB module has a higher deubiquitinase activity (Mohan et al. 2014), indicating that the *Drosophila* DUB module structure may be different from yeast. Further analyses are needed to reveal these questions.

1.4.2 SAGA modules are required for transcription

SAGA plays an important role in regulating transcription. In general, SAGA is recruited to promoters via transcription activators and the HAT module acetylates neighboring histones to open up the landscape of chromatin (Brown et al. 2001). The TBP interaction subunits facilitate TBP binding (Mohibullah and Hahn 2008, Laprade et al. 2007, Larschan and Winston 2001). During early elongation, the DUB module removes the ubiquitin from ubH2B, allowing the recruitment of Ctk1 to phosphorylate Pol II CTD for its further elongation (Wyce et al. 2007).

Many studies indicate that loss of SAGA subunits cause a change of transcription. Early studies using microarray showed that SAGA predominantly regulates ~10% of the measurable yeast genome, which are TATA-box containing genes and largely stress induced (Huisinga and Pugh 2004, Basehoar, Zanton and Pugh 2004). Determined by high-density oligonucleotide arrays, Gcn5, Spt3 and Spt20 affect the expression of 4%, 3% and 10% of yeast genes, respectively (Lee et al. 2000). Recently, a genome wide analysis revealed a global decrease of Pol II in Spt20Δ stain, suggesting that SAGA acts on the whole transcribed genome (Bonnet et al. 2014). In higher eukaryotes, SAGA is also essential for transcription. Loss of *Drosophila* Ada2b influences the expression of ~600 genes in larvae and ~900 genes in pupa (Pankotai et al. 2013, Zsindely et al. 2009). Non-stop, the *Drosophila* homolog of Ubp8, and Sgf11 regulate several hundred genes in 3rd instar larvae (Weake et al. 2008) and they coregulate a large number of genes in *Drosophila* larva glia (Ma et al. 2016). Microarray of *GCN5* knock–out neurosphere lines indicates that loss of GCN5 affects expression of about 5000 genes (Martinez-Cerdeno et al. 2012).

Different modules of SAGA can have distinct functions from each other in activating transcription. In *S. cerevisiae*, overlapped but distinct sets of genes change expression upon loss of Spt3, Spt20 or Gcn5 (Lee et al. 2000). Microarray assay shows that the profiles of *Ubp8*Δ and

*Sgf11*Δ are distinct from those of *Spt3*Δ and *Spt8*Δ, indicating that the DUB module has a discrete function from SPT module (Ingvarsdottir et al. 2005). More comprehensive genome-wide expression analyses on all viable SAGA deletion mutants in *S. pombe* reveal distinct functional classes of SAGA subunits (Helmlinger et al. 2011). Similarly, *Drosophila* DUB module subunits Non-stop and Sgf11 affect a different set of genes from the HAT module subunit Ada2b (Weake et al. 2008). In mammals, genome wide analysis of SAGA mutants needs to be done to reveal the transcriptional change upon loss of different subunits. However, some phenotypic analyses show that the different modules of SAGA may play distinct roles in regulating transcription. For example, spinocerebellar ataxia type 7 (SCA7) is a neurodegenerative disease that results from ATXN7 mutation. Although loss of Gcn5 can contribute to the severity of SCA7 phenotypes, it is not sufficient to cause severe cerebellar ataxia, suggesting that some genes which are specifically regulated by Ataxin-7 contribute to the pathology (Chen et al. 2012).

1.4.3 Function of SAGA in development and disease

1.4.3a SAGA is required for development

Normal development requires precise regulation of gene expression. SAGA, as a coactivator, controls many developmental processes. *Drosophila* and mice are the most common models used to study the roles of SAGA subunits in development. In *Drosophila*, loss of Gcn5 is pupa lethal and it is required for metamorphosis during this stage. Deletion of Gcn5 in ovary germline cells arrests oogenesis at an early stage, suggesting the requirement of Gcn5 for oogenesis (Carre et al. 2005). Another HAT module subunit Ada2b is also required for oogenesis and viability (Qi et al. 2004, Pankotai et al. 2005), and loss of Ada2b causes axon targeting

defects in the developing visual system of larvae (Weake et al. 2008). In addition to the HAT module, the DUB module subunits have been shown to control development. Mutation of Non-stop or Sgf11 leads to decreased number of glial cells present in the lamina, indicating that they are required for normal neural development (Martin et al. 1995, Poeck et al. 2001, Weake et al. 2008).

In a similar manner, mouse SAGA subunits are required for development. GCN5 null mouse embryos grow severely retarded by 8.5 d.p.c and fail to form dorsal mesoderm lineages and they die during embryogenesis (Xu et al. 2000). Deletion of GCN5 specifically in neural progenitor cells results in 25% reduction in brain mass, suggesting that GCN5 plays a key role in neural progenitor cells in the developing brain (Martinez-Cerdeno et al. 2012). An RNAi screen identifies GCN5 as a critical regulator of reprogramming initiation (Hirsch et al. 2015). USP22, the mammalian homolog of Ubp8, is critical for the early embryogenesis. *USP22* null embryos die before E10.5 and H&E staining reveals retardation in embryonic development (Lin et al. 2012). Reduction of USP22 levels significantly changes the frequency of differentiated cells in the small intestine and brain, providing evidence for the role for USP22 in controlling cell differentiation and lineage specification (Kosinsky et al. 2015).

1.4.3b The role of SAGA in disease

A number of studies indicate that SAGA is linked directly or indirectly to diseases and cancers. Polyglutamine expansions in ATXN7 are associated with the human neural degenerative disease: spinocerebellar ataxia type 7 (SCA7). SCA7 knock-in mice and *Drosophila* models confirm the contribution of polyQ-expanded ATXN7 to this disease (Yoo et al. 2003, Latouche

et al. 2007). Moreover, USP22, GCN5 and several other SAGA components are involved in cancers. USP22 was first identified in microarray screens as part of an 11-gene "signature" of poor prognosis in multiple types of cancers (Glinsky, Berezovska and Glinskii 2005). It may act as an oncogene in colorectal cancer (Liu et al. 2012) and its expression levels increase in multiple cancers (Liu et al. 2011, Zhang et al. 2011). However, it is not clear whether increased DUB activity is linked to these cancers. GCN5, STAF65γ (human homolog of Spt7) and TRRAP (human homolog of Tra1) interact with c-Myc oncoprotein and regulate its activity (McMahon, Wood and Cole 2000, Liu et al. 2003, Liu et al. 2008). Downregulation of rat SGF29 suppresses the expression of c-Myc target genes and inhibits metastasis, indicating that it could be involved in the c-Myc-mediated malignant transformation (Kurabe et al. 2007).

The roles of SAGA subunits in development and the links between SAGA and diseases indicate the importance of understanding the full range of functions of SAGA in multiple areas. Obtaining a mechanistic understanding of the ways SAGA contributes to development and cancers will be essential for preventing human birth defects and providing new therapies for cancers.

1.5 *Drosophila melanogaster*

1.5.1 Life cycle

The fruit fly *Drosophila melanogaster* is a popular model organism used in biomedical research for over a century. They are easy to handle in laboratory conditions and have short life cycles (roughly 10 days at 25°C). *Drosophila* undergoes a four-stage life cycle; embryo, larva, pupa, and fly. Embryonic development, which follows fertilization, takes about one day (25°C).

The embryos hatch to 1st instar larvae, and then the larvae eat, grow and undergo two molts over 5 days before becoming pupa. Then the pupa undergoes metamorphosis into the adult in four days.

1.5.2 Oogenesis

Drosophila oogenesis is a powerful model system for studying cell and developmental biology. A female has a pair of ovaries, which are made up of 12 to 16 ovarioles. In each ovariole, the germarium, containing stem cells, is at the anterior end and followed by the developing egg chambers arranged in a linear fashion with the mature egg chambers reaching the posterior end. Each egg chamber is composed of 16 germline cells (15 nurse cells and one oocyte), and is surrounded by a monolayer of epithelial follicle cells. Oogenesis takes about a week and can be divided into 14 stages, with stage 14 being the mature egg (Bastock and St Johnston 2008, He, Wang and Montell 2011, Kirilly and Xie 2007).

1.5.3 Embryogenesis

Drosophila embryogenesis takes about one day at 25°C and has been divided into 17 different stages. Some stages last several hours such as stage 17 (8 hours), while others like stage 6 only take 10 minutes (Bownes 1975). A series of developmental events occur at different stages giving rise to fully developed embryos.

After fertilization, nuclei divide thirteen times without cell division (stage 1 to stage 4). During these stages, the embryo is called a syncytial blastoderm. The first seven nuclear

divisions are centrally localized in the yolk, nuclei migrate to the cortex during nuclear cycle 8 and most of the nuclei arrive at the periphery at nuclear cycle 10. After their arrival, these nuclei undergo three more divisions before cellularization (Campos-Ortega and Hartenstein 2013, Kotadia et al. 2001).

By nuclear cycle 14 (stage 5), cellularization occurs by invagination of membrane furrows between blastoderm nuclei. This process is associated with microtubules, actin filaments, and myosin II and many genes are involved in this process (Mazumdar and Mazumdar 2002). During cycle 14, maternal RNAs are rapidly degraded and zygotic transcription increases (Tadros and Lipshitz 2009), this is called mid-blastula transition (MBT). Based on these facts, stage 5 embryos provide a good model to study the link between transcription regulation and developmental processes.

After cellularization, the embryos undergo gastrulation, germ band elongation, germ band shortening, dorsal closure, and head involution before hatching (Campos-Ortega and Hartenstein 2013).

1.6 Thesis overview

The intact SAGA complex has been well characterized for its function in transcription regulation and development. However, little is known about the roles of individual modules within SAGA and if they have any SAGA independent functions. Using *Drosophila*, we sought to determine whether 1) SAGA is required for transcription of all genes, 2) SAGA dependent genes require both the HAT and DUB modules, and 3) individual modules can function independently of SAGA.

In chapter 3, I demonstrate that the two enzymatic modules of *Drosophila* SAGA are differently required in oogenesis. Loss of the histone acetyltransferase (HAT) activity blocks oogenesis, while loss of the H2B deubiquitinase (DUB) activity does not. A large subset of genes require the HAT but not the DUB module during oogenesis. However, the DUB module regulates a subset of genes in early embryogenesis and loss of the DUB subunits causes defects in cellularization. Whole genome profiling by RNA-seq shows that transcription of a subset of genes, primarily those involved in development, are affected by loss of DUB module subunits. ChIP-seq analysis of early embryos reveals that both the DUB and HAT modules bind most SAGA target genes even though many of these targets do not require the DUB module for expression. Furthermore, we find that the DUB module can bind to chromatin and regulate transcription independently of the HAT module.

In chapter 4, I describe the primary findings of the SAGA TAF module. Loss of TATA-binding protein (TBP) interaction (TAF) module subunit WDA leads to severe defects during oogenesis and many genes change expression upon loss of WDA. ChIP-seq of early embryos reveals that the TAF module binds to both SAGA targets and non-SAGA targets.

In chapter 5, I discussed the findings from my studies.

In chapter 6, I summarize our observations and provide directions of future experiments.

Figure 1.1 Nucleosome with histone posttranslational modifications. Modified from (Tollervey and Lunyak 2012, Huang et al. 2014). Ph: phosphorylation; Ac: acetylation; Me: methylation; Ub: ubiquitination.

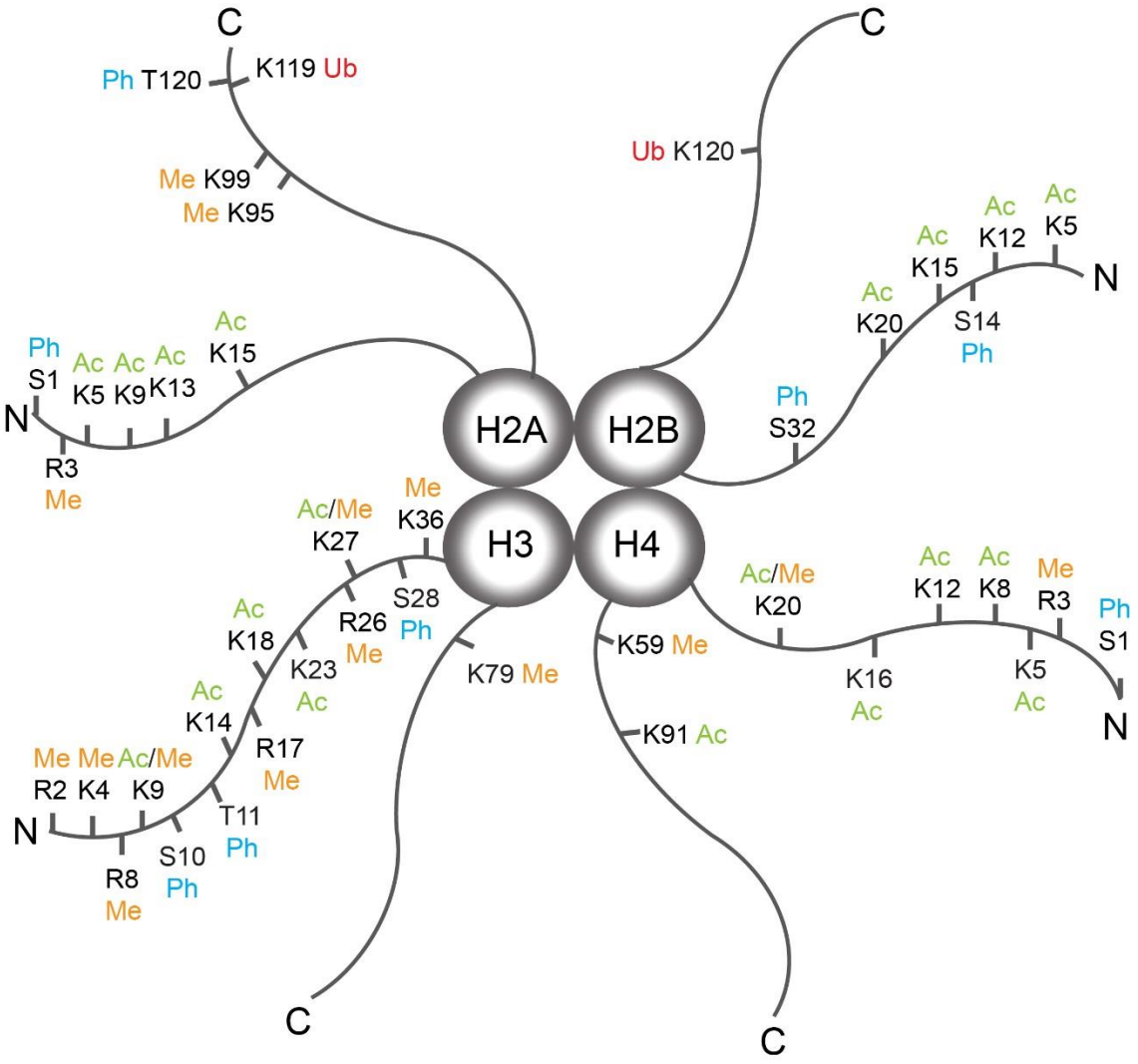

Figure 1.2 Schematic of *Drosophila* SAGA complex. Modified from (Mohan et al. 2014). The modular structure and composition is based on a model of yeast SAGA. The modules are indicated by the following color codes: green-HAT module; red-DUB module; yellow-SPT module; blue-TAF module.

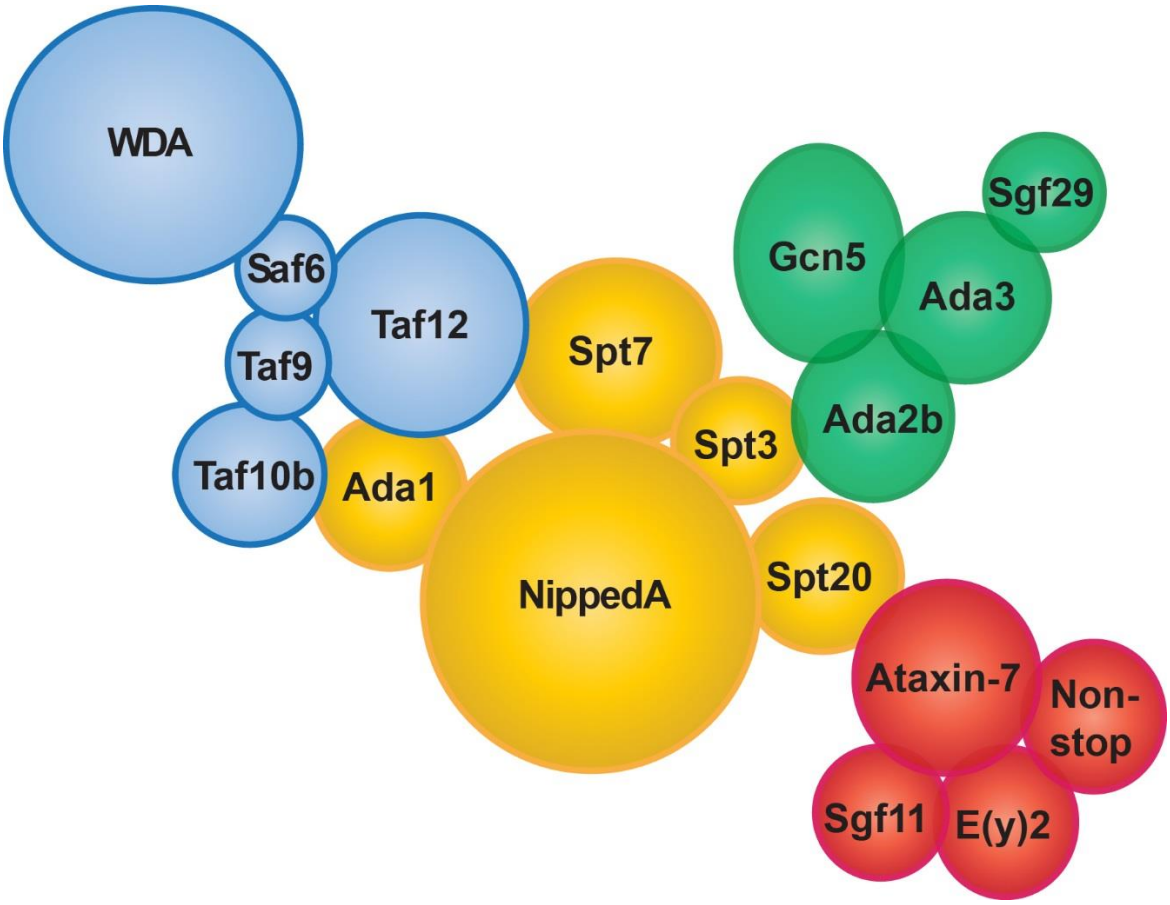

Table 1.1 Members of MYST and GNAT complexes. Modified from (Steunou, Rossetto and Côté 2014)

MYST complexes			
Complex	**Name**	**Organism**	**Acetyltransferase**
NuA4/Tip60	NuA4	*Saccharomyces cerevisiae*	Esa1
	TIP60	*Drosophila melanogaster*	TIP60
	TIP60	*Homo sapiens*	TIP60
MOF	MSL	*Drosophila melanogaster*	MOF
	MSL	*Homo sapiens*	MOF
	NSL	*Drosophila melanogaster*	MOF
	NSL	*Homo sapiens*	MOF
Sas3/MOZ	NuA3	*Saccharomyces cerevisiae*	Sas3
	MOZ/MORF	*Homo sapiens*	MOZ/MORF
Other	SAS	*Saccharomyces cerevisiae*	Sas2
	HBO1	*Homo sapiens*	HBO1
GNAT complexes			
Complex	**Name**	**Organisms**	**Acetyltransferase**
Gcn5/PCAF	ADA	*Saccharomyces cerevisiae*	Gcn5
	SAGA	*Saccharomyces cerevisiae*	Gcn5
	SAGA	*Drosophila melanogaster*	Gcn5
	STAGA	*Homo sapiens*	GCN5
	PCAF	*Homo sapiens*	PCAF
ATAC-type	ATAC	*Drosophila melanogaster*	Gcn5
	ATAC	*Homo sapiens*	GCN5/PCAF
Other	HATB	*Saccharomyces cerevisiae*	Hat1
	Elongator	*Saccharomyces cerevisiae*	Elp3

Table 1.2 subunits of SAGA in yeast, *Drosophila* and human. Modified from (Rodriguez-Navarro 2009)

Yeast	*Drosophila*	Human
Gcn5	Gcn5	GCN5
Ada2	Ada2b	ADA2B
Ada3	Ada3	ADA3
Sgf29	Sgf29	SGF29
Spt3	Spt3	SPT3
Spt7	Spt7	SPT7
Spt8		
Spt20	Spt20	SPT20
Ada1	Ada1	ADA1
Tra1	Nipped A	TRRAP
Taf5	Wda	TAF5L
Taf6	Saf6	TAF6L
Taf9	Taf9	TAF9
Taf10b	Taf10b	TAF10
Taf12	Taf12	TAF12
Ubp8	Non-stop	USP22
Sgf11	Sgf11	ATXN7L3
Sgf73	Ataxin-7	ATXN7
Sus1	E(y)2	ENY2

Chapter 2

Materials and Methods

2.1 Fly strains and culture

Drosophila melanogaster was grown on standard medium at 25°C unless stated otherwise. Females were conditioned with fresh yeast for 2–3 d before ovary dissection. Embryos were collected using standard apple juice plates with yeast. The *non-stop*^{02069} stock (*P{ry*$^{+t7.2}$ *= PZ}not*^{02069}*ry*^{506}*/TM6B, r*^{CB} *Tb*$^{+}$) was provided by the Bloomington Drosophila Stock Center at Indiana University (BL11553) (Martin et al. 1995, Poeck et al. 2001). The *ada2b*^{1} fly stock was provided by Matthias Mannervik (Qi et al. 2004). The *wda*^{11} fly stock was generated by the former Workman lab member Sebastia´n Guelman (Guelman et al. 2006b). The WDA RNAi line was provided by the Bloomington Drosophila Stock Center at Indiana University (BL32469).

2.2 Imprecise excision of P element KG02020

The *Ataxin-7*^{HO3} stock was generated by imprecise excision of the P-element of Bloomington stock: *y*^{1}*w*^{67c23}*; P{SUPor-P}Atxn7*^{KG02020} (BL14255). The P-element was excised by the standard protocols using the Δ2–3 transposase by Dr. Ryan Mohan. P-element excision was scored by the loss of the associated *white* gene, and homozygous lethal stocks were retained. Deletion of *Ataxin-7*^{HO3} was identified by PCR of genomic DNA from homozygous embryos. PCR primers were CCATCCCTAAGCAAATACAACGA (sense) and CTCGTGATCCTGAAGCTT (antisense). In *Ataxin-7*^{HO3}, a 1949bp-fragment from exon 1 to

exon 2 that included the translation start codon was deleted. Transcripts for this region were not observed by RNA-seq. No protein was detected in the mutants.

2.3 EMS mutagenesis

The *Ataxin-7*$^{2A-1}$ stock was generated by ethyl methanesulfonate (EMS). Adult males (Bloomington stock 23651: *w*; P{His2Av-mRFP1}II.2*) 3-5 days after eclosion were starved for 3h and transferred to vials saturated with 30mM EMS, 100mM Tris-HCl and 10% sucrose. After 20h, the males were transferred to fresh food for 3 changes to clear the EMS and mated to females (Bloomington 1672: w^{1118}; sna^{Sco}/*CyO, P{en1}*wg^{en11}) 2-6 days after eclosion. Progeny *CyO* males were mated to *Ataxin-7*^{HO3}/*CyO* females and non-complementing alleles were recovered. Genomic DNA were obtained from homozygous embryos. *Ataxin-7*$^{2A-1}$ was confirmed by PCR and sequencing. Primers were CGGCTACGTATGCAACGAATACC (sense) and CTTGCTCCTCGTTTGGAGGAAG (antisense). This allele contains a G to A point mutation at position 1787, introducing a nonsense mutation at aa142 (W to stop). Random mutations were removed by outcrossing the mutagenized chromosome for two generations to Oregon R before the phenotypic analysis.

2.4 Transgenic fly of Ada2b RNAi

The RNAi fly stock designed to target Ada2b (RNAi 2-T2) was made using the Valium20 vector according to Transgenic RNAi Project (TRiP) protocols, with oligo 5'-ctagcagtGCGAGGCAAGTTCAAATTCAAtagttatattcaagcataTTGAATTTGAACTTGCCTCGCgcg – 3' (Ni et al. 2011). The plasmid was injected to *y[1] v[1] P{y[+t7.7]=nos-*

phiC31\int.NLS}X; P{y[+t7.7]=CaryP}attP40 (BL25709) by Rainbow trangenic Flies, Inc. Transgenic flies were confirmed by the presence of the *vermilion* gene. Final stocks were validated by PCR and sequencing. This RNA hairpin was predicted to target all Ada2b transcripts with no off-targets.

2.5 Germline clone fly

For each mutant allele, FRT was recombined into the same chromosome arm to get stable stocks. Then FRT, ovoD stocks were crossed with the mutation, FRT stocks. For germline clone analyses, larvae from the crosses were heat-shocked for 2hr at 37°C for two days starting from the second day after hatching. Homozygous virgins were collected and used for further analyses.

2.6 Immunostaining

Embryos were collected from apple juice plates and dechorionated with 3% bleach for 3 mins. Dechorionated embryos were vigorously mixed in fixative (2% formaldehyde, 0.1M PIPES pH 6.9, 2mM $MgSO_4$ and 1mM EDTA) with an equal volume of Heptane for 18min at room temperature. After removal of the fixative, embryos in Heptane were devitellinized by vigorously mixing with an equal volume of Methanol:EGTA (9:1 Methanol:0.5M EGTA). Embryos were washed three times with Methanol:EGTA (9:1 Methanol:0.5M EGTA) and embryos were stored at -20°C before use.

For the immunostaining, embryos were washed in PBST (PBS + 0.5% Tween-20) 3 X 15mins at room temperature with rotation. Subsequently, embryos were blocked in PBST with

5% normal horse serum for 1h. All the immunostaining were performed in PBST with 5% normal horse serum.

Ovaries were dissected in Shields and Sang M3 insect medium within 30mins and fixed in PBS with 4% formaldehyde for 15min at room temperature with rotation. After fixation, ovaries were washed in PBST (PBS+0.2% Triton) 4 X 15mins and blocked in PBST with 5% normal horse serum for 1h. All the immunostaining were performed in PBST with 5% normal horse serum.

Primary antibody staining was performed at 4°C overnight and secondary antibody staining was performed at room temperature for 2-3h. Primary antibodies included Discs-large (1:20), Even-skipped (1:10), Enabled (1:500) and Fasciclin II (1:500) from the DSHB (Iowa City, IA). Twist (1:500), α-Tubulin (1:200; F2168, Sigma-Aldrich). Vasa (1:200; sc-30210) and Staufen (1:200; sc-15823) from Santa Cruz Biotechnology. H3K9ac (ab4441) and H3K14ac (ab52946) from Abcam. Alexa Fluor 647 Phalloidin (1:20; A22287, Thermo Fisher Scientific) was used to detect F-actin. The Myosin Heavy Chain monoclonal antibody (MHC, 1:1000) was obtained from D. Kiehart (Duke University Medical Ctr. Durham, NC). Alexa Fluor secondary antibodies (1:200) were obtained from Invitrogen. Colorimetric detection was performed using biotinylated anti-mouse secondary antibodies (1:200, Vector Laboratories) and the Vectastain ABC elite kit (Vector Laboratories). Cell nuclei were stained using DAPI (1µg/ml).

Images were taken using Zeiss LSM 510 VIS and LSM 700 Falcon confocal microscopes. Some embryo and ovary images were generated by max projection of selected confocal slices using ImageJ. Channel colors were altered in ImageJ for optimal viewing. Brightness and contrast were adjusted in ImageJ when necessary. Shape and volume were determined for Twist stained nuclei using the surface function of Imaris.

2.7 RNA purification and analysis

Stage 5 embryos were collected, dechorionated and hand sorted under microscopes. Ovaries from yeast conditioned 2-3d females were dissected in Shields and Sang M3 insect medium within 30 mins. Total RNA was extracted using the RNeasy Plus Mini Kit (Qiagen) according to the manufacturer's protocol, with biological triplicates for each genotype.

cDNA was generated using Superscript III First-Strand Synthesis according to the manufacturer's protocol. Quantitative PCR (real-time PCR) was performed from biological triplicates using 7900HT Real time system.

For RNA-seq analysis, biological triplicates were carried out for each genotype. Reads generated were 51-base-pair (bp) single-end, poly-A-selected, directional using the Illumina protocol. Resulting reads per gene were analyzed in R with the edgeR package using default methods. Differentially expressed genes (DEGs) were identified using the cutoff of P-value < 0.05 and FPKM>1. The cutoff of fold change more than 2 was applied for identifying down-regulated genes and up-regulated genes. Some of the analyses were done by Chris Seidel (Stowers Institute for Medical Research).

2.8 ChIP-seq analysis

Stage 4-6 embryos were collected and dechorionated. The embryo stage was confirmed microscopically. Embryos were fixed in 1.8% formaldehyde for 15 min at room temperature with shaking. Embryos were homogenized in buffer A1 (15 mM HEPES at pH 7.5, 15 mM NaCl, 60 mM KCl, 4 mM $MgCl_2$, 0.5% TritonX-100, 0.5 mM DTT) (0.1g embryos/1ml A1). The chromatin pellet was washed three times with 5ml buffer A1 and once with 5ml buffer A2

(15 mM HEPES at pH 7.5, 140 mM NaCl, 1 mM EDTA, 0.5 mM EGTA, 1% TritonX-100, 0.1% sodium deoxycholate, 0.1% SDS, 0.5% N-lauroyl sarcosine). The chromatin was sonicated in 250µL of buffer A2 (0.1g embryos/250ul A2) seven times for 10 sec (0.9s on/0.1s off for 10 times) at 30% power. After centrifugation at 14,000 rpm for 10 min at 4°C, soluble chromatin was incubated with antibodies at 4°C overnight. Antibody-bound chromatin was pulled down by protein A or protein G-conjugated Dynabeads (Invitrogen) at 4°C for 2h, and the beads were washed five times with RIPA buffer (50 mM HEPES at pH 7.5, 1 mM EDTA, 0.7% sodium deoxycholate, 1% NP-40, 0.5 M LiCl, 1 mM PMSF) and once with TE buffer containing 50 mM NaCl. The chromatin was eluted twice in TE buffer containing 1% SDS and 250 mM NaCl for 30 min at 65°C. After RNase A and proteinase K treatment, cross-linking was reversed overnight at 65°C. DNA was purified by phenol-chloroform extraction and ethanol precipitation.

The antibodies used for ChIP included 10 µg of rabbit α-Sgf11, 20 µg of rabbit α-Ada2b, 20 µg of rabbit α-Spt3, 20 µg of rabbit α-Non-stop, 20 µg of rabbit α-WDA, 3 µg mouse α-pol II (4H8) (ab5408, Abcam), 5 µg of mouse α-ubH2B (17-650, EMD millipore), 5 µg of rabbit α-H2B (ab1790, Abcam), 5 µg of rabbit α-H3K9ac (ab4441, Abcam), 5 µg of rabbit α-H3K14ac (ab52946, Abcam) and 5 µg of rabbit α-H3 (ab1791, Abcam).

Most of the analyses were done by Chris Seidel. Reads of 51 bases from an Illumina HiSeq 2500 were aligned to version dm3 of the *Drosophila* genome from UC Santa Cruz using bowtie parameters: --best --strata -k 1 -m 3. The resulting BAM files were analyzed in R using Bioconductor to generate coverage and normalize the data in Reads Per Million. Locations of enrichment for each protein were identified using MACS2 with default parameters. For each subunit, multiple biological replicates were carried out and peaks were called only if present in at least two replicates. SAGA peaks were called only if present in all subunits. The DUB module

peaks included only those sites in which Ada2b and Spt3 binding were absent in all biological replicates.

2.9 Antibody production

Affinity purified antibodies for ChIP analysis were generated by the GenScript Company following the PolyExpress Premium Antigen-Specific Affinity Purification Production protocol. Antigens included: full length Sgf11 and Spt3, aa 1-330 of Ada2b, aa 178-496 of Non-stop and aa 75-380 of WDA. For immunostaining, aa 1-320 of Twist was purified from *E.coli* and injected into guinea pigs by Pocono Rabbit Farm and Laboratory, and antiserum was affinity purified using the same antigen.

2.10 Differential interference contrast microscope

Differential interference contrast (DIC) images of ovaries were taken using a Zeiss Axioplan 2 microscope, and the Adobe Photoshop Photomerge function was used to generate composite images where necessary.

2.11 Acridine Orange staining

Live ovaries were dissected in PBS within 15mins and then stained with 1µg/ml acridine orange for 15min with rotation at room temperature (avoiding light). Ovaries were briefly washed with PBS and mounted in PBS.

2.12 Live imaging

To visualize nuclei, His2Av-mRFP was integrated into germline clone female chromosomes. Embryos (stage 1-2) were collected at 25°C and dechorionated before imaging. Embryos were incubated in PBS and immobilized in a custom made poly (dimethylsiloxane) microfluidic device at room temperature (Ghannad-Rezaie et al. 2012), and imaged with a LSM 780 confocal microscope using a 20x Plan-Apochromat (NA 0.8) objective. Images were acquired every 3 minutes with excitation from a 561nm laser. Fluorescence emission was collected across the entire visible range, the pixel time was 1.58 µs and the Z spacing was 1 µm.

2.13 Survival Quantitation

0-4h embryos were collected, transferred to standard apple juice plates and grown at 25°C. 1st instar larvae were counted one day after transfer. Dead embryos were confirmed by brown coloring. Three replicates of 100 embryos were carried for each genotype; unfertilized (white) embryos were subtracted from the total prior to quantitation.

2.14 Nuclear extracts and Western blot

Embryos were collected and dechorionated and then resuspended embryos in 200µl buffer I (15mM HEPES (Na+) pH 7.5, 10mM KCl, 5mM MgCl2, 0.1mM EDTA, 0.5mM EGTA, 350mM sucrose, 20µg/mL leupeptin, 20µg/mL pepstatin and 100µM PMSF). Nuclei were pelleted at 10400g for 15 min at 4ºC. Nuclei were suspended in 200µl buffer I and pelleted again at 10400g for 10 min at 4ºC. Nuclei were suspended in 200µl extract buffer (20mM HEPES

(Na+) pH 7.5, 10% glycerol, 0.35M NaCl, 1mM MgCl2, 0.1% Triton X-100, 20µg/mL leupeptin, 20µg/mL pepstatin and 100µM PMSF) at 4°C for 1h with rotation. The mixture was centrifuged at 14000 rpm for 10min at 4ºC to pellet chromatin. Protein concentration was measured using Bio-Rad protein assay.

Larvae were bulk-homogenized with a sterile Polypropylene (PP) pestle in 200 µl of CytEB 1X (15 mM Hepes-KOH pH 7.6, 10 mM KCl, 5 mM MgCl2, 0.1 mM EDTA pH 8.0, 10% Glycerol). The homogenate was centrifuged at 600g for 1min at 4 ºC and the supernatant was carefully removed and processed in further steps. About 150–200 µl of supernatant was centrifuged 5000g for 10min at 4 ºC. The dried pellet was washed with 150µl wash buffers WASH150 (CytEB 1X, 150mM sucrose) and 150µl WASH250 (CytEB 1X, 250mM sucrose). Finally, 150µl of NEB (350 mM Sucrose, 15 mM Hepes-KOH pH 7.6, 385 mM KCl, 5 mM MgCl2, 0.1 mM EDTA pH 8.0, 0.05% Tween 20, 10% Glycerol) was used to extract nuclear proteins and centrifuged at 14000g for 10min at 4 ºC. Protein concentration was measured using Bio-Rad protein assay (Lo Piccolo, Bonaccorso and Onorati 2015).

An equal amount of protein was subjected to Western blotting. Primary antibodies used for western bloting include: rabbit α-Non-stop (1/1000), rabbit α-Ataxin-7 (1/1000) and rabbit α-Ada2b (1/1000).

Chapter 3

Enzymatic modules of the SAGA chromatin-modifying complex play distinct roles in *Drosophila* gene expression and development

3.1 Abstract

The Spt-Ada-Gcn5-acetyltransferase (SAGA) chromatin-modifying complex is a transcriptional coactivator that contains four different modules of subunits. The intact SAGA complex has been well characterized for its function in transcription regulation and development. However, little is known about the roles of individual modules within SAGA and if they have any SAGA independent functions. Using *Drosophila*, we sought to determine whether 1) SAGA is required for transcription of all genes, 2) SAGA dependent genes require both the HAT and DUB modules, and 3) individual modules can function independently of SAGA. We generated germline clones of genes encoding subunits of several modules to eliminate maternal gene product and examined the requirement for SAGA in oogenesis and early embryogenesis. Morphological analysis was used to determine the developmental stage at which mutants of different SAGA modules exhibit defects. Whole transcriptome profiling was used to determine which genes require different SAGA subunits. Lastly, ChIP-seq analysis was used to identify the direct targets of SAGA and its submodules in early embryos. Here we demonstrate that the two enzymatic modules of *Drosophila* SAGA are differently required in oogenesis. Loss of the histone acetyltransferase (HAT) activity blocks oogenesis, while loss of the H2B deubiquitinase (DUB) activity does not. However, the DUB module regulates a subset of genes in early embryogenesis and loss of the DUB subunits causes defects in embryogenesis. ChIP-seq analysis

revealed that both the DUB and HAT modules bind most SAGA target genes even though many of these targets do not require the DUB module for their expression. Furthermore, we found that the DUB module can bind to chromatin and regulate transcription independently of the HAT module. Our results suggest that the DUB module has functions within SAGA as well as independent functions.

3.2 Introduction

Histone modifications, such as acetylation and ubiquitination, play a key role in facilitating a number of nuclear events, including transcriptional regulation. Acetylation of histones is largely associated with relaxing chromatin structures in order to support the entry of transcriptional machinery to the genomic loci for activation, while histone ubiquitination has been linked to both gene activation and repression (Brownell et al. 1996, Weake and Workman 2008). The histone modifying enzymes that catalyze these post-translational modifications are often integrated into large complexes to facilitate their enzymatic activity, substrate specificity and genomic localization.

SAGA is a 2 MDa transcription co-activator protein complex that contains several distinct modules of subunits. These include a transcription activator interaction module, a TATA-binding protein (TBP) interaction module and two enzymatic modules: a histone acetyltransferase (HAT) module and a deubiquitinase (DUB) module. Given the role of SAGA in transcription regulation, it is not surprising that some SAGA subunits are essential for development, especially subunits of the enzymatic modules. Gcn5 is the acetyltransferase subunit of SAGA and ADA (yeast) and ATAC (metazoans) complexes (Guelman et al. 2006a,

Grant et al. 1997, Martinez et al. 1998, Martinez et al. 2001, Demeny et al. 2007, Ogryzko et al. 1998). *Drosophila* Gcn5 is required for metamorphosis and oogenesis (Carre et al. 2005). In mice, GCN5 null embryos die during embryogenesis (Xu et al. 2000), and GCN5 HAT activity is critical for cranial neural tube closure (Bu et al. 2007). The SAGA specific HAT module subunit Ada2b, which is required for the HAT activity, is also essential for *Drosophila* viability (Pankotai et al. 2005, Qi et al. 2004, Kusch et al. 2003, Muratoglu et al. 2003, Zsindely et al. 2009).

The DUB module subunits also control developmental processes. In *Drosophila*, the deubiquitinase subunit Non-stop and an essential DUB module subunit Sgf11 function together in neural development (Weake et al. 2008). The mouse deubiquitinase subunit USP22 is critical for early embryogenesis (Lin et al. 2012) and it has also been shown to play a role in cell differentiation and lineage specification (Kosinsky et al. 2015).

Several studies have investigated the structural features of SAGA and how SAGA subunits integrate into the whole complex. The two enzymatic modules are anchored to core SAGA through other subunits. Combining deletions with affinity purification of tagged subunits and mass spectrometry initially revealed the organization of subunits into modules within yeast SAGA. The HAT module subunits were lost from SAGA when purified from an *ada2Δ* strain, suggesting that the Ada2 is essential to anchor the HAT module (Lee et al. 2011). Similarly, Sgf73 anchors the DUB module into SAGA (Lee et al. 2009). These results are confirmed by separate groups using EM (Electron Microscopy) analysis and cross-linking studies (Han et al. 2014, Setiaputra et al. 2015). Moreover, the N terminus of Sgf73 is necessary for DUB module activation and its recruitment to SAGA. (Kohler et al. 2010, Kohler et al. 2008). Notably, the DUB module can disassociate from SAGA under some conditions and remain stable. In yeast, a

functional DUB module can be separated from SAGA by the proteasome regulatory particle (Lim et al. 2013). In *Drosophila,* loss of the Sgf73 homolog Ataxin-7 leads to disassociation of an enzymatically active DUB module (Mohan et al. 2014). In humans, the DUB module is still stable in SPT20 knockdown cells. Thus, the integrity of the DUB module appears to be independent of SAGA, suggesting that it may be able to exist as a free form (Nagy et al. 2009).

In this study, we took advantage of genetic approaches in *Drosophila* to remove the maternal contribution and investigated the requirement for the SAGA HAT and DUB enzymatic modules in early development. We found that perturbation of the HAT module caused defects in oogenesis and a complete inability to form mature oocytes. By contrast, the DUB activity was expendable during oogenesis, and at least some early zygotic genes were transcriptionally active. Nevertheless it was essential for normal cellularization in these early embryos, and their survival through embryogenesis. It was also essential for wild-type levels of transcription. We identified binding sites for several SAGA subunits genome wide in early embryos and found coincident binding at most sites. Notably, the DUB module bound to chromatin with other SAGA subunits even when it was not required for transcription of the associated genes. More interestingly, we identified sites in which DUB module subunits bound chromatin independent of the core SAGA modules, where it regulated transcription.

3.3 Results

3.3.1 The HAT module is required for oogenesis, whereas the DUB is expendable

Since the SAGA complex contains distinct functional modules we sought to investigate whether all the modules of SAGA are required coordinately or if different modules play distinct roles during development. We focused on the two enzymatic modules, which contain the histone

acetyltransferase (HAT) activity and the deubiquitinase (DUB) activity. We first evaluated whether both the HAT and the DUB activity were required at the earliest stages of development, during oogenesis. For this analysis, it was necessary to eliminate maternally-provided transcript in the developing eggs. We used the *FLP/FRT/ovoD* system (Chou and Perrimon 1996) to delete subunits of the DUB and HAT modules in the germline cells of the germline clone (GLC) females ovaries. This analysis was carried out with null alleles of the SAGA-specific subunits Ada2b, which is required in the HAT module for its activity (Qi et al. 2004, Kusch et al. 2003, Muratoglu et al. 2003), Ataxin-7, which anchors the DUB module to the remainder of SAGA, and the deubiquitinase subunit Non-stop (Figure 3.1).

We found that oogenesis is blocked in *Ada2b* GLC females, which did not lay eggs. This result is consistent with previous data that *Ada2b* germ cells arrest at an early stage of oogenesis (Qi et al. 2004). To determine the stage at which Ada2b was required, we examined the morphology of dissected ovaries by Differential Interference Contrast (DIC) and confocal microscopy. Overall, *Ada2b* mutant egg chambers developed to stage 10, when nuclei began to exhibit degeneration (Figure 3.2A) and apoptotic cell death was observed (Figure 3.3). DIC images also revealed degeneration of the oocyte prior to maturity (Figure 3.4). By contrast with the *Ada2b* mutants, oogenesis proceeded normally in both the *Ataxin-7* and *non-stop* GLC females, suggesting that oogenesis is not dramatically affected by disrupting the DUB activity of SAGA. Moreover, nuclei in these developing oocytes were normal (Figure 3.2), and the females laid eggs. Whole dissected ovaries show the dramatic impact of loss of Ada2b, and the normal state of the *non-stop* and *Ataxin-7* GLCs (Figure 3.5). Egg laying rates for germline clone females are shown in Table 3.1.

To examine these mutant ovaries in more detail and begin to assess requirements for gene expression, we stained ovaries with the germline markers Vasa and Staufen, which play critical roles in germ plasm assembly during oogenesis (Brendza et al. 2000, Wilkie, Dickson and Gray 2003, Johnstone and Lasko 2001). Interestingly, we detected weak localized Vasa protein but no localized Staufen protein in the degenerating *Ada2b* germline cells (Figure 3.2). However, Staufen was detected and localized to the posterior end of earlier stage oocytes (Figure 3.6). These results suggest that *vasa* and *staufen* mRNA transcription still occurs in the absence of Ada2b. Not surprising, in *Ataxin-7* and *non-stop* GLC females ovaries, those two proteins were still expressed and localized at the right places. Taken together, we conclude that the HAT module is required for normal oogenesis, but not for transcription of all genes. However, oocytes lacking Non-stop or Ataxin-7 in the DUB module develop normally.

3.3.2 The HAT module plays a critical role in transcriptional regulation in the ovary

Although clearly some transcription occurred in ovary germ cells lacking Ada2b, as evidenced by the expression of Staufen and Vasa, the degeneration of these oocytes prompted us to investigate transcription defects genome-wide using RNA-seq. We hypothesized that comparison of gene expression in oocytes lacking Ada2b to those lacking Ataxin-7 or Non-stop would allow us to identify genes requiring the SAGA HAT activity but not the DUB activity for their expression. The ovaries include both the germline derived oocytes and overlying somatic follicle cells. The latter are wild-type for these SAGA subunits in the germline clones. We were therefore unable to evaluate changes in expression of some genes in the oocytes if their expression in follicle cells was higher. However, this analysis did reveal those genes that differ between the HAT and the DUB modules in the ovary germline cells. Consistent with the severe

phenotype, more than a thousand genes changed expression in *Ada2b* GLC ovaries. In contrast, expression of only a few hundred genes was affected by absence of Ataxin-7 or Non-stop (Figure 3.7A). We also found that very few genes overlapped between the three mutants, suggesting the possibility that the DUB module is exclusively required for the expression of some genes. Because of the presence of the overlying wild type follicle cells, we are unable to identify genes that do not require the HAT module in the ovary. Nevertheless, these studies reveal different requirements for the DUB and the HAT modules in developing oocytes, with the latter playing a greater role.

To determine whether specific gene networks and pathways have a common requirement for the HAT activity during oogenesis, we performed Gene Ontology (GO) term analysis (Figure 3.7B). Genes involved in DNA replication, eggshell formation and chromosome organization were significantly down-regulated in the absence of Ada2b. Specifically, genes involved in DNA repair were down-regulated in *Ada2b* GLC ovaries, which may explain the nuclear degeneration phenotype (Table 3.2). Similar analysis in the *Ataxin-7* or *non-stop* GLC ovaries revealed no significant enrichment of any particular pathways, including those noted above for Ada2b. These data correspond well with the different phenotypes shown earlier, and support our earlier observations that nuclei degenerate in *Ada2b* oocytes and that the DUB module is expendable for oogenesis.

3.3.3 Early patterning still occurs in embryos lacking Ataxin-7 or non-stop

To investigate whether the DUB module play a role in embryogenesis, we examined the fertilized embryos from *Ataxin-7* and *non-stop* GLC females. We focused on Stage 5 embryos

and confirmed from RNA-seq analysis that no maternal load or zygotic transcripts of *Ataxin-7* or *non-stop* were yet detectable (Figure 3.1). Therefore, we inferred that the presence of a wild type zygotic copy from the male upon fertilization did not impact analysis at this early stage. We then examined the Anterior-Posterior (A-P) and Dorsal-Ventral (D-V) axes of these embryos. The pair rule gene *even-skipped* (*eve*) contributes to axis specification and its zygotic expression is visible in a 7-stripe pattern along the A-P axis (Macdonald, Ingham and Struhl 1986). The bHLH factor *twist* is one of the earliest zygotically active genes along the D-V axis and its expression along the ventral side of the embryos specifies mesoderm (Thisse, el Messal and Perrin-Schmitt 1987). As shown in Figure 3.8, Eve was apparent in a 7-stripe pattern in *Ataxin-7* and *non-stop* GLC embryos in a pattern that is reminiscent of WT, suggesting both that *eve* is expressed and that the A-P axis forms in the absence of DUB module subunits. We also found that *twist* was expressed in the presumptive mesoderm and localized on the ventral side, indicating formation of an early D-V axis. We therefore conclude that transcription of some early zygotic genes occurs in early embryogenesis independent of the DUB module of SAGA.

3.3.4 Loss of DUB module subunits affects cellularization and gene expression

Although expression of some zygotic genes was initiated and early patterning occurred, we did observe defects in cellularization. Normally, the newly fertilized embryo undergoes several rounds of nuclear divisions without cytokinesis and remains syncytial. The nuclei then migrate to the periphery of the embryo, at which time they become surrounded by individual cell membranes (Mazumdar and Mazumdar 2002). In WT embryos, nuclei at the surface of the embryos formed an organized pattern (Figure 3.8B-C). However, in *Ataxin-7* and *non-stop* GLC embryos, nuclear Twist staining revealed a disorganized pattern, with the absence of nuclei in

some locations. Expression of the membrane marker Discs-large (Dlg) revealed misshapen membranes in these regions. DAPI staining of all nuclei indicated that these defects were not limited to the ventral side (Figure 3.9). Notably, we are unable to distinguish the male chromosome provided to the egg upon fertilization by heterozygous mutant males and the genotype of the resulting embryos at this stage (m-/-, z-/- vs m-/-, z-/+). However, the above defects were observed in all embryos independent of the zygotic copy provided by the male. Lastly, the ovary and embryonic phenotypes of *Ataxin-7*^{HO3} were confirmed with *Ataxin-7*$^{2A-1}$ (Figure 3.10). Thus, we conclude that these defects are a consequence of the absence of maternal Ataxin-7 or Non-stop.

Interestingly, we noted the presence of mislocalized nuclei in the internal of the embryo underneath the distorted regions (Figure 3.9). We hypothesized that these nuclei might be unable to complete migration or anchor to the periphery. However, time lapse imaging revealed that these nuclei were actually able to migrate to the periphery but did not maintain this position and fell back into the internal of the embryos. Despite the ability of most nuclei to remain at the periphery, these nuclei also exhibited defects in cellularization. Tubulin and Enabled revealed that cell membrane invagination was defective in GLC embryos (Figure 3.9A). Real-time PCR showed that genes known to be involved in cellularization and nuclear anchoring (*kuk, slam, bnk, Sry-α, nullo*) (Chen et al. 2013, Pritchard and Schubiger 1996, Schejter and Wieschaus 1993, Brandt et al. 2006, Pilot et al. 2006, Stein et al. 2002, Ibnsouda et al. 1993) depend on the DUB module and change expression in *non-stop* and *Ataxin-7* GLC embryos. In conjunction with similar loss of function phenotypes for *kuk*, *non-stop* and *Ataxin-7*, we conclude that cellularization and nuclear anchoring are abnormal as a consequence of these decreases in expression. As shown in Figure 3.9B, transcript levels of these genes changed in the absence of

Ataxin-7 or Non-stop (Primer sequences Table 3.3). Therefore, we conclude that the DUB module plays an important role in regulating transcription prior to cellularization.

We examined the muscle, central nervous system, H3K9ac and H3K14ac in stage 16 *Ada2b* zygotic mutant embryos. The levels of H3K9ac and H3K14ac were reduced, indicating that the HAT module affects acetylation during embryogenesis as previously shown (Qi et al. 2004). However, decreased acetylation at this stage does not result in phenotypic defects, possibly indicating that maternal Ada2b is sufficient for early transcription and specification (Figure 3.11A). We also identified Ada2b knock down conditions that allowed oogenesis to proceed and examined the phenotype of the resulting embryos. The embryos exhibited defects in cellularization, indicating a role for Ada2b in early embryogenesis and suggesting that reduction in Ada2b has similar consequences to loss of Ataxin-7 and Non-stop (Figure 3.11B). Interesting ly, RNA-seq of *Ada2b* knock-down embryos shows that genes (*kuk*, *slam*, *bnk*, *nullo*) which changed expression in the DUB mutants were also down-regulated in the *Ada2b* mutants. These data indicate that the entire SAGA complex is required for cellularization.

We also noted that most nuclei in *Ataxin-7* and *non-stop* GLC embryos were misshapen. To better visualize these shapes and quantitate their volumes, we used the surfacing function of Imaris software. It revealed that a large number of nuclei, both at the surface and internal, did not adopt the elongated shape characteristic of WT (Figure 3.9C). The defective nuclei in GLC embryos appeared larger than WT (Figure 3.8C), but Imaris surfacing indicates they are only modestly smaller (Figure 3.9D). Given that all *Ada2b* GLC oocyte nuclei appeared to degenerate, we then asked whether these misshapen embryo nuclei in *Ataxin-7* and *non-stop* GLCs were also degenerated. We examined the DNA damage marker γH2Av in *Ataxin-7* GLC embryos but this marker revealed no damaged nuclei (data not shown). Consistent with this finding, the early

defects in embryos lacking the DUB module subunits could be rescued by zygotic expression of a wild type copy of the gene contributed by the male. This rescue was apparent in the muscle pattern of *Ataxin-7* (m-/-, z-/+) embryos despite their early defects (Figure 3.12A). In fact, 25% of these embryos survived to 1st instar larvae (Figure 3.12B). Thus, we conclude that the distorted shape and defective cellularization described above is not associated with degeneration of the nuclei and, moreover, that the embryo must be able to accommodate or correct these defects.

Despite the modest impact of the absence of DUB module subunits in early development, Ataxin-7 and Non-stop are important for embryogenesis. Notably, 75% of *Ataxin-7* (m-/-, z-/+) embryos and 100% of *non-stop* (m-/-, z-/+) embryos died during embryogenesis (Figure 3.12B). More significantly, zygotic expression is essential since embryos lacking both maternal and zygotic expression exhibited dramatic defects later in embryogenesis (Figure 3.12A), suggesting that the presence of the DUB module subunits is critical for embryogenesis.

Altogether, these data demonstrate the importance of the DUB module for wild-type levels of gene expression in the early embryo and overt embryogenesis.

3.3.5 The DUB module regulates a subset of genes in early embryogenesis

Based on the known role of the DUB module in deubiquitination of H2B and the effect of its mutation on expression of several genes above, we wished to explore whether dependence on the DUB module at this stage extended beyond genes associated with cellularization. RNA-seq revealed expression of approximately 6000 genes at stage 5 as expected (RPKM > 1), but only 40% of those genes changed expression in *Ataxin-7* and *non-stop* GLC embryos (Figure 3.13A).

These data support our phenotypic results that while defects were observed, initial patterning of the early embryos was relatively normal.

The similar cellularization defects in *Ataxin-7* and *non-stop* GLC embryos shown above suggests that these proteins function together within the DUB module to regulate transcription. To address this hypothesis, we compared the patterns of gene expression in these GLC embryos and found that approximately 50% of those genes that changed expression are similarly affected in both mutants (Figure 3.13A & Figure 3.14). We then performed GO term analysis of the genes that are commonly changed (764 down-regulated genes and 713 up regulated genes). As shown in Figure 3.13B & Table 3.4, down-regulated genes were enriched in several pathways, primarily those involved in embryonic development and tissue morphogenesis, indicating that these processes were highly dependent on the DUB module. Only genes associated with metabolic processes were enriched in the commonly up-regulated genes. As suggested by the GO term analysis (Table 3.5), some of the up-regulated genes may be secondary effects of down-regulated repressors in the DUB mutants. Combined with the results of our phenotypic analysis, these findings demonstrate that the DUB module of SAGA regulates a subset of genes during early embryogenesis.

Previous studies have suggested that loss of DUB module subunits does not impair HAT activity and the integrity of the rest of SAGA (Weake et al. 2008, Mohan et al. 2014, Lee et al. 2011). To examine the HAT activity in *Ataxin-7* GLC embryos, we performed ChIP-seq of H3K9ac and H3K14ac and found no significant changes in *Ataxin-7* GLC embryos. Moreover, Ada2b binding sites did not change in *Ataxin-7* GLC embryos (Figure 3.15). Comparison of the patterns of genes expression of the DUB GLC embryos and *Ada2b* knock-down embryos indicates that there is only a small degree of overlap between the DUB mutants and *Ada2b*

(Figure 3.16). We also examined H3K9ac and H3K14ac in the germline cells of *Ataxin-7* and *non-stop* GLC ovaries, and observed similar levels to those seen in WT (Figure 3.17). Taken together, these data suggest that the DUB module subunits are not essential for the HAT activity of SAGA and the two enzymatic modules are required by different subset of genes.

3.3.6 Identification of SAGA-bound genes in early embryos

To establish which genes were direct targets of SAGA, ChIP-seq (Chromatin Immunoprecipitation Sequencing) assays were performed to determine occupancy in WT embryos. We chose subunits from each of three different SAGA modules: Ada2b in the HAT module, Spt3 in the SPT module and Sgf11 in the DUB module. Multiple biological replicates were carried out, and peaks were called only if present in at least two replicates. We identified 3033 Ada2b peaks, 2382 Spt3 peaks and 5425 Sgf11 peaks. To identify sites that are likely bound by the intact SAGA, we compared the binding patterns of these three factors for overlap and found good congruence (Figure 3.18A). Hereafter we refer to the 1650 common peaks as SAGA peaks. Next, we assigned these peaks to the nearest transcription start sites (TSS) and identified 1998 genes in which SAGA bound within 500bp of the TSS. Note that the number of target genes is greater than the number of peaks due to the fact that binding can occur within 500bp of the TSS of one, two or, in rare cases, three genes. As shown in Figure 3.18B & Figure 3.14B, only some of the differentially expressed genes were bound by SAGA. These indirect targets may be secondary effects of down-regulated transcriptional activators in DUB mutants (Table 3.5). Of the SAGA-bound targets, some showed expression changes in the DUB mutant (Differentially Expressed in DUB mutants; hereafter referred to as DUB DE), but, interestingly, many others did not change (Figure 3.18B). Thus, the DUB module binds to SAGA targets as a

part of SAGA even though it is not always required for the expression of the target genes (Figure 3.18C). We conclude that SAGA binds to many target genes as a whole complex in early embryos, but the DUB module is only required by a subset of these genes for their expression.

3.3.7 The DUB module binds and regulates gene expression independent of the HAT module

As noted in the introduction, some studies suggest that a stable DUB module exists independent of SAGA under some conditions. However, these studies did not address whether this module can bind to genomic chromatin independent of other SAGA modules under wild type conditions. Whereas most of the Sgf11 peaks overlapped with Ada2b and Spt3, we noticed 2382 target sites where only Sgf11 was bound (Figure 3.18A). We reevaluated peaks using high stringency criteria, including only those sites in which Ada2b and Spt3 binding were absent in all biological replicates. This analysis identified 647 Sgf11 peaks independent of Ada2b and Spt3 (Figure 3.19A). MEME analysis showed that these sites include fork head domain and homeobox domain motifs, and are particularly enriched for Zinc Finger (Znf) binding motifs (Table 3.6). To address whether these Sgf11 bound sites reflected binding of the entire DUB module, we carried out ChIP analysis of Non-stop binding and found that about 90% of all Sgf11 peaks were also bound by Non-stop (Figure 3.20). Since Non-stop was bound at 80% of the unique Sgf11 peaks, we inferred that these peaks represent SAGA-independent binding of an intact DUB module.

To examine the role of the DUB module in regulating transcription of novel targets, we assigned the 647 Sgf11-only peaks to the nearest TSS. Like SAGA, we found a similar binding

preference of the DUB module near the TSS, with 345 of these sites within 500bp of a TSS (Figure 3.19B). Of the 345 DUB target genes (as identified by Sgf11 ChIP-seq), 56 genes required DUB subunits for their expression (Figure 3.19C). Although the DUB module prefers to bind to TSS like SAGA, it binds to genes with different types of promoters (Figure 3.21).

To examine the correlation of ubH2B and gene expression in the DUB mutants for the DUB targets and SAGA targets, we performed ChIP-seq of ubH2B in WT and *Ataxin-7* GLCs. As shown in Figure 3.22, downregulated SAGA target genes have slightly decreased ubH2B in the coding regions in the absence of Ataxin-7, while upregulated SAGA target genes have increased ubH2B in both promoters and coding regions (Figure 3.22B). By contrast, downregulated DUB target genes showed decreased ubH2B in the coding regions in the absence of Ataxin-7, whereas upregulated genes showed increased ubH2B in their promoters (Figure 3.22A). Thus, loss of Ataxin-7 leads to: 1) increased ubH2B at up-regulated genes bound by either SAGA or DUB module subunits and 2) decreased ubH2B at down-regulated genes bound by either SAGA or DUB module subunits. This finding is consistent with an overall activating role of ubH2B. The different distribution of ubH2B in upregulated genes in the DUB module targets (promoters) versus the SAGA targets (promoters and gene bodies) suggest that the DUB module plays distinct roles at those two sets of target genes.

We noticed throughout our analysis that a large portion of SAGA or DUB module target genes did not require the DUB module for their expression. We therefore wished to determine whether the SAGA target genes and the DUB target genes that did not require DUB for expression nevertheless had Pol II bound. The majority of these genes were indeed bound by Pol II (Figure 3.19D). To further characterize the difference of the DUB DE and DUB independent genes, we performed promoter analysis (Chen et al. 2013). As shown in Figure 3.20, for both

SAGA targets and DUB targets, DUB DE genes and DUB independent genes have distinct promoter types, indicating that different promoter types of genes have different requirements for the DUB module. DUB DE DUB targets are enriched for DPE and Inr promoter classes while DUB independent DUB targets are enriched for DRE and Ohler6. DUB DE SAGA targets are enriched for TATA, Inr, and MTE, while DUB independent SAGA targets are enriched for DRE and Ohler1. Moreover, GO terms analysis of SAGA targets suggested that dynamically expressed patterning genes are more likely to require the DUB module, while metabolic process genes tend to be independent of the DUB module (Figure 3.23). Using intensity of H2B binding to monitor nucleosome occupancy between different classes of genes, we found no difference between DUB DE and DUB independent targets for either DUB specific or SAGA targets (Figure 3.21B).

Lastly, we examined the level of Pol II binding at expressed genes (Figure 3.19E). Compared to all Pol II peaks of expressed genes (gray box), much higher levels of Pol II were present at SAGA bound sites (orange box), consistent with previous findings (Weake et al. 2011). Pol II binding was not elevated at robustly expressed DUB target genes (pink box). However, the DUB module clearly facilitates Pol II binding genome wide, possibly reflecting a role for the DUB module in the regulation of paused Pol II and elongation (Figure 3.24).

In summary, we conclude that the DUB module binds to chromatin as a part of SAGA and also independently of SAGA. Its presence is essential for transcription of some of these genes.

3.4 Discussion

Our results reveal the developmental stages at which the DUB and HAT modules of the SAGA chromatin modifying complex are first required. Whereas the HAT module is required during oogenesis and mutant oocytes degenerate by Stage 10, the DUB module is not required for this process and ovaries lacking Non-stop or Ataxin-7 are normal. Moreover, the dorsal-ventral and anterior-posterior axes form in these embryos. The first defect observed in embryos lacking these DUB module subunits is at the stage of cellularization.

Numerous studies have explored the phenotypic consequences of mutations in SAGA DUB and/or HAT module subunits at other stages of *Drosophila* development and in other organisms. In some cases, loss of the two enzymatic modules has the same phenotypic impact, while in other cases, their loss has different consequences. For example, in yeast, DUB module subunits Ubp8 and Sgf73 contribute to centromere stability, while the HAT module subunits Gcn5 and Ada3 do not (Canzonetta et al. 2015). An RNAi screen found that mouse GCN5 regulates reprogramming initiation in embryonic stem cells, whereas the DUB module appears to play no role in this process (Hirsch et al. 2015). In contrast, loss of the *Drosophila* DUB module subunits Non-stop and Sgf11 and the HAT module subunit Ada2b cause similar defects in axon guidance in the eye imaginal disc (Weake et al. 2008). As we have shown for Ada2b, loss of Gcn5 blocks oogenesis and metamorphosis (Carre et al. 2005), and zygotic Ada2b is also essential for viability (Qi et al. 2004, Pankotai et al. 2005). Though their mutant phenotypes have not been compared, the mouse SAGA deubiquitinase USP22 and HAT module subunits GCN5 or ADA3 null embryos all die during embryogenesis (Mohibi et al. 2012, Xu et al. 2000, Lin et al. 2012). Additionally, GCN5 HAT activity is critical for cranial neural tube closure (Bu et al. 2007). Interestingly, loss of the *Drosophila* Ataxin-7 in the eye and adult brain results in neural degeneration (Mohan et al. 2014). Similarly, mammalian Ataxin-7 plays a primary role in the

neurodegenerative disease Spinocerebellar ataxia type 7 (David et al. 1997, David et al. 1998, Del-Favero et al. 1998, Johansson et al. 1998), and some genes which are regulated by Ataxin-7 contribute to the pathology (Chen et al. 2012).

It is important to note in many of the above analyses that several SAGA subunits are present in multiple complexes. For example, Gcn5 is also present in the ADA (yeast) and the ATAC (metazoans) complex. Thus, the greater severity of Gcn5 mutants in many of these examples may result from the loss of these other complexes. Our studies with SAGA-specific HAT and DUB module subunits allow direct comparison of their requirements, with regard to genetic phenotype, expression profiles and target genes.

Many studies show that loss of SAGA subunits affects expression of a subset of genes and that different subunits seem to regulate distinct genes. In yeast, SAGA predominates at more regulated non-housekeeping genes (de Jonge et al. 2017), and is preferentially used by those with TATA boxes, including those associated with stress (Huisinga and Pugh 2004, Basehoar et al. 2004). A more comprehensive genome-wide analysis of all viable SAGA deletion mutants suggests that different modules regulate different sets of genes (Helmlinger et al. 2011). Spt3 and Spt20 regulate 3% and 10% of yeast genes, respectively. Gcn5, by contrast, has been reported to regulate between 1.1% and 4%, most of which are distinct from those regulated by Spt3 or Spt20 (Lee et al. 2000, Helmlinger et al. 2008). Bonnet and colleagues suggested that SAGA is required for all transcribed genes based on Pol II recruitment, and nascent mRNA synthesis at select genes (Bonnet et al. 2014). Gene expression profiling has also been reported for later stages in the *Drosophila* life cycle. Loss of zygotic Ada2b only influences the expression of ~600 genes in larvae and ~900 genes in pupa (Pankotai et al. 2013, Pahi et al. 2015, Zsindely et al. 2009). Similar to yeast, many genes in *Drosophila* larvae require SAGA for their expression,

but some are dependent on the DUB module while others require the HAT module (Weake et al. 2008). Our results suggest that genes transcribed in the *Drosophila* ovary also have distinct requirements for the two enzymatic modules. Consistent with the defective ovaries observed in the absence of Ada2b but not Non-stop or Ataxin-7, many genes require Ada2b in the ovary, while only a small number are affected by the loss of DUB module subunits.

Loss of these subunits alters transcription of many genes, while others exhibit robust expression that is unaffected. As noted above, we observed a reduction in expression of a subset of genes that are important for cellularization, which is likely responsible for the mutant phenotype. Among the cellularization genes reduced in the absence of both Ataxin-7 and Non-stop is *Kugelkern* (*kuk*), which has a similar mutant phenotype (Pilot et al. 2006). Curiously, loss of zygotic Ataxin-7 causes larval lethality that is partially rescued by reducing Non-stop, raising questions of whether critical genes impacted by the loss of Non-stop are affected differently by the loss of Ataxin-7 in all larval tissues (Mohan et al. 2014). By comparison, our analysis showed that many genes are influenced by loss of only one of the subunits, but consistent with their similar embryonic phenotypes, roughly 50% of those genes impacted by the loss of Ataxin-7 or Non-stop are similarly affected in both mutants (Figure 3.13A).

Previous genome wide studies have used binding of a single SAGA subunit to infer targets of the entire complex. For example, Ada2b binding identified putative SAGA targets in *Drosophila* larvae muscle and neurons (Weake et al. 2011), and SPT20 was shown to bind to a subset of transcribed genes in human cell lines (Krebs et al. 2011). In contrast to our analysis, these studies did not evaluate binding differences between modules. We used three SAGA-specific subunits for three different modules in our whole genome analysis of early embryos. Interestingly, we found that the DUB module subunits bound with HAT and SPT module

subunits to SAGA targets, even though it was not always required for their expression. In addition, the DUB module bound to novel targets without the HAT or SPT modules in WT embryos. While we are unable to eliminate the possibility that the unique Sgf11 peaks reflect a robust antibody and are not actually devoid of HAT components, we note that different promoter types are enriched in SAGA targets and DUB specific targets. This finding supports our view that the DUB targets are distinct from those of SAGA.

The studies described in Chapter 3 of this dissertation was published on *Genes and Development* (Li et al. 2017).

Figure 3.1 Null alleles of *Ada2b, Ataxin-7* and *non-stop*. (*A*) Schematic representation of mutant alleles of each genes. Exons are shown as blue rectangles. The translation start codon is labeled as ATG. Red arrow points to the P-element insertion. (*B*) Ovaries RNA-seq tracks show transcription of $Ada2b^{1}$, $Ataxin\text{-}7^{HO3}$ and $non\text{-}stop^{02069}$ in WT and GLC ovaries. (*C*) Stage 5 embryos RNA-seq tracks show transcription of *Ataxin-7* and *non-stop* in WT and GLC embryos. (*D*) Western blots confirm the absence of protein for each reported null allele. Nuclear proteins were extracted from stage 5-9 $Ataxin\text{-}7^{HO3}$ GLC embryos, $non\text{-}stop^{02069}$ GLC embryos and $Ada2b^{1}$ homozygous 3rd instar larvae. Ponceau S is provided as a loading control.

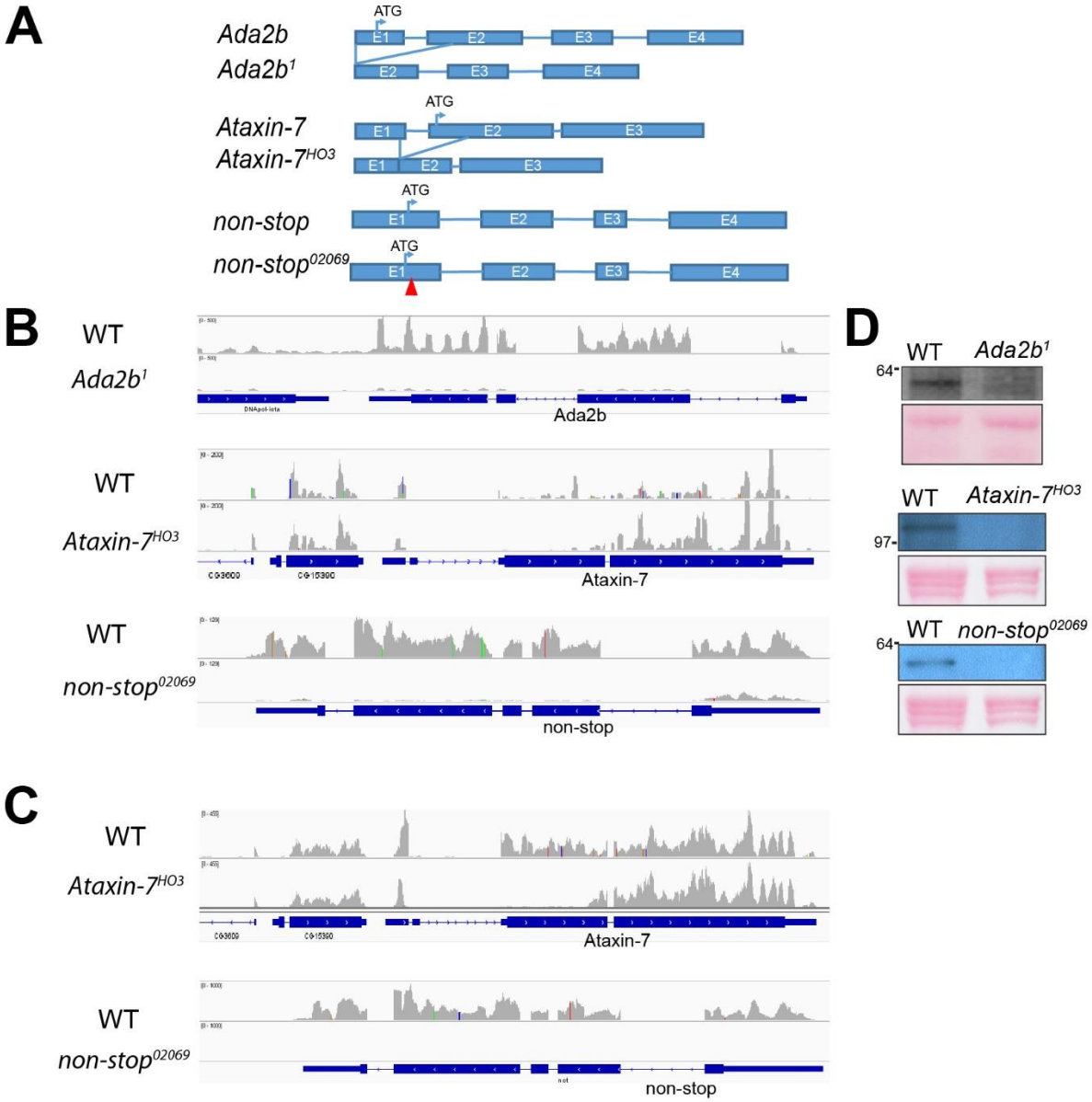
A
Ada2b
Ada2b1
ATG
E1
E2
E3
E4
Ataxin-7
Ataxin-7HO3
non-stop
non-stop02069
B
WT
Ada2b1
Ada2b
WT
Ataxin-7HO3
Ataxin-7
WT
non-stop02069
non-stop
C
WT
Ataxin-7HO3
Ataxin-7
WT
non-stop02069
non-stop
D
WT
Ada2b1
64-
WT
Ataxin-7HO3
97-
WT
non-stop02069
64-

Figure 3.2 The HAT module is required for oogenesis, whereas the DUB is expendable. (*A*) Whole ovaries were stained with Phalloidin (red) for actin and DAPI (green) for nuclei. Posterior is to the right in all panels. (*B*) Vasa protein was observed in the anterior end of stage 10 oocytes for all genotypes (red; arrowhead). Staufen was observed at the posterior end of WT, *Ataxin-7^{HO3}* and *non-stop^{02069}* GLC oocytes (green; arrow). (The muscle sheath that surrounds the ovariole shows prominent but likely nonspecific staining with the Staufen antibody). DAPI (blue) revealed degenerating germline nurse cell nuclei in *Ada2b^{1}* egg chambers (highlighted by white box). The genotypes of GLC ovaries were as follows: Oregon R (WT); *hs-Flp/+; ada2b^{1}, FRT^{82B}/FRT^{82B}, ovo^{D1-18}* (*Ada2b^{1}*); *hs-Flp/+; non-stop^{02069}, FRT^{2A}/FRT^{2A}, ovo^{D1-18}* (*non-stop^{02069}*); *hs-Flp/+; Ataxin-7^{HO3}, FRT^{40A}/FRT^{40A}, ovo^{D1-18}* (*Ataxin-7^{HO3}*). Bars: *A–B*, 50 µm. (The images in panel A were generated by Leanne Well from Stowers Institute)

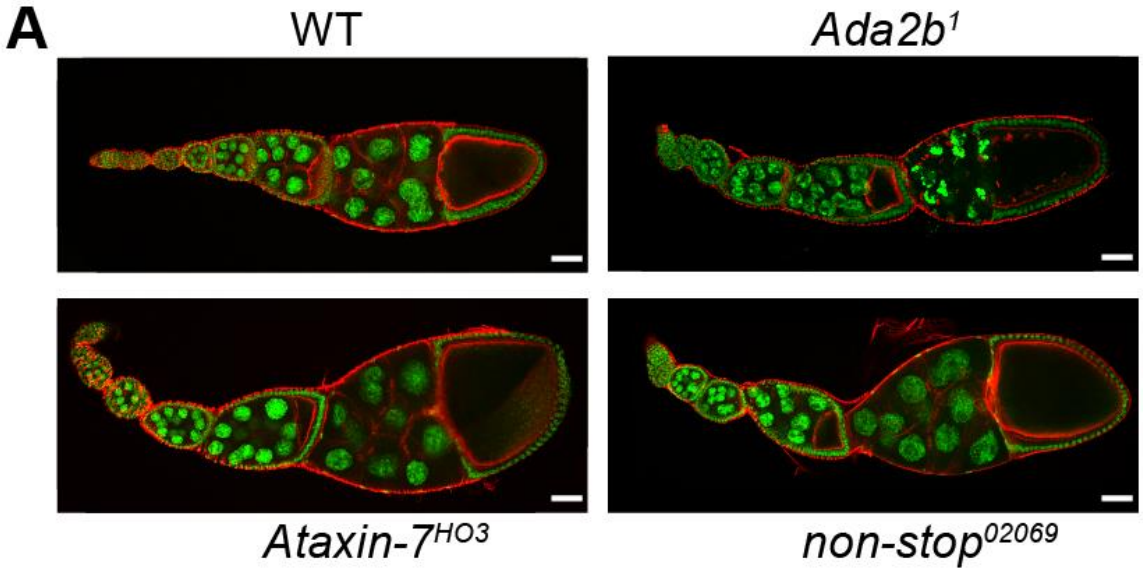
A
WT
Ada2b1
Ataxin-7HO3
non-stop02069

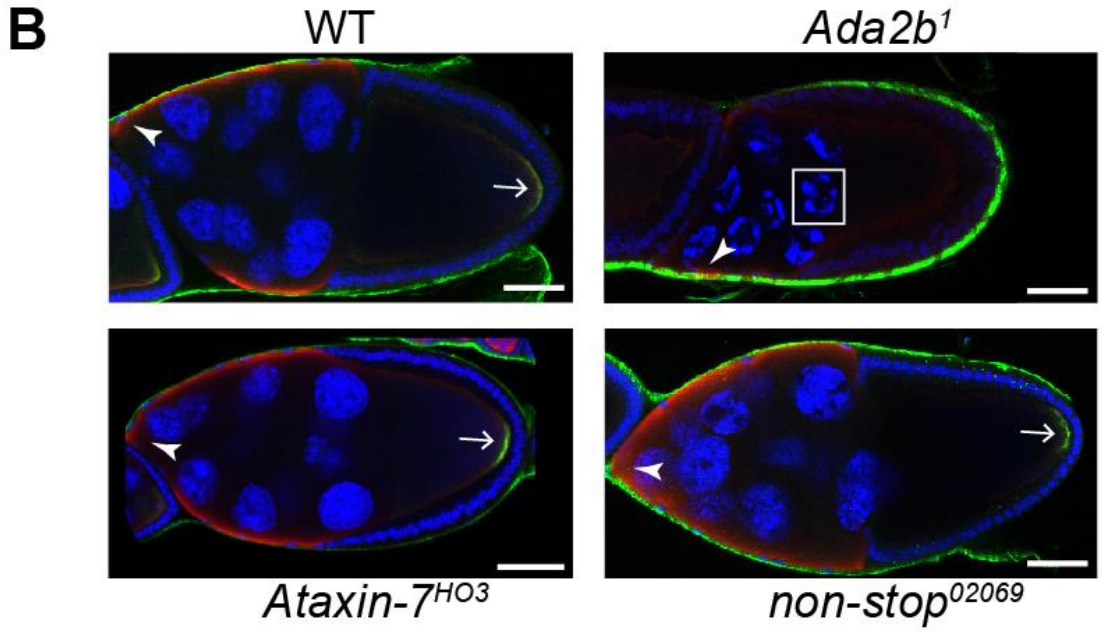
B
WT
Ada2b1
Ataxin-7HO3
non-stop02069

Figure 3.3 Cell death in *Ada2b*^{1} GLC ovaries occurs by apoptosis. (*A*) DAPI staining of ovaries shows the nuclei degeneration in *Ada2b*^{1} GLC. (*B*) Detection of apoptosis in *Ada2b*^{1} GLC ovaries by using acridine orange. *Ada2b*^{1} GLC egg chambers have higher levels of acridine orange than WT at stage 10 (Arrow). However, early stage (stage 7) *Ada2b*^{1} egg chambers developed normally as they had similar levels of acridine orange as in WT egg chambers (Arrow head). Bars: *A–B*, 50 µm.

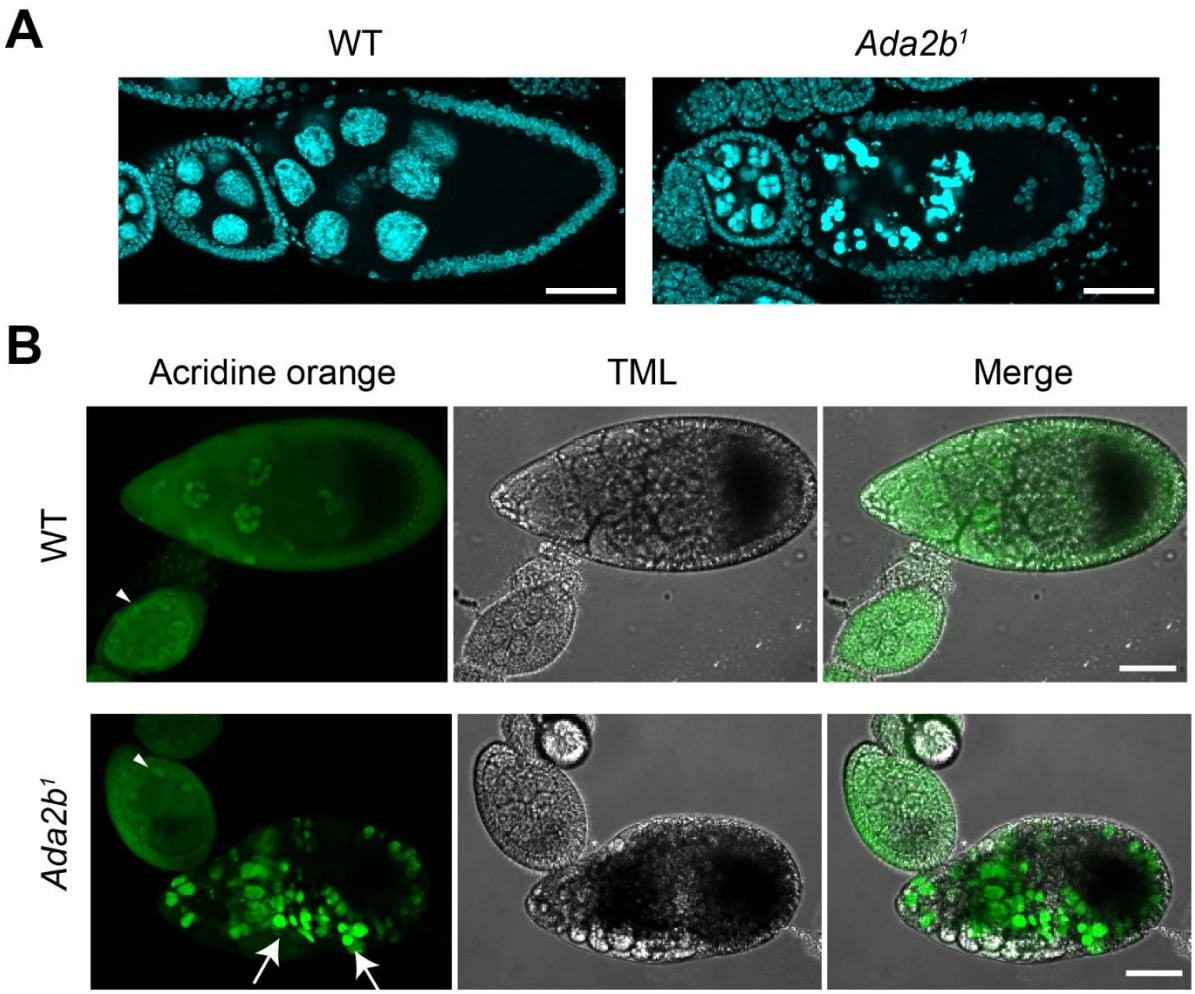

Figure 3.4 *Ada2b* GLC oocytes show degeneration at late stage while *Ataxin-7* and *non-stop* GLCs are fine. Differential interference contrast (DIC) images of ovaries showing the morphology of the ovaries of each genotype. The genotypes were the same as Figure 3.2. Bars: 50µm. (The images in this figure were taken by Leanne Well)

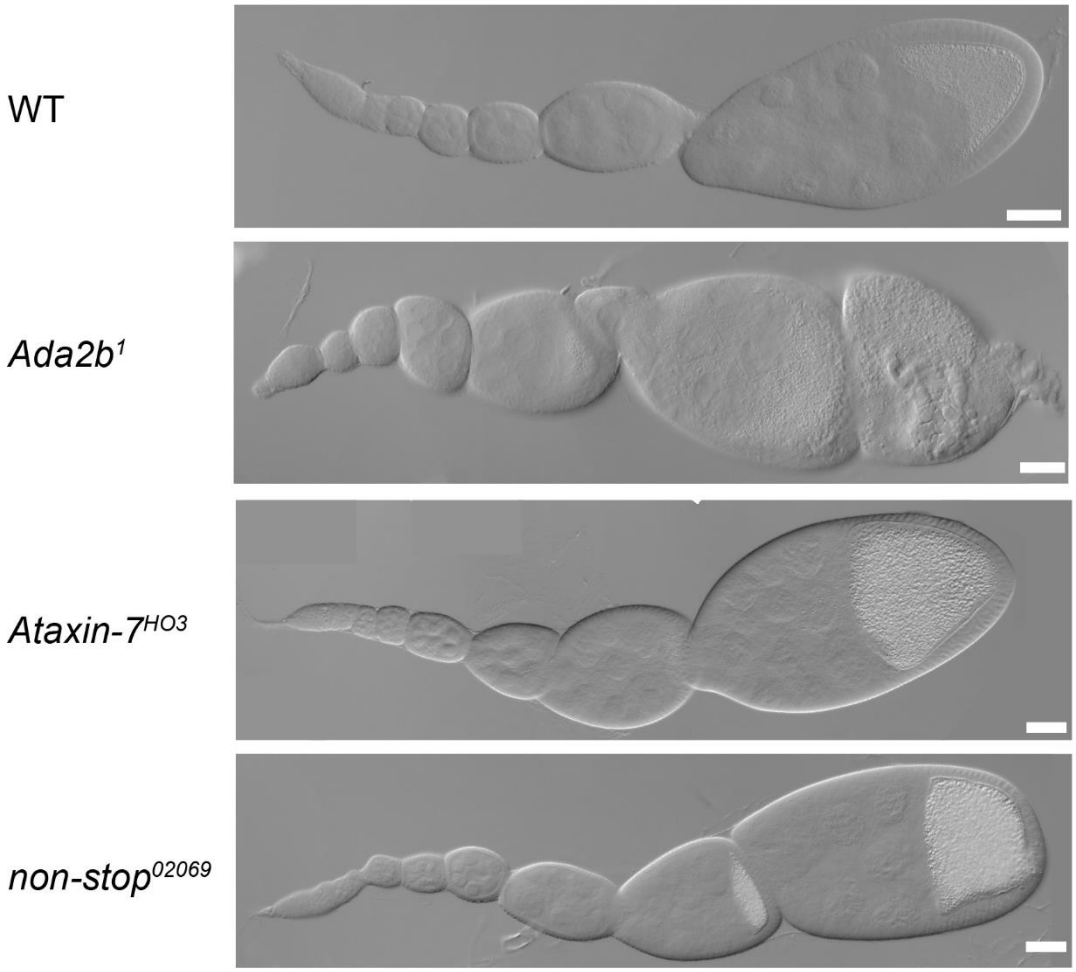

Figure 3.5 Low magnification pictures showing the size of the ovaries of each genotype. The genotypes were the same as Figure 3.2. All pictures are taken by dissection microscope under the same magnification. *Ataxin-7^{HO3}* and *non-stop^{02069}* GLC ovaries have similar size as WT, *Ada2b^{1}* GLC ovaries are smaller than WT.

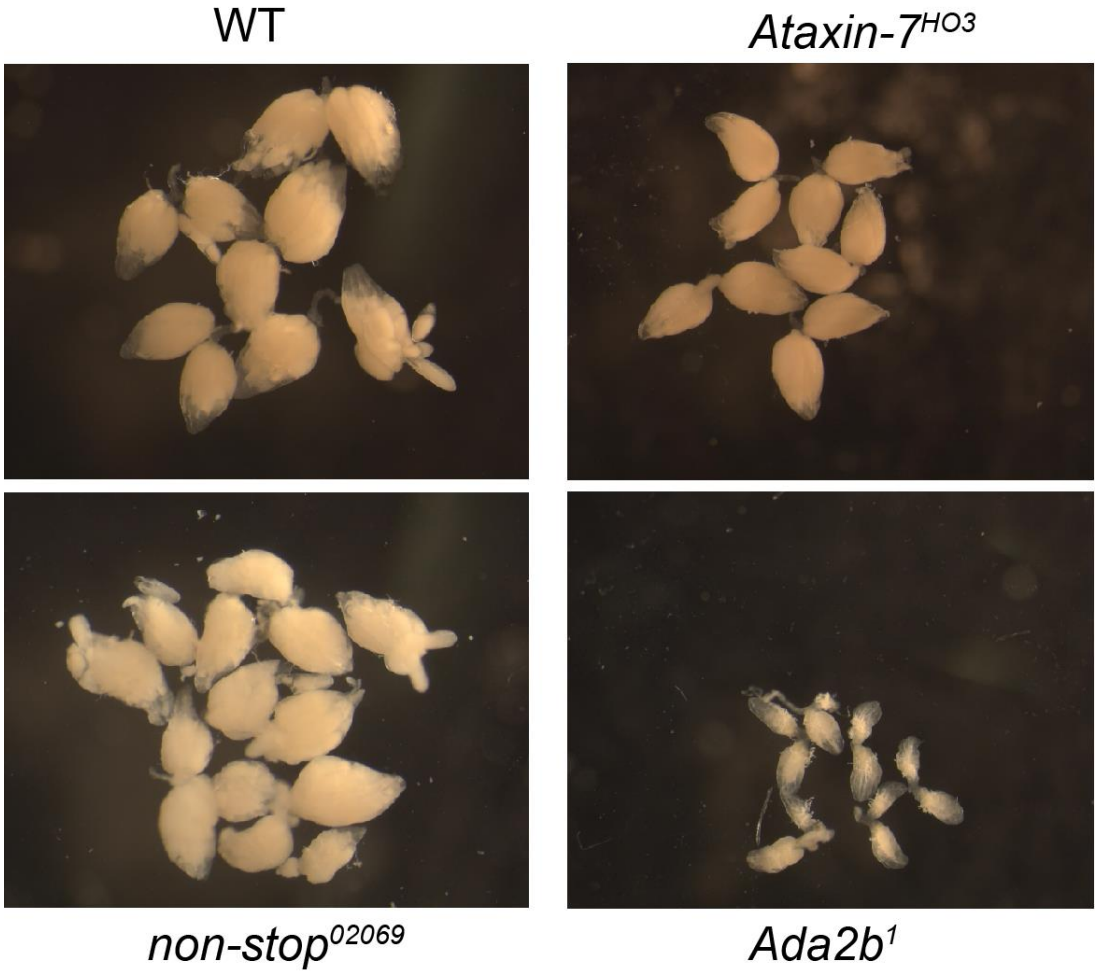

Figure 3.6 Staufen expresses and localizes to the posterior end of earlier stage oocytes. *Ada2b*^{1} GLC oocytes were stained with Staufen (green) and DAPI (blue). Arrow points to Staufen at the posterior end of egg chambers.

Figure 3.7 RNA-seq analysis reveals that the HAT module plays a critical role in transcriptional regulation in the ovary. (*A*) Venn diagrams showing the overlapping genes with decreased or increased transcript levels in *Ada2b*^{1}, *Ataxin-7*^{HO3} and *non-stop*^{02069} GLC ovaries (Fold change > 2, P < 0.05, FPKM > 1). (*B*) GO term analysis of biological process (BP) of genes down- or up-regulated in *Ada2b*^{1} GLC ovaries. A complete list of enriched GO terms with Adjusted *P*-value < 0.05 is provided in Table 3.2.

A

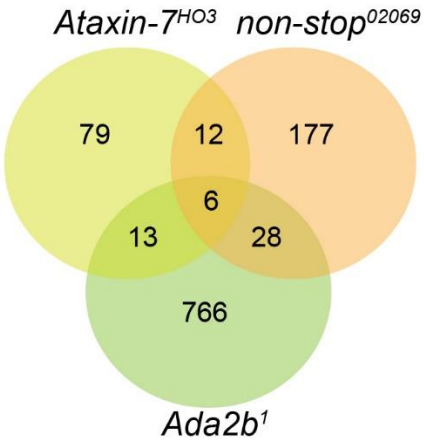

Down >2 fold, P<0.05

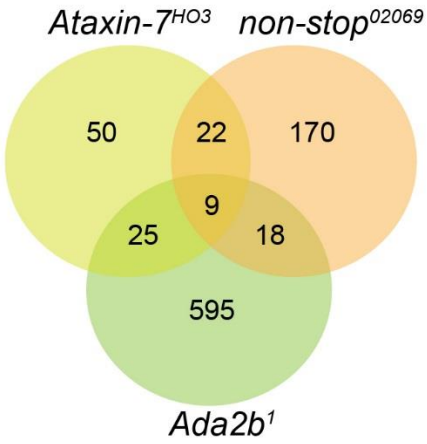

Up >2 fold, P<0.05

B

Ada2b¹ down

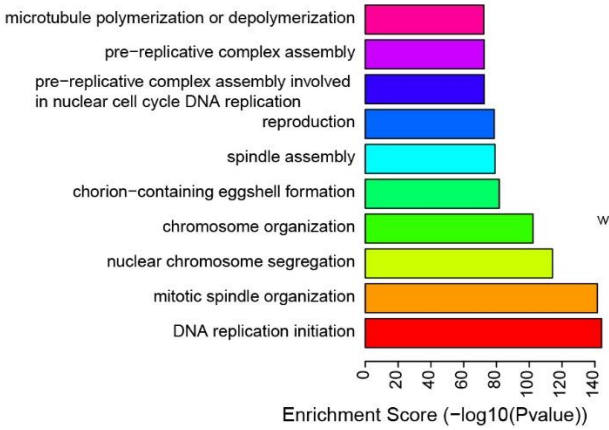

Ada2b¹ up

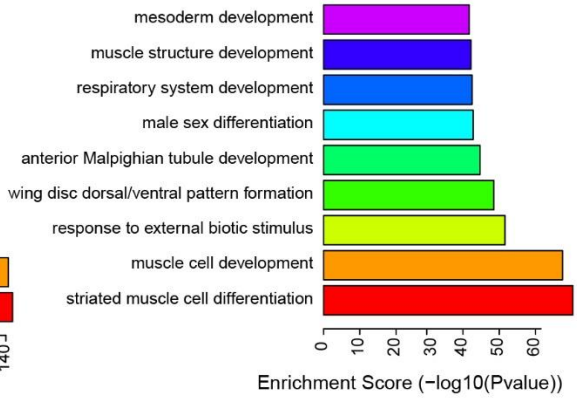

Figure 3.8 Anterior-posterior patterning, segmentation and mesoderm specification occurs in *Ataxin-7* and *non-stop* GLC embryos, but these embryos exhibit defects in cellularization. (*A*) Even-skipped (red) staining was observed in the expected 7 stripe pattern in stage 5 GLC embryos, and Twist staining (green) revealed specified mesoderm on the ventral side of these embryos. Anterior is to the left and ventral is to the bottom. (*B*) Stage 5 GLC embryos were stained with Discs-large (red) to mark membranes, Twist (green) to mark mesodermal nuclei and DAPI (blue) to mark all nuclei. A ventral view with anterior to the left is shown. Disruptions in the organization of Twist-expressing nuclei are apparent at this low magnification. (*C*) High magnification of stage 5 embryos shows defects in organization of the migrated nuclei at the time of cellularization. Staining was as in panel *B*. Boxes denote positions in which nuclei on the surface appear to be absent. The embryos were collected from crosses as follows: Oregon R (WT); *Ataxin-7* GLC females crossed to *Ataxin-7*^{HO3}*/Cyo* (*Ataxin-7*^{HO3}); *non-stop* GLC females crossed to *non-stop*^{02069}*/TM3* (*non-stop*^{02069}). Bars: *A–B*, 50 µm. *C*, 10 µm.

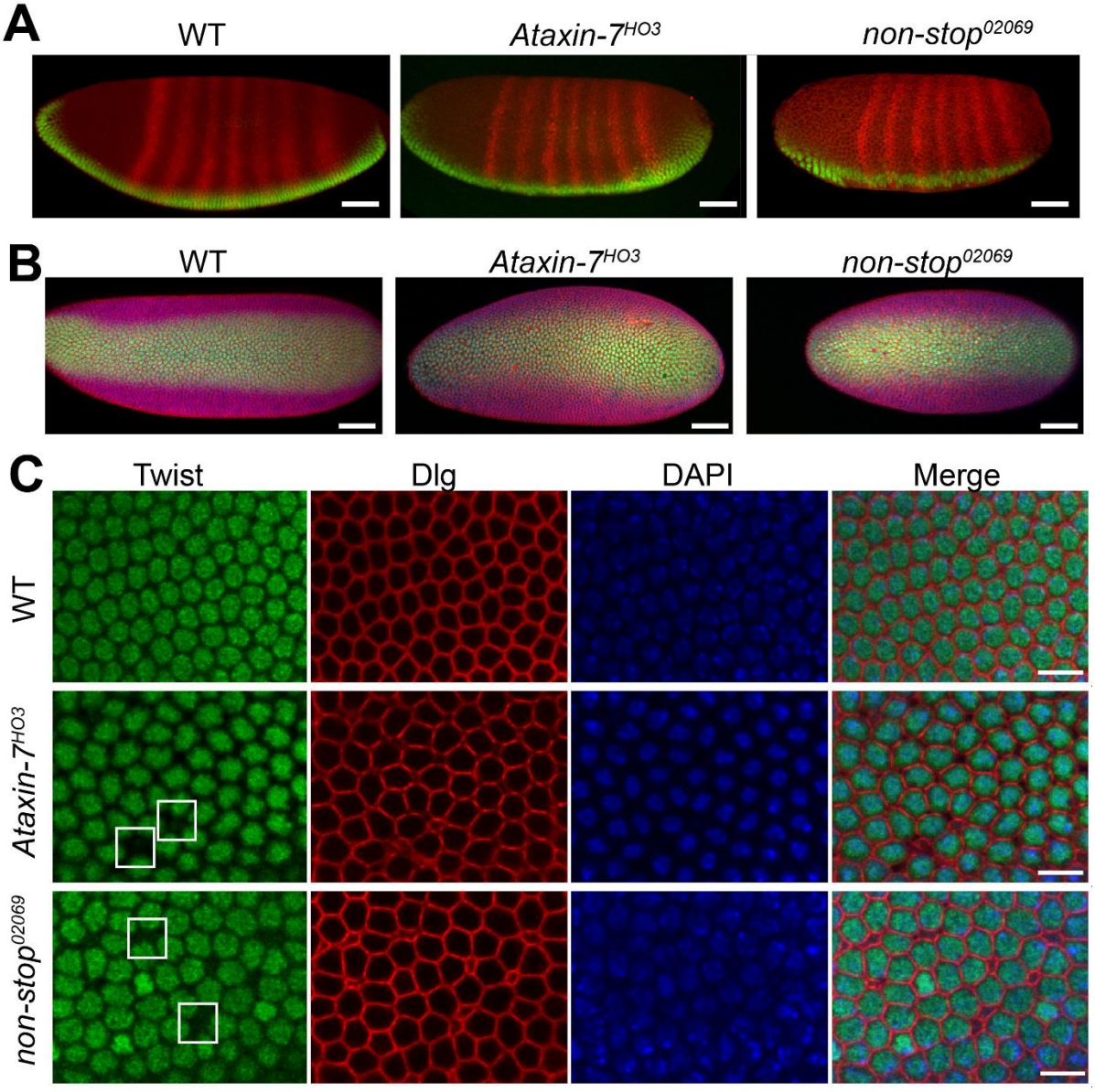
A
WT
Ataxin-7HO3
non-stop02069
B
WT
Ataxin-7HO3
non-stop02069
C
Twist
Dlg
DAPI
Merge
WT
Ataxin-7HO3
non-stop02069

Figure 3.9 Similar defects in cellularization, gene expression and nuclear shape are observed upon loss of the DUB module subunits Ataxin-7 and Non-stop. (*A*) Stage 5 embryos were stained with α-Tubulin (green) and Enabled (red) to visualize invaginating membranes during cellularization. DAPI (gray) marked nuclei. (*B*) Real-time PCR was performed on cDNA isolated from stage 5 WT, *Ataxin-7*^{HO3} and *non-stop*^{02069} GLC embryos, and expression of genes associated with cellularization was assessed. *Actin5C* was used as the normalization control. (*C*) Screenshots of confocal data analyzed in 3D using Imaris to determine shape and volume for Twist-expressing nuclei. The embryo surface is at the top and internal is at the bottom. Arbitrary coloring highlights nuclei at the surface (cyan), mislocalized nuclei (pink) and differences in nuclear shape (yellow). (*D*) Quantification of nuclear volume of stage 5 embryos for each genotype, obtained from the Imaris analysis in *C*. Genotypes in *A-D* were the same as Figure 3.8. Bars: *A*, 10 µm. *C*, 5 µm

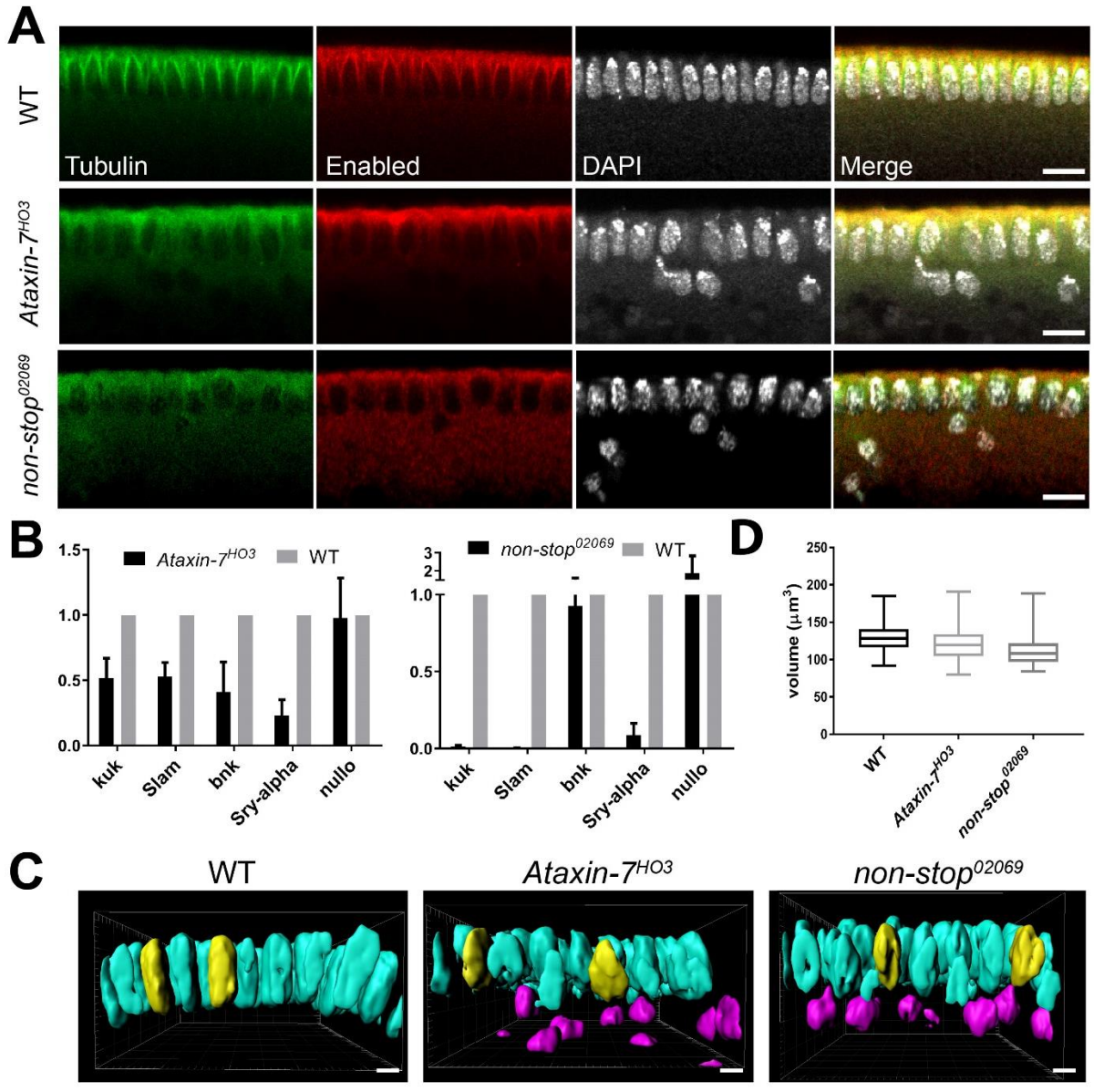
A
WT
Ataxin-7HO3
non-stop02069
Tubulin
Enabled
DAPI
Merge
B
Ataxin-7HO3
WT
non-stop02069
WT
kuk
Slam
bnk
Sry-alpha
nullo
D
volume (µm3)
WT
Ataxin-7HO3
non-stop 02069
C
WT
Ataxin-7HO3
non-stop02069

Figure 3.10 *Ataxin-7*$^{2A-1}$ has the same phenotype as *Ataxin-7*^{HO3}. (*A*) Schematic representation of mutant alleles of *Ataxin-7*$^{2A-1}$. Exons are shown as blue rectangles. Translation start codon is labeled as ATG. Red arrow points to the point mutation. (*B*) Ovaries were stained as in Figure 1A. (*C*) Ovaries were stained as in Figure 1B. Vasa (red) was observed in the anterior and Staufen (green) was observed in the posterior. (*D*) Stage 5 embryos were stained as in Figure 3C. The genotype of germline females was: *hs-Flp/+; Ataxin-7*$^{2A-1}$, *FRT*^{40A}/*FRT*^{40A}, *ovo*$^{D1-18}$. The embryos were collected from cross: *Ataxin-7* GLC females crossed to *Ataxin-7*$^{2A-1}$/*Cyo*. Bars: *A*–*B*, 50 µm. *C*, 10 µm.

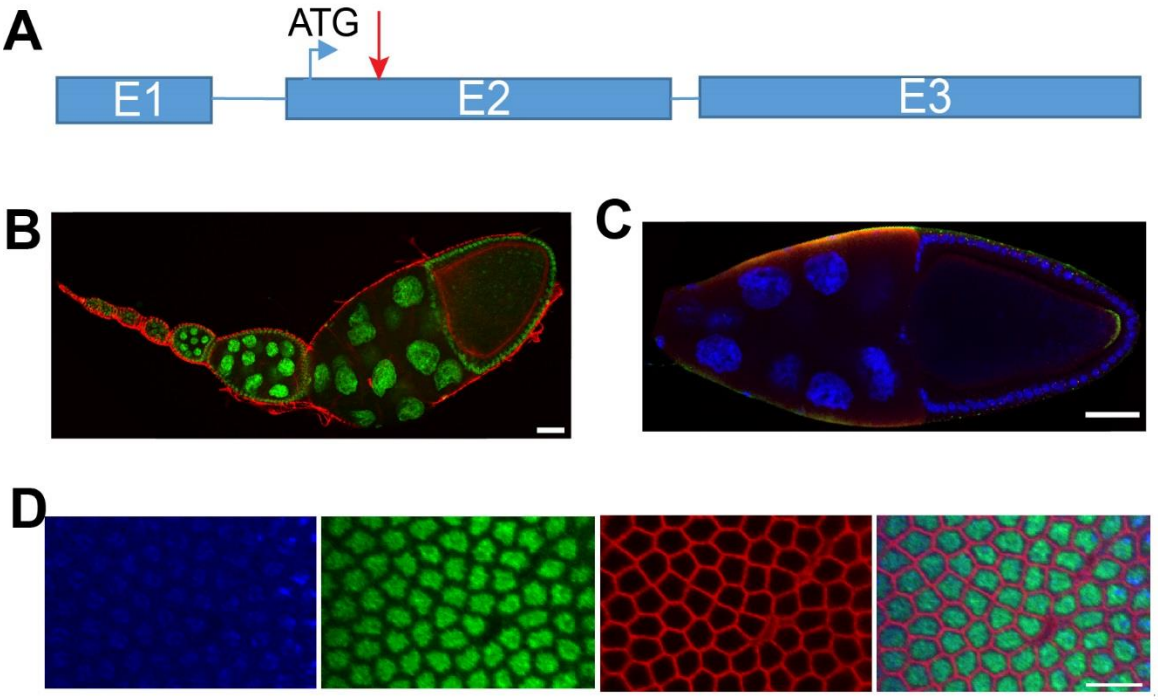

Figure 3.11 Ada2b is important for HAT activity in embryogenesis and Ada2b knock down embryos shows similar defects as DUB mutants. (*A*) H3K9ac level is reduced in *Ada2b*^{1} mutant embryos. Stage 16 embryos were stained with H3K9ac (red), muscle heavy chain (MHC) (purple) and DAPI (blue). Ventral side is to the middle. The genotypes of embryos were *ada2b*^{1}/*ada2b*^{1}. (*B*) H3K14ac level is reduced in *Ada2b*^{1} mutant embryos. Stage 16 embryos were stained with H3K14ac (Red), central nerve system (CNS) (Purple) and DAPI (Blue). Ventral side is to the middle. The genotypes of embryos were *ada2b*^{1}/*ada2b*^{1}. (*C*) Stage 5 embryos were stained with Discs-large (red) to mark membranes, Twist (green) to mark mesodermal nuclei and DAPI (blue) to mark all nuclei. A ventral view with anterior to the left is shown. Disruptions in the organization of Twist-expressing nuclei are apparent at this low magnification. (*D*) High magnification of Stage 5 embryos shows defects in organization of the migrated nuclei at the time of cellularization. Staining was as in panel *B*. Boxes denote positions in which nuclei on the surface appear to be absent. The embryos in *C-D* were collected from crosses as follows at 29°C: *P{w[+mC]=otu-GAL4::VP16.R}1, w[*]; P{w[+mC]=GAL4-nos.NGT}40; P{w[+mC]=GAL4::VP16-nos.UTR}CG6325[MVD1]/ y[1] sc[*] v[1]; P{y[+t7.7] v[+t1.8]=Ada2b RNAi 2-T2} attP40 cross to w[*]; P{w[+mC]=GAL4-Hsp70.PB}89-2-1*. Bars: *A–C*, 50 µm. *D*, 10 µm.

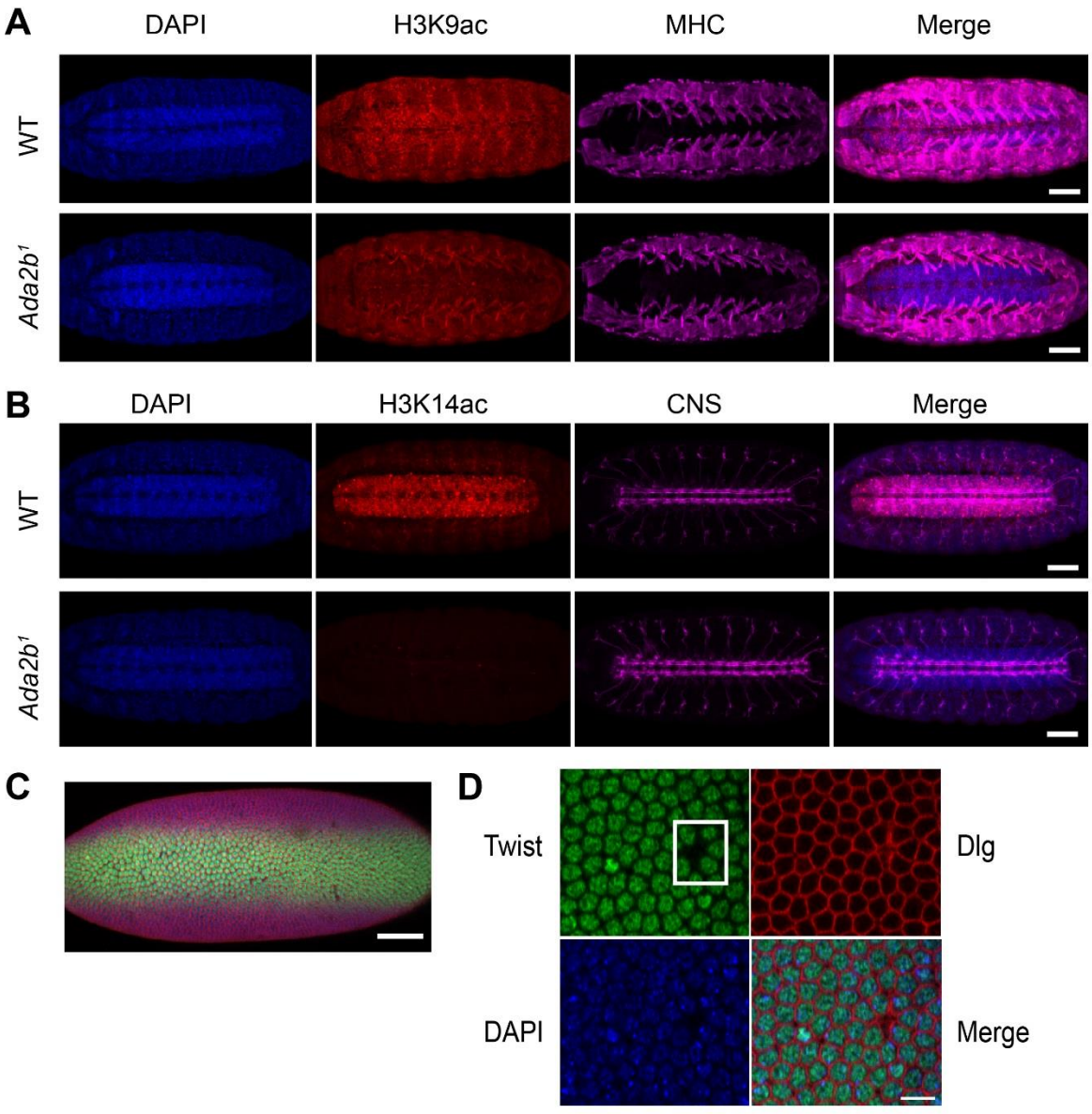
A
DAPI
H3K9ac
MHC
Merge
WT
Ada2b1
B
DAPI
H3K14ac
CNS
Merge
WT
Ada2b1
C
D
Twist
Dlg
DAPI
Merge

Figure 3.12 The DUB module is required for embryogenesis and survival. (*A*) Stage 16 embryos were stained with MHC to visualize muscles. Embryos were collected from cross: *Ataxin-7* GLC females crossed to *Ataxin-7^{HO3}/Cyo-GFP*. Embryos were stained with GFP and were hand sorted GFP positive (m-/-, z-/+) vs GFP negative (m-/-, z-/-) before being stained with MHC. (*B*) Survival test of zygotic rescued embryos hatching to 1st instar larvae. Embryos were collected from crosses: GLC females crossed to WT. Bars: *A*, 20µm.

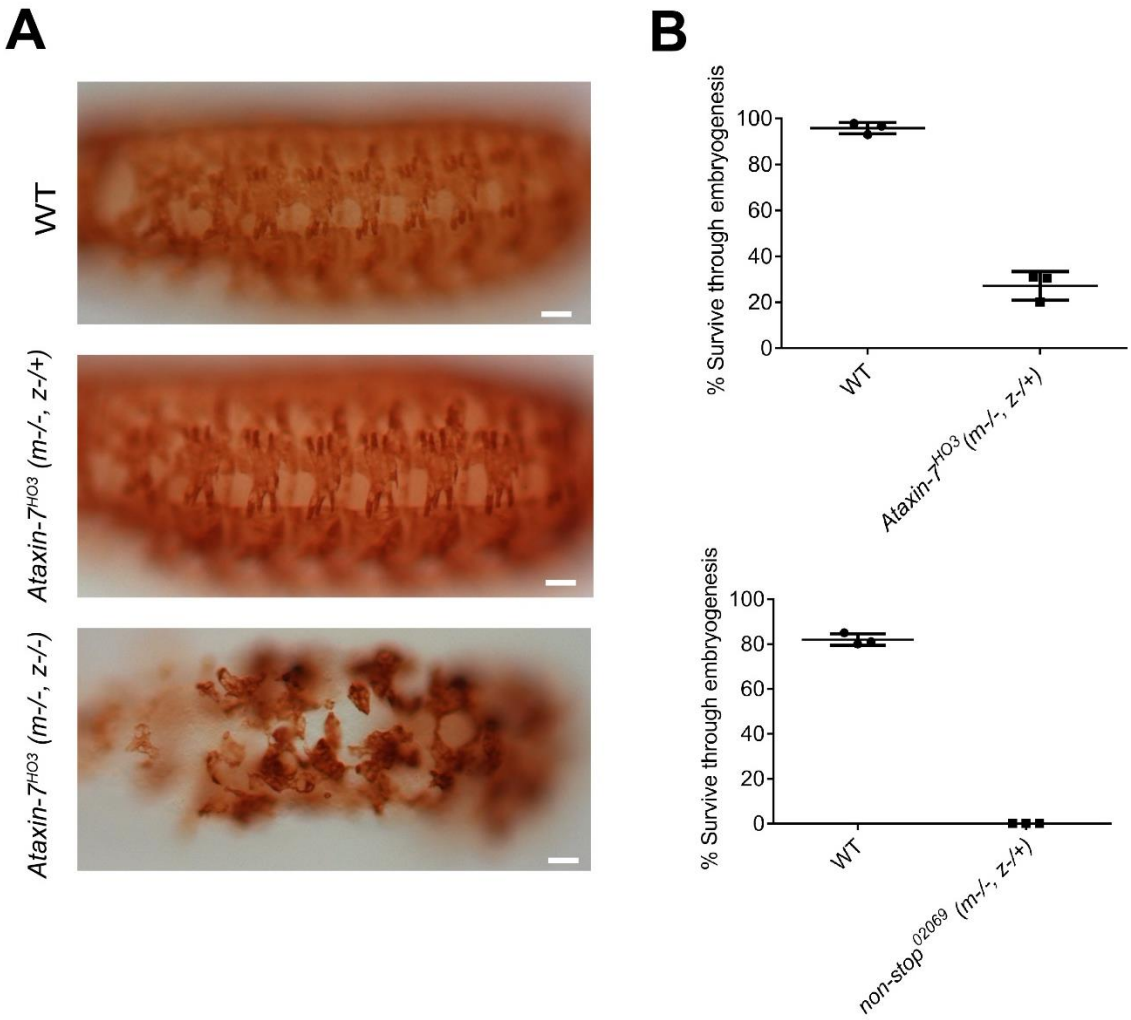

Figure 3.13 RNA-seq analysis reveals that the DUB module regulates expression of a subset of early genes in embryogenesis. (*A*) Venn diagrams showing the overlapping genes with decreased or increased transcript levels in stage 5 *Ataxin-7*^{HO3} and *non-stop*^{02069} GLC embryos (Fold change >2, P < 0.05, FPKM > 1). A large portion of genes were similarly affected in both mutants. (*B*) GO term analysis of biological process (BP) of genes commonly changed in both GLC embryos. A complete list of enriched GO terms with Adjusted *P*-value < 0.05 is provided in Table 3.4.

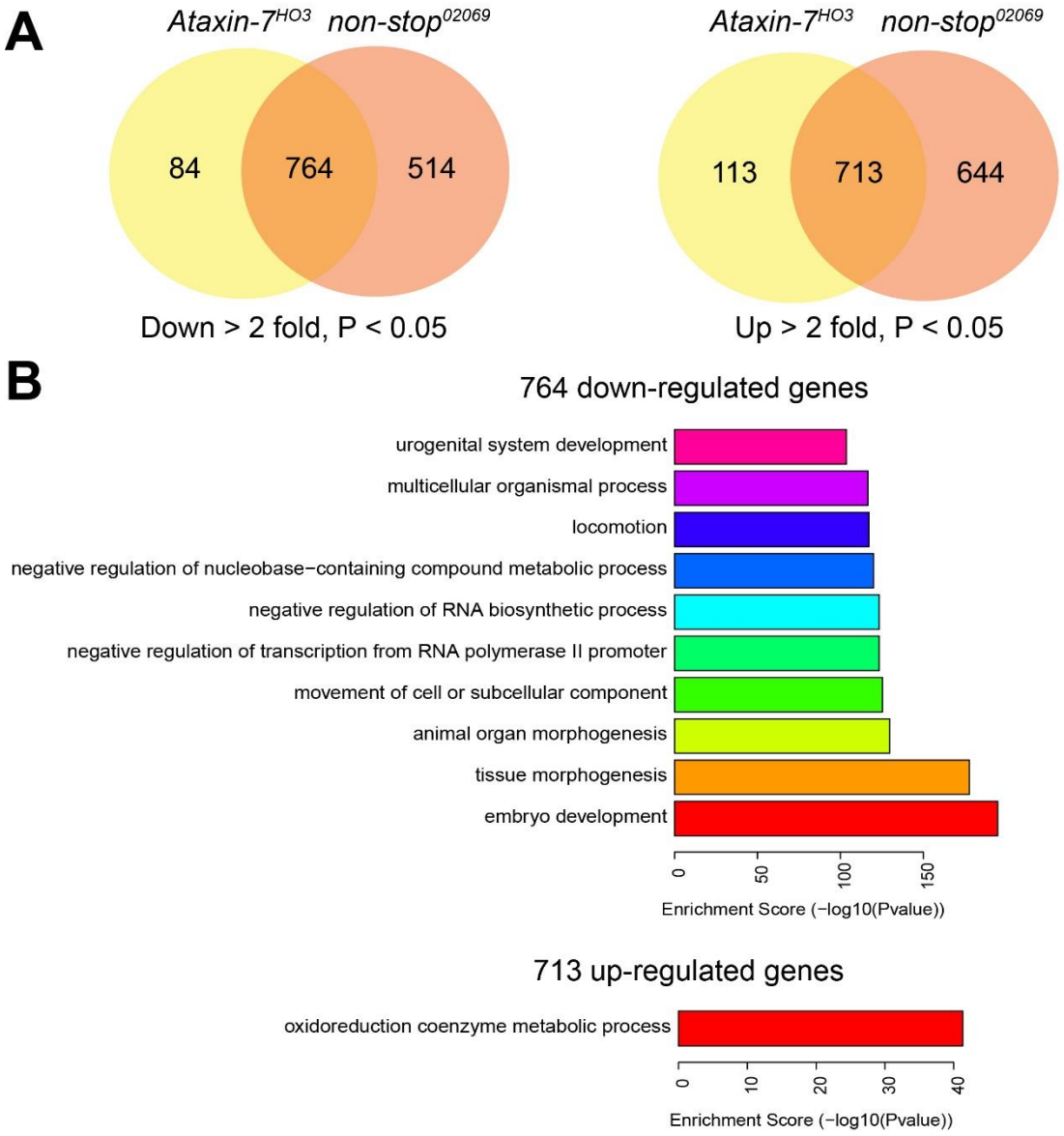
A
Ataxin-7HO3
non-stop02069
84
764
514
Down > 2 fold, P < 0.05
Ataxin-7HO3
non-stop02069
113
713
644
Up > 2 fold, P < 0.05
B
764 down-regulated genes
urogenital system development
multicellular organismal process
locomotion
negative regulation of nucleobase−containing compound metabolic process
negative regulation of RNA biosynthetic process
negative regulation of transcription from RNA polymerase II promoter
movement of cell or subcellular component
animal organ morphogenesis
tissue morphogenesis
embryo development
0
50
100
150
Enrichment Score (−log10(Pvalue))
713 up-regulated genes
oxidoreduction coenzyme metabolic process
0
10
20
30
40
Enrichment Score (−log10(Pvalue))

Figure 3.14 Only a few genes change expression oppositely in the absence of Ataxin-7 and non-stop and some of the differentially expressed genes are direct targets of SAGA or the DUB module. (*A*) Venn diagrams showing the overlapping genes with increased transcripts levels in *Ataxin-7*^{HO3} GLC embryos and decreased transcripts levels in *non-stop*^{02069} ones (Fold change > 2, P < 0.05, FPKM > 1). (*B*) Venn diagrams showing the overlapping genes with decreased transcripts levels in *Ataxin-7*^{HO3} GLC embryos and increased transcripts levels in *non-stop*^{02069} ones (Fold change > 2, P < 0.05, FPKM > 1). (*C*) Statistical analysis of SAGA bound genes or DUB module bound genes overlapped with DUB DE genes (genes have FPKM >1 were analyzed). Commonly down-regulated genes in both *Ataxin-7* and *non-stop* GLC embryos are significant overlapped with SAGA targets, whereas commonly up-regulated genes are not. However, commonly up-regulated genes are significantly overlapped with the DUB targets, but not for commonly down-regulated genes.

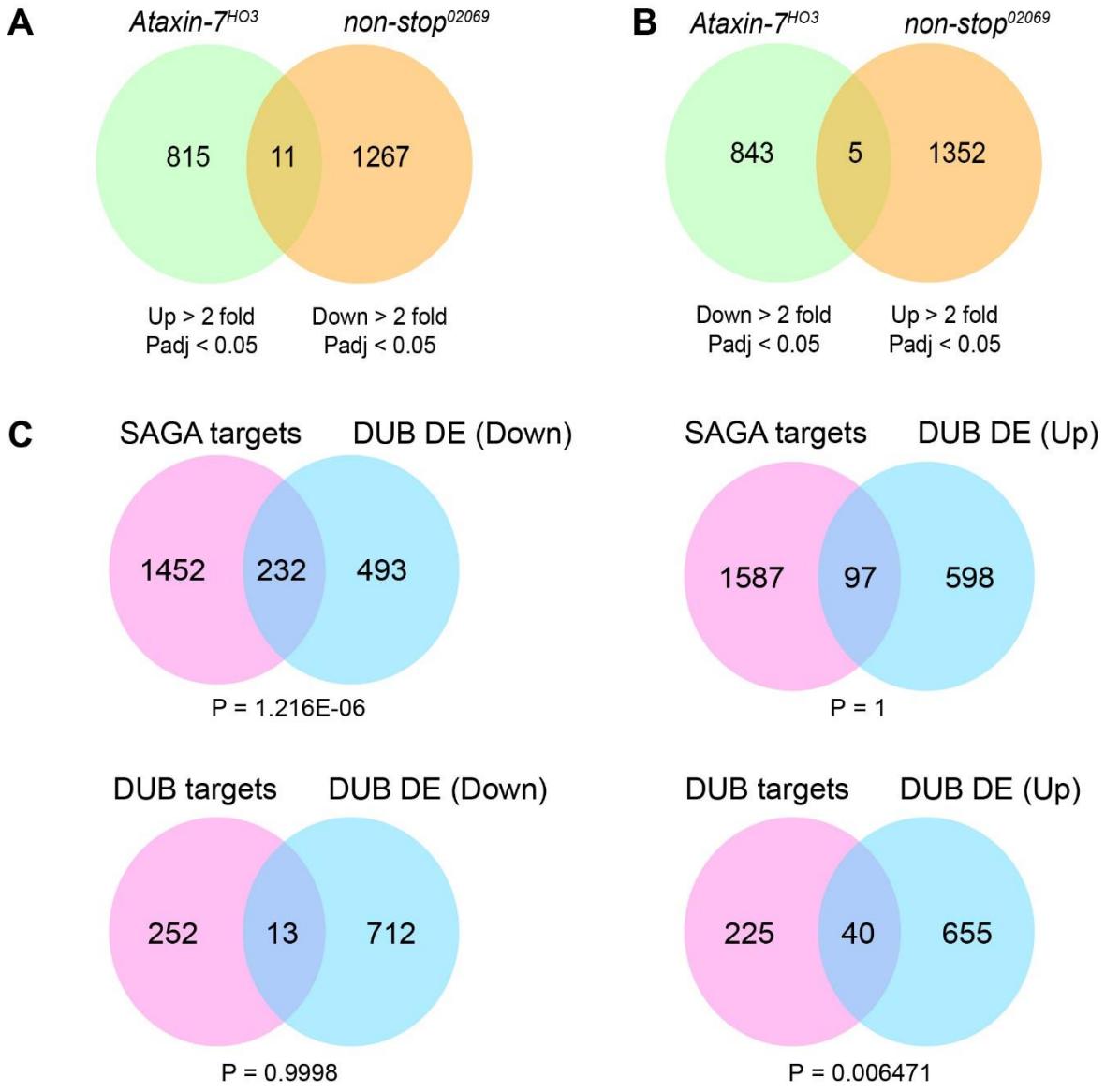
A
Ataxin-7HO3
non-stop02069
815
11
1267
Up > 2 fold
Padj < 0.05
Down > 2 fold
Padj < 0.05
B
Ataxin-7HO3
non-stop02069
843
5
1352
Down > 2 fold
Padj < 0.05
Up > 2 fold
Padj < 0.05
C
SAGA targets
DUB DE (Down)
1452
232
493
P = 1.216E-06
SAGA targets
DUB DE (Up)
1587
97
598
P = 1
DUB targets
DUB DE (Down)
252
13
712
P = 0.9998
DUB targets
DUB DE (Up)
225
40
655
P = 0.006471

Figure 3.15 H3K9ac or H3K14ac level did not change in *Ataxin-7*^{HO3} GLC embryos. (*A*) Average profiles depicting H3K9ac distribution on gene bodies. No significant change of H3K9ac in DUB DE genes. (*B*) Average profiles depicting H3K14ac distribution on gene bodies. No significant change of H3K14ac in DUB DE genes. (*C*) Average profiles depicting H3K9ac and H3K14ac distribution on SAGA target genes (*D*) Venn diagram showing the overlapping Ada2b peaks between WT and *Ataxin-7* GLC embryos.

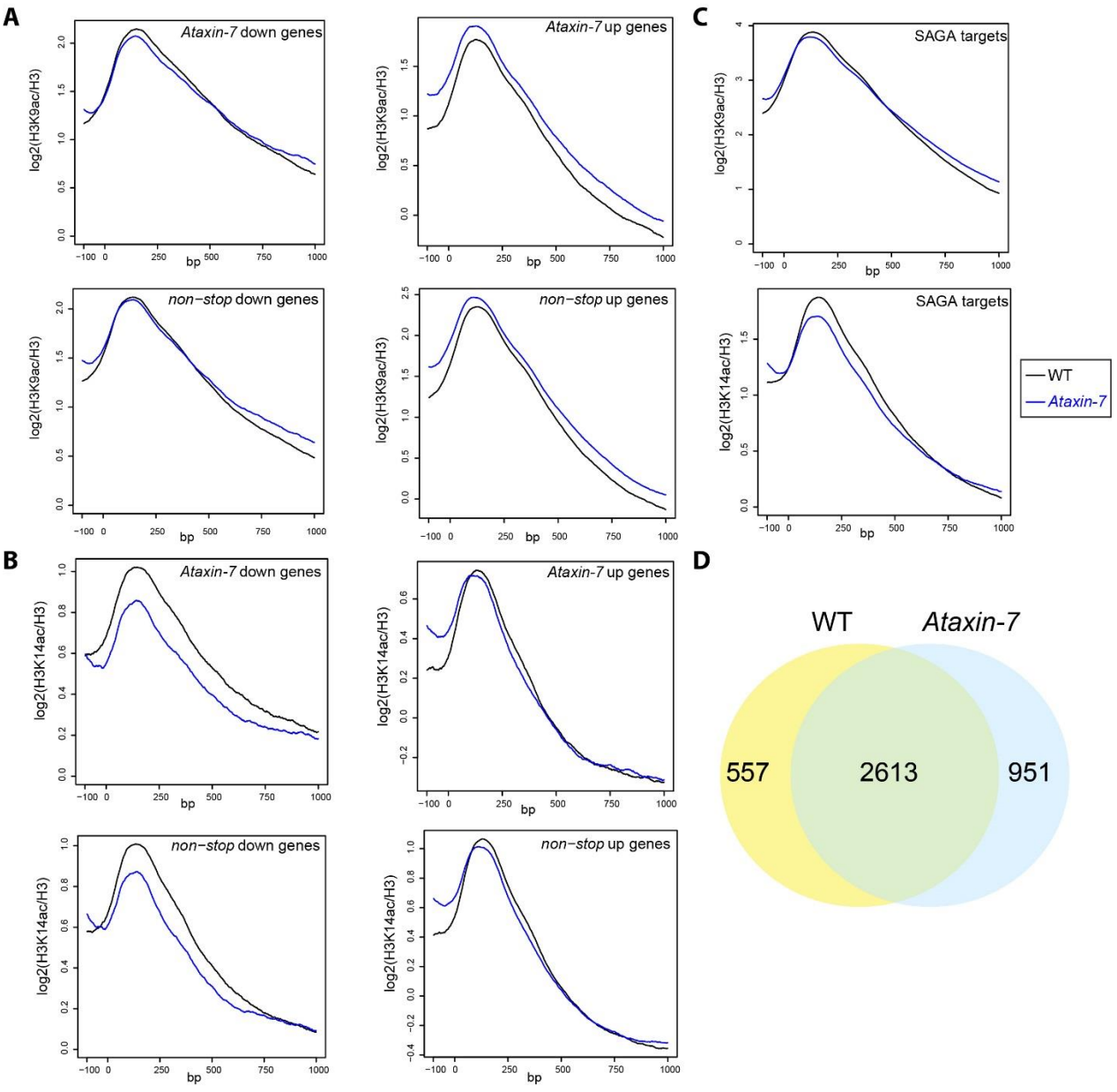
A
Ataxin-7 down genes
Ataxin-7 up genes
non−stop down genes
non−stop up genes
log2(H3K9ac/H3)
bp
B
Ataxin-7 down genes
Ataxin-7 up genes
non−stop down genes
non−stop up genes
log2(H3K14ac/H3)
bp
C
SAGA targets
SAGA targets
log2(H3K9ac/H3)
log2(H3K14ac/H3)
bp
WT
Ataxin-7
D
WT
Ataxin-7
557
2613
951

Figure 3.16 RNA-seq analysis reveals that the HAT and DUB modules regulate different subsets of genes. Venn diagrams showing the overlapping genes with decreased or increased transcript levels in *Ada2b*^{1}, *Ataxin-7*^{HO3} and *non-stop*^{02069} embryos (Fold change > 2, P < 0.05, FPKM > 1).

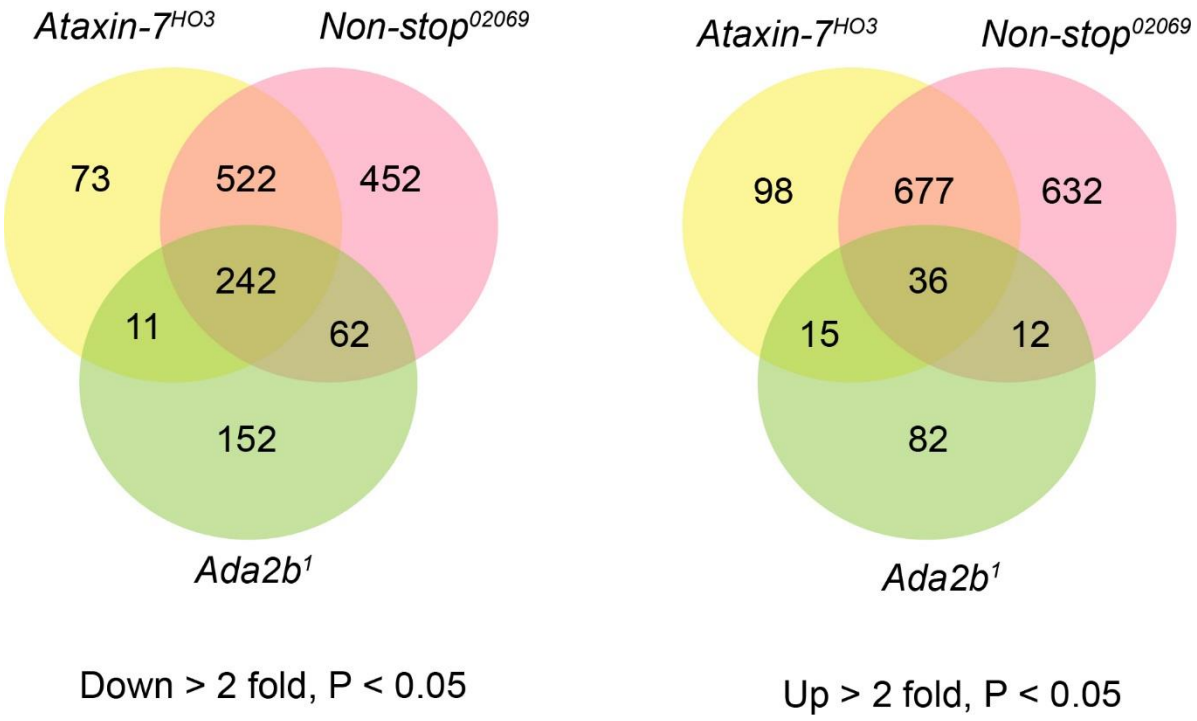

Figure 3.17 H3K9ac or H3K14ac is not impaired in DUB mutants. (*A*) Whole ovaries were stained with H3K9ac (green) and DAPI (cyan). Boxes highlight the germline nurse cells. *Ada2b* germline nurse cells have reduced H3K9ac, while *Ataxin-7* and *non-stop* germline nurse cells have similar H3K9ac levels as WT. (*B)* Whole ovaries were stained with H3K14ac (green) and DAPI (cyan). Boxes highlight the germline nurse cells. *Ada2b* germline nurse cells have reduced H3K14ac, *Ataxin-7* and *non-stop* germline nurse cells have similar H3K14ac levels as WT. The genotypes are the same as Figure 3.2. Bars: 50 μm.

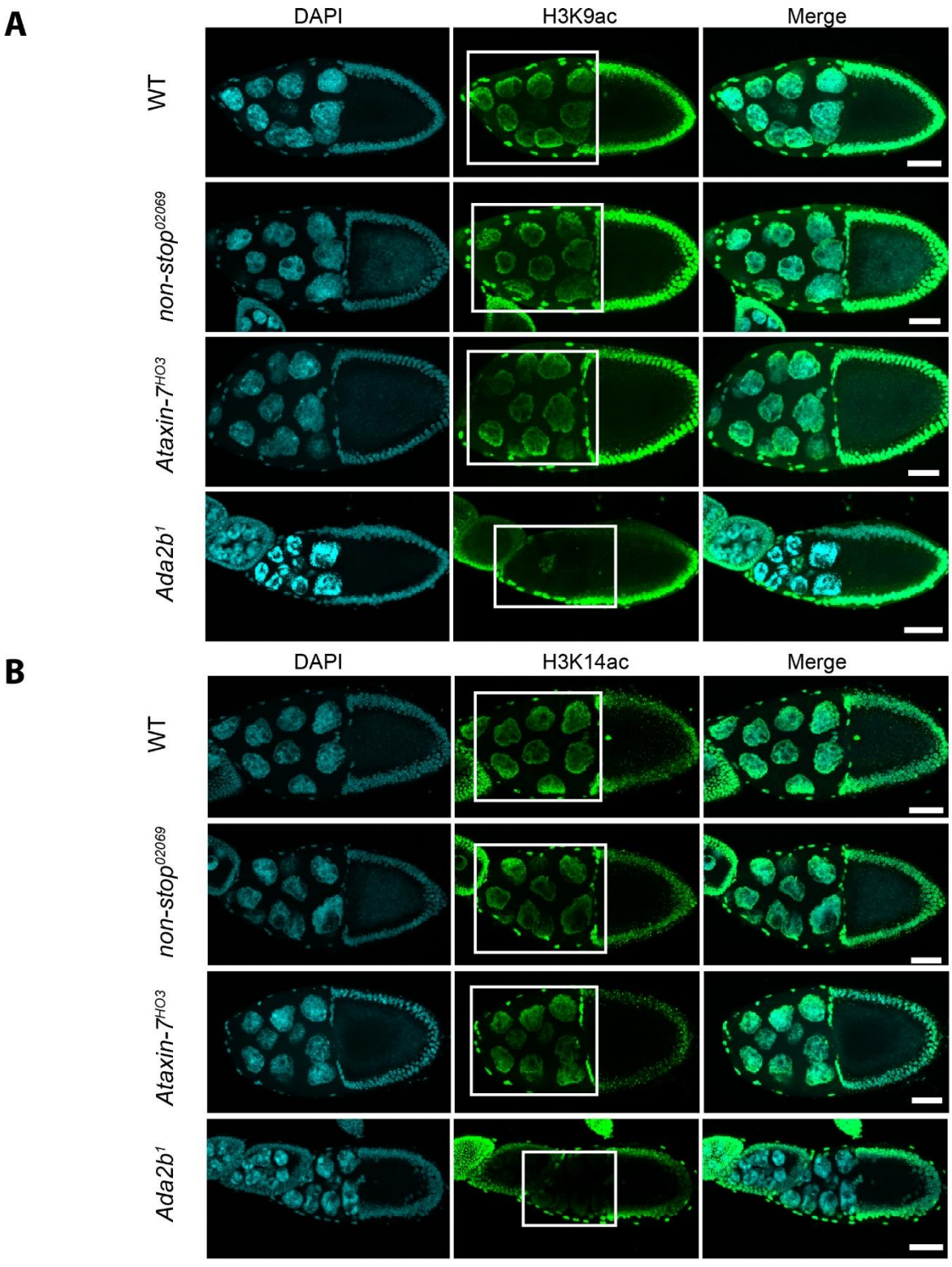
A
DAPI
H3K9ac
Merge
WT
non-stop02069
Ataxin-7HO3
Ada2b1
B
DAPI
H3K14ac
Merge
WT
non-stop02069
Ataxin-7HO3
Ada2b1

Figure 3.18 ChIP-seq analysis reveals that the DUB module binds to SAGA targets as a part of the whole complex, but it is only required by a subset of these genes for their expression. (*A*) Venn diagram showing the overlapping ChIP-seq peaks between Sgf11, Ada2b and Spt3. The overlapped peaks are referred to as SAGA peaks. (*B*) MA plots showing gene expression in *non-stop* and *Ataxin-7* GLC embryos (Genes with FPKM <1 in WT have been removed). Fold changes > 2 are marked in red, fold changes < -2 are marked in green. Genes bound by SAGA are marked in black. (*C*) Example genes show that the DUB module binds to SAGA targets even though it is not always required for their expression. Binding profiles for Sgf11 (purple), Ada2b (green) and Spt3 (orange) are shown at the *dgo* (DUB DE gene) and *Csp* (DUB independent gene) loci.

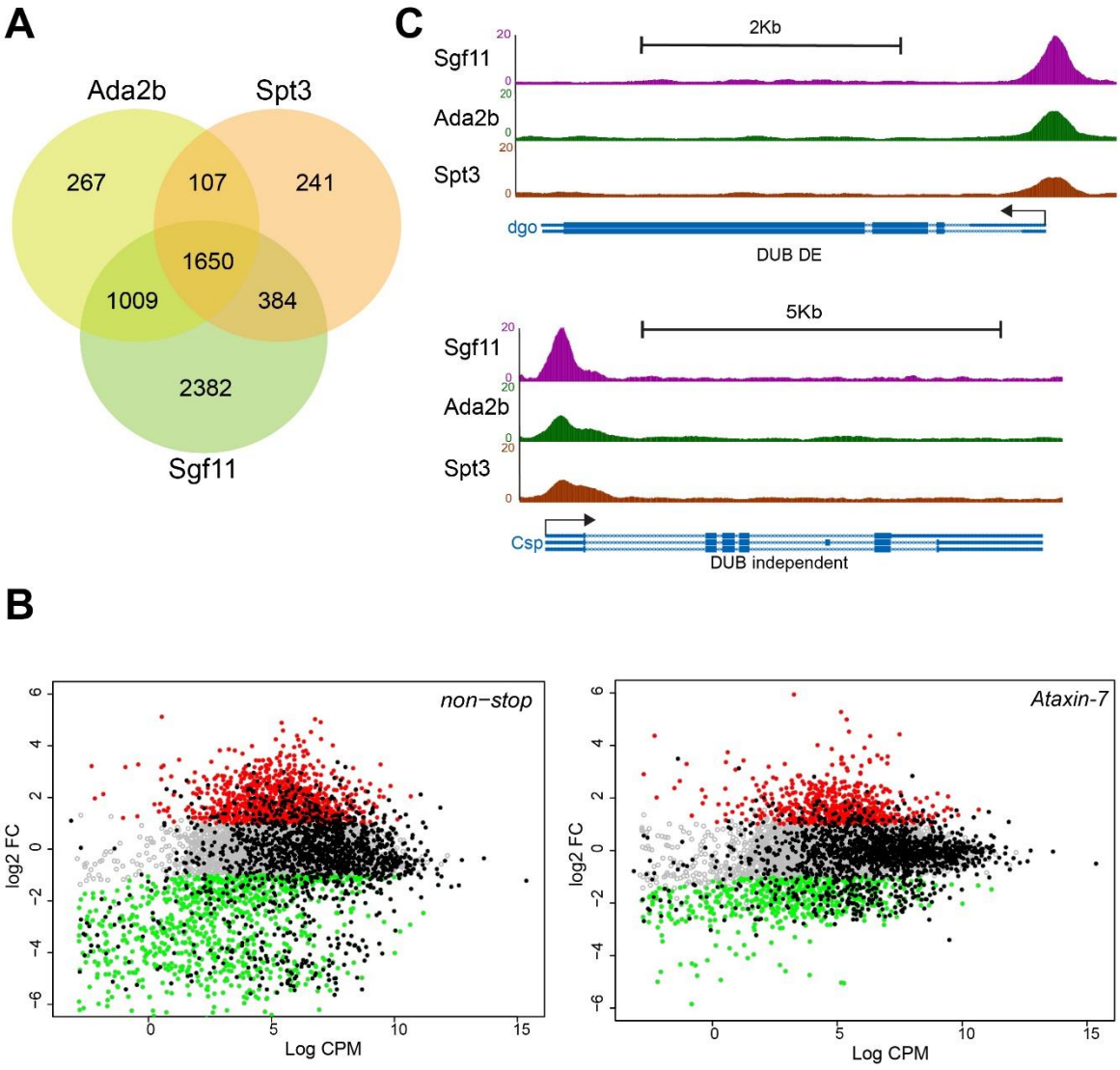
A
Ada2b
Spt3
267
107
241
1650
1009
384
2382
Sgf11
C
2Kb
Sgf11
Ada2b
Spt3
dgo
DUB DE
5Kb
Sgf11
Ada2b
Spt3
Csp
DUB independent
B
non−stop
Ataxin-7
log2 FC
Log CPM

Figure 3.19 The DUB module binds and regulates gene expression independent of the HAT module. (*A*) Genome browser of ChIP-seq tracks at a representative region revealed that the DUB module binds to some genes without the HAT or SPT modules. Red arrow points to the Sgf11 only peak. (*B*) Histograms of distance (from -5000bp to +5000bp) to the transcription start sites (TSS) for SAGA peaks and the DUB module peaks. (*C*) MA plots showing gene expression in *non-stop* and *Ataxin-7* GLC embryos (Genes with FPKM <1 in WT have been removed). Fold changes > 2 are marked in red, fold changes < -2 are marked in green. Genes bound by the DUB module are marked in black. (*D*) Barplot showing that the SAGA target genes or the DUB module target genes which did not require the DUB module at this stage are bound by RNA polymerase II. (*E*) To compare the Pol II levels at different sites, the log10 of Pol II peaks of expressed genes with an FPKM >1 was plotted.

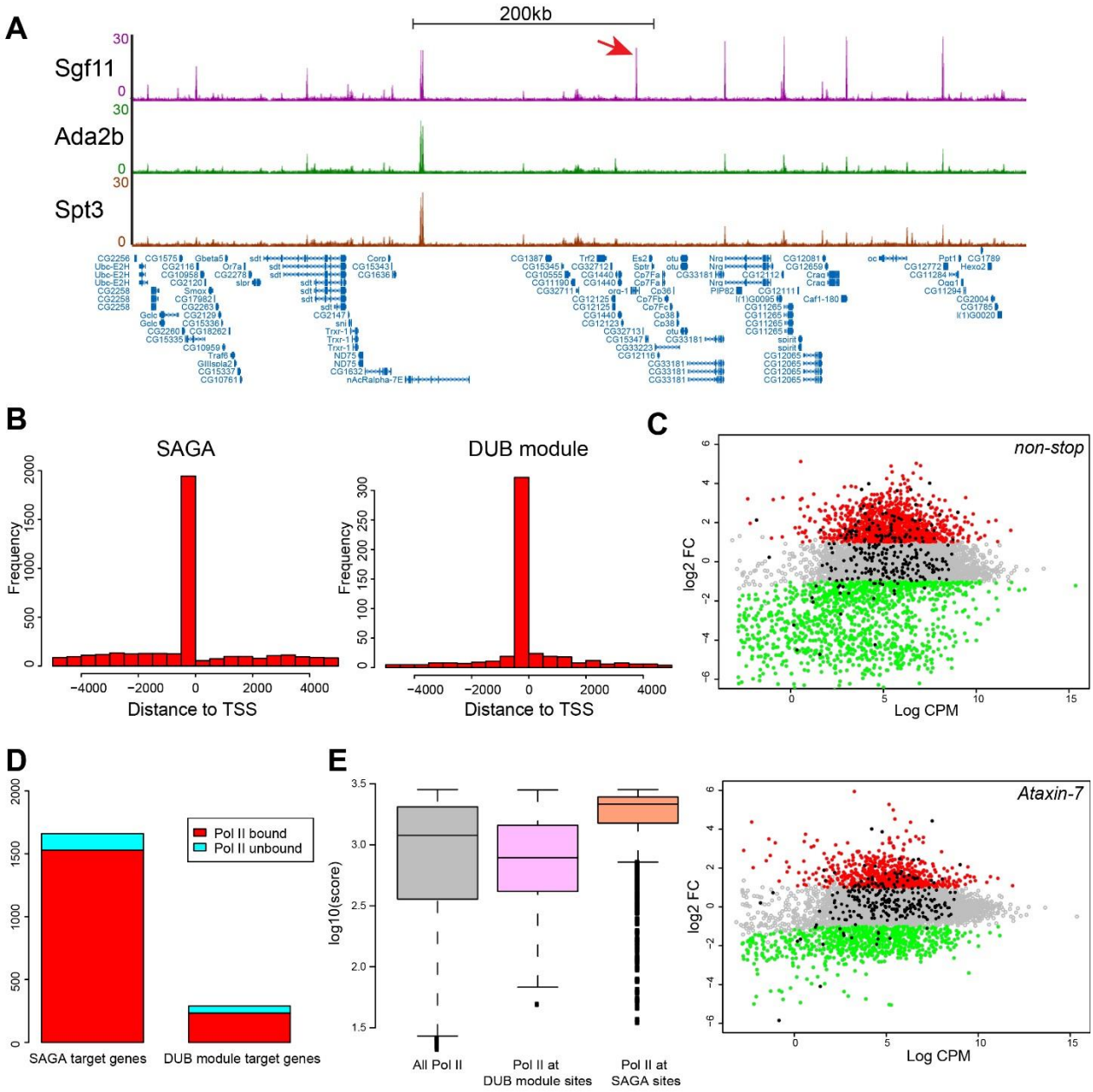
A
200kb
Sgf11
Ada2b
Spt3
30
0
B
SAGA
DUB module
Frequency
Distance to TSS
C
non-stop
log2 FC
Log CPM
D
Pol II bound
Pol II unbound
SAGA target genes
DUB module target genes
E
log10(score)
All Pol II
Pol II at DUB module sites
Pol II at SAGA sites
Ataxin-7

Figure 3.20 The Sgf11 bound sites are also bound by Non-stop. ChIP-seq data of Non-stop shows that the majority of Sgf11 peaks overlap with Non-stop peaks, indicating that these peaks represent SAGA-independent binding of an intact DUB module.

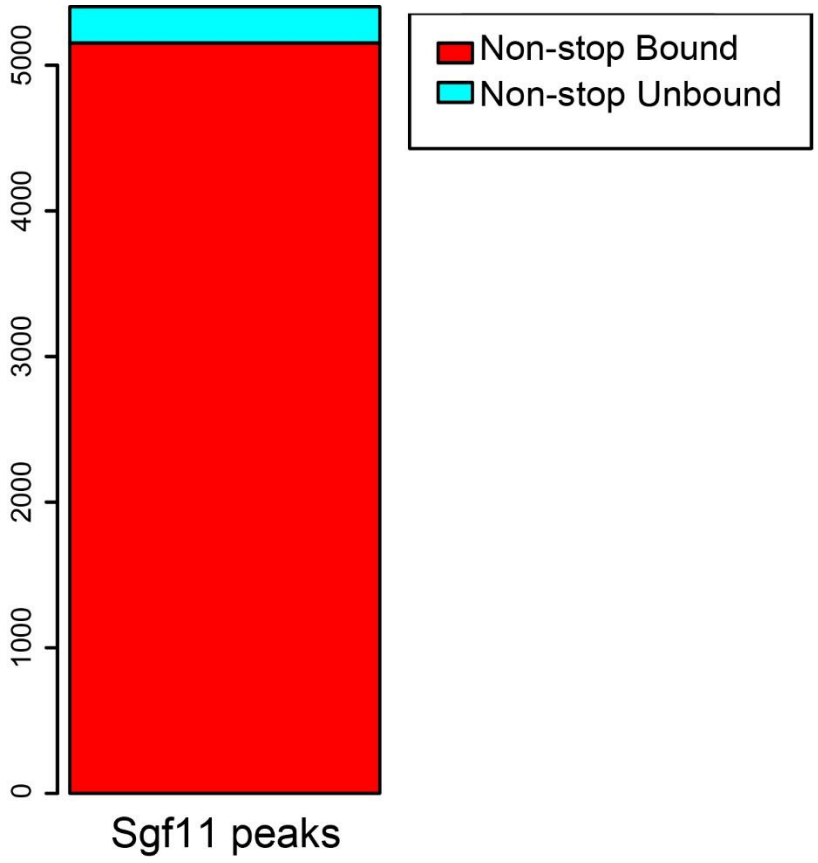

Figure 3.21 Promoter enrichment and histone density analysis of SAGA and DUB target genes. (*A*) Comparison of promoter types of different classes of genes. (*B*) Histone H2B occupancy in different classes of genes. No difference between DUB DE and DUB independent targets for either DUB specific or SAGA targets.

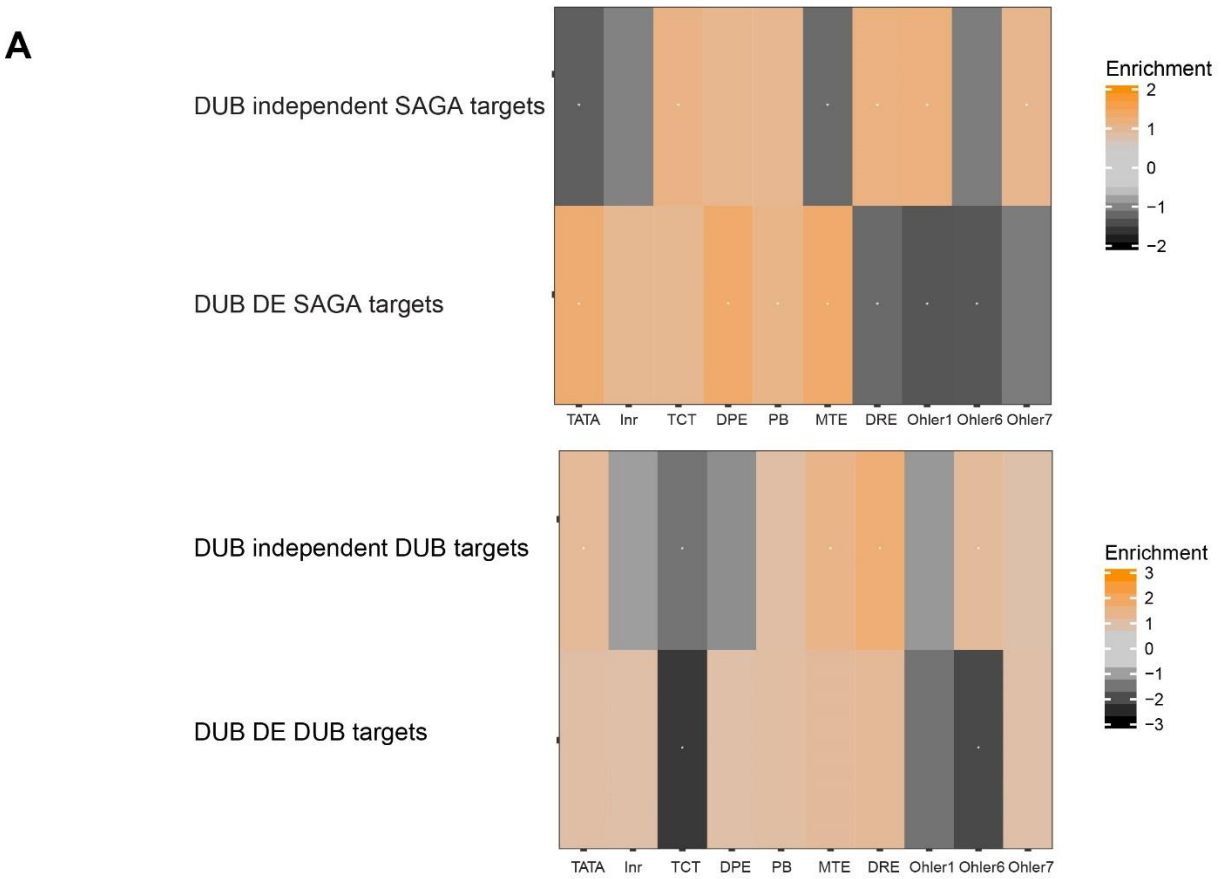
A
DUB independent SAGA targets
DUB DE SAGA targets
TATA Inr TCT DPE PB MTE DRE Ohler1 Ohler6 Ohler7
Enrichment
2
1
0
−1
−2
DUB independent DUB targets
DUB DE DUB targets
TATA Inr TCT DPE PB MTE DRE Ohler1 Ohler6 Ohler7
Enrichment
3
2
1
0
−1
−2
−3

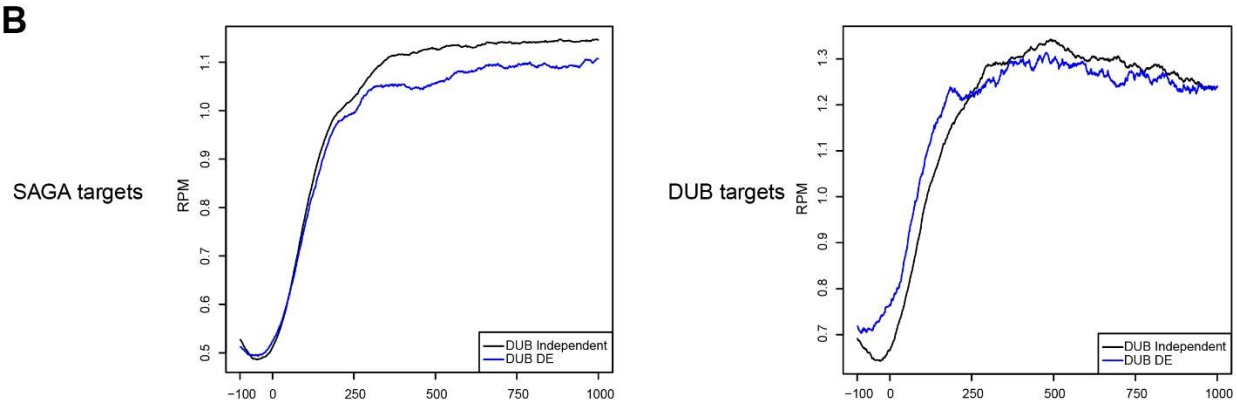
B
SAGA targets
RPM
DUB Independent
DUB DE
−100 0 250 500 750 1000
DUB targets
RPM
DUB Independent
DUB DE
−100 0 250 500 750 1000

Figure 3.22 UbH2B level changes in *Ataxin-7^{HO3}* GLC embryos. (*A*) Average profiles depicting ubH2B distribution on gene bodies of the DUB module target genes which are differentially expressed in *Ataxin-7* or *non-stop* GLC embryos. (*B*) Average profiles depicting ubH2B distribution on gene bodies of SAGA target genes which are differentially expressed in *Ataxin-7* or *non-stop* GLC embryos.

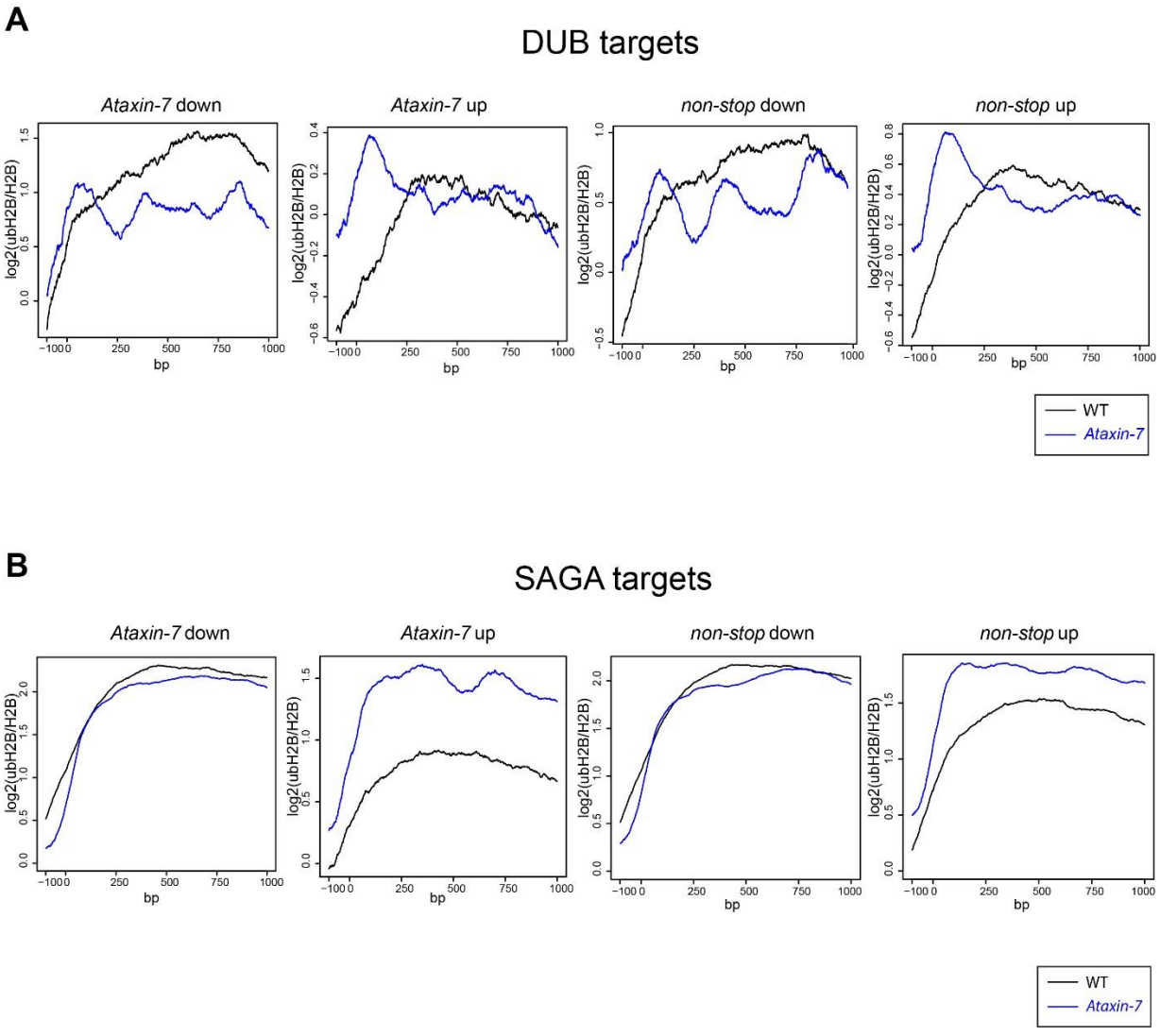

Figure 3.23 GO term analysis of SAGA targets. (*A*) GO term analysis of biological processes (BP) of SAGA target genes which are differentially expressed in DUB mutant. Those genes were enriched for many patterning genes. (*B*) GO term analysis of biological processes (BP) of DUB independent SAGA target genes.

A

DUB DE genes

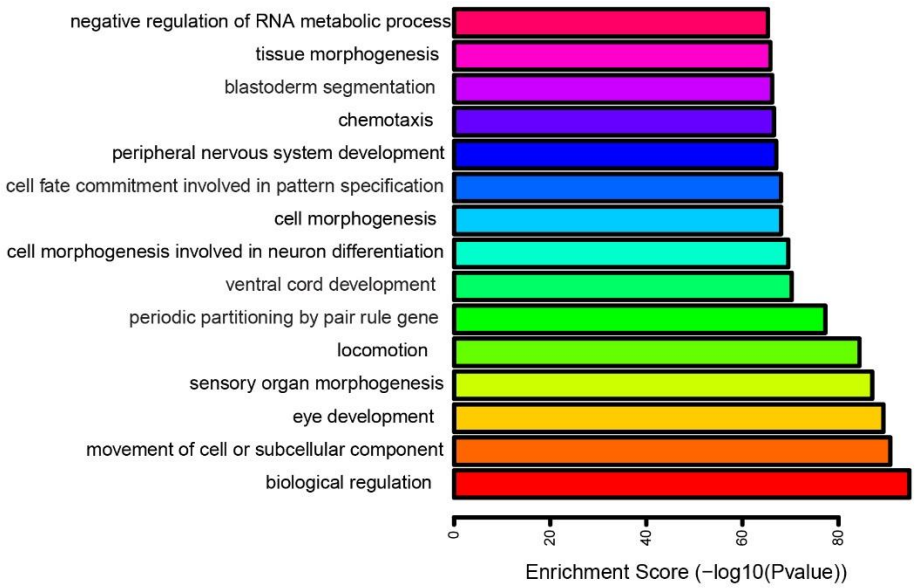

B

DUB independent genes

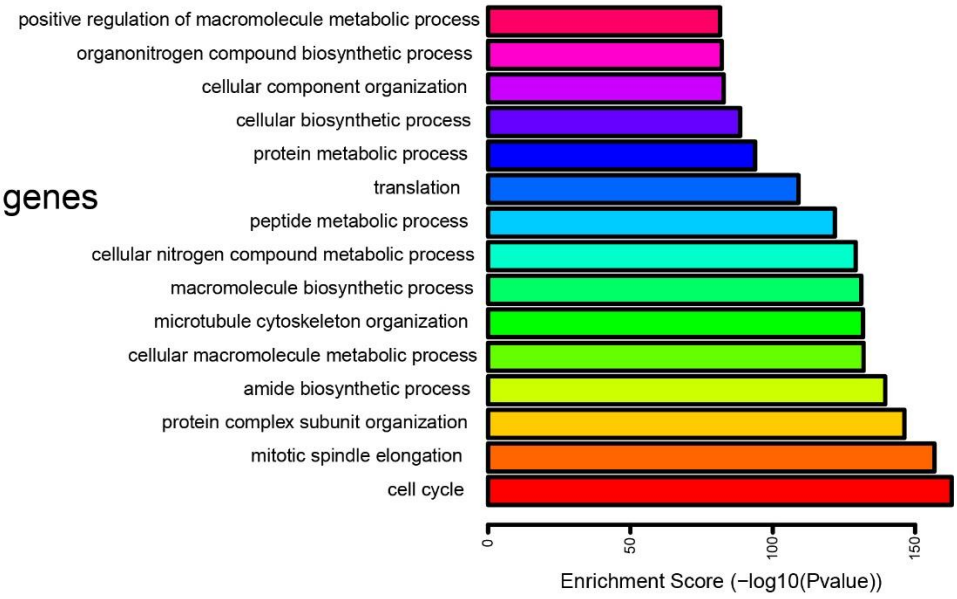

Figure 3.24 Enrichment Pol II peaks at different sites. To compare the Pol II levels at different sites, the log10 of Pol II peaks scores was plotted. Pol II levels are higher at SAGA bound sites (orange) and DUB module bound sites (pink) than in the entire genome (gray). Quadruple-asterisks indicate significance of $P < 0.0001$.

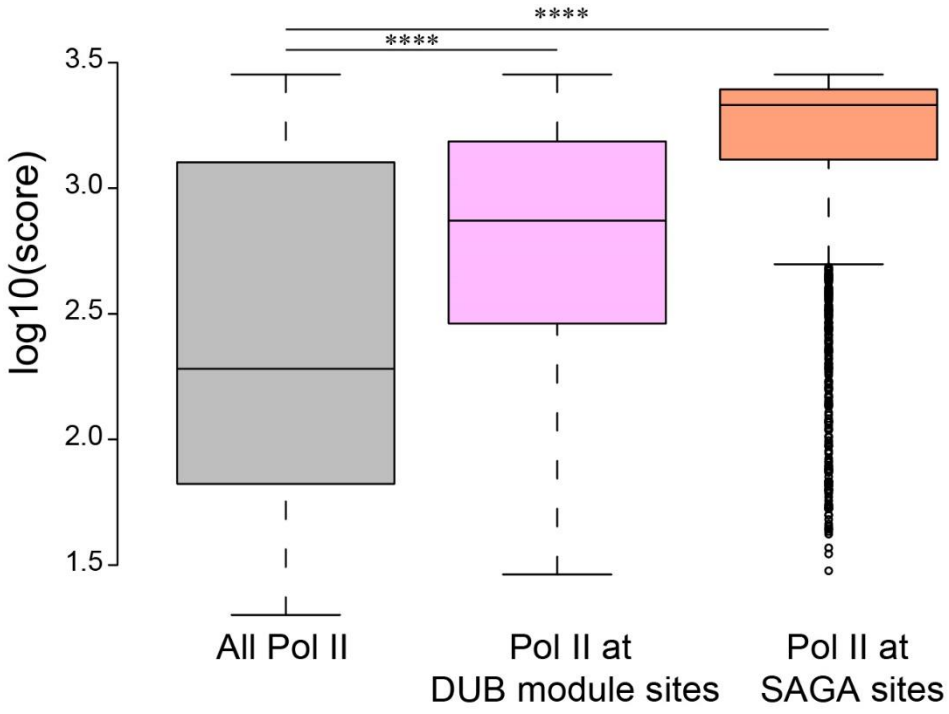

Table 3.1 Egg laying rate of germline clone females

WT	140 eggs/100 females/hr
Non-stop	20 eggs/100 females/hr
Ataxin-7	60 eggs/100 females/hr
Ada2b	0 eggs/100 females/hr

Table 3.2 A complete list of enriched biological processes GO terms with Adjusted *P*-value < 0.05 in *Ada2b*^{1} GLC ovaries.

Down-regulated genes			
GOBPID	P value	Adjust P value	Term
GO:0006270	3.88E-15	1.55E-12	DNA replication initiation
GO:0007052	6.90E-15	2.75E-12	mitotic spindle organization
GO:0098813	3.84E-12	1.52E-09	nuclear chromosome segregation
GO:0051276	5.88E-11	2.33E-08	chromosome organization
GO:0007304	6.72E-09	2.65E-06	chorion-containing eggshell formation
GO:0051225	1.22E-08	4.81E-06	spindle assembly
GO:0000003	1.36E-08	5.34E-06	reproduction
GO:0006267	5.59E-08	2.19E-05	pre-replicative complex assembly involved in nuclear cell cycle DNA replication
GO:0036388	5.59E-08	2.19E-05	pre-replicative complex assembly
GO:0031109	5.85E-08	2.28E-05	microtubule polymerization or depolymerization
GO:0019953	1.91E-07	7.43E-05	sexual reproduction
GO:0000280	2.02E-07	7.84E-05	nuclear division
GO:0006281	6.06E-07	0.000235	DNA repair
GO:0010965	8.66E-07	0.000334	regulation of mitotic sister chromatid separation
GO:1902099	1.01E-06	0.000389	regulation of metaphase/anaphase transition of cell cycle
GO:0007076	1.85E-06	0.00071	mitotic chromosome condensation
GO:0044786	3.79E-06	0.001452	cell cycle DNA replication
GO:0007088	4.31E-06	0.001646	regulation of mitotic nuclear division
GO:0007020	5.08E-06	0.001935	microtubule nucleation
GO:0048609	5.19E-06	0.001972	multicellular organismal reproductive process
GO:0007057	6.64E-06	0.002517	spindle assembly involved in female meiosis I
GO:0006261	7.54E-06	0.00285	DNA-dependent DNA replication
GO:0031577	9.25E-06	0.003487	spindle checkpoint
GO:0033048	9.25E-06	0.003487	negative regulation of mitotic sister chromatid segregation
GO:0045841	9.25E-06	0.003487	negative regulation of mitotic metaphase/anaphase transition
GO:0006260	1.27E-05	0.00475	DNA replication
GO:0051985	1.82E-05	0.006789	negative regulation of chromosome segregation
GO:0048477	3.32E-05	0.01235	oogenesis
GO:0051784	3.35E-05	0.012429	negative regulation of nuclear division
GO:0032837	3.68E-05	0.013616	distributive segregation
GO:1901988	5.43E-05	0.020037	negative regulation of cell cycle phase transition
GO:0000070	5.53E-05	0.02035	mitotic sister chromatid segregation

GO:2001251	5.82E-05	0.021359	negative regulation of chromosome organization
GO:0007094	5.82E-05	0.021359	mitotic spindle assembly checkpoint
GO:0002066	6.66E-05	0.024309	columnar/cuboidal epithelial cell development
GO:0048646	7.14E-05	0.02599	anatomical structure formation involved in morphogenesis
GO:0035044	7.23E-05	0.026245	sperm aster formation
GO:0050000	7.67E-05	0.027765	chromosome localization
GO:0016321	8.14E-05	0.029385	female meiosis chromosome segregation
GO:0051704	0.0001	0.036081	multi-organism process
Up regulated genes			
GO:0051146	1.33E-07	5.27E-05	striated muscle cell differentiation
GO:0055001	2.57E-07	0.000101	muscle cell development
GO:0043207	9.96E-06	0.003925	response to external biotic stimulus
GO:0048190	2.02E-05	0.00792	wing disc dorsal/ventral pattern formation
GO:0061327	4.87E-05	0.019074	anterior Malpighian tubule development
GO:0046661	7.49E-05	0.029301	male sex differentiation
GO:0060541	7.98E-05	0.031141	respiratory system development
GO:0061061	8.64E-05	0.033613	muscle structure development
GO:0007498	9.52E-05	0.036942	mesoderm development

Table 3.3 Primer sequences for real-time PCR.

oligos for real-time PCR	sense	antisense
kuk	AATGGCTAGCAACACAAGCGGCG	TCCGCGGTTGGTTGCTCTTT
bnk	ACTACAAGCTTAGCCCGTCC	CTCCATGGACCAGCGTTTCT
slam	TGGTCCTAAGCAATTCCACGCCG	CGGTCAGGAAGCGATCATCATCC
Sry-alpha	GCAGTGAGCTGATTGCAGAG	GCACAGGAAGATGGTCTCCA
nullo	ATGGGCAGCACACATTCCGC	GGAGATGCTTGGAGCGCTTG
Act5C	CGAAGAAGTTGCTGCTCTGG	ACGAGTCCTTCTGGCCCATG

Table 3.4 A complete list of enriched biological processes GO terms with Adjusted *P*-value < 0.05 of genes commonly down-regulated or up-regulated in both *Ataxin-7*^{HO3} and *Non-stop*^{02069} GLC embryos.

Down-regulated genes			
GOBPID	P value	Adjust P value	Term
GO:0009790	3.31E-20	1.86E-17	embryo development
GO:0048729	1.69E-18	9.47E-16	tissue morphogenesis
GO:0009887	1.08E-13	6.02E-11	animal organ morphogenesis
GO:0006928	2.97E-13	1.66E-10	movement of cell or subcellular component
GO:0000122	4.61E-13	2.57E-10	negative regulation of transcription from RNA polymerase II promoter
GO:1902679	4.66E-13	2.59E-10	negative regulation of RNA biosynthetic process
GO:0045934	1.03E-12	5.70E-10	negative regulation of nucleobase-containing compound metabolic process
GO:0040011	1.94E-12	1.08E-09	locomotion
GO:0032501	2.24E-12	1.24E-09	multicellular organismal process
GO:0001655	4.41E-11	2.44E-08	urogenital system development
GO:0060255	1.56E-10	8.58E-08	regulation of macromolecule metabolic process
GO:0034654	1.78E-10	9.79E-08	nucleobase-containing compound biosynthetic process
GO:0009890	2.24E-10	1.23E-07	negative regulation of biosynthetic process
GO:0051674	3.03E-10	1.66E-07	localization of cell
GO:0045944	3.05E-10	1.67E-07	positive regulation of transcription from RNA polymerase II promoter
GO:0001703	5.99E-10	3.27E-07	gastrulation with mouth forming first
GO:0061326	8.23E-10	4.48E-07	renal tubule development
GO:0007369	1.14E-09	6.22E-07	gastrulation
GO:0007417	1.29E-09	7.01E-07	central nervous system development
GO:0007423	3.29E-09	1.79E-06	sensory organ development
GO:0007419	4.33E-09	2.34E-06	ventral cord development
GO:0007432	5.01E-09	2.70E-06	salivary gland boundary specification
GO:0007398	5.92E-09	3.19E-06	ectoderm development
GO:0048865	9.05E-09	4.87E-06	stem cell fate commitment
GO:0060429	1.63E-08	8.75E-06	epithelium development
GO:1903508	1.72E-08	9.21E-06	positive regulation of nucleic acid-templated transcription
GO:0048565	2.15E-08	1.15E-05	digestive tract development
GO:0002165	2.33E-08	1.24E-05	instar larval or pupal development
GO:0048569	2.38E-08	1.27E-05	post-embryonic animal organ development

GO:0007494	3.80E-08	2.02E-05	midgut development
GO:0031175	3.80E-08	2.02E-05	neuron projection development
GO:0048737	3.91E-08	2.07E-05	imaginal disc-derived appendage development
GO:0035220	4.03E-08	2.13E-05	wing disc development
GO:0051254	5.61E-08	2.96E-05	positive regulation of RNA metabolic process
GO:0048858	7.04E-08	3.71E-05	cell projection morphogenesis
GO:0007560	9.46E-08	4.98E-05	imaginal disc morphogenesis
GO:0006935	1.49E-07	7.82E-05	chemotaxis
GO:0035290	1.71E-07	8.99E-05	trunk segmentation
GO:0010557	1.93E-07	0.000101	positive regulation of macromolecule biosynthetic process
GO:0007350	2.00E-07	0.000104	blastoderm segmentation
GO:0001709	3.65E-07	0.00019	cell fate determination
GO:0010628	3.98E-07	0.000207	positive regulation of gene expression
GO:0031328	4.77E-07	0.000247	positive regulation of cellular biosynthetic process
GO:0007402	4.93E-07	0.000255	ganglion mother cell fate determination
GO:0046845	4.93E-07	0.000255	branched duct epithelial cell fate determination, open tracheal system
GO:0007479	6.36E-07	0.000328	leg disc proximal/distal pattern formation
GO:0014019	6.36E-07	0.000328	neuroblast development
GO:0007498	6.61E-07	0.00034	mesoderm development
GO:0051173	6.94E-07	0.000356	positive regulation of nitrogen compound metabolic process
GO:0007411	7.61E-07	0.000389	axon guidance
GO:0007165	7.89E-07	0.000403	signal transduction
GO:0060322	7.96E-07	0.000406	head development
GO:0097659	7.97E-07	0.000406	nucleic acid-templated transcription
GO:0007366	1.35E-06	0.000683	periodic partitioning by pair rule gene
GO:0001708	1.56E-06	0.000791	cell fate specification
GO:0008586	1.69E-06	0.000856	imaginal disc-derived wing vein morphogenesis
GO:0007167	1.77E-06	0.000894	enzyme linked receptor protein signaling pathway
GO:0022008	2.02E-06	0.001017	neurogenesis
GO:0061458	2.05E-06	0.001033	reproductive system development
GO:0060581	2.13E-06	0.001068	cell fate commitment involved in pattern specification
GO:0007548	2.54E-06	0.001272	sex differentiation
GO:0023052	2.56E-06	0.001281	signaling
GO:0007509	3.93E-06	0.001964	mesoderm migration involved in gastrulation
GO:0008406	4.81E-06	0.002395	gonad development
GO:0035289	8.61E-06	0.004278	posterior head segmentation
GO:0046552	8.66E-06	0.004298	photoreceptor cell fate commitment
GO:0035160	8.82E-06	0.004364	maintenance of epithelial integrity, open tracheal system

GO:0007420	9.00E-06	0.004444	brain development
GO:0007474	9.29E-06	0.004581	imaginal disc-derived wing vein specification
GO:0001667	9.67E-06	0.004757	ameboidal-type cell migration
GO:0007422	1.01E-05	0.004969	peripheral nervous system development
GO:0021782	1.06E-05	0.005208	glial cell development
GO:0048523	1.21E-05	0.005928	negative regulation of cellular process
GO:0007523	1.41E-05	0.006882	larval visceral muscle development
GO:0006355	1.50E-05	0.007308	regulation of transcription, DNA-templated
GO:2001141	1.50E-05	0.007308	regulation of RNA biosynthetic process
GO:0008354	1.73E-05	0.008415	germ cell migration
GO:0035225	3.30E-05	0.015952	determination of genital disc primordium
GO:0007375	3.51E-05	0.016938	anterior midgut invagination
GO:0035310	3.51E-05	0.016938	notum cell fate specification
GO:0048522	6.49E-05	0.031224	positive regulation of cellular process
GO:0007482	6.78E-05	0.032539	haltere development
GO:0009605	7.34E-05	0.035149	response to external stimulus
GO:0065007	8.43E-05	0.040293	biological regulation
GO:0048646	8.72E-05	0.041574	anatomical structure formation involved in morphogenesis
Up-regulated genes			
GO:0006733	7.36E-05	0.026876	oxidoreduction coenzyme metabolic process

Table 3.5 A complete list of enriched molecular functions GO terms with Adjusted P-value < 0.05 of genes commonly down-regulated in both *Ataxin-7^{HO3}* and *Non-stop^{02069}* GLC embryos.

GOMFID	P value	Adjust P value	Term
GO:0003705	9.98E-13	1.20E-10	transcription factor activity, RNA polymerase II distal enhancer sequence-specific binding
GO:0043565	3.23E-12	3.85E-10	sequence-specific DNA binding
GO:0044212	7.27E-08	8.58E-06	transcription regulatory region DNA binding
GO:0001067	8.87E-08	1.04E-05	regulatory region nucleic acid binding
GO:1990837	2.85E-06	0.000331	sequence-specific double-stranded DNA binding
GO:0001078	5.45E-06	0.000627	transcriptional repressor activity, RNA polymerase II core promoter proximal region sequence-specific binding
GO:0003700	4.74E-05	0.005404	transcription factor activity, sequence-specific DNA binding
GO:0000980	5.23E-05	0.00591	RNA polymerase II distal enhancer sequence-specific DNA binding
GO:0042803	0.00014	0.015641	protein homodimerization activity
GO:0030676	0.000146	0.016171	Rac guanyl-nucleotide exchange factor activity
GO:0001158	0.000212	0.023342	enhancer sequence-specific DNA binding
GO:0050840	0.000416	0.045377	extracellular matrix binding
GO:0005515	0.000437	0.047145	protein binding

Table 3.6 Motif analysis of Sgf11-specific sites. The set of 647 Sgf11 stringent sites was used as input to MEME. Motifs found by MEME were then subject to comparison to known motifs via tomtom. Protein Domains/Motifs information are from flybase.org.

Symbol	Annotation symbol	Protein Domains/Motifs
dati	CG2052	Zinc finger C2H2-type
br	CG11491	BTB/POZ domain; SKP1/BTB/POZ domain; Tetratricopeptide-like helical domain; Zinc finger, RING/FYVE/PHD-type; Zinc finger C2H2-type
CG4328	CG4328	Homeobox domain; Zinc finger, LIM-type; Homeobox domain-like; Homeobox, conserved site
Blimp-1	CG5249	SET domain; Zinc finger, RING/FYVE/PHD-type; Zinc finger C2H2-type
pnr	CG3978	Zinc finger, GATA-type; Armadillo-like helical; Zinc finger, NHR/GATA-type; WD40/YVTN repeat-like-containing domain
Dref	CG5838	Zinc finger, BED-type; Ribonuclease H-like domain; Zinc finger C2H2-type
BEAF-32	CG10159	Zinc finger, BED-type; BESS motif; Zinc finger C2H2-type
odd	CG3851	Zinc finger, RING/FYVE/PHD-type; Zinc finger C2H2-type
slp1	CG16738	Fork head domain; Winged helix-turn-helix DNA-binding domain; Fork head domain conserved site1; Fork head domain conserved site 2
bin	CG18647	Fork head domain; Winged helix-turn-helix DNA-binding domain; Fork head domain conserved site 2
croc	CG5069	Fork head domain; Winged helix-turn-helix DNA-binding domain; Fork head domain conserved site1; Fork head domain conserved site 2
slp2	CG2939	Fork head domain; Winged helix-turn-helix DNA-binding domain; Fork head domain conserved site1; Fork head domain conserved site 2
fd59A	CG3668	Fork head domain; Winged helix-turn-helix DNA-binding domain; Fork head domain conserved site1; Fork head domain conserved site 2
CHES-1-like	CG12690	Fork head domain; Winged helix-turn-helix DNA-binding domain; WD40/YVTN repeat-like-containing domain; Fork head domain conserved site1; Fork head domain conserved site 2
FoxP	CG43067	Fork head domain; Winged helix-turn-helix DNA-binding domain; Fork head domain conserved site 2; FOXP, coiled-coil domain
hbn	CG33152	Homeobox domain; Homeobox domain-like; Homeobox, conserved site
H2.0	CG11607	Homeobox domain; Homeobox domain-like; Homeobox, conserved site; Homeobox domain, metazoa

abd-A	CG10325	Homeobox domain; Homeobox domain-like; WD40/YVTN repeat-like-containing domain; Homeobox, conserved site; Homeobox domain, metazoa; Homeobox protein
abd-B	CG11648	Homeobox domain; Homeobox domain-like; Homeobox, conserved site; Homeobox domain, metazoa
onecut	CG1922	Homeobox domain; CUT domain; Homeobox domain-like; Lambda repressor-like, DNA-binding domain
toe	CG10704	Homeobox domain; Paired domain; Homeobox domain-like; Winged helix-turn-helix DNA-binding domain; Homeobox, conserved site
eyg	CG10488	Homeobox domain; Paired domain; Homeobox domain-like; Tetratricopeptide-like helical domain; Winged helix-turn-helix DNA-binding domain; Homeobox, conserved site
Antp	CG1028	Homeobox domain; Homeobox protein, antennapedia type, conserved site; Homeobox domain-like; Armadillo-like helical; Homeobox, conserved site; Homeobox protein, antennapedia type; Homeobox domain, metazoa
cad	CG1759	Helix-turn-helix motif; Homeobox domain; Homeobox domain-like; Homeobox, conserved site; Homeobox domain, metazoa
vvl	CG10037	POU-specific domain; Homeobox domain; Homeobox domain-like; Lambda repressor-like, DNA-binding domain; Tetratricopeptide-like helical domain; POU domain; WD40/YVTN repeat-like-containing domain; POU-domain transcription factor, class 3; Homeobox, conserved site
z	CG7803	Armadillo-like helical; Myb/SANT-like DNA-binding domain
Hsf	CG5748	Heat shock factor (HSF)-type, DNA-binding; Vertebrate heat shock transcription factor, C-terminal domain; Winged helix-turn-helix DNA-binding domain; Heat shock factor protein 1; Heat shock transcription factor family

Chapter 4

In *Drosophila*, TAF module may have SAGA-independent function

4.1 Abstract

The Spt-Ada-Gcn5-acetyltransferase (SAGA) chromatin-modifying complex is a transcriptional coactivator that contains four different modules of subunits. The TATA binding protein-associated factors (TAF) module serves important roles in maintaining the integrity of SAGA and certain TAF proteins are required for SAGA-dependent nucleosomal HAT activity. We generated a germline clone of WDA to eliminate the maternal gene product and examined the requirement for WDA in oogenesis. Morphological analysis and whole transcriptome profiling were used to determine the requirement of WDA during oogenesis. Lastly, ChIP-seq analysis was used to identify the direct targets of WDA in early embryos. Here we demonstrate that WDA or the TAF module is required for normal oogenesis and a large subset of genes change expression in *wda* germline clone ovaries. WDA regulates the cellularization process during early embryogenesis. WDA binds to SAGA targets as a part of SAGA and non-SAGA targets where no other modules bind. Moreover, WDA-only sites are found at both the transcription start sites (TSS) and the gene body.

4.2 Introduction

The TATA binding protein-associated factors (TAFs) were originally discovered as components of the conserved general transcription factor TFIID. By mass spectrometry and

immunoblotting, Grant and his colleagues first identified in yeast that several TAFs (Taf5, Taf6, Taf9, Taf10 and Taf12) are integral components of the SAGA complex being required for HAT activity and transcription activation (Grant et al. 1998). Later, many groups show that *Drosophila* SAGA has the orthologs of most components of yeast SAGA (Kusch et al. 2003, Muratoglu et al. 2003, Kurshakova et al. 2007, Weake et al. 2008). Although the composition of SAGA is highly conserved across species, there are some difference in *Drosophila*. For example, in yeast, the TAF module subunits in SAGA are shared with TFIID. However, *Drosophila* SAGA contains SAGA-specific TAF module subunits: WDA (will decrease acetylation) and SAF6 (SAGA factor-like TAF6). These subunits provide a way to separate the function of the TAF module in SAGA from TFIID.

Using affinity purification with MudPIT and coimmunoprecipitation analyses, the Workman group identified that a new protein called WDA is a subunit of SAGA. Moreover, MudPIT analysis of WDA affinity purified complex does not identify TFIID-exclusive TAFs, suggesting that WDA is not a TAF (Guelman et al. 2006b). The WDA protein has six WD40 repeats which are necessary for it to incorporate into SAGA. *Wda* zygotic mutants are larvae lethal and homozygous embryos have decreased H3 acetylation. However, co-IP and gel filtration data indicate that the SAGA integrity has no change in the *wda* mutant, suggesting that WDA is not required for the structure of SAGA (Guelman et al. 2006b).

Using this same strategy, the Workman group identified another bona fide SAGA TAF module subunit SAF6. SAF6 is a homolog but not ortholog of yeast TAF6 because it is not in TFIID. Unlike WDA, SAF6 is not required for SAGA HAT or DUB activity (Weake et al. 2009). However, zygotic SAF6 is essential for *Drosophila* development and *saf6* homozygous mutant larvae die during the second instar stage. Loss of SAF6 causes transcriptional change of

some SAGA-regulated genes, indicating that it plays a role in the coactivator function of SAGA, independent of the enzymatic activities (Weake et al. 2009).

The conformation of the TAF module within SAGA is based on yeast studies. Electron microscopy and cross-linking mass spectrometry analyses reveal that the TAF module is likely located at the center of SAGA, combining with the SPT module to form a central core with highly interconnected subunits (Wu et al. 2004, Han et al. 2014, Setiaputra et al. 2015). However, given the difference between yeast and *Drosophila* TAF subunits, it is not clear whether the *Drosophila* TAF module has the same localization and conformation in SAGA.

In this study, we removed the maternal contribution of WDA and investigated the requirement for WDA (the TAF module) in early development. We found that perturbation of WDA caused more severe defects than loss of the HAT module and a large subset of genes changed expression upon loss of WDA in oogenesis. Reduction of WDA in early embryos gave rise to a similar defects as DUB and HAT mutants. We also identified WDA binding sites in wild-type embryos and found that WDA can bind to chromatin independent of the core SAGA modules and a large portion of these WDA-only sites are in the gene body.

4.3 Results

4.3.1 WDA is required for oogenesis

As we discussed in Chapter 3, the HAT module is required for oogenesis while the DUB module is expendable. We then asked whether the non-enzymatic modules of SAGA play any role in oogenesis. To answer this question, we chose the SAGA specific TAF module subunit WDA. We used the *FLP/FRT/ovoD* system to remove WDA in germline cells of the germline

clone (GLC) female's ovaries. This analysis was carried out with null alleles of WDA (Guelman et al. 2006b). In wild type, egg chambers increase in size toward the posterior of the ovary. However, loss of WDA arrested development around stage 7, generating egg chambers obviously smaller than WT (Figure 4.1A). To examine the requirements of WDA for gene expression, we stained ovaries with the germline markers Vasa and Staufen, which play critical roles in germ plasm assembly during oogenesis. Unlike the DUB mutant ovaries described in chapter 3, no Staufen was detected in *wda* GLC ovaries (Figure 4.1B). There are two explanations for the phenotypes: 1) transcription of the gene was down-regulated upon loss of WDA. 2) The *wda* GLC ovaries did not develop to the stage when *staufen* gene starts transcription. Taken together, we conclude that WDA is required for normal oogenesis.

4.3.2 WDA regulates many more genes than Ada2b in ovaries

A previous study demonstrates that WDA is required for SAGA HAT activity (Guelman et al. 2006b). However, based on the severe defects we showed above, we hypothesize that WDA has a HAT-independent function in regulating transcription. To test this, RNA-seq analysis was performed in *wda* GLC ovaries to examine patterns of gene expression. Consistent with the phenotypic results, there were about 2500 genes that changed expression upon loss of WDA in germline cells (~1400 genes down-regulated and ~1000 genes up-regulated) (Figure 4.2A). By comparing the transcription profiles of *wda* and *Ada2b* mutants, we found that more than 80% of the Ada2b-dependent genes were also dependent on WDA (Figure 4.2A). This result indicates that WDA and Ada2b may function together to regulate the SAGA HAT activity and transcription of a subset of genes. We also noticed that there were about 1100 WDA-only dependent genes which were not coregulated by HAT or DUB modules. To determine whether

specific gene networks and pathways have requirements for WDA specifically during oogenesis, we performed Gene Ontology (GO) term analysis of WDA-only dependent genes. Genes involved in egg coat formation, eggshell formation and oocyte differentiation were enriched in the down-regulated genes, which may cause the arrest phenotype in the *wda* mutants (Figure 4.2B). These data correspond well with the different phenotypes shown earlier, and support our hypothesis that WDA has a HAT-independent function in regulating transcription, which could be a coactivator function of SAGA or a SAGA-independent function.

4.3.3 WDA is required for cellularization

Given the severe defects during oogenesis, we wanted to test whether WDA has functions in embryogenesis. Due to the sterility of *wda* GLC females, we could not examine the phenotypes of *wda* GLC embryos. However, we identified WDA knock down conditions that allowed oogenesis to proceed and examined the phenotype of the resulting embryos. Interestingly, we found that *wda* mutant embryos have similar cellularization defects as the DUB or HAT module mutants (Figure 4.3). These observations suggest that the early defects are due to loss of the SAGA function but not to a particular module. To test whether loss of WDA causes similar effects on RNA levels as other SAGA subunits, RNA-seq analysis of these mutant embryos is needed.

4.3.4 WDA can bind to SAGA and non-SAGA target genes in wild type embryos

To examine the binding profile of WDA and compare it to other SAGA modules, we generated a WDA antibody for ChIP-seq and identified its binding sites in wild type embryos.

We compared these sites to other SAGA modules. Overall, the SAGA sites (identified by Sgf11, Spt3 and Ada2b) were also bound by WDA (Figure 4.4). The genome wide ChIP-seq data are consistent with previous biochemical results that WDA is a bona fide subunit of SAGA (Guelman et al. 2006b). Surprisingly, we found that 4913 WDA peaks were not colocalized with Ada2b or Spt3 (Figure 4.4B). Since we already identified some DUB module-only targets as we discussed last chapter, we then asked whether WDA binds to non-SAGA targets with the DUB module. After comparing to Sgf11, we found that 2027 Sgf11 and WDA peaks did colocalize without Ada2b or Spt3, indicating that WDA may interact with the DUB module without other SAGA modules (Figure 4.4B).

Interestingly, there were 2886 targets sites where only WDA was bound (Figure 4.4B), we reevaluated peaks using high stringency criteria which we used to identify the DUB targets last chapter. We included only those WDA sites in which Ada2b, Sgf11 and Spt3 binding were absent in all biological replicates. This analysis identified 1580 WDA-only peaks independent of any other SAGA modules (Figure 4.4A). We then asked where these WDA unique peaks are located. As we showed previously, the majority of SAGA and DUB module peaks are at TSS. However, only ~20% of the WDA-only peaks localized at TSS and many peaks were at the gene body, suggesting that the free WDA may have functions in both transcription activation and elongation (Figure 4.4C).

4.4 Discussion

Our preliminary results reveal the requirement for WDA during oogenesis and embryogenesis and the SAGA-independent binding of WDA in early embryos. Loss of WDA

arrests oogenesis at early stage and ~2500 genes in the ovaries require WDA for their expression. WDA is required for normal cellularization. In wild type conditions, WDA can bind to non-SAGA target genes, either with the DUB module or without any other SAGA modules.

Wda GLC females had severe defects and loss of WDA caused mis-regulation of a large subset of genes in oogenesis. However, this phenotype could be due to another gene CG13827. The *wda* allele we used in this study was generated by imprecise excision of P-element located upstream of *wda* gene. The hop-out event caused a deletion of CG13827, adjacent to *wda* (Guelman et al. 2006b). Although the lethality of *wda* flies was not caused by the CG13827, we could not rule out the possibility that CG13827 plays an essential role in oogenesis and the severe defects are due to the deletion of both genes. However, the expression of CG13827 is very low in ovaries, so the chance that the oogenesis defects are caused by loss of CG13827 is very low. Nevertheless, to test the role of WDA and get a more solid conclusion, a new *wda* allele is needed.

To test whether the defects in oogenesis and embryogenesis are due to the TAF module or WDA itself, future experiments of other TAF module subunits are necessary. SAF6 has been shown to be a SAGA specific subunit (Weake et al. 2009), therefore, the analyses of *saf6* mutants will address this issue. The third TAF module subunit Taf10b might be used too. However, no clear data demonstrate that Taf10b is SAGA specific and unpublished purification data showed that Taf10b was associated with TFIID. It is possible that the *taf10b* mutant defects are caused by disturbing SAGA and TFIID.

In our ChIP-seq experiments, we identified many WDA-only peaks without any other SAGA modules. To examine whether those peaks are non-specific binding during the process of ChIP, we performed high salt condition ChIP. Under this condition, we washed the antibody-

beads-extract mixture with high salt buffer before elution in order to remove non-specific binding. Compared to the normal (low salt) ChIP, there was no difference in WDA enrichment at the WDA-only peaks, supporting that these peaks are real (Figure 4.5).

It is still not clear whether the TAF module can bind to non-SAGA targets by just showing the WDA data. To confirm that the WDA unique peaks are bound by the entire TAF module, ChIP-seq of SAF6 will be performed.

Although we used a more stringent method to identify the WDA unique peaks, we are still unable to eliminate the possibility that the unique WDA peaks reflect a robust antibody and are not actually devoid of other SAGA components. However, we note the different binding preference in SAGA targets and WDA specific targets: TSS versus TSS & gene body. This finding supports our view that the WDA targets are distinct from those of SAGA.

The mechanism by which WDA is recruited to chromatin is still under investigation. At present, we cannot distinguish whether WDA binds on its own or binds in association with novel proteins. It may bind to chromatin through other proteins and its WD40 repeats may serve as a rigid scaffold for protein interactions. Further affinity-purification of WDA is needed.

Figure 4.1 WDA is required for oogenesis. (*A*) Differential interference contrast (DIC) images of ovaries showing the morphology of the ovaries of each genotype. The genotypes of ovaries were as follows: Oregon R (WT); *hs-Flp/+; wda*^{11}, *FRT*^{82B}/*FRT*^{82B}, *ovo*$^{D1-18}$ (*wda*). (*B*) WT and *Wda* GLC ovaries were stained with Vasa (red), Staufen (green) and DAPI (cyan). No Staufen was detected. Bars: *A–B*, 50 µm. (The images in panel A were generated by Leanne Well)

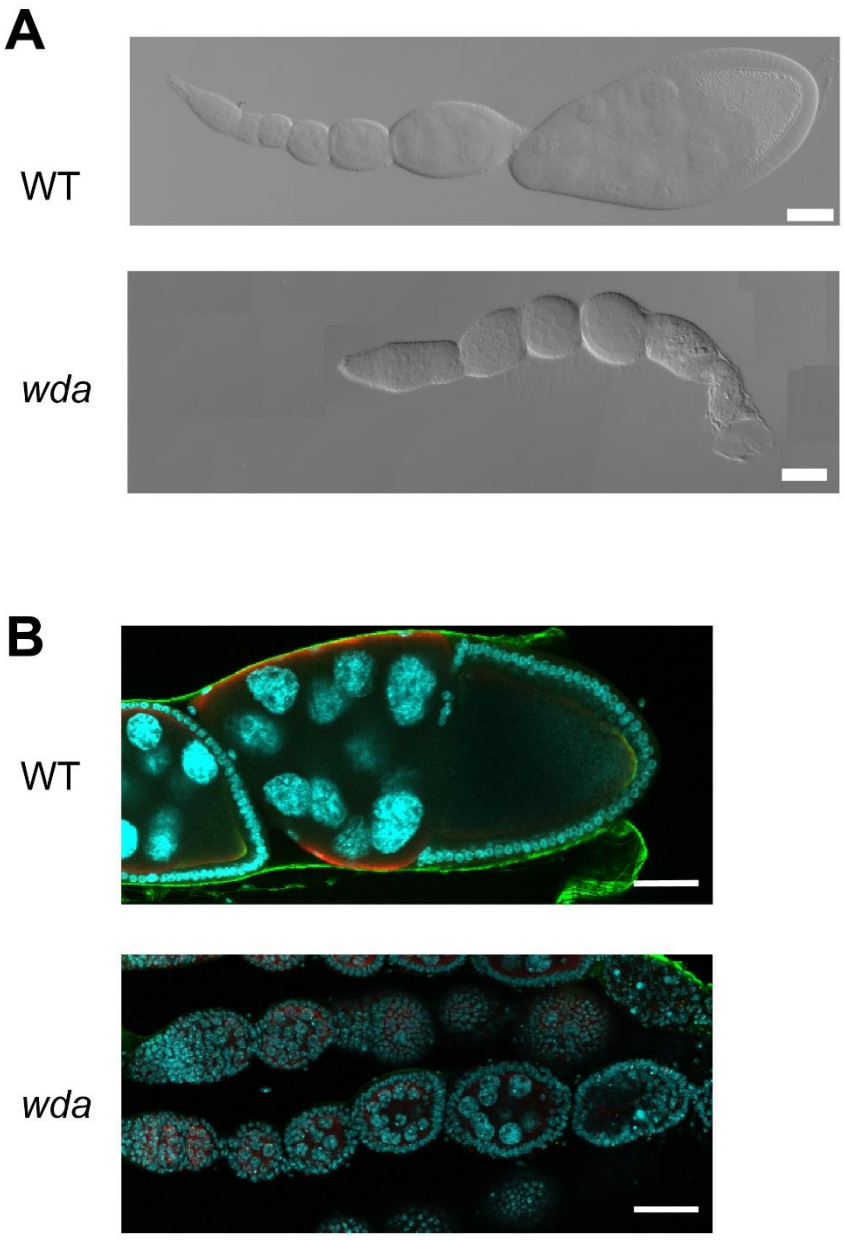

Figure 4.2 WDA regulated transcription of a large subset of genes during oogenesis. (*A*) Venn diagrams showing the overlapping genes with decreased or increased transcript levels in *wda*, *Ada2b*, *Ataxin-7* and *non-stop* GLC ovaries (Fold change > 2, P < 0.05, FPKM > 1). (*B*) GO term analysis of biological process (BP) of genes specifically down-regulated in *wda* GLC ovaries. Adjusted *P*-value < 0.05. A complete list of enriched GO terms with Adjusted *P*-value < 0.05 is provided in Table 4.1

A

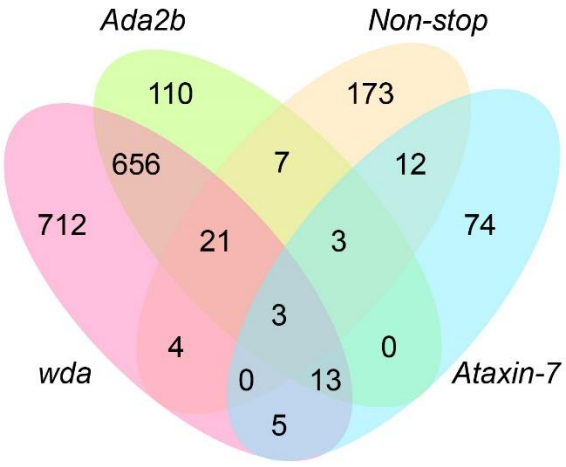

Down > 2 fold, P < 0.05

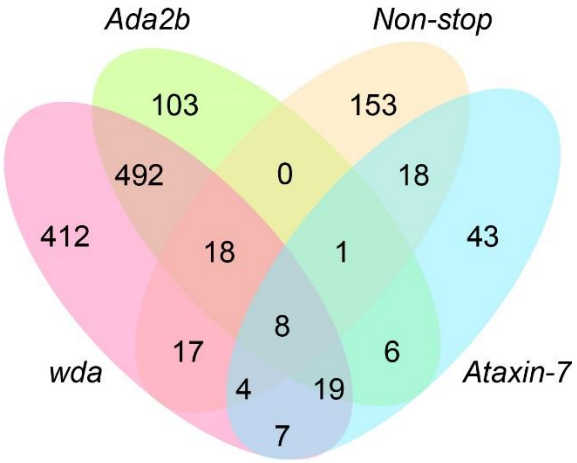

Up > 2 fold, P < 0.05

B

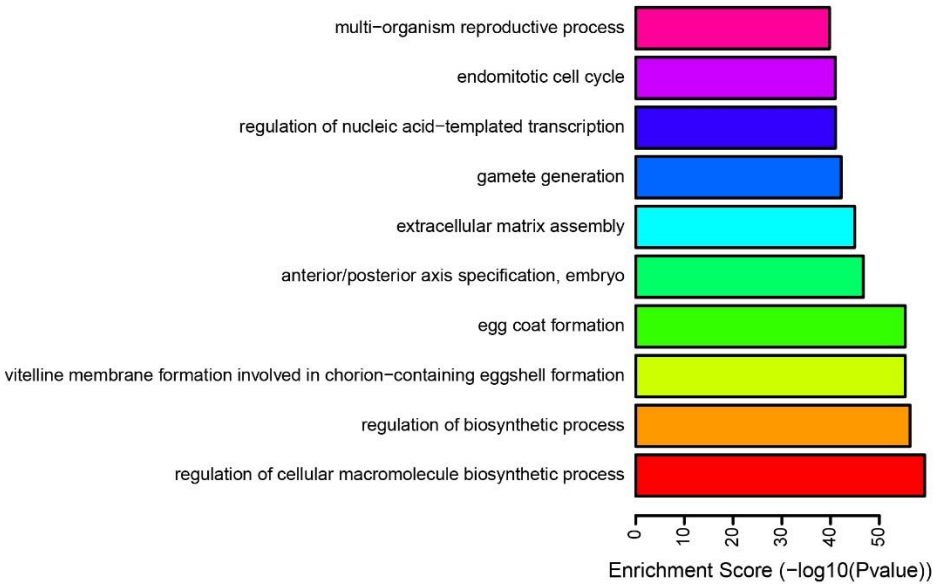

Figure 4.3 WDA is required for cellularization. Stage 5 embryos were stained with Discs-large (red) to mark membranes, Twist (green) to mark mesodermal nuclei and DAPI (blue) to mark all nuclei. A ventral view with anterior to the left is shown. Disruptions in the organization of Twist-expressing nuclei are apparent in *wda* embryos. The *wda* embryos in were collected from crosses as follows at 29°C: *P{w[+mC]=otu-GAL4::VP16.R}1, w[*]; P{w[+mC]=GAL4-nos.NGT}40; P{w[+mC]=GAL4::VP16-nos.UTR}CG6325[MVD1]/ y[1] sc[*] v[1]; P{y[+t7.7] v[+t1.8]=Ada2b RNAi 2-T2} attP40 cross to y[1] sc[*] v[1]; P{y[+t7.7] v[+t1.8]=TRiP.HMS00469}attP2*. Bars: 50 µm.

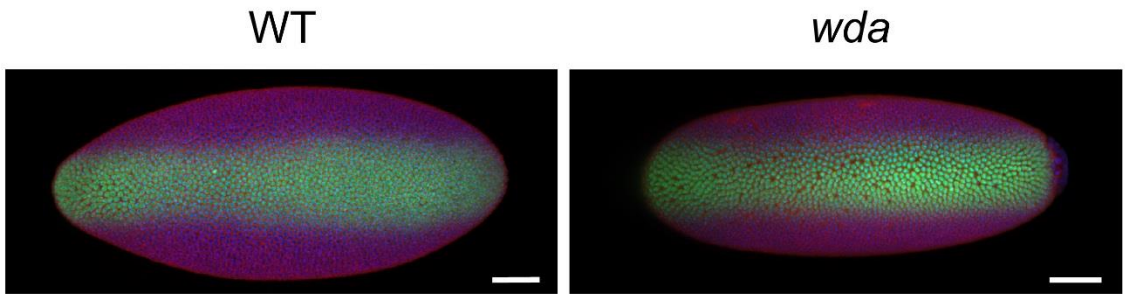

Figure 4.4 WDA binds to target genes independent of SAGA. (*A*) Genome browser of ChIP-seq tracks at a representative region revealed that WDA binds to some genes without other SAGA modules. The red arrow points to the WDA only peak. (*B*) Venn diagram showing the overlapping ChIP-seq peaks between WDA, Sgf11, Ada2b and Spt3. (*C*) Histograms of distance (from -5000bp to +5000bp) to the transcription start sites (TSS) for the WDA-only peaks. Many peaks are located at the gene body.

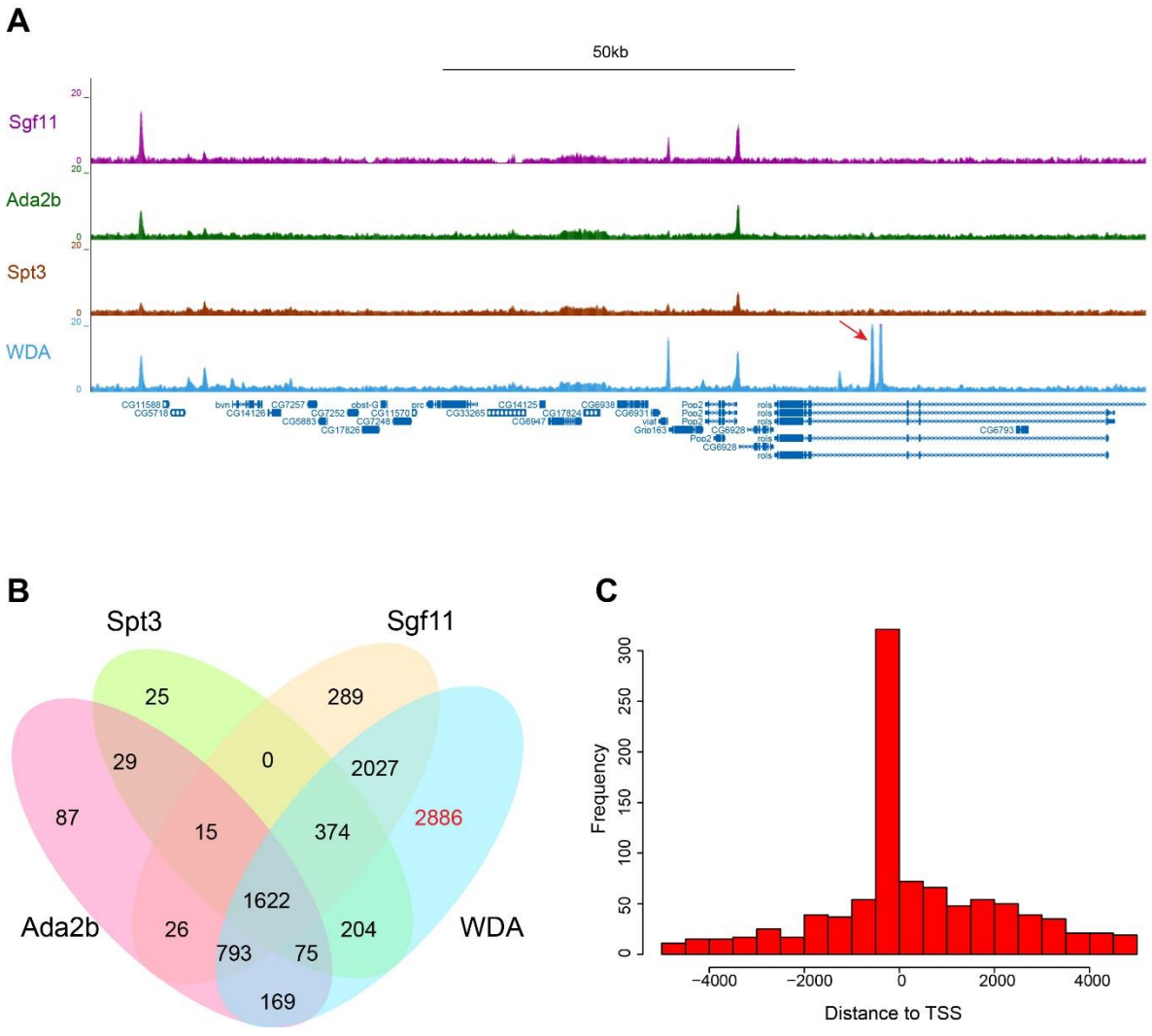

Figure 4.5 Test the specificity of WDA antibody by ChIP-qPCR. ChIP was performed under normal conditions (low salt) and stringent conditions (high salt). The enrichment of WDA-only peaks was the same under both conditions.

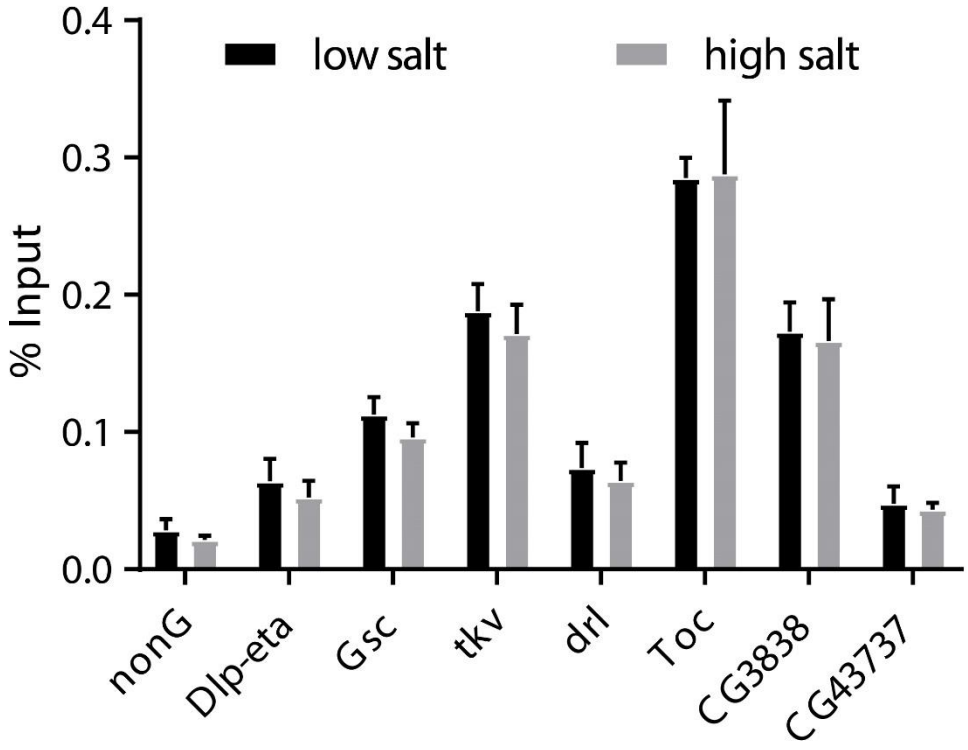

Table 4.1 A complete list of enriched biological processes GO terms with Adjusted *P*-value < 0.05 in genes only down-regulated in *wda* GLC ovaries.

GOBPID	P value	Adjust P value	Term
GO:2000112	1.17E-06	0.000463	regulation of cellular macromolecule biosynthetic process
GO:0009889	2.33E-06	0.00092	regulation of biosynthetic process
GO:0007305	2.93E-06	0.001153	vitelline membrane formation involved in chorion-containing eggshell formation
GO:0035803	2.93E-06	0.001153	egg coat formation
GO:0008595	2.12E-05	0.008321	anterior/posterior axis specification, embryo
GO:0085029	3.20E-05	0.012515	extracellular matrix assembly
GO:0007276	6.03E-05	0.02353	gamete generation
GO:1903506	7.87E-05	0.030624	regulation of nucleic acid-templated transcription
GO:0007113	7.94E-05	0.030824	endomitotic cell cycle
GO:0044703	0.000105	0.040556	multi-organism reproductive process
GO:0045934	0.000119	0.045856	negative regulation of nucleobase-containing compound metabolic process
GO:1902679	0.000123	0.047454	negative regulation of RNA biosynthetic process

Chapter 5

Discussion

In this study, I demonstrate that the individual modules of SAGA complex do not always function together, as shown for transcription regulation, development and chromatin binding. To the best of our knowledge, this is the first work that dissects the roles of individual modules instead of the whole SAGA complex, which adds new pieces of knowledge of this well characterized chromatin-modifying complex. Additionally, similar studies may reveal the functions of individual modules of other modular complexes. Comprehensive knowledge of these complexes will help us understand how cells utilize different modules efficiently during evolution.

5.1 SAGA submodules regulate different subsets of genes

Numerous studies have explored the phenotypic consequences of mutations in SAGA submodule subunits at other stages of *Drosophila* development and in other organisms. In some cases, the loss of certain subunits lead to different phenotypes and distinct transcriptional changes. For example, expression analyses in *S. pombe* revealed distinct functional classes of SAGA subunits (Helmlinger et al. 2011). The *Drosophila* DUB module affects different sets of genes from the HAT module subunit Ada2b in late stage larvae (Weake et al. 2008). These observations indicate that different modules of SAGA may have distinct functions in regulating transcription and development. In agreement with these previous data, we found that whereas the

HAT and TAF modules are required during oogenesis, the DUB module is not required for this process and ovaries lacking Non-stop or Ataxin-7 are normal. Moreover, although HAT and DUB module mutant embryos have similar defects in nuclear anchoring and cellularization, RNA-seq reveals that mutations affecting DUB module subunits have overlapping but distinct effects in transcription compared to the HAT module in early embryogenesis. These results suggest that although, in most cases, SAGA binds to target genes as a complex, individual modules are not equally essential for expression of all targets. The different requirement for each module might be due to expression level, promoter types, nucleosomal occupancy or response to changes in histone modification levels of the target genes. It will be very interesting to further investigate the molecular mechanisms that cause the differences.

5.2 Why is Non-stop expendable in ovaries?

This interesting observation that the DUB module is expendable in ovaries leads us to consider the possibility that SAGA may have alternative components in certain tissues. Until now, most data of *Drosophila* SAGA subunits are derived from yeast SAGA and biochemical studies in *Drosophila* S2 cells. Although SAGA is highly conserved and almost all of the subunits (except Spt8) of yeast SAGA have been identified in S2 cells, it is possible that *Drosophila* SAGA has different conformations or components in different tissues than S2 cells. Other multi-subunit complexes such as the SWI/SNF complex have tissue specific subunits. Interestingly, in the mammalian system, other DUBs (USP27X and USP51) can compete with USP22 for binding to DUB subunits ATXN7L3 and ENY2 to form a complex, although they cannot substitute for USP22 in SAGA (Atanassov et al. 2016). There appear to be 23 candidate deubiquitinases in *Drosophila,* several with significant homology to Non-stop and some are able

to deubiquitinate ubH2B (van der Knaap et al. 2005, Buszczak et al. 2009). Based on this evidence, it would be interesting to examine whether SAGA has alternative compositions in ovaries compared to other tissues, in which Non-stop is not the DUB subunit of SAGA or other DUBs can substitute for Non-stop when it is deleted. The deeper biochemical investigation of the potential new components of SAGA in *Drosophila* will help us to understand the evolution of SAGA in higher eukaryotes.

5.3 SAGA submodules have SAGA independent functions

The investigation of the modularity of SAGA and the implications that these modules are involved in transcriptional regulation may give us hints about how the SAGA modules integrate into a complex. Previous studies suggest that the yeast HAT and DUB modules are stable even though the integrity of SAGA is impaired (Lee et al. 2011) and this is true for the DUB module in mammalian cells (Nagy et al. 2009). In the fly, a hyperactive DUB module can bind to chromatin after disassociation from SAGA (Mohan et al. 2014). More interestingly, under wild type condition in yeast, the DUB module can be separated from SAGA by the proteasome chaperones (Lim et al. 2013). The DUB module subunit Sus1 is in the mRNA export complex TREX-2 (Rodriguez-Navarro et al. 2004) and Sgf73 mediates the stable interaction between the TREX subunits (Kohler et al. 2008). The *Drosophila* Sus1 homolog E(y)2 is also required for mRNA export (Kurshakova et al. 2007). These studies have established links between transcription and mRNA export, leading to more efficient RNA synthesis.

Our ChIP-seq data not only support their observation that submodules can exist without having to associate with SAGA in wild type conditions, but also prove that they can bind to

chromatin and regulate transcription. We do not understand the mechanisms by which these modules bind to chromatin yet; they may bind to chromatin by themselves or have novel partners for their binding. Sgf11 is a Znf protein and can bind to nucleosomal DNA (Koehler et al. 2014). Although WDA has not been shown to bind to chromatin yet, other WD40 repeats containing proteins can interact with methylated H3 (Wysocka et al. 2005). These suggest that Sgf11 and WDA may interact with chromatin and recruit these submodules without additional help. Supporting this hypothesis, we found that Znf binding sites are enriched in the Sgf11-specific targets (Table 3.6). Moreover, non-SAGA proteins could interact with these submodules for their binding. For example, the WD40 repeats of WDA may serve as a rigid scaffold for protein interactions. Interestingly, we found that Sgf11-specific target sites are also enriched for fork head domain and homeobox domain protein-binding motifs, suggesting that these submodules can interact with novel complexes besides SAGA and may have additional functions besides transcriptional activation.

It will be very interesting to examine if new protein complexes can be found to interact with these submodules. These new findings will link transcription with other biological processes and broaden our views of how cells utilize different complexes efficiently to tether different processes together.

5.4 SAGA is required for a subset of genes

SAGA, as a transcription coactivator, has been shown to be important for transcription. However, there is an ongoing debate regarding the question of whether SAGA is required for transcription of all or only a subset of genes. Various groups using different methods have

reported opposite conclusions: microarray data suggest that SAGA only regulates 10% of yeast genes and is preferentially used by those with TATA boxes, including those associated with stress, while the other 90% of genes are TFIID-dominant (Huisinga and Pugh 2004, Basehoar et al. 2004). However, Bonnet and colleagues examined changes of histone modification and Pol II enrichment by ChIP-seq in SAGA mutants and demonstrate that SAGA is required for all transcribed genes for both yeast and human (Bonnet et al. 2014). Recently, two groups demonstrated that SAGA and TFIID are not alternative factors but both are required for almost all the yeast genes (Baptista et al. 2017, Warfield et al. 2017, Taatjes 2017). However, ChIP-seq of SAGA in fly muscle cells reveals that only 40% of Pol II bound genes are bound by SAGA (Weake et al. 2011). In mice, both TFIID and SAGA complexes are dispensable for early paraxial mesoderm development (Bardot et al. 2017), arguing against the global role of SAGA in transcription. Why do different groups get different conclusions? Possible explanations are: 1) SAGA in different organisms may behave differently. 2) Loss of different subunits of SAGA has different effects on transcription and conclusions may vary from different mutations. For example, the microarray data examined a *spt3Δ* strain, whereas the ChIP-seq data of histone modification changes were from *gcn5* and *ubp8* mutants. 3) Changes in histone modifications could be a secondary effect of both SAGA and other histone modifying complexes, which are regulated by SAGA. If so, examining the histone modifications may not be the best way to reveal roles of SAGA in regulating transcription. 4) Gcn5 is also present in the ADA (yeast) and the ATAC (metazoan) complexes. Thus, the greater severity of Gcn5 mutants in many of these examples may result from the loss of other complexes. 5) The definition of "global" from different groups could be different. For example, based on the data that SAGA binds to both SAGA- and TFIID-dominant genes and genes in both groups change expression upon loss of

SAGA subunits, Baptista et al demonstrated that SAGA is a general cofactor. However, in genome wide studies, less than half of the genes are bound by SAGA and only 70% of these genes change expression in SAGA mutants (Baptista et al. 2017), arguing that SAGA is not required for all genes.

Using multiple SAGA specific subunits and combining ChIP-seq, RNA-seq and morphological analyses in ovaries and early embryos, our data suggest that SAGA binds to and regulates a subset of genes in the *Drosophila* genome. These results are consistent with most published ChIP-seq data that SAGA localizes to a subset of genes and not all the transcribed genes change expression upon loss of SAGA subunits (Lee et al. 2000, Helmlinger et al. 2011, Krebs et al. 2011, Weake et al. 2008). Together, our comprehensive studies about SAGA indicate that it is an important coactivator for a subset of *Drosophila* genes.

5.5 Only a few nuclei have anchoring defects in the DUB mutants

Loss of Ataxin-7 or Non-stop caused global defects of membrane invagination and nuclear shape. Surprisingly, these global defects led to only a few nuclei dropping from the surface of the embryos. To explain that, we need to consider that all living organisms are in a state of dynamic balance and have thresholds for any changes. Although expression of some critical genes for cellularizatIon were misregulated in the DUB mutants, many genes regulating cellularization may not depend on the DUB module for their expression. The normal expression of these genes may cover up the loss of others in some nuclei and the total change in these nuclei do not reach the threshold necessary for nuclei dropping. Whereas the misregulated genes have greater effects in the other nuclei that reach the threshold; thus the nuclei could not stay on the

surface. Moreover, at this stage, there is a transition from one cell to multiple cells. The microenvironments of each nuclei with the surrounding forming cells could be different. However, individual cells are not formed yet during cellularization and we could not predict which nuclei drop from the surface. It will be very difficult to examine the transcription of individual cells.

5.6 ubH2B levels change in the *Ataxin-7* mutant embryos

SAGA has been shown to activate transcription in many cases. However, we found that many up-regulated SAGA target genes had higher ubH2B levels in the *Ataxin-7* mutants. This indicates that SAGA (the DUB module) could be a transcriptional repressor for some target genes dependent on gene contents.

Additionally, we found that the down-regulated SAGA targets in the DUB mutants did not have dramatic changes in ubH2B levels, suggesting that ubH2B levels were not the main reason for their down-regulation. We also found that the HAT activity was not affected in the *Ataxin-7* mutants. Given the role of Ataxin-7 in anchoring the DUB module and interacting with core subunits of other modules (such as Spt20), we hypothesize that down-regulation of these genes may be caused by impairing SAGA non-enzymatic modules upon loss of Ataxin-7. To verify this, ubH2B levels of mutant embryos from non-enzymatic modules need to be examined.

5.7 Whether Ataxin-7 and Non-stop have opposite roles

Loss of zygotic Ataxin-7 causes larval lethality that is partially rescued by reducing Non-stop expression, suggesting that these two proteins have opposite effects (Mohan et al. 2014). By comparison, our analysis showed that the two mutant embryos had similar defects during cellularization and roughly 50% of the genes impacted by the loss of Ataxin-7 or Non-stop were similarly affected in both mutants. How to explain the different conclusions? Firstly, lethality only reflects one part of development and transcription. It is possible that genes essential for survival are oppositely affected by Ataxin-7 and Non-stop, while many other genes are co-regulated by these two proteins. Secondly, larval and early embryos are different developmental stages and Ataxin-7 and Non-stop could have different functions at different stages. Finally, loss of Ataxin-7 and Non-stop could have opposite effects on ubH2B levels, but both ubH2B changes cause similar transcriptional change and developmental defects. To examine this hypothesis, we can do double mutant of Ataxin-7 and Non-stop in early embryos and check the phenotypes.

5.8 The findings of the DUB module in *Drosophila* may help explain neural disease

Polyglutamine expansions in Ataxin-7 are associated with the human neural degenerative disease: spinocerebellar ataxia type 7 (SCA7). Ataxin-7, but not GCN5, plays a primary role in the neurodegenerative disease SCA 7 (David et al. 1997, David et al. 1998, Del-Favero et al. 1998, Johansson et al. 1998, Chen et al. 2012). The mechanism(s) responsible for this neural defect are not entirely clear. Mohan et al found that loss of Ataxin-7 in the fly leads to a similar neural degeneration phenotype as polyglutamine expansion (Mohan et al. 2014), raising the possibility that polyQ expansion and Ataxin7 loss of function could impair the same molecular process. The N terminus of Sgf73 (yeast Ataxin-7) is necessary for DUB recruitment to SAGA (Kohler et al. 2010, Kohler et al. 2008) and this region is subject to the polyQ expansion. Thus,

perhaps the polyQ expansion changes the structure of Ataxin-7 such that it cannot anchor the DUB module into SAGA. The disassociated and misregulated DUB module may cause SCA7. So Ataxin-7 mutants will provide a good model system to understand the mechanisms of SCA7. This disassociated and misregulated DUB module may cause SCA7 in a similar manner to the absence of Ataxin-7 in *Drosophila*. Alternatively, the dissociation of the DUB module by either means might simply compromise SAGA function. This latter mechanism is supported by our observation that the same set of genes is impacted by loss of the deubiquitinase itself as well as Ataxin-7. It is also strengthened by our observation that the DUB module still binds to the same sites as other SAGA subunits in the *Ataxin-7* mutant, though perhaps this interaction is not as stable and compromises SAGA function. Lastly, the neurodegenerative defect may be a combination of both of these effects, both reduced SAGA function and novel DUB activity.

In any case, loss of Ataxin-7 and Non-stop causes down-regulation of several genes involved in neural development (Table 3.4), indicating that neural genes are dependent on the DUB module. It is possible that polyQ expansion of Ataxin-7 causes similar changes in gene expression and these changes lead to degeneration. Further analysis of genes that depend on the DUB module for their expression and the ubH2B level changes that occur upon loss of Ataxin-7 may help us to understand the basis for the disease phenotype. The ability to discern the impact of SAGA perturbation on the molecular mechanisms that give rise to neurodegeneration in the fly may provide insights into SCA7 disease, and lead to potential therapies for this disease.

5.9 Evolutional view of SAGA

Some other histone modifying complexes have modularity similar to SAGA. An interesting example is the metazoan TIP60 complex, which is the fusion of two yeast complexes. In my studies, we identified the SAGA-independent functions of submodules. It is possible that the SAGA modules are evolved from small complexes. Interestingly, the ADA complex, which contains the HAT module of SAGA and two other non-SAGA subunits, present in yeast but not in higher eukaryotes. This leads us to wonder that whether SAGA is derived from ADA during evolution. The presence of the DUB module and TAF module in other complexes suggests that these modules may exist as individual complexes in prokaryotes and fuse together as needed during evolution. Gradually, these small complexes are replaced by big complexes and become less abundant.

During evolution, gene duplications have occurred for many SAGA subunits (such as WDA) and more subunits became SAGA specific, thus loss of SAGA subunits will not affect the function of other complexes. Also, SAGA-like complexes arose in metazoans (such as ATAC) and regulate distinct gene sets from SAGA. These changes may benefit metazoans during evolution: the reduction of the effects of SAGA in transcription and development may increase the chance of survival upon loss of SAGA subunits.

Chapter 6

Conclusions and future directions

6.1 Conclusions

In my dissertation project, I used *Drosophila* as a model to investigate the role of SAGA submodules in gene expression and development. I have the following conclusions:

6.1.1 The *Drosophila* HAT, TAF and DUB module subunits are required at different stages of development

HAT and TAF modules are required for oogenesis, whereas the DUB module is expendable. Here I show that loss of the HAT module subunit Ada2b or the TAF module subunit WDA causes defects in oogenesis and the GLC females cannot lay eggs. However, the DUB module subunits Ataxin-7 and Non-stop are not required for normal oogenesis and the *Ataxin-7* and *Non-stop* GLC females lay fertilized embryos. RNA-seq analyses of these GLC ovaries indicate that there are many more genes dependent on the HAT or TAF module than genes dependent on the DUB module, which is consistent with the phenotypic results. Moreover, *wda* GLC females have the most severe ovary defects, suggesting that WDA may have HAT-independent functions.

6.1.2 Early patterns still form in the DUB mutants

I have explored the requirement for DUB module subunits during embryogenesis. Here I show that the *Ataxin-7* or *Non-stop* GLC embryos still form the dorsal-ventral and anterior-posterior axes. Based on Even-skipped and Twist staining, segmentation and mesoderm specification still occur in the mutants. I therefore conclude that transcription of some early zygotic genes occurs in early embryogenesis independent of the DUB module of SAGA.

6.1.3 The DUB module is required for embryogenesis

At stage 5, the *Ataxin-7* or *Non-stop* GLC embryos show cellularization defects. Here I show that membrane invagination is abnormal upon loss of the DUB subunits, as evidenced by the staining of Tubulin and Enabled. Some nuclei cannot anchor to the periphery of the embryos and fall off after their arrival, leaving a disorganized pattern on the surface. Moreover, all the nuclei (surface and internal) are misshapen in the *Ataxin-7* and *Non-stop* GLC embryos, suggesting that loss of the DUB module subunits causes global defects during cellularization. Despite the modest impact of the absence of DUB module subunits in early development, Ataxin-7 and Non-stop are important for embryogenesis. In a lethality test, 75% of *Ataxin-7* (m-/-, z-/+) embryos and 100% of *non-stop* (m-/-, z-/+) embryos died during embryogenesis. Altogether, I demonstrate that the DUB module is important for overt embryogenesis.

6.1.4 The DUB subunits control expression of a subset of genes

RNA-seq of the *Ataxin-7* or *Non-stop* GLC embryos reveal that loss of these subunits alters transcription of many genes, while others genes exhibit robust expression that is unaffected. There is a large degree of overlap between the effects of the *Ataxin-7* or *Non-stop*

GLC embryos. This result indicates that Ataxin-7 or Non-stop function together to regulate transcription of a subset of genes. Particularly, genes involved in embryo development are highly enriched in the commonly down-regulated genes, indicating the essential role of the DUB module during embryogenesis.

6.1.5 In most cases, SAGA binds to chromatin as a whole complex

We generated antibodies against SAGA subunits from all four modules: Sgf11 in the DUB module, Ada2b in the HAT module, Spt3 in the SPT module and WDA in the TAF module. I performed ChIP-seq to identify the target sites of individual modules. By comparing the binding sites of the four modules, I demonstrate that in most cases, SAGA binds to targets as a whole complex even though some of them do not require all SAGA modules for their expression. These genome wide data confirms previous biochemical results that SAGA acts as a whole complex.

6.1.6 The DUB and TAF module can bind to chromatin without the entire SAGA

Besides binding with the entire SAGA complex, the DUB and TAF module also bind to non-SAGA targets. The DUB module still binds to TSS and it can regulate the expression of some target genes. However, different promoter types are enriched in SAGA targets and DUB specific targets. The DUB module facilitates Pol II binding genome wide, possibly reflecting a role for the DUB module in the regulation of paused Pol II and elongation. The TAF module binds to many non-SAGA targets. It has distinct binding preferences from SAGA and the DUB module: many WDA-only peaks are in the gene body.

6.2 Future directions

Since the first discovery of the SAGA complex many years ago, numerous studies have been carried out to explore the function of SAGA in regulating transcription and development. In this study, I have characterized the requirement of individual modules of SAGA and provided novel insights into the function of these submodules. However, there are still many interesting questions awaiting exploration.

6.2.1 To investigate the role of TAF module in oogenesis

I removed the maternal WDA in germline cells of ovaries and investigated the phenotypes and expression profiles. However, WDA by itself, cannot reflect the requirement of the entire TAF module in oogenesis. It is highly possible that WDA has non-SAGA functions, which cause the severe defects I observed above. To answer this question, examining another TAF module subunit SAF6 is needed. SAF6 can be deleted in ovaries by a germline clone method or knock down. EMS mutagenesis or CRISPR/Cas9 can be used to generate a new *saf6* allele. Knock-down of SAF6 in ovaries gives similar defects as *wda* mutants, further RNA-seq of *saf6* mutant ovaries needs to be performed.

6.2.2 To investigate the binding sites of SAGA submodules in ovaries

I have shown that the different SAGA submodules have different requirements in oogenesis. I identified the binding sites of individual modules in embryos. However, I do not know how these submodules behave in ovaries. There are questions realted to SAGA in ovaries:

1) Does the TAF module bind to non-SAGA targets and regulate transcription? 2) Does the DUB module bind to SAGA targets where they do not need it? 3) Does the ubH2B level change in the DUB mutant? To answer these questions, ChIP-seq of ovaries is needed. Since the antibodies have been tested in embryos, they should work in ovaries.

6.2.3 To investigate the role of the TAF module in embryogenesis

The morphology analysis suggests that WDA is required for cellularization. However, I do not know the requirement of WDA in transcription. RNA-seq of the *wda* knock-down embryos is needed to address it. Moreover, I identified many WDA-only genes in wild type embryos, but I do not know whether WDA or the TAF module regulate transcription of these genes. Comparing RNA-seq results of *wda* knock-down embryos and WDA ChIP-seq will answer this question.

Additionally, it is interesting to examine whether the TAF module regulates enzymatic activities of SAGA. ChIP-seq of H3K9ac, H3K14ac and ubH2B in *wda* or *saf6* mutant embryos will answer these questions.

6.2.4 To confirm that the binding sites of WDA are TAF module targets

Sgf11 and Non-stop ChIP-seq results support the idea that the entire DUB module binds to novel targets. Although I identified WDA-only targets, I cannot conclude that these sites are free TAF module targets. To address whether these WDA bound sites reflect binding of the

entire TAF module, ChIP analysis of SAF6 will be carried out (the SAF6 antibody has been tested and works for ChIP).

6.2.5 To investigate the mechanism by which the DUB and TAF modules are recruited to chromatin

In this study, I used ChIP-seq to identify that the DUB module and the TAF module (WDA) bind to both SAGA and non-SAGA genes. Comparison of ChIP-seq data of Sgf11 and WDA reveals that they colocalize at many non-SAGA targets. This interesting result indicates that these two modules may interact with each other outside of SAGA for their binding. To examine the direct interaction of the two modules, the baculoviral system can be used to express Sgf11 and WDA without other SAGA subunits. Alternatively, knock out of Spt20, which is required for the integrity of SAGA complex (Nagy et al. 2009), in S2 cells can be tried. Coimmunoprecipitation assays of Sgf11 and WDA can be performed in the *spt20* knockout cells. If Sgf11 and WDA have direct interactions, this suggests that the DUB and TAF module may form a small complex and facilitate each other's binding to chromatin.

From motif analysis (Table 3.6), we found that the DUB module binds to many ZnF-protein targets, indicating that the DUB module may be recruited to chromatin by the Sgf11-ZnF domain. To verify this interaction, mutations of the Sgf11 ZnF-domain or the target motif sequences can be used. If the DUB module cannot bind to target genes in the mutant conditions, we can conclude that the Sgf11 ZnF-domain is crucial for the recruitment of the DUB module to chromatin.

CRISPR/Cas9 can be used to delete the ZnF-domain in Sgf11. In yeast and mammals, the ZnF domain of Sgf11 is not essential for the assembly of the DUB module (Lang et al. 2011, Kohler et al. 2010) and the loss of Ataxin-7 and Non-stop do not arrest oogenesis in *Drosophila*. We think the loss of the Sgf11 ZnF-domain will not cause disassembly of the DUB module nor oogenesis defects. ChIP-seq of Nonstop will be performed in Sgf11 ZnFΔ embryos and compared to WT. Alternatively, *in vitro* assays can be used to examine the role of the ZnF domain of Sgf11 in DNA binding. The baculoviral system can be used to express the DUB module subunits. DNA sequences of WT or mutant ZnF-binding motifs can be obtained in vitro. Then Gel Shift assay can be used to test the binding of the recombinant DUB module and ZnF-binding motifs.

To identify potential binding partners of the DUB and TAF modules, affinity-purification of tagged Sgf11 or WDA followed by mass spec is necessary. FLAG-tagged Sgf11 and Flag-tagged WDA transgenic flies will be generated by CRISPR/Cas9. FLAG-tagged S2 cell lines are alternative systems to do the biochemical experiments. Affinity purification of WDA or Sgf11 followed by mass spec will be used to identify the potential non-SAGA candidates which interact with Sgf11 or WDA. Further *in vivo* immunoprecipitation experiments can be used to confirm their interactions. The next step is to generate antibodies (by the GenScript Company) against these candidates and perform ChIP-seq in embryos to test whether they bind to the same target genes as the DUB and TAF modules.

6.2.6 To investigate the ubH2B level change in *Non-stop* mutant embryos and examine *Ataxin-7, Non-stop* double mutants.

The similar defects and great overlap of *Ataxin-7* and *Non-stop* GLC embryos indicate that these two subunits may have the same effects on transcription. We examined the change of chromatin ubH2B level in *Ataxin-7* GLC embryos and hypothesized that *Non-stop* GLC embryos are the same. However, loss of Ataxin-7 and Non-stop may not change chromatin ubH2B level in a similar way. Loss of Non-stop, which is the deubiquitinase, causes higher ubH2B (Weake et al. 2008). Whereas loss of Ataxin-7 frees the DUB module from SAGA and leads to lower ubH2B (Mohan et al. 2014). My preliminary ChIP-seq results of *Ataxin-7* GLC embryos revealed that the DUB and HAT modules still bind to the same target sites as in WT conditions (Figure 5.1), suggesting that most of the SAGA target genes are still bound by the two enzymatic modules upon loss of Ataxin-7 (although the two modules may not be associated together). It is possible that loss of Ataxin-7 and Non-stop have different effects on chromatin ubH2B but it will be very interesting if they cause similar changes in chromatin ubH2B levels. I was unable to get sufficient *non-stop* GLC embryos because of the overall health of the mothers. An alternative approach is to knock down Non-stop in ovaries and early embryos using the Gal4/UAS system (MTD-Gal4 and Non-stop RNAi stocks are available). ChIP-seq of ubH2B in these embryos will be performed to study the correlation between the genes with expression change in the DUB mutants and the genes with an altered state of ubH2B.

It will be interesting to examine phenotypes and transcription in double mutant embryos. It is almost impossible to delete both genes using the traditional GLC method. However, CRISPR/Cas9 technology makes it feasible. FRT sites can be integrated into both 5’ and 3’ ends of genes of interest (Ataxin-7 and Non-stop). Similarly, the hsflp gene driven by an ovary specific enhancer can integrate into the same stock using CRISPR/Cas9. Deletion of both genes

will be induced by heat shock in late stage larvae or adults. Phenotypic and genome-wide analyses of the mutant ovaries and embryos can be performed.

6.2.7 To investigate the role of other deubiquitinases in development

The possibility that other deubiquitinases can substitute for Non-stop remains a formal possibility. There appear to be 23 candidate deubiquitinases in *Drosophila*, several with significant homology to Non-stop. Scrawny and USP7 have been reported to have activity on ubH2B (van der Knaap et al. 2005, Buszczak et al. 2009). Scrawny encodes the *Drosophila* homologue of yeast Ubp10, which has been reported to deubiquitinate ubH2b in the coding sequence (Schulze et al. 2011). It remains to be determined whether any of these can substitute for SAGA in the absence of Non-stop or whether another complex might provide this activity.

Mutant stocks of Scrawny or USP7 can be obtained by CRISPR/Cas9 or EMS methods and GLC females can be made. RNA-seq of these GLC ovaries will be performed and compared to *Non-stop* mutants. To examine whether Non-stop and other deubiquitinases have overlapping functions in oogenesis, double deletion of Non-stop and Scrawny (Non-stop and USP7) in ovaries can be obtained by CRISPR/Cas9 as discussed earlier. Phenotypical analyses and RNA-seq will be performed in these double mutants.

Figure 6.1 In *Ataxin-7* GLC embryos, the HAT and DUB modules still bind to the same target sites as WT. (*A*) Venn diagram showing the overlapping Ada2b or Sgf11 ChIP-seq peaks between WT and *Ataxin-7* GLC embryos. (*B*) Genome browser of ChIP-seq tracks at a representative region revealed that Sgf11 and Ada2b bind to the same target sites in WT and *Ataxin-7* GLC embryos.

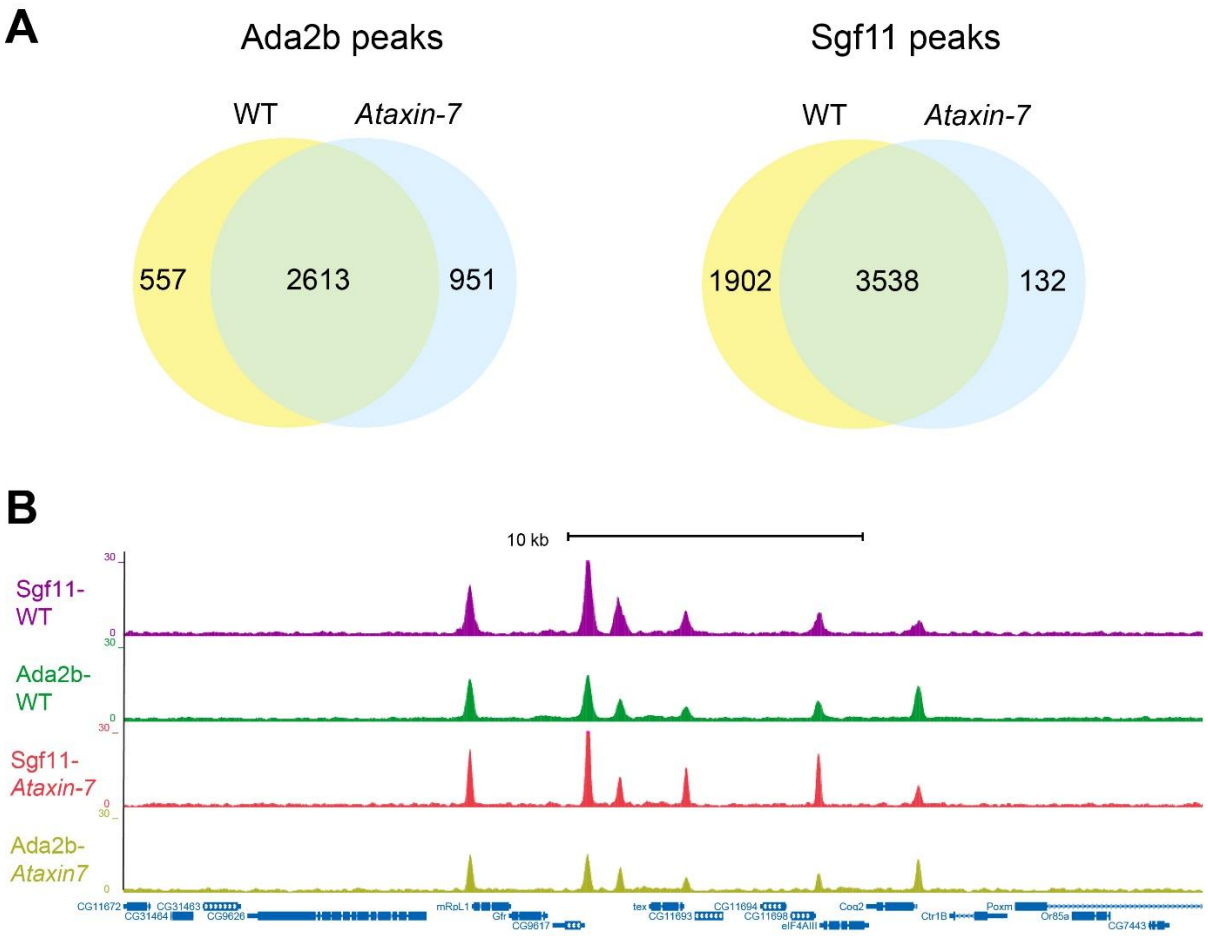

Appendix A: Up-regulated genes in *Ada2b* GLC ovaries

FBgn0013686	FBgn0261113	FBgn0031675	FBgn0040238	FBgn0027930	FBgn0260660	FBgn0036926	FBgn0038631
FBgn0005391	FBgn0033188	FBgn0002789	FBgn0035039	FBgn0261673	FBgn0039678	FBgn0065032	FBgn0040357
FBgn0004045	FBgn0263916	FBgn0010222	FBgn0002528	FBgn0032943	FBgn0024980	FBgn0260767	FBgn0034200
FBgn0013678	FBgn0028373	FBgn0261674	FBgn0031489	FBgn0052196	FBgn0063649	FBgn0039431	FBgn0030662
FBgn0013675	FBgn0000964	FBgn0004003	FBgn0026061	FBgn0051997	FBgn0027596	FBgn0063497	FBgn0263397
FBgn0040007	FBgn0014906	FBgn0010039	FBgn0001341	FBgn0086608	FBgn0261647	FBgn0033785	FBgn0264695
FBgn0004047	FBgn0030079	FBgn0029714	FBgn0010383	FBgn0029766	FBgn0040718	FBgn0031571	FBgn0035084
FBgn0015221	FBgn0004646	FBgn0038720	FBgn0040687	FBgn0050273	FBgn0082967	FBgn0037547	FBgn0030332
FBgn0015222	FBgn0034761	FBgn0050197	FBgn0024234	FBgn0039205	FBgn0051216	FBgn0262104	FBgn0030828
FBgn0262952	FBgn0023542	FBgn0260722	FBgn0030485	FBgn0000320	FBgn0037956	FBgn0002609	FBgn0085249
FBgn0013681	FBgn0039115	FBgn0050344	FBgn0086602	FBgn0052850	FBgn0260866	FBgn0032666	FBgn0062978
FBgn0065053	FBgn0263619	FBgn0027364	FBgn0085819	FBgn0025693	FBgn0024321	FBgn0029507	FBgn0264562
FBgn0015393	FBgn0020513	FBgn0261284	FBgn0033421	FBgn0033919	FBgn0038774	FBgn0040832	FBgn0037853
FBgn0000409	FBgn0263510	FBgn0027572	FBgn0011591	FBgn0086672	FBgn0034085	FBgn0250871	FBgn0040763
FBgn0014184	FBgn0005612	FBgn0010246	FBgn0259938	FBgn0060296	FBgn0032156	FBgn0003366	FBgn0035023
FBgn0033548	FBgn0043364	FBgn0030052	FBgn0085765	FBgn0026878	FBgn0038679	FBgn0037433	FBgn0033817
FBgn0002868	FBgn0037443	FBgn0040813	FBgn0030218	FBgn0034909	FBgn0020385	FBgn0035976	FBgn0264490
FBgn0015795	FBgn0030040	FBgn0038869	FBgn0082988	FBgn0053126	FBgn0028420	FBgn0036288	FBgn0030160
FBgn0005278	FBgn0003328	FBgn0083005	FBgn0085354	FBgn0052364	FBgn0046776	FBgn0032405	FBgn0038147
FBgn0004404	FBgn0043841	FBgn0033926	FBgn0034602	FBgn0003731	FBgn0038826	FBgn0031678	FBgn0031630
FBgn0082919	FBgn0042094	FBgn0039430	FBgn0033584	FBgn0053099	FBgn0034198	FBgn0035431	FBgn0040600
FBgn0031285	FBgn0001224	FBgn0026562	FBgn0039313	FBgn0051955	FBgn0050428	FBgn0024179	FBgn0031501
FBgn0031913	FBgn0010019	FBgn0010434	FBgn0031305	FBgn0003089	FBgn0002733	FBgn0035727	FBgn0000406
FBgn0031381	FBgn0038183	FBgn0051869	FBgn0032297	FBgn0028540	FBgn0086365	FBgn0260486	FBgn0025632
FBgn0035763	FBgn0045800	FBgn0013688	FBgn0050104	FBgn0003053	FBgn0033494	FBgn0085376	FBgn0029712
FBgn0261560	FBgn0036121	FBgn0083000	FBgn0037856	FBgn0040532	FBgn0033304	FBgn0030234	FBgn0051781
FBgn0029148	FBgn0016123	FBgn0010388	FBgn0038981	FBgn0004456	FBgn0086664	FBgn0004647	FBgn0000046
FBgn0063391	FBgn0261975	FBgn0036770	FBgn0003890	FBgn0259209	FBgn0030653	FBgn0264617	FBgn0083990
FBgn0264504	FBgn0027594	FBgn0024320	FBgn0000635	FBgn0263200	FBgn0000448	FBgn0039486	FBgn0038353
FBgn0035541	FBgn0031756	FBgn0000044	FBgn0050269	FBgn0031907	FBgn0050015	FBgn0035089	FBgn0025712
FBgn0042174	FBgn0036091	FBgn0032149	FBgn0001168	FBgn0027106	FBgn0038638	FBgn0000723	FBgn0051370
FBgn0082929	FBgn0082953	FBgn0025879	FBgn0052687	FBgn0038088	FBgn0004893	FBgn0034925	FBgn0264618
FBgn0034443	FBgn0000636	FBgn0250788	FBgn0082978	FBgn0035767	FBgn0039756	FBgn0063491	FBgn0035949
FBgn0082948	FBgn0000299	FBgn0086603	FBgn0015872	FBgn0000394	FBgn0010424	FBgn0035049	FBgn0001227
FBgn0053199	FBgn0030955	FBgn0038243	FBgn0022160	FBgn0029693	FBgn0014903	FBgn0259697	FBgn0025111
FBgn0044508	FBgn0053051	FBgn0020762	FBgn0034638	FBgn0031909	FBgn0031322	FBgn0015575	FBgn0036169
FBgn0027108	FBgn0037279	FBgn0037906	FBgn0038460	FBgn0031412	FBgn0033204	FBgn0027578	FBgn0065064
FBgn0082945	FBgn0042112	FBgn0261800	FBgn0031813	FBgn0031245	FBgn0050115	FBgn0085773	FBgn0261642
FBgn0085742	FBgn0001234	FBgn0031998	FBgn0026602	FBgn0004169	FBgn0011746	FBgn0040071	FBgn0020299
FBgn0034399	FBgn0010038	FBgn0083015	FBgn0035710	FBgn0031011	FBgn0016797	FBgn0037166	FBgn0034438
FBgn0025683	FBgn0036373	FBgn0030357	FBgn0014380	FBgn0033134	FBgn0260964	FBgn0030237	FBgn0038420

FBgn0086039	FBgn0038465	FBgn0083120	FBgn0013680	FBgn0036756	FBgn0051313	FBgn0085412	FBgn0032472
FBgn0086082	FBgn0031250	FBgn0051360	FBgn0003149	FBgn0035917	FBgn0263873	FBgn0035282	FBgn0041096
FBgn0085759	FBgn0032264	FBgn0035868	FBgn0261451	FBgn0050026	FBgn0034126	FBgn0023023	FBgn0259736
FBgn0010228	FBgn0036460	FBgn0021874	FBgn0032006	FBgn0033214	FBgn0031745	FBgn0003312	FBgn0039129
FBgn0061198	FBgn0034758	FBgn0037265	FBgn0033504	FBgn0000210	FBgn0050460	FBgn0033274	FBgn0013685
FBgn0052448	FBgn0032298	FBgn0037883	FBgn0065055	FBgn0038341	FBgn0037835	FBgn0005771	FBgn0028988
FBgn0013272	FBgn0032036	FBgn0031717	FBgn0039155	FBgn0039529	FBgn0040658	FBgn0038652	FBgn0085475
FBgn0039218	FBgn0040364	FBgn0033153	FBgn0034639	FBgn0035158	FBgn0033799	FBgn0027586	FBgn0039525
FBgn0034232	FBgn0002354	FBgn0261548	FBgn0003997	FBgn0019643	FBgn0010651	FBgn0036616	FBgn0050409
FBgn0063449	FBgn0044047	FBgn0004797	FBgn0003067	FBgn0033483	FBgn0015541	FBgn0033880	FBgn0052702
FBgn0033485	FBgn0036752	FBgn0020439	FBgn0083048	FBgn0031220	FBgn0013988	FBgn0263470	FBgn0020521
FBgn0259993	FBgn0039109	FBgn0032805	FBgn0083047	FBgn0050441	FBgn0033132	FBgn0263316	FBgn0032774
FBgn0083027	FBgn0028894	FBgn0001297	FBgn0040367	FBgn0010385	FBgn0034920	FBgn0053494	FBgn0039297
FBgn0039714	FBgn0260942	FBgn0086666	FBgn0002526	FBgn0040491	FBgn0002772	FBgn0011296	FBgn0051676
FBgn0037007	FBgn0052091	FBgn0082925	FBgn0030876	FBgn0036196	FBgn0015399	FBgn0026160	FBgn0035636
FBgn0030519	FBgn0040949	FBgn0000568	FBgn0012037	FBgn0086910	FBgn0040732	FBgn0028491	FBgn0031080
FBgn0004629	FBgn0083123	FBgn0030731	FBgn0030676	FBgn0025631	FBgn0036945	FBgn0046696	FBgn0033205
FBgn0083124	FBgn0040827	FBgn0261555	FBgn0037092	FBgn0028707	FBgn0029771	FBgn0002930	FBgn0031908
FBgn0262686	FBgn0082582	FBgn0032218	FBgn0037012	FBgn0004117	FBgn0033661	FBgn0037046	FBgn0039897
FBgn0029975	FBgn0030350	FBgn0011695	FBgn0263930	FBgn0041184	FBgn0036381	FBgn0036992	FBgn0010423
FBgn0033571	FBgn0003206	FBgn0034225	FBgn0050345	FBgn0033786	FBgn0028956	FBgn0017482	FBgn0010387
FBgn0082949	FBgn0023549	FBgn0022709	FBgn0003486	FBgn0011274	FBgn0032075	FBgn0035427	FBgn0259977
FBgn0037819	FBgn0040575	FBgn0028970	FBgn0086708	FBgn0001145	FBgn0002773	FBgn0034512	FBgn0015039
FBgn0082931	FBgn0083004	FBgn0039114	FBgn0004028	FBgn0082980	FBgn0025680	FBgn0036759	FBgn0043806
FBgn0032167	FBgn0086558	FBgn0038966	FBgn0033787	FBgn0047000	FBgn0038881	FBgn0047095	FBgn0260653
FBgn0003888	FBgn0030816	FBgn0015513	FBgn0047133	FBgn0011674	FBgn0263459	FBgn0085474	FBgn0000490
FBgn0025456	FBgn0039266	FBgn0033905	FBgn0030629	FBgn0026872	FBgn0263472	FBgn0033820	FBgn0035090
FBgn0030309	FBgn0262004	FBgn0035904	FBgn0013683	FBgn0083049	FBgn0037845	FBgn0035490	FBgn0030796
FBgn0034611	FBgn0083003	FBgn0030759	FBgn0033438	FBgn0030976	FBgn0051777	FBgn0050089	FBgn0029580
FBgn0040609	FBgn0259832	FBgn0001123	FBgn0264478	FBgn0016076	FBgn0039927	FBgn0035656	FBgn0038761
FBgn0014011	FBgn0032715	FBgn0038312	FBgn0034194	FBgn0004859	FBgn0037565	FBgn0033654	FBgn0003162
FBgn0038610	FBgn0038321	FBgn0038079	FBgn0031645	FBgn0037560	FBgn0038550	FBgn0036454	FBgn0002565
FBgn0039233	FBgn0037439	FBgn0261565	FBgn0086408	FBgn0083050	FBgn0035755	FBgn0034275	FBgn0015033
FBgn0030596	FBgn0029838	FBgn0030403	FBgn0040398	FBgn0051807	FBgn0264494	FBgn0039208	FBgn0037275
FBgn0082927	FBgn0013953	FBgn0261258	FBgn0036101	FBgn0020908	FBgn0051826	FBgn0051217	FBgn0032452
FBgn0033814	FBgn0262945	FBgn0038842	FBgn0262353	FBgn0030941	FBgn0040765	FBgn0001250	FBgn0036106
FBgn0024183	FBgn0037577	FBgn0032497	FBgn0032713	FBgn0033649	FBgn0052582	FBgn0027608	FBgn0034219
FBgn0010611	FBgn0045064	FBgn0004133	FBgn0032899	FBgn0033128	FBgn0051352	FBgn0001230	FBgn0029588
FBgn0038983	FBgn0039776	FBgn0038294	FBgn0037213	FBgn0035975	FBgn0262970	FBgn0032612	FBgn0024293
FBgn0033459	FBgn0029118	FBgn0029648	FBgn0040091	FBgn0034723	FBgn0039685	FBgn0000119	

Appendix B: Down-regulated genes in *Ada2b* GLC ovaries

FBgn0000355	FBgn0004106	FBgn0035959	FBgn0024956	FBgn0033762	FBgn0025808	FBgn0029935	FBgn0037742
FBgn0000360	FBgn0036927	FBgn0036620	FBgn0012058	FBgn0037368	FBgn0037028	FBgn0029970	FBgn0053926
FBgn0000359	FBgn0259979	FBgn0039465	FBgn0031947	FBgn0051365	FBgn0014127	FBgn0037025	FBgn0263048
FBgn0011761	FBgn0032783	FBgn0024732	FBgn0032422	FBgn0033990	FBgn0044046	FBgn0024993	FBgn0005624
FBgn0000357	FBgn0030501	FBgn0021761	FBgn0086855	FBgn0030710	FBgn0036660	FBgn0039731	FBgn0010194
FBgn0000358	FBgn0038453	FBgn0262619	FBgn0027070	FBgn0034728	FBgn0029861	FBgn0039696	FBgn0034321
FBgn0001225	FBgn0015565	FBgn0032105	FBgn0005596	FBgn0013732	FBgn0086908	FBgn0051522	FBgn0003292
FBgn0004419	FBgn0036938	FBgn0260243	FBgn0027559	FBgn0259676	FBgn0031405	FBgn0030170	FBgn0051388
FBgn0014076	FBgn0002183	FBgn0032482	FBgn0264291	FBgn0086711	FBgn0039117	FBgn0037646	FBgn0038047
FBgn0001149	FBgn0260985	FBgn0011604	FBgn0261065	FBgn0027570	FBgn0039061	FBgn0037664	FBgn0000808
FBgn0022893	FBgn0038972	FBgn0032955	FBgn0027903	FBgn0052251	FBgn0011660	FBgn0259789	FBgn0053258
FBgn0250848	FBgn0036272	FBgn0031996	FBgn0038974	FBgn0034946	FBgn0033971	FBgn0052207	FBgn0050334
FBgn0034753	FBgn0033757	FBgn0029676	FBgn0039098	FBgn0038115	FBgn0020445	FBgn0003268	FBgn0000567
FBgn0004362	FBgn0030817	FBgn0037372	FBgn0051658	FBgn0033692	FBgn0085428	FBgn0033718	FBgn0041160
FBgn0041775	FBgn0010097	FBgn0030943	FBgn0039301	FBgn0031739	FBgn0033569	FBgn0260955	FBgn0036369
FBgn0001092	FBgn0037376	FBgn0027526	FBgn0038692	FBgn0011774	FBgn0030242	FBgn0002901	FBgn0262636
FBgn0040309	FBgn0027512	FBgn0000251	FBgn0035593	FBgn0086253	FBgn0032934	FBgn0039594	FBgn0035957
FBgn0000356	FBgn0036690	FBgn0032157	FBgn0005696	FBgn0086695	FBgn0039164	FBgn0035902	FBgn0250907
FBgn0014466	FBgn0030322	FBgn0029924	FBgn0052438	FBgn0011606	FBgn0260817	FBgn0051262	FBgn0033674
FBgn0000579	FBgn0086266	FBgn0037770	FBgn0034354	FBgn0032910	FBgn0000376	FBgn0017448	FBgn0025382
FBgn0011823	FBgn0039640	FBgn0027335	FBgn0040290	FBgn0039004	FBgn0036240	FBgn0027490	FBgn0038098
FBgn0001226	FBgn0015929	FBgn0035969	FBgn0052822	FBgn0027660	FBgn0034569	FBgn0034186	FBgn0032211
FBgn0033631	FBgn0032864	FBgn0262609	FBgn0029738	FBgn0030439	FBgn0000063	FBgn0264326	FBgn0085421
FBgn0259682	FBgn0025390	FBgn0002542	FBgn0038099	FBgn0036991	FBgn0003733	FBgn0053107	FBgn0037759
FBgn0261987	FBgn0003087	FBgn0036486	FBgn0260771	FBgn0031848	FBgn0017561	FBgn0024510	FBgn0029821
FBgn0001091	FBgn0000927	FBgn0053156	FBgn0039379	FBgn0051163	FBgn0034853	FBgn0000075	FBgn0033702
FBgn0032127	FBgn0032374	FBgn0037203	FBgn0024227	FBgn0051015	FBgn0041721	FBgn0036480	FBgn0027343
FBgn0033879	FBgn0026430	FBgn0051661	FBgn0040283	FBgn0035918	FBgn0033258	FBgn0003450	FBgn0263608
FBgn0264696	FBgn0035209	FBgn0030743	FBgn0035997	FBgn0005683	FBgn0037149	FBgn0261567	FBgn0030593
FBgn0086254	FBgn0050118	FBgn0010313	FBgn0036382	FBgn0033884	FBgn0039680	FBgn0038740	FBgn0038337
FBgn0035694	FBgn0035425	FBgn0025633	FBgn0013756	FBgn0015271	FBgn0264384	FBgn0030945	FBgn0260005
FBgn0032789	FBgn0010314	FBgn0027500	FBgn0058469	FBgn0052452	FBgn0035312	FBgn0032025	FBgn0030757
FBgn0003178	FBgn0017577	FBgn0023515	FBgn0038478	FBgn0027513	FBgn0038390	FBgn0039908	FBgn0033443
FBgn0041709	FBgn0015625	FBgn0022702	FBgn0038381	FBgn0015396	FBgn0037338	FBgn0263667	FBgn0037519
FBgn0028688	FBgn0037810	FBgn0031252	FBgn0000307	FBgn0259791	FBgn0030646	FBgn0263047	FBgn0264310
FBgn0086355	FBgn0052644	FBgn0000996	FBgn0033656	FBgn0061476	FBgn0040928	FBgn0028647	FBgn0035968
FBgn0002780	FBgn0041186	FBgn0039099	FBgn0034490	FBgn0027504	FBgn0032382	FBgn0031070	FBgn0039663
FBgn0014464	FBgn0004107	FBgn0038575	FBgn0039338	FBgn0023395	FBgn0026148	FBgn0086027	FBgn0033627
FBgn0010431	FBgn0003022	FBgn0030373	FBgn0039125	FBgn0004795	FBgn0011020	FBgn0263831	FBgn0038279
FBgn0010288	FBgn0013576	FBgn0002645	FBgn0032929	FBgn0050463	FBgn0040382	FBgn0045035	FBgn0030576
FBgn0037607	FBgn0036428	FBgn0026257	FBgn0033845	FBgn0024251	FBgn0033698	FBgn0036777	FBgn0003996

FBgn0087040	FBgn0010247	FBgn0003044	FBgn0023180	FBgn0031464	FBgn0036715	FBgn0263256	FBgn0030331
FBgn0041252	FBgn0029161	FBgn0038608	FBgn0264704	FBgn0028476	FBgn0033935	FBgn0050001	FBgn0033836
FBgn0038252	FBgn0020370	FBgn0086356	FBgn0015270	FBgn0034098	FBgn0034903	FBgn0031734	FBgn0032116
FBgn0014869	FBgn0035397	FBgn0003114	FBgn0016792	FBgn0262895	FBgn0031554	FBgn0038889	FBgn0033079
FBgn0035328	FBgn0029696	FBgn0023169	FBgn0027783	FBgn0011802	FBgn0015568	FBgn0029966	FBgn0003174
FBgn0029568	FBgn0014417	FBgn0002673	FBgn0034067	FBgn0035761	FBgn0033740	FBgn0046225	FBgn0038296
FBgn0004649	FBgn0052412	FBgn0010877	FBgn0260484	FBgn0010113	FBgn0028997	FBgn0026432	FBgn0039591
FBgn0264493	FBgn0034021	FBgn0263236	FBgn0036689	FBgn0030500	FBgn0003701	FBgn0033993	FBgn0032730
FBgn0051641	FBgn0035955	FBgn0032705	FBgn0260632	FBgn0031549	FBgn0040347	FBgn0001090	FBgn0085245
FBgn0000182	FBgn0003525	FBgn0039250	FBgn0000140	FBgn0261385	FBgn0023513	FBgn0037540	FBgn0260475
FBgn0000404	FBgn0017551	FBgn0028700	FBgn0022772	FBgn0033890	FBgn0034433	FBgn0037520	FBgn0038247
FBgn0051928	FBgn0261524	FBgn0004584	FBgn0039066	FBgn0002948	FBgn0037624	FBgn0039449	FBgn0052823
FBgn0034403	FBgn0020633	FBgn0015544	FBgn0015391	FBgn0031434	FBgn0002906	FBgn0034797	FBgn0039170
FBgn0014465	FBgn0030863	FBgn0051926	FBgn0031664	FBgn0259113	FBgn0032295	FBgn0030065	FBgn0030912
FBgn0038469	FBgn0029879	FBgn0031483	FBgn0030320	FBgn0015371	FBgn0004378	FBgn0024944	FBgn0054046
FBgn0052642	FBgn0028408	FBgn0024984	FBgn0051109	FBgn0027509	FBgn0034618	FBgn0052645	FBgn0264273
FBgn0011703	FBgn0020415	FBgn0039065	FBgn0035558	FBgn0003187	FBgn0063492	FBgn0034249	FBgn0039530
FBgn0030438	FBgn0039563	FBgn0039293	FBgn0052676	FBgn0035035	FBgn0036116	FBgn0050295	FBgn0033744
FBgn0032788	FBgn0029733	FBgn0031452	FBgn0030758	FBgn0037746	FBgn0038549	FBgn0036875	FBgn0034322
FBgn0035726	FBgn0011481	FBgn0030241	FBgn0003598	FBgn0037109	FBgn0037920	FBgn0033354	FBgn0050194
FBgn0031677	FBgn0027889	FBgn0260986	FBgn0034447	FBgn0261004	FBgn0002899	FBgn0035891	FBgn0029710
FBgn0002921	FBgn0010342	FBgn0030938	FBgn0036574	FBgn0028916	FBgn0031741	FBgn0263414	FBgn0083977
FBgn0031111	FBgn0032126	FBgn0032698	FBgn0002924	FBgn0037515	FBgn0011739	FBgn0038827	FBgn0264331
FBgn0039972	FBgn0003076	FBgn0016122	FBgn0026431	FBgn0026433	FBgn0041629	FBgn0003751	FBgn0035948
FBgn0023167	FBgn0051852	FBgn0002567	FBgn0023181	FBgn0004876	FBgn0015600	FBgn0003934	FBgn0035040
FBgn0263979	FBgn0051453	FBgn0036008	FBgn0030787	FBgn0031655	FBgn0040232	FBgn0026315	FBgn0033763
FBgn0004507	FBgn0011725	FBgn0040206	FBgn0003071	FBgn0050440	FBgn0035475	FBgn0036688	FBgn0030666
FBgn0016053	FBgn0002525	FBgn0264561	FBgn0040477	FBgn0030805	FBgn0040514	FBgn0262167	FBgn0027600
FBgn0063494	FBgn0030268	FBgn0039073	FBgn0000147	FBgn0027375	FBgn0035073	FBgn0036857	FBgn0037972
FBgn0001248	FBgn0004698	FBgn0037215	FBgn0086350	FBgn0036994	FBgn0030420	FBgn0031865	FBgn0250862
FBgn0000615	FBgn0260991	FBgn0030973	FBgn0003545	FBgn0261625	FBgn0019990	FBgn0029831	FBgn0262352
FBgn0038395	FBgn0032997	FBgn0000351	FBgn0014032	FBgn0003159	FBgn0026876	FBgn0001206	FBgn0052029
FBgn0003124	FBgn0035978	FBgn0035253	FBgn0034406	FBgn0029822	FBgn0002715	FBgn0036368	FBgn0050046
FBgn0002719	FBgn0004913	FBgn0033526	FBgn0043900	FBgn0086697	FBgn0030421	FBgn0034217	FBgn0082585
FBgn0036661	FBgn0004598	FBgn0032078	FBgn0034314	FBgn0263038	FBgn0037212	FBgn0038412	FBgn0040726
FBgn0035768	FBgn0051075	FBgn0038011	FBgn0264382	FBgn0032521	FBgn0260006	FBgn0030925	FBgn0031127
FBgn0010173	FBgn0027603	FBgn0037106	FBgn0037364	FBgn0032523	FBgn0002707	FBgn0043854	FBgn0263836
FBgn0031769	FBgn0031529	FBgn0038772	FBgn0086358	FBgn0034999	FBgn0031597	FBgn0030583	FBgn0029753
FBgn0000644	FBgn0025815	FBgn0027521	FBgn0031682	FBgn0030510	FBgn0035435	FBgn0051053	FBgn0004959
FBgn0032906	FBgn0037807	FBgn0027580	FBgn0035210	FBgn0050377	FBgn0034704	FBgn0250755	FBgn0036939
FBgn0032014	FBgn0014861	FBgn0004643	FBgn0036735	FBgn0004379	FBgn0034425	FBgn0261285	FBgn0026439
FBgn0022213	FBgn0030054	FBgn0031886	FBgn0001612	FBgn0022786	FBgn0259112	FBgn0263093	FBgn0010401
FBgn0038293	FBgn0037555	FBgn0032213	FBgn0051108	FBgn0037144	FBgn0015376	FBgn0032752	FBgn0029603

FBgn0013763	FBgn0037405	FBgn0036053	FBgn0001276	FBgn0259990	FBgn0032303	FBgn0038207
FBgn0033979	FBgn0027949	FBgn0036141	FBgn0002872	FBgn0015926	FBgn0035539	FBgn0038815
FBgn0029512	FBgn0035641	FBgn0027565	FBgn0259734	FBgn0263855	FBgn0034908	FBgn0028527
FBgn0262743	FBgn0039754	FBgn0263352	FBgn0030507	FBgn0032907	FBgn0025807	FBgn0034452
FBgn0029094	FBgn0250850	FBgn0036893	FBgn0015553	FBgn0029896	FBgn0038118	FBgn0052602
FBgn0050497	FBgn0024332	FBgn0031893	FBgn0262647	FBgn0010497	FBgn0264574	FBgn0035189
FBgn0260780	FBgn0030208	FBgn0027515	FBgn0263600	FBgn0035033	FBgn0039355	FBgn0032869
FBgn0026144	FBgn0027948	FBgn0039559	FBgn0034187	FBgn0259876	FBgn0026598	FBgn0036765
FBgn0003023	FBgn0001086	FBgn0035697	FBgn0038551	FBgn0022359	FBgn0058006	FBgn0031961
FBgn0016070	FBgn0036761	FBgn0025781	FBgn0085290	FBgn0030228	FBgn0025185	
FBgn0022338	FBgn0030093	FBgn0031878	FBgn0039210	FBgn0035627	FBgn0034063	
FBgn0038611	FBgn0032189	FBgn0000826	FBgn0039638	FBgn0013995	FBgn0034808	
FBgn0027936	FBgn0031969	FBgn0031875	FBgn0038167	FBgn0036354	FBgn0037781	
FBgn0052774	FBgn0026143	FBgn0030871	FBgn0039632	FBgn0033233	FBgn0036397	
FBgn0035640	FBgn0037377	FBgn0031267	FBgn0024991	FBgn0023540	FBgn0031575	
FBgn0029697	FBgn0010382	FBgn0003495	FBgn0032161	FBgn0034997	FBgn0031191	
FBgn0050359	FBgn0035766	FBgn0263697	FBgn0031435	FBgn0259985	FBgn0050467	
FBgn0036619	FBgn0031001	FBgn0034053	FBgn0034943	FBgn0030389	FBgn0051674	
FBgn0029137	FBgn0032522	FBgn0030116	FBgn0259210	FBgn0039167	FBgn0037931	
FBgn0051475	FBgn0039704	FBgn0036323	FBgn0034647	FBgn0033049	FBgn0034733	
FBgn0262145	FBgn0033031	FBgn0030244	FBgn0259164	FBgn0037290	FBgn0034454	
FBgn0031906	FBgn0030437	FBgn0261363	FBgn0032180	FBgn0032343	FBgn0031816	

Appendix C: Up-regulated genes in *Ataxin-7* GLC ovaries

FBgn0000055	FBgn0035049	FBgn0062928
FBgn0000241	FBgn0035484	FBgn0065046
FBgn0001224	FBgn0035880	FBgn0065055
FBgn0001227	FBgn0036101	FBgn0082953
FBgn0002773	FBgn0036294	FBgn0082959
FBgn0003933	FBgn0036382	FBgn0082967
FBgn0004183	FBgn0036616	FBgn0082988
FBgn0004187	FBgn0036857	FBgn0083987
FBgn0004959	FBgn0037518	FBgn0085195
FBgn0010038	FBgn0037577	FBgn0086669
FBgn0010263	FBgn0037841	FBgn0250755
FBgn0010388	FBgn0037930	FBgn0259927
FBgn0013688	FBgn0038243	FBgn0260388
FBgn0015558	FBgn0038744	FBgn0261839
FBgn0015568	FBgn0038914	FBgn0262945
FBgn0015569	FBgn0039208	FBgn0263093
FBgn0017448	FBgn0039226	FBgn0263414
FBgn0019952	FBgn0039350	FBgn0263468
FBgn0020385	FBgn0039678	FBgn0263477
FBgn0023023	FBgn0039748	FBgn0263492
FBgn0023507	FBgn0039856	FBgn0264310
FBgn0025693	FBgn0040321	FBgn0264385
FBgn0028523	FBgn0040348	FBgn0264504
FBgn0029507	FBgn0040370	FBgn0264617
FBgn0029738	FBgn0040609	FBgn0264676
FBgn0029990	FBgn0040717	FBgn0264702
FBgn0030187	FBgn0040718	
FBgn0030598	FBgn0040813	
FBgn0030925	FBgn0040832	
FBgn0031190	FBgn0041721	
FBgn0031313	FBgn0044047	
FBgn0031923	FBgn0045761	
FBgn0032129	FBgn0050101	
FBgn0032666	FBgn0050334	
FBgn0033134	FBgn0051279	
FBgn0033188	FBgn0051313	
FBgn0033257	FBgn0051807	
FBgn0033815	FBgn0052207	
FBgn0033875	FBgn0052625	
FBgn0034075	FBgn0058002	

Appendix D: Down-regulated genes in *Ataxin-7* GLC ovaries

FBgn0001230	FBgn0033093	FBgn0051217
FBgn0001321	FBgn0033304	FBgn0051612
FBgn0002121	FBgn0033785	FBgn0051619
FBgn0003996	FBgn0033960	FBgn0051898
FBgn0010225	FBgn0034053	FBgn0052205
FBgn0013771	FBgn0034406	FBgn0052364
FBgn0013813	FBgn0034761	FBgn0052595
FBgn0015040	FBgn0034839	FBgn0054010
FBgn0015714	FBgn0035311	FBgn0058378
FBgn0016054	FBgn0035431	FBgn0083990
FBgn0020493	FBgn0035727	FBgn0085352
FBgn0023531	FBgn0035770	FBgn0085736
FBgn0024366	FBgn0035904	FBgn0085789
FBgn0026570	FBgn0035949	FBgn0086676
FBgn0027070	FBgn0036091	FBgn0086898
FBgn0027654	FBgn0036323	FBgn0259164
FBgn0029161	FBgn0036330	FBgn0260874
FBgn0029588	FBgn0036670	FBgn0261404
FBgn0029712	FBgn0037163	FBgn0261567
FBgn0029766	FBgn0037290	FBgn0262003
FBgn0029924	FBgn0037581	FBgn0262101
FBgn0030319	FBgn0037742	FBgn0262104
FBgn0030593	FBgn0037844	FBgn0262352
FBgn0030653	FBgn0037934	FBgn0262822
FBgn0030852	FBgn0037936	FBgn0262854
FBgn0030999	FBgn0037975	FBgn0263219
FBgn0031001	FBgn0038012	FBgn0263220
FBgn0031224	FBgn0038550	FBgn0264508
FBgn0031296	FBgn0038681	FBgn0264675
FBgn0031343	FBgn0039006	FBgn0264727
FBgn0031365	FBgn0039098	
FBgn0031489	FBgn0039170	
FBgn0031530	FBgn0039313	
FBgn0031741	FBgn0039585	
FBgn0031801	FBgn0039941	
FBgn0032082	FBgn0040091	
FBgn0032125	FBgn0047000	
FBgn0032180	FBgn0050401	
FBgn0032211	FBgn0050424	
FBgn0032235	FBgn0051054	

Appendix E: Up-regulated genes in *Non-stop* GLC ovaries

FBgn0000166	FBgn0030598	FBgn0035109	FBgn0039944	FBgn0085298	FBgn0025740
FBgn0000241	FBgn0030676	FBgn0035113	FBgn0039958	FBgn0086027	FBgn0026238
FBgn0000355	FBgn0030839	FBgn0035424	FBgn0040005	FBgn0086558	FBgn0026401
FBgn0000357	FBgn0030925	FBgn0035484	FBgn0040321	FBgn0086655	FBgn0026616
FBgn0001180	FBgn0030931	FBgn0035617	FBgn0040323	FBgn0259112	FBgn0027101
FBgn0001224	FBgn0031170	FBgn0035642	FBgn0040348	FBgn0259247	FBgn0027865
FBgn0001227	FBgn0031182	FBgn0035678	FBgn0040600	FBgn0260799	FBgn0028397
FBgn0001230	FBgn0031313	FBgn0035702	FBgn0040823	FBgn0260932	FBgn0028622
FBgn0002354	FBgn0031343	FBgn0035833	FBgn0040832	FBgn0261363	FBgn0028743
FBgn0002466	FBgn0031516	FBgn0035842	FBgn0040994	FBgn0261383	FBgn0029504
FBgn0002521	FBgn0031675	FBgn0036152	FBgn0041100	FBgn0261404	FBgn0029813
FBgn0002932	FBgn0031703	FBgn0036196	FBgn0041180	FBgn0261617	FBgn0029840
FBgn0003459	FBgn0031894	FBgn0036294	FBgn0041252	FBgn0261688	FBgn0029866
FBgn0003482	FBgn0031961	FBgn0036324	FBgn0041604	FBgn0261954	FBgn0029996
FBgn0003934	FBgn0031974	FBgn0036374	FBgn0046696	FBgn0261984	FBgn0030048
FBgn0003935	FBgn0032079	FBgn0036501	FBgn0050054	FBgn0262117	FBgn0030294
FBgn0003997	FBgn0032249	FBgn0036620	FBgn0050441	FBgn0262123	FBgn0030347
FBgn0004183	FBgn0032303	FBgn0036670	FBgn0051279	FBgn0262124	FBgn0030361
FBgn0004191	FBgn0032452	FBgn0036906	FBgn0051807	FBgn0262866	FBgn0030421
FBgn0004395	FBgn0032730	FBgn0036942	FBgn0051875	FBgn0262945	
FBgn0004837	FBgn0032789	FBgn0037000	FBgn0051926	FBgn0263001	
FBgn0004875	FBgn0032820	FBgn0037076	FBgn0051998	FBgn0263027	
FBgn0005386	FBgn0032979	FBgn0037518	FBgn0052099	FBgn0263110	
FBgn0010263	FBgn0033079	FBgn0037521	FBgn0052133	FBgn0263414	
FBgn0010316	FBgn0033234	FBgn0037623	FBgn0052163	FBgn0263607	
FBgn0011259	FBgn0033252	FBgn0037742	FBgn0052196	FBgn0263660	
FBgn0013984	FBgn0033304	FBgn0037838	FBgn0052350	FBgn0263836	
FBgn0014342	FBgn0033479	FBgn0037918	FBgn0052373	FBgn0264307	
FBgn0015025	FBgn0033627	FBgn0037972	FBgn0052594	FBgn0264310	
FBgn0015569	FBgn0033799	FBgn0038330	FBgn0052625	FBgn0264385	
FBgn0016974	FBgn0033836	FBgn0038490	FBgn0052642	FBgn0264439	
FBgn0020385	FBgn0033984	FBgn0038589	FBgn0052644	FBgn0264449	
FBgn0022359	FBgn0034075	FBgn0038740	FBgn0052767	FBgn0264481	
FBgn0022710	FBgn0034093	FBgn0039129	FBgn0052822	FBgn0264500	
FBgn0024251	FBgn0034113	FBgn0039226	FBgn0053062	FBgn0264504	
FBgn0024291	FBgn0034255	FBgn0039462	FBgn0053108	FBgn0264617	
FBgn0024732	FBgn0034789	FBgn0039464	FBgn0053180	FBgn0264676	
FBgn0025382	FBgn0034976	FBgn0039525	FBgn0065046	FBgn0264678	
FBgn0025632	FBgn0035084	FBgn0039590	FBgn0083956	FBgn0264702	
FBgn0025693	FBgn0035106	FBgn0039920	FBgn0085271	FBgn0264704	

Appendix F: Down-regulated genes in *Non-stop* GLC ovaries

FBgn0000299	FBgn0020910	FBgn0031489	FBgn0035824	FBgn0039419	FBgn0250876
FBgn0000566	FBgn0022355	FBgn0031664	FBgn0035844	FBgn0039430	FBgn0259164
FBgn0001168	FBgn0022774	FBgn0031745	FBgn0035933	FBgn0039452	FBgn0259173
FBgn0002609	FBgn0023507	FBgn0031756	FBgn0035949	FBgn0039638	FBgn0260004
FBgn0002645	FBgn0023549	FBgn0031805	FBgn0036168	FBgn0039678	FBgn0260386
FBgn0002733	FBgn0024989	FBgn0031837	FBgn0036169	FBgn0039682	FBgn0260660
FBgn0002869	FBgn0025393	FBgn0031907	FBgn0036271	FBgn0039748	FBgn0260767
FBgn0003068	FBgn0026061	FBgn0031944	FBgn0036381	FBgn0039914	FBgn0260768
FBgn0003312	FBgn0026430	FBgn0031955	FBgn0036545	FBgn0040030	FBgn0260955
FBgn0003486	FBgn0026878	FBgn0032021	FBgn0036550	FBgn0040089	FBgn0261567
FBgn0003867	FBgn0027080	FBgn0032075	FBgn0036646	FBgn0040357	FBgn0261596
FBgn0003890	FBgn0027364	FBgn0032318	FBgn0036652	FBgn0040606	FBgn0261673
FBgn0003961	FBgn0027585	FBgn0032889	FBgn0036690	FBgn0041096	FBgn0261963
FBgn0003996	FBgn0027600	FBgn0032891	FBgn0036732	FBgn0043806	FBgn0261975
FBgn0004507	FBgn0027611	FBgn0032913	FBgn0036875	FBgn0043841	FBgn0261990
FBgn0004893	FBgn0027843	FBgn0033047	FBgn0037213	FBgn0044046	FBgn0262112
FBgn0005390	FBgn0028420	FBgn0033093	FBgn0037409	FBgn0050021	FBgn0262686
FBgn0005592	FBgn0028886	FBgn0033483	FBgn0037607	FBgn0050026	FBgn0262886
FBgn0005771	FBgn0028993	FBgn0033528	FBgn0037644	FBgn0050104	FBgn0262887
FBgn0010038	FBgn0029161	FBgn0033654	FBgn0037721	FBgn0050410	FBgn0263046
FBgn0010387	FBgn0029603	FBgn0033817	FBgn0037723	FBgn0050428	FBgn0263200
FBgn0010431	FBgn0029838	FBgn0033926	FBgn0038147	FBgn0050440	FBgn0263219
FBgn0010452	FBgn0029879	FBgn0033958	FBgn0038277	FBgn0050456	FBgn0263440
FBgn0011206	FBgn0030077	FBgn0034126	FBgn0038337	FBgn0050460	
FBgn0011770	FBgn0030357	FBgn0034262	FBgn0038412	FBgn0050489	
FBgn0013688	FBgn0030482	FBgn0034406	FBgn0038658	FBgn0051217	
FBgn0013717	FBgn0030562	FBgn0034997	FBgn0038681	FBgn0051370	
FBgn0014396	FBgn0030583	FBgn0034999	FBgn0038717	FBgn0051704	
FBgn0014455	FBgn0030593	FBgn0035035	FBgn0038718	FBgn0052687	
FBgn0015288	FBgn0030662	FBgn0035094	FBgn0038804	FBgn0052702	
FBgn0015399	FBgn0030666	FBgn0035164	FBgn0038983	FBgn0060296	
FBgn0015568	FBgn0030899	FBgn0035186	FBgn0039006	FBgn0063485	
FBgn0015575	FBgn0030914	FBgn0035189	FBgn0039040	FBgn0085195	
FBgn0016075	FBgn0030999	FBgn0035308	FBgn0039061	FBgn0085313	
FBgn0016076	FBgn0031224	FBgn0035422	FBgn0039232	FBgn0085359	
FBgn0016123	FBgn0031227	FBgn0035638	FBgn0039301	FBgn0085400	
FBgn0016684	FBgn0031299	FBgn0035656	FBgn0039311	FBgn0085736	
FBgn0019936	FBgn0031305	FBgn0035695	FBgn0039312	FBgn0086365	
FBgn0020415	FBgn0031397	FBgn0035726	FBgn0039313	FBgn0086661	
FBgn0020618	FBgn0031412	FBgn0035770	FBgn0039319	FBgn0086710	

Appendix G: Up-regulated genes in *wda* GLC ovaries

FBgn0036262	FBgn0020299	FBgn0028499	FBgn0035917	FBgn0032713	FBgn0004370	FBgn0260768	FBgn0030519
FBgn0039525	FBgn0264618	FBgn0033304	FBgn0016076	FBgn0263240	FBgn0031717	FBgn0045064	FBgn0035334
FBgn0001228	FBgn0035023	FBgn0029771	FBgn0051807	FBgn0032006	FBgn0262108	FBgn0053051	FBgn0010228
FBgn0039129	FBgn0035755	FBgn0035638	FBgn0260746	FBgn0053126	FBgn0030357	FBgn0033188	FBgn0005634
FBgn0003162	FBgn0002930	FBgn0031993	FBgn0263974	FBgn0261555	FBgn0083048	FBgn0036373	FBgn0025682
FBgn0016032	FBgn0029813	FBgn0035727	FBgn0052280	FBgn0004028	FBgn0052174	FBgn0004914	FBgn0013272
FBgn0040805	FBgn0039467	FBgn0024321	FBgn0033214	FBgn0032497	FBgn0028970	FBgn0037443	FBgn0086051
FBgn0025712	FBgn0036454	FBgn0085813	FBgn0014388	FBgn0032943	FBgn0010434	FBgn0034501	FBgn0034232
FBgn0086367	FBgn0033817	FBgn0030828	FBgn0261545	FBgn0032899	FBgn0015513	FBgn0040786	FBgn0033340
FBgn0035264	FBgn0034588	FBgn0040732	FBgn0040491	FBgn0035849	FBgn0034312	FBgn0030350	FBgn0030292
FBgn0034439	FBgn0031530	FBgn0037057	FBgn0020385	FBgn0035085	FBgn0033421	FBgn0010222	FBgn0033485
FBgn0035090	FBgn0052702	FBgn0085376	FBgn0011274	FBgn0085452	FBgn0015872	FBgn0001624	FBgn0083983
FBgn0000490	FBgn0000046	FBgn0047095	FBgn0038079	FBgn0030485	FBgn0034420	FBgn0030955	FBgn0052448
FBgn0034219	FBgn0035186	FBgn0039006	FBgn0036196	FBgn0264718	FBgn0022709	FBgn0031764	FBgn0262686
FBgn0036106	FBgn0035844	FBgn0040383	FBgn0032431	FBgn0004364	FBgn0002528	FBgn0034500	FBgn0063449
FBgn0034756	FBgn0032253	FBgn0264494	FBgn0262353	FBgn0013688	FBgn0034225	FBgn0037439	FBgn0052069
FBgn0004360	FBgn0029712	FBgn0041184	FBgn0030852	FBgn0050345	FBgn0036663	FBgn0003328	FBgn0014163
FBgn0043806	FBgn0040958	FBgn0050428	FBgn0034436	FBgn0035791	FBgn0035868	FBgn0032202	FBgn0035772
FBgn0032075	FBgn0036821	FBgn0260660	FBgn0031245	FBgn0030066	FBgn0030040	FBgn0083049	FBgn0025683
FBgn0000928	FBgn0040658	FBgn0083121	FBgn0029766	FBgn0032793	FBgn0030759	FBgn0037011	FBgn0027590
FBgn0015011	FBgn0030347	FBgn0263873	FBgn0031220	FBgn0262820	FBgn0052138	FBgn0029118	FBgn0039218
FBgn0037547	FBgn0035949	FBgn0052756	FBgn0035189	FBgn0262112	FBgn0041180	FBgn0010019	FBgn0260745
FBgn0052476	FBgn0017482	FBgn0035338	FBgn0264507	FBgn0037633	FBgn0262886	FBgn0003206	FBgn0034248
FBgn0032129	FBgn0035490	FBgn0033274	FBgn0033134	FBgn0037602	FBgn0040238	FBgn0033951	FBgn0034399
FBgn0028675	FBgn0004449	FBgn0033799	FBgn0039748	FBgn0263782	FBgn0030403	FBgn0035321	FBgn0001941
FBgn0038674	FBgn0030976	FBgn0037513	FBgn0039529	FBgn0263459	FBgn0032499	FBgn0040609	FBgn0082945
FBgn0037447	FBgn0030011	FBgn0004569	FBgn0053108	FBgn0031489	FBgn0040813	FBgn0037279	FBgn0016926
FBgn0033033	FBgn0013988	FBgn0031745	FBgn0034142	FBgn0037391	FBgn0030218	FBgn0261113	FBgn0262742
FBgn0031646	FBgn0026160	FBgn0016797	FBgn0046696	FBgn0038981	FBgn0020414	FBgn0035696	FBgn0032897
FBgn0259736	FBgn0051313	FBgn0034920	FBgn0032022	FBgn0030960	FBgn0038811	FBgn0035298	FBgn0000083
FBgn0030160	FBgn0085474	FBgn0003312	FBgn0052850	FBgn0261552	FBgn0039430	FBgn0029002	FBgn0027108
FBgn0000406	FBgn0035084	FBgn0063649	FBgn0039118	FBgn0037525	FBgn0032264	FBgn0040364	FBgn0025839
FBgn0010389	FBgn0035049	FBgn0015541	FBgn0028622	FBgn0261873	FBgn0029838	FBgn0002354	FBgn0034443
FBgn0051781	FBgn0039756	FBgn0033786	FBgn0037548	FBgn0051915	FBgn0051360	FBgn0036091	FBgn0035763
FBgn0015033	FBgn0086901	FBgn0038037	FBgn0039232	FBgn0053111	FBgn0030808	FBgn0036126	FBgn0053199
FBgn0010395	FBgn0038347	FBgn0034606	FBgn0025693	FBgn0082986	FBgn0032430	FBgn0001234	FBgn0035541
FBgn0261563	FBgn0038652	FBgn0038088	FBgn0036589	FBgn0039419	FBgn0031401	FBgn0030309	FBgn0085742
FBgn0031146	FBgn0051217	FBgn0086708	FBgn0051536	FBgn0031975	FBgn0020762	FBgn0040575	FBgn0023477
FBgn0036169	FBgn0011296	FBgn0262104	FBgn0085432	FBgn0013683	FBgn0260748	FBgn0051800	FBgn0082942
FBgn0037166	FBgn0036381	FBgn0004893	FBgn0035767	FBgn0042111	FBgn0033584	FBgn0036121	FBgn0000116
FBgn0020521	FBgn0027586	FBgn0035089	FBgn0030876	FBgn0014396	FBgn0037016	FBgn0001224	FBgn0085759

FBgn0015039	FBgn0039809	FBgn0040297	FBgn0033987	FBgn0003997	FBgn0082987	FBgn0031250	FBgn0083027
FBgn0263973	FBgn0034199	FBgn0028420	FBgn0046258	FBgn0085475	FBgn0085819	FBgn0039776	FBgn0082944
FBgn0037853	FBgn0031322	FBgn0038638	FBgn0039678	FBgn0000635	FBgn0031777	FBgn0047114	FBgn0030521
FBgn0050418	FBgn0031501	FBgn0034085	FBgn0040718	FBgn0030899	FBgn0032805	FBgn0027594	FBgn0003275
FBgn0035282	FBgn0035308	FBgn0020493	FBgn0050269	FBgn0031813	FBgn0025879	FBgn0016075	FBgn0031913
FBgn0039226	FBgn0000119	FBgn0032779	FBgn0040398	FBgn0051997	FBgn0013771	FBgn0028490	FBgn0015924
FBgn0062978	FBgn0031299	FBgn0023023	FBgn0023095	FBgn0050456	FBgn0038877	FBgn0042094	FBgn0261560
FBgn0030029	FBgn0001227	FBgn0026319	FBgn0013733	FBgn0034638	FBgn0086665	FBgn0083123	FBgn0259238
FBgn0029723	FBgn0263397	FBgn0034909	FBgn0000163	FBgn0031413	FBgn0051373	FBgn0014141	FBgn0033635
FBgn0035636	FBgn0029507	FBgn0011746	FBgn0000210	FBgn0259209	FBgn0037883	FBgn0032311	FBgn0053155
FBgn0035691	FBgn0024179	FBgn0025680	FBgn0264478	FBgn0050104	FBgn0032149	FBgn0036460	FBgn0082949
FBgn0038420	FBgn0083990	FBgn0028956	FBgn0000320	FBgn0259170	FBgn0034758	FBgn0036318	FBgn0031285
FBgn0011706	FBgn0040071	FBgn0001145	FBgn0038341	FBgn0033945	FBgn0261800	FBgn0043841	FBgn0003514
FBgn0038516	FBgn0036616	FBgn0263115	FBgn0051119	FBgn0262160	FBgn0000229	FBgn0043364	FBgn0003660
FBgn0003463	FBgn0031571	FBgn0034198	FBgn0033926	FBgn0022160	FBgn0037478	FBgn0058469	FBgn0031505
FBgn0053062	FBgn0010385	FBgn0003149	FBgn0033483	FBgn0085408	FBgn0031998	FBgn0030362	FBgn0031381
FBgn0032452	FBgn0036945	FBgn0019643	FBgn0004117	FBgn0037856	FBgn0260722	FBgn0011764	FBgn0004921
FBgn0051676	FBgn0033880	FBgn0040600	FBgn0035101	FBgn0004167	FBgn0052486	FBgn0020304	FBgn0029148
FBgn0028550	FBgn0031908	FBgn0036501	FBgn0027106	FBgn0032218	FBgn0010246	FBgn0032167	FBgn0029506
FBgn0262979	FBgn0042175	FBgn0038550	FBgn0262947	FBgn0085354	FBgn0030057	FBgn0032595	FBgn0063391
FBgn0030317	FBgn0259163	FBgn0062928	FBgn0050441	FBgn0010225	FBgn0024958	FBgn0085279	FBgn0004404
FBgn0031630	FBgn0037560	FBgn0050273	FBgn0028707	FBgn0002526	FBgn0036279	FBgn0032298	FBgn0015795
FBgn0000395	FBgn0030653	FBgn0004647	FBgn0035888	FBgn0039155	FBgn0021874	FBgn0082928	FBgn0259993
FBgn0050016	FBgn0030958	FBgn0034706	FBgn0037708	FBgn0053555	FBgn0024320	FBgn0034611	FBgn0262116
FBgn0010423	FBgn0038881	FBgn0034723	FBgn0004456	FBgn0004133	FBgn0038720	FBgn0033555	FBgn0004687
FBgn0034126	FBgn0030234	FBgn0026872	FBgn0041092	FBgn0052687	FBgn0027287	FBgn0033717	FBgn0262954
FBgn0029588	FBgn0024980	FBgn0036926	FBgn0001168	FBgn0003067	FBgn0026199	FBgn0260388	FBgn0035499
FBgn0028988	FBgn0030993	FBgn0260932	FBgn0013680	FBgn0085236	FBgn0029959	FBgn0262945	FBgn0002868
FBgn0050089	FBgn0051352	FBgn0040832	FBgn0029693	FBgn0028572	FBgn0086602	FBgn0000299	FBgn0031453
FBgn0036168	FBgn0264695	FBgn0039328	FBgn0037163	FBgn0032001	FBgn0250789	FBgn0030079	FBgn0005278
FBgn0004652	FBgn0039431	FBgn0083940	FBgn0085736	FBgn0003963	FBgn0250788	FBgn0042112	FBgn0034398
FBgn0036759	FBgn0085799	FBgn0004583	FBgn0036756	FBgn0034523	FBgn0002968	FBgn0034709	FBgn0014184
FBgn0040765	FBgn0035431	FBgn0027578	FBgn0034075	FBgn0024277	FBgn0030048	FBgn0003401	FBgn0082929
FBgn0035427	FBgn0039486	FBgn0082997	FBgn0038788	FBgn0261258	FBgn0003345	FBgn0083004	FBgn0033548
FBgn0034789	FBgn0262970	FBgn0037956	FBgn0030745	FBgn0000568	FBgn0032694	FBgn0028373	FBgn0086068
FBgn0264677	FBgn0028491	FBgn0046776	FBgn0031011	FBgn0001297	FBgn0030052	FBgn0024183	FBgn0013684
FBgn0040349	FBgn0263316	FBgn0030662	FBgn0039641	FBgn0024234	FBgn0259832	FBgn0004657	FBgn0000409
FBgn0025632	FBgn0036288	FBgn0050460	FBgn0261859	FBgn0011591	FBgn0083919	FBgn0026088	FBgn0000043
FBgn0032774	FBgn0031918	FBgn0063497	FBgn0060296	FBgn0040827	FBgn0039360	FBgn0031037	FBgn0004907
FBgn0035113	FBgn0260767	FBgn0035158	FBgn0034194	FBgn0037552	FBgn0013953	FBgn0037007	FBgn0262952
FBgn0259977	FBgn0035975	FBgn0027596	FBgn0085774	FBgn0011695	FBgn0261284	FBgn0038183	FBgn0015222
FBgn0004858	FBgn0050115	FBgn0033661	FBgn0000244	FBgn0033446	FBgn0036752	FBgn0263510	FBgn0015221
FBgn0041096	FBgn0036732	FBgn0051955	FBgn0052196	FBgn0037251	FBgn0082999	FBgn0035020	FBgn0065053

FBgn0065032	FBgn0034925	FBgn0051116	FBgn0026878	FBgn0016762	FBgn0031675	FBgn0004646	FBgn0013981
FBgn0250871	FBgn0034262	FBgn0038774	FBgn0000394	FBgn0001123	FBgn0050197	FBgn0001332	FBgn0013681
FBgn0031574	FBgn0027585	FBgn0262563	FBgn0038460	FBgn0034958	FBgn0086672	FBgn0085271	FBgn0086039
FBgn0034438	FBgn0004959	FBgn0031170	FBgn0004055	FBgn0038294	FBgn0027364	FBgn0025456	FBgn0002590
FBgn0003366	FBgn0260964	FBgn0033649	FBgn0250876	FBgn0038536	FBgn0262871	FBgn0263916	FBgn0065071
FBgn0035656	FBgn0087002	FBgn0002733	FBgn0011592	FBgn0030676	FBgn0039266	FBgn0014011	FBgn0052230
FBgn0050409	FBgn0037835	FBgn0004859	FBgn0033153	FBgn0051324	FBgn0024754	FBgn0035770	FBgn0013679
FBgn0037046	FBgn0259697	FBgn0033919	FBgn0036155	FBgn0034639	FBgn0052091	FBgn0033972	FBgn0013697
FBgn0037433	FBgn0260027	FBgn0003091	FBgn0003731	FBgn0032681	FBgn0086558	FBgn0014906	FBgn0032518
FBgn0023001	FBgn0025631	FBgn0011674	FBgn0004169	FBgn0261451	FBgn0026562	FBgn0032407	FBgn0010408
FBgn0264490	FBgn0262887	FBgn0033128	FBgn0039313	FBgn0038243	FBgn0032228	FBgn0083003	FBgn0034743
FBgn0261642	FBgn0032405	FBgn0032744	FBgn0003053	FBgn0032297	FBgn0016123	FBgn0010406	FBgn0260441
FBgn0051826	FBgn0050026	FBgn0031270	FBgn0262475	FBgn0036910	FBgn0038869	FBgn0003888	FBgn0013675
FBgn0025111	FBgn0005771	FBgn0086608	FBgn0012037	FBgn0026061	FBgn0262579	FBgn0020249	FBgn0040007
FBgn0034275	FBgn0033132	FBgn0037831	FBgn0034602	FBgn0021953	FBgn0028494	FBgn0010611	FBgn0033912
FBgn0039208	FBgn0032156	FBgn0002609	FBgn0033504	FBgn0015777	FBgn0083000	FBgn0041789	FBgn0262608
FBgn0030237	FBgn0033785	FBgn0083039	FBgn0038721	FBgn0030638	FBgn0000044	FBgn0031008	FBgn0013678
FBgn0031973	FBgn0083978	FBgn0033787	FBgn0040532	FBgn0016694	FBgn0002789	FBgn0033459	FBgn0002579
FBgn0030532	FBgn0063491	FBgn0052369	FBgn0047133	FBgn0014380	FBgn0038321	FBgn0036147	FBgn0030136
FBgn0008654	FBgn0035678	FBgn0030941	FBgn0035710	FBgn0259938	FBgn0023549	FBgn0033875	FBgn0005533
FBgn0038761	FBgn0038744	FBgn0036551	FBgn0036545	FBgn0035132	FBgn0032036	FBgn0013263	FBgn0261606
FBgn0032612	FBgn0260866	FBgn0261647	FBgn0040091	FBgn0012051	FBgn0027610	FBgn0034761	FBgn0003274
FBgn0030574	FBgn0085412	FBgn0031909	FBgn0039205	FBgn0085446	FBgn0032451	FBgn0035542	FBgn0086472
FBgn0033204	FBgn0260486	FBgn0067905	FBgn0037934	FBgn0052163	FBgn0037709	FBgn0022382	FBgn0010078
FBgn0001230	FBgn0000723	FBgn0083047	FBgn0263200	FBgn0003890	FBgn0262004	FBgn0004629	FBgn0032987
FBgn0264617	FBgn0039927	FBgn0085773	FBgn0010383	FBgn0261565	FBgn0030294	FBgn0082925	FBgn0013672
FBgn0000542	FBgn0050015	FBgn0038826	FBgn0263930	FBgn0031305	FBgn0030816	FBgn0038369	FBgn0023170
FBgn0052582	FBgn0034512	FBgn0086910	FBgn0027930	FBgn0030099	FBgn0083005	FBgn0082919	FBgn0013704
FBgn0040763	FBgn0029881	FBgn0002773	FBgn0045842	FBgn0037265	FBgn0030482	FBgn0039233	FBgn0013674
FBgn0001250	FBgn0036834	FBgn0034886	FBgn0250835	FBgn0030731	FBgn0082582	FBgn0037819	FBgn0013676
FBgn0037565	FBgn0261703	FBgn0036101	FBgn0050021	FBgn0038842	FBgn0003391	FBgn0033571	FBgn0066084
FBgn0035976	FBgn0037845	FBgn0010651	FBgn0033438	FBgn0020439	FBgn0039509	FBgn0061198	FBgn0013686
FBgn0032533	FBgn0015399	FBgn0040348	FBgn0033240	FBgn0040850	FBgn0038465	FBgn0029854	
FBgn0261053	FBgn0032666	FBgn0031907	FBgn0086408	FBgn0031968	FBgn0005612	FBgn0001296	
FBgn0039738	FBgn0033079	FBgn0261260	FBgn0037213	FBgn0038312	FBgn0037577	FBgn0039714	
FBgn0053494	FBgn0010424	FBgn0038679	FBgn0039945	FBgn0035904	FBgn0000636	FBgn0034724	
FBgn0033654	FBgn0053087	FBgn0002772	FBgn0044419	FBgn0039114	FBgn0085802	FBgn0014029	
FBgn0085450	FBgn0031313	FBgn0030511	FBgn0037670	FBgn0033905	FBgn0028894	FBgn0037912	
FBgn0031488	FBgn0031678	FBgn0051777	FBgn0044047	FBgn0035347	FBgn0030749	FBgn0022774	

Appendix H: Down-regulated genes in *wda* GLC ovaries

FBgn0014395	FBgn0037717	FBgn0035435	FBgn0022786	FBgn0032262	FBgn0000140	FBgn0039465	FBgn0011770
FBgn0053207	FBgn0039631	FBgn0032123	FBgn0259985	FBgn0011666	FBgn0030787	FBgn0029696	FBgn0263106
FBgn0032522	FBgn0032656	FBgn0033075	FBgn0033916	FBgn0086695	FBgn0002778	FBgn0030938	FBgn0032374
FBgn0083951	FBgn0030010	FBgn0030170	FBgn0000581	FBgn0036991	FBgn0032886	FBgn0024371	FBgn0033209
FBgn0261843	FBgn0034217	FBgn0033392	FBgn0034997	FBgn0031434	FBgn0036958	FBgn0051661	FBgn0003732
FBgn0033048	FBgn0038588	FBgn0035812	FBgn0042185	FBgn0033692	FBgn0036333	FBgn0039156	FBgn0263351
FBgn0053223	FBgn0004187	FBgn0032486	FBgn0023540	FBgn0038167	FBgn0039125	FBgn0027526	FBgn0000927
FBgn0030666	FBgn0026318	FBgn0000352	FBgn0029911	FBgn0031051	FBgn0039066	FBgn0086251	FBgn0025390
FBgn0051475	FBgn0050381	FBgn0030420	FBgn0031655	FBgn0263490	FBgn0027495	FBgn0037377	FBgn0038453
FBgn0036323	FBgn0003751	FBgn0001180	FBgn0033766	FBgn0010575	FBgn0016696	FBgn0003044	FBgn0039350
FBgn0263001	FBgn0035106	FBgn0037188	FBgn0036336	FBgn0001337	FBgn0002924	FBgn0262619	FBgn0031030
FBgn0026439	FBgn0028525	FBgn0032135	FBgn0031091	FBgn0034046	FBgn0012058	FBgn0036620	FBgn0038535
FBgn0035743	FBgn0033993	FBgn0034425	FBgn0031820	FBgn0034098	FBgn0027903	FBgn0002567	FBgn0015929
FBgn0044048	FBgn0035518	FBgn0037920	FBgn0259990	FBgn0051109	FBgn0030871	FBgn0030093	FBgn0035987
FBgn0029137	FBgn0030581	FBgn0032863	FBgn0031384	FBgn0010497	FBgn0039712	FBgn0020224	FBgn0010097
FBgn0259164	FBgn0050295	FBgn0030121	FBgn0043458	FBgn0003187	FBgn0005596	FBgn0027335	FBgn0000644
FBgn0052698	FBgn0003862	FBgn0032303	FBgn0036519	FBgn0037760	FBgn0003638	FBgn0030241	FBgn0038476
FBgn0019985	FBgn0263414	FBgn0024909	FBgn0032354	FBgn0036710	FBgn0037737	FBgn0053138	FBgn0052473
FBgn0028991	FBgn0043854	FBgn0026876	FBgn0030396	FBgn0264712	FBgn0033887	FBgn0264693	FBgn0032643
FBgn0040726	FBgn0036368	FBgn0027518	FBgn0086442	FBgn0261786	FBgn0029738	FBgn0039877	FBgn0030932
FBgn0259210	FBgn0039067	FBgn0035411	FBgn0053052	FBgn0038569	FBgn0003495	FBgn0011604	FBgn0038611
FBgn0031127	FBgn0034062	FBgn0029935	FBgn0037134	FBgn0037084	FBgn0033845	FBgn0000996	FBgn0026144
FBgn0012042	FBgn0038827	FBgn0034389	FBgn0010356	FBgn0030049	FBgn0003598	FBgn0036764	FBgn0036239
FBgn0030244	FBgn0262167	FBgn0035229	FBgn0035312	FBgn0013773	FBgn0027506	FBgn0264389	FBgn0037614
FBgn0037889	FBgn0263831	FBgn0264384	FBgn0029861	FBgn0250786	FBgn0030803	FBgn0035766	FBgn0033757
FBgn0039704	FBgn0033354	FBgn0033616	FBgn0040347	FBgn0030805	FBgn0031947	FBgn0027603	FBgn0037024
FBgn0030716	FBgn0032752	FBgn0030680	FBgn0030628	FBgn0038115	FBgn0036893	FBgn0014037	FBgn0027936
FBgn0264562	FBgn0029831	FBgn0002707	FBgn0036004	FBgn0260012	FBgn0022772	FBgn0037770	FBgn0086266
FBgn0034053	FBgn0036818	FBgn0260397	FBgn0086908	FBgn0023395	FBgn0259745	FBgn0032189	FBgn0036272
FBgn0250862	FBgn0024975	FBgn0040514	FBgn0035033	FBgn0043900	FBgn0028343	FBgn0086356	FBgn0002183
FBgn0031001	FBgn0035891	FBgn0036116	FBgn0029819	FBgn0051365	FBgn0037844	FBgn0033349	FBgn0029704
FBgn0264546	FBgn0036688	FBgn0037802	FBgn0030030	FBgn0002948	FBgn0035997	FBgn0021761	FBgn0037843
FBgn0035948	FBgn0037540	FBgn0058006	FBgn0027539	FBgn0028476	FBgn0039532	FBgn0027500	FBgn0039640
FBgn0261688	FBgn0052645	FBgn0031575	FBgn0000384	FBgn0033884	FBgn0261065	FBgn0038575	FBgn0261278
FBgn0016974	FBgn0046225	FBgn0037117	FBgn0003415	FBgn0039538	FBgn0036008	FBgn0026083	FBgn0029697
FBgn0030120	FBgn0030945	FBgn0085428	FBgn0040230	FBgn0028708	FBgn0053181	FBgn0026143	FBgn0011327
FBgn0010223	FBgn0264324	FBgn0035073	FBgn0031549	FBgn0262647	FBgn0264652	FBgn0024732	FBgn0035640
FBgn0050101	FBgn0038548	FBgn0038223	FBgn0037379	FBgn0003687	FBgn0033224	FBgn0051852	FBgn0023529
FBgn0037888	FBgn0038766	FBgn0036812	FBgn0026206	FBgn0039638	FBgn0014075	FBgn0030054	FBgn0050359
FBgn0033763	FBgn0038889	FBgn0263463	FBgn0036483	FBgn0030794	FBgn0039338	FBgn0002542	FBgn0030038
FBgn0039167	FBgn0036374	FBgn0015376	FBgn0037515	FBgn0036043	FBgn0034313	FBgn0033309	FBgn0086691

FBgn0029753	FBgn0026432	FBgn0043796	FBgn0264495	FBgn0259791	FBgn0062449	FBgn0001086	FBgn0027512
FBgn0031900	FBgn0034304	FBgn0034114	FBgn0017561	FBgn0039210	FBgn0011474	FBgn0035641	FBgn0029996
FBgn0020908	FBgn0039449	FBgn0004101	FBgn0030500	FBgn0061476	FBgn0039767	FBgn0051092	FBgn0032242
FBgn0010401	FBgn0045035	FBgn0085423	FBgn0039487	FBgn0011606	FBgn0039379	FBgn0000251	FBgn0019686
FBgn0054046	FBgn0005386	FBgn0050169	FBgn0000376	FBgn0086384	FBgn0038251	FBgn0029924	FBgn0020392
FBgn0036939	FBgn0243513	FBgn0063492	FBgn0032523	FBgn0042085	FBgn0010269	FBgn0031535	FBgn0030328
FBgn0032180	FBgn0031573	FBgn0038593	FBgn0003733	FBgn0028471	FBgn0039831	FBgn0035907	FBgn0037533
FBgn0261839	FBgn0029789	FBgn0002715	FBgn0263855	FBgn0001078	FBgn0034447	FBgn0010300	FBgn0003655
FBgn0083977	FBgn0051522	FBgn0040232	FBgn0003464	FBgn0039632	FBgn0035945	FBgn0086779	FBgn0029092
FBgn0039530	FBgn0263047	FBgn0260941	FBgn0014127	FBgn0035807	FBgn0039250	FBgn0032955	FBgn0000250
FBgn0053926	FBgn0033806	FBgn0037212	FBgn0030970	FBgn0037368	FBgn0036053	FBgn0036761	FBgn0032721
FBgn0052823	FBgn0030008	FBgn0032120	FBgn0026428	FBgn0003545	FBgn0029676	FBgn0260243	FBgn0036927
FBgn0034322	FBgn0030499	FBgn0029896	FBgn0085224	FBgn0036850	FBgn0051249	FBgn0039644	FBgn0033081
FBgn0038337	FBgn0260458	FBgn0051457	FBgn0022359	FBgn0004650	FBgn0016792	FBgn0031529	FBgn0040064
FBgn0262352	FBgn0003480	FBgn0026573	FBgn0023506	FBgn0011774	FBgn0039301	FBgn0031969	FBgn0030817
FBgn0030116	FBgn0034186	FBgn0026598	FBgn0030013	FBgn0042177	FBgn0031878	FBgn0039942	FBgn0259979
FBgn0264307	FBgn0030660	FBgn0036715	FBgn0035405	FBgn0014032	FBgn0023215	FBgn0053156	FBgn0053303
FBgn0052029	FBgn0044046	FBgn0264574	FBgn0036039	FBgn0031739	FBgn0263352	FBgn0037655	FBgn0022338
FBgn0083956	FBgn0032796	FBgn0002899	FBgn0036660	FBgn0032748	FBgn0001257	FBgn0011826	FBgn0022213
FBgn0050194	FBgn0264707	FBgn0036240	FBgn0263929	FBgn0034763	FBgn0032078	FBgn0034451	FBgn0028692
FBgn0260475	FBgn0036777	FBgn0040928	FBgn0030242	FBgn0051163	FBgn0040384	FBgn0250850	FBgn0032783
FBgn0033815	FBgn0034249	FBgn0035475	FBgn0036801	FBgn0037364	FBgn0039293	FBgn0011705	FBgn0050497
FBgn0037519	FBgn0030090	FBgn0035642	FBgn0013765	FBgn0030812	FBgn0034067	FBgn0032105	FBgn0038293
FBgn0032116	FBgn0028974	FBgn0027620	FBgn0010762	FBgn0260632	FBgn0000826	FBgn0029801	FBgn0015565
FBgn0038412	FBgn0017448	FBgn0036356	FBgn0032521	FBgn0263600	FBgn0027070	FBgn0010382	FBgn0025352
FBgn0035040	FBgn0027490	FBgn0037716	FBgn0020445	FBgn0036621	FBgn0011818	FBgn0025633	FBgn0010173
FBgn0262636	FBgn0053172	FBgn0039860	FBgn0260484	FBgn0263993	FBgn0040208	FBgn0032482	FBgn0031769
FBgn0003174	FBgn0028743	FBgn0036397	FBgn0030330	FBgn0262473	FBgn0038099	FBgn0004882	FBgn0028695
FBgn0039591	FBgn0035902	FBgn0031377	FBgn0039251	FBgn0087008	FBgn0036372	FBgn0003447	FBgn0260780
FBgn0051121	FBgn0029966	FBgn0031351	FBgn0039733	FBgn0032251	FBgn0038772	FBgn0037203	FBgn0036661
FBgn0038247	FBgn0028647	FBgn0052365	FBgn0004049	FBgn0039227	FBgn0038478	FBgn0027949	FBgn0001142
FBgn0000448	FBgn0028895	FBgn0037855	FBgn0034008	FBgn0031059	FBgn0037106	FBgn0034962	FBgn0039562
FBgn0083987	FBgn0032763	FBgn0028387	FBgn0031405	FBgn0051108	FBgn0263108	FBgn0035969	FBgn0262743
FBgn0033443	FBgn0031698	FBgn0030346	FBgn0039240	FBgn0036689	FBgn0015522	FBgn0027948	FBgn0250906
FBgn0040994	FBgn0037620	FBgn0261625	FBgn0023097	FBgn0033607	FBgn0034918	FBgn0024332	FBgn0038395
FBgn0030576	FBgn0035414	FBgn0038549	FBgn0013759	FBgn0024991	FBgn0010421	FBgn0023515	FBgn0035768
FBgn0033234	FBgn0083068	FBgn0026148	FBgn0003159	FBgn0264382	FBgn0031886	FBgn0002783	FBgn0032014
FBgn0250907	FBgn0036480	FBgn0011739	FBgn0033996	FBgn0035025	FBgn0032698	FBgn0037555	FBgn0028325
FBgn0038207	FBgn0002641	FBgn0033713	FBgn0052654	FBgn0003410	FBgn0036141	FBgn0035936	FBgn0015321
FBgn0029863	FBgn0039528	FBgn0000479	FBgn0011802	FBgn0030738	FBgn0263697	FBgn0035959	FBgn0033979
FBgn0020300	FBgn0260006	FBgn0032154	FBgn0004876	FBgn0051342	FBgn0030973	FBgn0005695	FBgn0263979
FBgn0038279	FBgn0023130	FBgn0034628	FBgn0037788	FBgn0052438	FBgn0032034	FBgn0030863	FBgn0003023
FBgn0031816	FBgn0038853	FBgn0031554	FBgn0001169	FBgn0023180	FBgn0039073	FBgn0037354	FBgn0030551

FBgn0038098	FBgn0035420	FBgn0031741	FBgn0010830	FBgn0031464	FBgn0038974	FBgn0260991	FBgn0016070
FBgn0032211	FBgn0036032	FBgn0039680	FBgn0039272	FBgn0026317	FBgn0002283	FBgn0262609	FBgn0010100
FBgn0039170	FBgn0031608	FBgn0037606	FBgn0029905	FBgn0001612	FBgn0031875	FBgn0036967	FBgn0051928
FBgn0041160	FBgn0037554	FBgn0032204	FBgn0031895	FBgn0026326	FBgn0027580	FBgn0025815	FBgn0031677
FBgn0082585	FBgn0029713	FBgn0037773	FBgn0003210	FBgn0052479	FBgn0031267	FBgn0004913	FBgn0052642
FBgn0030757	FBgn0261383	FBgn0041721	FBgn0010825	FBgn0259734	FBgn0003520	FBgn0052644	FBgn0032788
FBgn0029128	FBgn0035923	FBgn0033740	FBgn0038649	FBgn0002872	FBgn0005674	FBgn0032876	FBgn0023167
FBgn0260005	FBgn0039594	FBgn0263440	FBgn0261274	FBgn0027660	FBgn0039098	FBgn0027348	FBgn0042134
FBgn0030331	FBgn0085478	FBgn0032295	FBgn0026375	FBgn0038722	FBgn0030373	FBgn0011481	FBgn0035726
FBgn0032730	FBgn0000075	FBgn0036395	FBgn0037924	FBgn0039634	FBgn0028360	FBgn0035955	FBgn0004507
FBgn0085245	FBgn0027083	FBgn0028997	FBgn0028980	FBgn0038551	FBgn0027951	FBgn0004698	FBgn0035121
FBgn0086898	FBgn0003450	FBgn0030465	FBgn0259676	FBgn0034314	FBgn0263144	FBgn0035402	FBgn0039972
FBgn0033674	FBgn0260789	FBgn0034808	FBgn0052251	FBgn0027783	FBgn0005390	FBgn0027889	FBgn0063494
FBgn0038296	FBgn0263667	FBgn0039589	FBgn0035035	FBgn0027570	FBgn0263933	FBgn0028425	FBgn0010488
FBgn0033836	FBgn0028397	FBgn0085281	FBgn0032172	FBgn0030758	FBgn0000541	FBgn0014861	FBgn0003124
FBgn0003934	FBgn0031597	FBgn0035047	FBgn0003475	FBgn0036735	FBgn0039559	FBgn0039186	FBgn0038469
FBgn0035957	FBgn0259112	FBgn0036614	FBgn0025186	FBgn0035998	FBgn0039065	FBgn0039994	FBgn0011703
FBgn0029821	FBgn0031070	FBgn0036746	FBgn0030228	FBgn0031435	FBgn0051926	FBgn0039563	FBgn0053129
FBgn0037759	FBgn0003042	FBgn0002906	FBgn0029822	FBgn0032910	FBgn0015544	FBgn0017551	FBgn0031111
FBgn0037290	FBgn0037936	FBgn0037028	FBgn0028955	FBgn0040477	FBgn0261016	FBgn0036690	FBgn0015778
FBgn0000567	FBgn0032723	FBgn0039705	FBgn0032904	FBgn0039212	FBgn0035253	FBgn0028554	FBgn0051641
FBgn0263027	FBgn0042178	FBgn0000533	FBgn0037144	FBgn0001087	FBgn0010313	FBgn0024841	FBgn0034403
FBgn0034454	FBgn0024510	FBgn0034691	FBgn0010113	FBgn0035558	FBgn0031452	FBgn0030740	FBgn0016053
FBgn0039244	FBgn0000166	FBgn0034618	FBgn0015360	FBgn0028468	FBgn0261854	FBgn0051075	FBgn0000615
FBgn0038047	FBgn0039696	FBgn0037184	FBgn0086253	FBgn0041087	FBgn0027515	FBgn0035872	FBgn0005630
FBgn0039663	FBgn0035842	FBgn0033935	FBgn0050377	FBgn0029893	FBgn0045862	FBgn0263112	FBgn0020653
FBgn0032082	FBgn0033636	FBgn0011020	FBgn0000810	FBgn0030710	FBgn0028380	FBgn0030268	FBgn0001120
FBgn0032084	FBgn0264326	FBgn0040752	FBgn0033316	FBgn0023181	FBgn0013756	FBgn0035209	FBgn0003015
FBgn0260955	FBgn0034270	FBgn0030646	FBgn0004379	FBgn0034187	FBgn0000351	FBgn0010342	FBgn0086265
FBgn0033049	FBgn0030963	FBgn0261397	FBgn0030930	FBgn0036450	FBgn0263236	FBgn0023528	FBgn0014465
FBgn0037742	FBgn0030833	FBgn0015240	FBgn0015271	FBgn0086350	FBgn0025335	FBgn0030276	FBgn0029568
FBgn0002891	FBgn0030421	FBgn0023513	FBgn0037746	FBgn0037922	FBgn0024921	FBgn0004598	FBgn0002781
FBgn0051674	FBgn0053107	FBgn0038488	FBgn0033639	FBgn0040030	FBgn0033737	FBgn0032026	FBgn0014464
FBgn0053970	FBgn0033673	FBgn0052767	FBgn0036382	FBgn0013732	FBgn0030943	FBgn0037248	FBgn0000114
FBgn0030583	FBgn0053182	FBgn0032934	FBgn0026575	FBgn0003964	FBgn0010877	FBgn0028408	FBgn0038252
FBgn0038418	FBgn0037031	FBgn0033258	FBgn0027504	FBgn0031682	FBgn0033526	FBgn0037807	FBgn0264493
FBgn0263975	FBgn0039466	FBgn0034569	FBgn0032485	FBgn0023526	FBgn0086855	FBgn0034091	FBgn0035328
FBgn0261698	FBgn0033994	FBgn0011232	FBgn0053116	FBgn0086358	FBgn0037878	FBgn0029879	FBgn0010288
FBgn0030266	FBgn0263355	FBgn0033698	FBgn0004832	FBgn0015391	FBgn0086372	FBgn0011725	FBgn0000182
FBgn0036765	FBgn0024993	FBgn0002775	FBgn0001974	FBgn0015396	FBgn0028646	FBgn0029152	FBgn0041252
FBgn0037520	FBgn0034300	FBgn0051224	FBgn0027513	FBgn0037481	FBgn0000183	FBgn0033374	FBgn0014869
FBgn0034321	FBgn0025874	FBgn0041629	FBgn0015371	FBgn0039385	FBgn0030790	FBgn0051716	FBgn0041709
FBgn0000808	FBgn0033718	FBgn0034433	FBgn0034158	FBgn0037755	FBgn0039741	FBgn0010282	FBgn0032127

FBgn0032449	FBgn0004381	FBgn0035627	FBgn0034999	FBgn0004795	FBgn0028563	FBgn0261524	FBgn0010431
FBgn0026616	FBgn0002901	FBgn0026313	FBgn0003310	FBgn0038011	FBgn0040239	FBgn0260399	FBgn0004649
FBgn0031182	FBgn0036386	FBgn0034853	FBgn0014007	FBgn0052676	FBgn0003114	FBgn0035978	FBgn0030608
FBgn0031422	FBgn0037944	FBgn0050055	FBgn0033233	FBgn0040290	FBgn0028700	FBgn0262737	FBgn0261014
FBgn0033437	FBgn0031191	FBgn0263602	FBgn0261845	FBgn0033656	FBgn0262126	FBgn0042693	FBgn0000404
FBgn0052137	FBgn0037025	FBgn0023508	FBgn0261986	FBgn0000273	FBgn0024984	FBgn0020633	FBgn0028688
FBgn0031865	FBgn0039296	FBgn0030174	FBgn0028916	FBgn0038206	FBgn0027521	FBgn0035397	FBgn0061515
FBgn0038589	FBgn0039355	FBgn0025808	FBgn0026433	FBgn0260771	FBgn0025777	FBgn0003138	FBgn0086355
FBgn0263048	FBgn0051262	FBgn0260817	FBgn0030018	FBgn0020248	FBgn0260743	FBgn0031047	FBgn0032789
FBgn0035002	FBgn0020312	FBgn0030510	FBgn0263077	FBgn0037758	FBgn0004584	FBgn0259978	FBgn0087040
FBgn0002932	FBgn0038564	FBgn0034308	FBgn0034728	FBgn0005617	FBgn0033773	FBgn0010314	FBgn0085362
FBgn0035290	FBgn0000286	FBgn0034629	FBgn0036144	FBgn0031664	FBgn0259174	FBgn0002652	FBgn0086254
FBgn0034452	FBgn0035150	FBgn0030439	FBgn0034946	FBgn0052484	FBgn0004643	FBgn0003612	FBgn0003178
FBgn0052602	FBgn0029894	FBgn0038872	FBgn0013548	FBgn0037021	FBgn0033039	FBgn0036938	FBgn0261987
FBgn0039045	FBgn0263005	FBgn0037624	FBgn0033890	FBgn0026619	FBgn0031842	FBgn0023423	FBgn0033879
FBgn0005624	FBgn0052707	FBgn0030314	FBgn0036994	FBgn0015553	FBgn0030456	FBgn0003076	FBgn0033631
FBgn0047000	FBgn0041147	FBgn0000063	FBgn0036522	FBgn0260959	FBgn0031126	FBgn0030438	FBgn0001226
FBgn0031961	FBgn0025185	FBgn0022768	FBgn0026597	FBgn0035697	FBgn0031252	FBgn0035425	FBgn0001218
FBgn0032343	FBgn0002873	FBgn0033569	FBgn0037722	FBgn0027559	FBgn0041171	FBgn0036316	FBgn0001091
FBgn0261567	FBgn0034410	FBgn0036266	FBgn0263768	FBgn0030320	FBgn0035866	FBgn0014417	FBgn0264696
FBgn0034797	FBgn0010398	FBgn0261238	FBgn0029685	FBgn0031893	FBgn0038608	FBgn0022981	FBgn0259682
FBgn0020379	FBgn0037781	FBgn0035145	FBgn0032223	FBgn0032870	FBgn0031483	FBgn0260795	FBgn0011823
FBgn0024944	FBgn0038740	FBgn0033971	FBgn0005683	FBgn0038692	FBgn0032705	FBgn0040493	FBgn0033663
FBgn0030065	FBgn0003268	FBgn0039966	FBgn0050389	FBgn0034894	FBgn0026257	FBgn0052412	FBgn0014466
FBgn0039068	FBgn0029970	FBgn0037185	FBgn0039141	FBgn0029157	FBgn0035016	FBgn0027567	FBgn0000405
FBgn0036906	FBgn0025807	FBgn0038390	FBgn0013995	FBgn0001108	FBgn0030468	FBgn0037810	FBgn0000427
FBgn0035267	FBgn0038118	FBgn0001099	FBgn0023083	FBgn0040372	FBgn0002673	FBgn0026370	FBgn0000579
FBgn0036423	FBgn0262730	FBgn0001085	FBgn0033990	FBgn0030507	FBgn0264561	FBgn0034181	FBgn0041775
FBgn0037205	FBgn0259789	FBgn0050440	FBgn0033762	FBgn0004462	FBgn0037081	FBgn0014133	FBgn0001092
FBgn0040465	FBgn0031610	FBgn0035021	FBgn0052452	FBgn0015270	FBgn0003028	FBgn0003022	FBgn0250848
FBgn0085435	FBgn0027342	FBgn0039164	FBgn0086711	FBgn0031217	FBgn0037405	FBgn0004107	FBgn0034753
FBgn0263745	FBgn0035851	FBgn0015600	FBgn0004655	FBgn0086694	FBgn0033236	FBgn0036815	FBgn0001149
FBgn0031734	FBgn0036814	FBgn0037338	FBgn0031848	FBgn0037482	FBgn0020386	FBgn0038437	FBgn0003887
FBgn0083985	FBgn0262895	FBgn0050183	FBgn0259113	FBgn0032929	FBgn0001222	FBgn0050118	FBgn0000356
FBgn0001206	FBgn0037646	FBgn0030512	FBgn0051015	FBgn0000307	FBgn0005694	FBgn0003525	FBgn0014076
FBgn0250755	FBgn0263865	FBgn0039459	FBgn0086697	FBgn0003071	FBgn0052043	FBgn0003087	FBgn0001225
FBgn0034634	FBgn0028421	FBgn0000017	FBgn0033206	FBgn0025781	FBgn0028953	FBgn0029161	FBgn0004419
FBgn0035151	FBgn0039731	FBgn0011660	FBgn0026431	FBgn0260986	FBgn0261710	FBgn0052774	FBgn0000358
FBgn0036875	FBgn0016641	FBgn0031885	FBgn0259876	FBgn0005696	FBgn0036505	FBgn0014427	FBgn0011761
FBgn0003292	FBgn0034704	FBgn0039223	FBgn0264704	FBgn0035593	FBgn0033482	FBgn0034021	FBgn0000359
FBgn0030925	FBgn0050467	FBgn0021818	FBgn0030717	FBgn0036574	FBgn0022936	FBgn0029733	FBgn0004045
FBgn0038815	FBgn0037186	FBgn0039061	FBgn0261004	FBgn0028470	FBgn0035529	FBgn0020370	FBgn0000360
FBgn0030100	FBgn0037664	FBgn0038401	FBgn0037109	FBgn0038381	FBgn0016122	FBgn0041186	FBgn0003980

FBgn0040153	FBgn0032587	FBgn0024994	FBgn0042180	FBgn0034401	FBgn0032157	FBgn0037376	FBgn0000357
FBgn0031519	FBgn0002552	FBgn0033155	FBgn0035918	FBgn0025639	FBgn0030864	FBgn0029969	FBgn0005391
FBgn0034859	FBgn0067102	FBgn0003701	FBgn0085290	FBgn0037239	FBgn0037236	FBgn0002962	FBgn0003983
FBgn0001090	FBgn0031696	FBgn0032907	FBgn0050463	FBgn0000147	FBgn0026576	FBgn0017577	FBgn0003979
FBgn0032869	FBgn0038619	FBgn0260862	FBgn0036028	FBgn0030336	FBgn0036486	FBgn0026430	FBgn0000355
FBgn0000158	FBgn0029756	FBgn0036565	FBgn0015926	FBgn0052822	FBgn0010786	FBgn0015625	
FBgn0033186	FBgn0003218	FBgn0263038	FBgn0039271	FBgn0051658	FBgn0022702	FBgn0028734	

Appendix I: Up-regulated genes in *Ataxin-7* GLC embryos

FBgn0053474	FBgn0033310	FBgn0015268	FBgn0039350	FBgn0260399	FBgn0036196	FBgn0030608	FBgn0263093
FBgn0042134	FBgn0264504	FBgn0052626	FBgn0052350	FBgn0039153	FBgn0034897	FBgn0034804	FBgn0010611
FBgn0028427	FBgn0032730	FBgn0016693	FBgn0015614	FBgn0024238	FBgn0036906	FBgn0034989	FBgn0029801
FBgn0038830	FBgn0262579	FBgn0035964	FBgn0034261	FBgn0033713	FBgn0030347	FBgn0015568	FBgn0026718
FBgn0037110	FBgn0040236	FBgn0030018	FBgn0038279	FBgn0035807	FBgn0037144	FBgn0032731	FBgn0022382
FBgn0261276	FBgn0000405	FBgn0028499	FBgn0263355	FBgn0050010	FBgn0053138	FBgn0003870	FBgn0003023
FBgn0020626	FBgn0038815	FBgn0028434	FBgn0036366	FBgn0058160	FBgn0030276	FBgn0024991	FBgn0010288
FBgn0014018	FBgn0259978	FBgn0028703	FBgn0002906	FBgn0038672	FBgn0052484	FBgn0037607	FBgn0037345
FBgn0260934	FBgn0052822	FBgn0011703	FBgn0016641	FBgn0261983	FBgn0023507	FBgn0029866	FBgn0031885
FBgn0033465	FBgn0039537	FBgn0025621	FBgn0040064	FBgn0039944	FBgn0036257	FBgn0003204	FBgn0023094
FBgn0022709	FBgn0038769	FBgn0028497	FBgn0032957	FBgn0028336	FBgn0031377	FBgn0039938	FBgn0030478
FBgn0039461	FBgn0031119	FBgn0035444	FBgn0022097	FBgn0001248	FBgn0261845	FBgn0032820	FBgn0033635
FBgn0032259	FBgn0002778	FBgn0030512	FBgn0029858	FBgn0040294	FBgn0031188	FBgn0030740	FBgn0083986
FBgn0262617	FBgn0261068	FBgn0005694	FBgn0032587	FBgn0038344	FBgn0041150	FBgn0029831	FBgn0052412
FBgn0038686	FBgn0032397	FBgn0038206	FBgn0022772	FBgn0039223	FBgn0005632	FBgn0042213	FBgn0023477
FBgn0261049	FBgn0023407	FBgn0039126	FBgn0020309	FBgn0259178	FBgn0039588	FBgn0035630	FBgn0030737
FBgn0038893	FBgn0014469	FBgn0085370	FBgn0034965	FBgn0032084	FBgn0000166	FBgn0029155	FBgn0000008
FBgn0011769	FBgn0035586	FBgn0034543	FBgn0037142	FBgn0030362	FBgn0015522	FBgn0037248	FBgn0052732
FBgn0031995	FBgn0035537	FBgn0010438	FBgn0017549	FBgn0010808	FBgn0014455	FBgn0016078	FBgn0030432
FBgn0035989	FBgn0260003	FBgn0010263	FBgn0035065	FBgn0052625	FBgn0032194	FBgn0261938	FBgn0033457
FBgn0043458	FBgn0038268	FBgn0037117	FBgn0053230	FBgn0034032	FBgn0024509	FBgn0052196	FBgn0030805
FBgn0085638	FBgn0034763	FBgn0036341	FBgn0037239	FBgn0260743	FBgn0039109	FBgn0263598	FBgn0017448
FBgn0039341	FBgn0041203	FBgn0263768	FBgn0029131	FBgn0052226	FBgn0033989	FBgn0038912	FBgn0038575
FBgn0039385	FBgn0030268	FBgn0025832	FBgn0031161	FBgn0031189	FBgn0000808	FBgn0002948	FBgn0001137
FBgn0033783	FBgn0039942	FBgn0029997	FBgn0032704	FBgn0037338	FBgn0263005	FBgn0022786	FBgn0040309
FBgn0051119	FBgn0033519	FBgn0263110	FBgn0037757	FBgn0016070	FBgn0264305	FBgn0064115	FBgn0035642
FBgn0037472	FBgn0021800	FBgn0036786	FBgn0036144	FBgn0050491	FBgn0263706	FBgn0002641	FBgn0010431
FBgn0052163	FBgn0040752	FBgn0031126	FBgn0031357	FBgn0001091	FBgn0041164	FBgn0035039	FBgn0035978
FBgn0023441	FBgn0036188	FBgn0033309	FBgn0041582	FBgn0263773	FBgn0026619	FBgn0024957	FBgn0039156
FBgn0040005	FBgn0034854	FBgn0001186	FBgn0031312	FBgn0053123	FBgn0041721	FBgn0014141	FBgn0039737
FBgn0263025	FBgn0036685	FBgn0261383	FBgn0036992	FBgn0000579	FBgn0010316	FBgn0026315	FBgn0050392
FBgn0052264	FBgn0026479	FBgn0034535	FBgn0052676	FBgn0039751	FBgn0023508	FBgn0261560	FBgn0063494
FBgn0023216	FBgn0001316	FBgn0021761	FBgn0041180	FBgn0020653	FBgn0086674	FBgn0010786	FBgn0038316
FBgn0033224	FBgn0001226	FBgn0020513	FBgn0039836	FBgn0019982	FBgn0000382	FBgn0000114	FBgn0051044
FBgn0032204	FBgn0020930	FBgn0263120	FBgn0262124	FBgn0264090	FBgn0032249	FBgn0038577	FBgn0031405
FBgn0067102	FBgn0038223	FBgn0023181	FBgn0036488	FBgn0045862	FBgn0033273	FBgn0029854	FBgn0038828
FBgn0000719	FBgn0264481	FBgn0260972	FBgn0015589	FBgn0011745	FBgn0000346	FBgn0026738	FBgn0024315
FBgn0038349	FBgn0264704	FBgn0263199	FBgn0000826	FBgn0039637	FBgn0015036	FBgn0033996	FBgn0030932
FBgn0003964	FBgn0027287	FBgn0030791	FBgn0038277	FBgn0004510	FBgn0259834	FBgn0003028	FBgn0038347
FBgn0034618	FBgn0028516	FBgn0030581	FBgn0033918	FBgn0264574	FBgn0034688	FBgn0004598	FBgn0050005
FBgn0032172	FBgn0003525	FBgn0263555	FBgn0037632	FBgn0050440	FBgn0261553	FBgn0015794	FBgn0250907

FBgn0028507	FBgn0262126	FBgn0061515	FBgn0061476	FBgn0004397	FBgn0083968	FBgn0036331	FBgn0032374
FBgn0038424	FBgn0035589	FBgn0039417	FBgn0005596	FBgn0262468	FBgn0033717	FBgn0025628	FBgn0026593
FBgn0014906	FBgn0259735	FBgn0036333	FBgn0086475	FBgn0038683	FBgn0243512	FBgn0082980	FBgn0052816
FBgn0031011	FBgn0033738	FBgn0035960	FBgn0016031	FBgn0036237	FBgn0004868	FBgn0035802	FBgn0037755
FBgn0030431	FBgn0050291	FBgn0010350	FBgn0039958	FBgn0001233	FBgn0029092	FBgn0031703	FBgn0028670
FBgn0029944	FBgn0039665	FBgn0023506	FBgn0033205	FBgn0030286	FBgn0053558	FBgn0033744	FBgn0029823
FBgn0053169	FBgn0033010	FBgn0026620	FBgn0029912	FBgn0037063	FBgn0260946	FBgn0032679	FBgn0042174
FBgn0038381	FBgn0010315	FBgn0031051	FBgn0004167	FBgn0262738	FBgn0264385	FBgn0051262	FBgn0034583
FBgn0045063	FBgn0259203	FBgn0027356	FBgn0036199	FBgn0050463	FBgn0037513	FBgn0026433	FBgn0039679
FBgn0034245	FBgn0002909	FBgn0037610	FBgn0032032	FBgn0031150	FBgn0029936	FBgn0031317	FBgn0032805
FBgn0051151	FBgn0024920	FBgn0037383	FBgn0010397	FBgn0037739	FBgn0039118	FBgn0028952	FBgn0035891
FBgn0039994	FBgn0259709	FBgn0040823	FBgn0030421	FBgn0031213	FBgn0034312	FBgn0035892	FBgn0037890
FBgn0086347	FBgn0035016	FBgn0027359	FBgn0030330	FBgn0053554	FBgn0038049	FBgn0262103	FBgn0000351
FBgn0039876	FBgn0039634	FBgn0037747	FBgn0261285	FBgn0027529	FBgn0263278	FBgn0003943	FBgn0040370
FBgn0024329	FBgn0032904	FBgn0030735	FBgn0045842	FBgn0022344	FBgn0031516	FBgn0010591	FBgn0260747
FBgn0035760	FBgn0037912	FBgn0000376	FBgn0259734	FBgn0004369	FBgn0264307	FBgn0034585	FBgn0010097
FBgn0042092	FBgn0037913	FBgn0000057	FBgn0030724	FBgn0039959	FBgn0033673	FBgn0001120	FBgn0261987
FBgn0029821	FBgn0030420	FBgn0039073	FBgn0039972	FBgn0002354	FBgn0035083	FBgn0002719	FBgn0031974
FBgn0051935	FBgn0039507	FBgn0033413	FBgn0036843	FBgn0027329	FBgn0029911	FBgn0010053	FBgn0033257
FBgn0037718	FBgn0034029	FBgn0021750	FBgn0003475	FBgn0038043	FBgn0037242	FBgn0027342	FBgn0034354
FBgn0034816	FBgn0015247	FBgn0034371	FBgn0050398	FBgn0038197	FBgn0259711	FBgn0005671	FBgn0263462
FBgn0035825	FBgn0035936	FBgn0026084	FBgn0036622	FBgn0033451	FBgn0036942	FBgn0038325	FBgn0027512
FBgn0263974	FBgn0033653	FBgn0028397	FBgn0040237	FBgn0036053	FBgn0014869	FBgn0010235	FBgn0035173
FBgn0025335	FBgn0259112	FBgn0037525	FBgn0261787	FBgn0058042	FBgn0031779	FBgn0004611	FBgn0035266
FBgn0036043	FBgn0029905	FBgn0031971	FBgn0026206	FBgn0033906	FBgn0052099	FBgn0037445	FBgn0037574
FBgn0035400	FBgn0038321	FBgn0085281	FBgn0013563	FBgn0031659	FBgn0036749	FBgn0037070	FBgn0004183
FBgn0037027	FBgn0261397	FBgn0022359	FBgn0030502	FBgn0261556	FBgn0037138	FBgn0040056	FBgn0030964
FBgn0040366	FBgn0033232	FBgn0051658	FBgn0040382	FBgn0032791	FBgn0263077	FBgn0035475	FBgn0031998
FBgn0032986	FBgn0033984	FBgn0263507	FBgn0032513	FBgn0015239	FBgn0260027	FBgn0028494	FBgn0001092
FBgn0039186	FBgn0029704	FBgn0004913	FBgn0085216	FBgn0041775	FBgn0035839	FBgn0003744	FBgn0262559
FBgn0003071	FBgn0000183	FBgn0058045	FBgn0033391	FBgn0035169	FBgn0001220	FBgn0051249	FBgn0011274
FBgn0053172	FBgn0029174	FBgn0263350	FBgn0004101	FBgn0051156	FBgn0039877	FBgn0050377	FBgn0263847
FBgn0020270	FBgn0011570	FBgn0027106	FBgn0031483	FBgn0024994	FBgn0034255	FBgn0015571	FBgn0036008
FBgn0086359	FBgn0032407	FBgn0037606	FBgn0036760	FBgn0037602	FBgn0040334	FBgn0263112	FBgn0039932
FBgn0011656	FBgn0085279	FBgn0040298	FBgn0038401	FBgn0023458	FBgn0000241	FBgn0028509	FBgn0011826
FBgn0031589	FBgn0262737	FBgn0000392	FBgn0036142	FBgn0260780	FBgn0032029	FBgn0250848	FBgn0040348
FBgn0015229	FBgn0038478	FBgn0085339	FBgn0014427	FBgn0032018	FBgn0037838	FBgn0036336	FBgn0015245
FBgn0027552	FBgn0035592	FBgn0015781	FBgn0041087	FBgn0035449	FBgn0259749	FBgn0025702	FBgn0037779
FBgn0031678	FBgn0033757	FBgn0002781	FBgn0053129	FBgn0038432	FBgn0000032	FBgn0027843	FBgn0003178
FBgn0024273	FBgn0011211	FBgn0002901	FBgn0000084	FBgn0003187	FBgn0039464	FBgn0037944	FBgn0087040
FBgn0262526	FBgn0033683	FBgn0033692	FBgn0016053	FBgn0000063	FBgn0015776	FBgn0032161	FBgn0065046
FBgn0004654	FBgn0015553	FBgn0263602	FBgn0041781	FBgn0036777	FBgn0000052	FBgn0039869	FBgn0086254
FBgn0031457	FBgn0069969	FBgn0086784	FBgn0010905	FBgn0003016	FBgn0036893	FBgn0015924	FBgn0025693

FBgn0030551	FBgn0034918	FBgn0022936	FBgn0030345	FBgn0036099	FBgn0036152	FBgn0024846	FBgn0035641
FBgn0031117	FBgn0011660	FBgn0035953	FBgn0000053	FBgn0005695	FBgn0031820	FBgn0003655	FBgn0032026
FBgn0014133	FBgn0015282	FBgn0036889	FBgn0083987	FBgn0038252	FBgn0016970	FBgn0003423	FBgn0003015
FBgn0050161	FBgn0015582	FBgn0035515	FBgn0032873	FBgn0052446	FBgn0038241	FBgn0033624	FBgn0039856
FBgn0039668	FBgn0052365	FBgn0035473	FBgn0086358	FBgn0017414	FBgn0052056	FBgn0259227	FBgn0000615
FBgn0038627	FBgn0025820	FBgn0042135	FBgn0030963	FBgn0041147	FBgn0260817	FBgn0040030	FBgn0000055
FBgn0030966	FBgn0038286	FBgn0005654	FBgn0038721	FBgn0036815	FBgn0004876	FBgn0032474	FBgn0086355
FBgn0031044	FBgn0038588	FBgn0028325	FBgn0036770	FBgn0023215	FBgn0039451	FBgn0259682	FBgn0032783
FBgn0026252	FBgn0050000	FBgn0052485	FBgn0023083	FBgn0036334	FBgn0028380	FBgn0029879	FBgn0035040
FBgn0037391	FBgn0039269	FBgn0043001	FBgn0040347	FBgn0039226	FBgn0034629	FBgn0011705	FBgn0011761
FBgn0038467	FBgn0036551	FBgn0037518	FBgn0031969	FBgn0030514	FBgn0261550	FBgn0051793	FBgn0001149
FBgn0039882	FBgn0036772	FBgn0032943	FBgn0031912	FBgn0030346	FBgn0039641	FBgn0001225	FBgn0032453
FBgn0031766	FBgn0260435	FBgn0032350	FBgn0040321	FBgn0032262	FBgn0032400	FBgn0040259	FBgn0264439
FBgn0030183	FBgn0010309	FBgn0030087	FBgn0032889	FBgn0033196	FBgn0026143	FBgn0261244	FBgn0002868
FBgn0034628	FBgn0261445	FBgn0027521	FBgn0025469	FBgn0038763	FBgn0051641	FBgn0050403	
FBgn0035402	FBgn0028665	FBgn0030612	FBgn0001612	FBgn0034951	FBgn0058263	FBgn0029504	
FBgn0087013	FBgn0004432	FBgn0023515	FBgn0037379	FBgn0013759	FBgn0031575	FBgn0037646	
FBgn0036896	FBgn0250850	FBgn0001224	FBgn0031194	FBgn0263975	FBgn0022710	FBgn0086608	
FBgn0033474	FBgn0036689	FBgn0001128	FBgn0029711	FBgn0086372	FBgn0040397	FBgn0259247	
FBgn0033179	FBgn0032705	FBgn0038928	FBgn0051807	FBgn0029895	FBgn0037203	FBgn0014417	

Appendix J: Down-regulated genes in *Ataxin-7* GLC embryos

FBgn0085273	FBgn0000659	FBgn0041184	FBgn0261434	FBgn0037797	FBgn0003430	FBgn0024236	FBgn0031621
FBgn0035245	FBgn0050489	FBgn0003984	FBgn0035674	FBgn0032691	FBgn0032633	FBgn0035849	FBgn0001247
FBgn0035246	FBgn0052982	FBgn0002631	FBgn0036350	FBgn0038150	FBgn0050383	FBgn0045761	FBgn0015600
FBgn0038647	FBgn0003145	FBgn0038977	FBgn0038385	FBgn0026570	FBgn0002873	FBgn0043854	FBgn0003396
FBgn0036986	FBgn0034937	FBgn0052372	FBgn0038981	FBgn0001965	FBgn0053526	FBgn0034504	FBgn0040392
FBgn0038773	FBgn0038804	FBgn0000071	FBgn0035725	FBgn0082931	FBgn0021875	FBgn0043841	FBgn0036882
FBgn0015399	FBgn0032682	FBgn0036287	FBgn0082926	FBgn0010238	FBgn0014163	FBgn0034083	FBgn0031536
FBgn0004174	FBgn0001123	FBgn0001234	FBgn0029114	FBgn0010109	FBgn0046253	FBgn0027108	FBgn0033528
FBgn0039419	FBgn0000157	FBgn0051710	FBgn0050089	FBgn0261111	FBgn0031592	FBgn0262418	FBgn0031760
FBgn0052214	FBgn0262405	FBgn0039590	FBgn0016054	FBgn0264707	FBgn0005634	FBgn0020546	FBgn0024230
FBgn0039343	FBgn0263467	FBgn0053555	FBgn0003900	FBgn0259936	FBgn0051161	FBgn0029128	FBgn0033107
FBgn0038944	FBgn0001168	FBgn0030675	FBgn0019968	FBgn0003042	FBgn0033087	FBgn0003053	FBgn0051118
FBgn0039585	FBgn0082961	FBgn0039000	FBgn0002633	FBgn0027793	FBgn0051004	FBgn0000463	FBgn0040344
FBgn0037974	FBgn0052104	FBgn0026320	FBgn0019650	FBgn0087007	FBgn0259745	FBgn0030361	FBgn0259113
FBgn0003091	FBgn0039937	FBgn0262867	FBgn0263256	FBgn0063261	FBgn0033988	FBgn0016984	FBgn0052829
FBgn0032666	FBgn0004635	FBgn0004052	FBgn0041160	FBgn0034964	FBgn0039167	FBgn0031549	FBgn0041094
FBgn0041156	FBgn0013272	FBgn0033174	FBgn0003683	FBgn0026160	FBgn0034126	FBgn0262109	FBgn0050466
FBgn0036338	FBgn0031129	FBgn0028373	FBgn0082958	FBgn0004956	FBgn0263873	FBgn0034322	FBgn0031238
FBgn0052115	FBgn0003328	FBgn0036503	FBgn0039727	FBgn0033526	FBgn0034879	FBgn0033859	FBgn0262517
FBgn0034462	FBgn0027364	FBgn0011723	FBgn0002528	FBgn0035824	FBgn0037753	FBgn0037085	FBgn0036369
FBgn0004892	FBgn0259244	FBgn0261269	FBgn0036791	FBgn0035436	FBgn0001324	FBgn0033871	FBgn0033240
FBgn0038012	FBgn0033649	FBgn0030796	FBgn0085243	FBgn0053653	FBgn0025830	FBgn0031157	FBgn0040234
FBgn0262577	FBgn0000489	FBgn0003896	FBgn0085412	FBgn0050296	FBgn0262166	FBgn0261823	FBgn0001174
FBgn0002121	FBgn0012037	FBgn0036715	FBgn0019886	FBgn0025790	FBgn0037007	FBgn0033241	FBgn0020300
FBgn0004878	FBgn0038172	FBgn0053200	FBgn0263610	FBgn0036844	FBgn0003963	FBgn0032348	FBgn0005410
FBgn0063386	FBgn0053207	FBgn0264601	FBgn0026063	FBgn0020414	FBgn0050441	FBgn0036810	FBgn0033962
FBgn0025776	FBgn0032335	FBgn0262719	FBgn0039738	FBgn0035236	FBgn0044328	FBgn0041161	FBgn0035704
FBgn0051997	FBgn0031001	FBgn0023001	FBgn0263971	FBgn0040296	FBgn0029959	FBgn0038071	FBgn0040297
FBgn0032048	FBgn0000576	FBgn0082941	FBgn0031053	FBgn0014342	FBgn0035608	FBgn0015949	FBgn0037561
FBgn0039941	FBgn0004595	FBgn0001077	FBgn0037363	FBgn0045064	FBgn0264332	FBgn0036545	FBgn0036547
FBgn0051909	FBgn0015773	FBgn0005672	FBgn0034724	FBgn0034822	FBgn0261830	FBgn0034631	FBgn0041627
FBgn0035348	FBgn0038191	FBgn0260745	FBgn0082979	FBgn0264270	FBgn0038146	FBgn0082953	FBgn0004367
FBgn0024244	FBgn0034479	FBgn0264089	FBgn0260935	FBgn0003719	FBgn0035987	FBgn0000413	FBgn0033809
FBgn0037375	FBgn0261873	FBgn0051536	FBgn0004646	FBgn0000116	FBgn0037149	FBgn0028983	FBgn0050285
FBgn0083003	FBgn0000542	FBgn0037213	FBgn0034013	FBgn0036450	FBgn0261800	FBgn0083973	FBgn0262656
FBgn0014388	FBgn0040759	FBgn0031897	FBgn0262029	FBgn0034275	FBgn0264469	FBgn0037105	FBgn0034501
FBgn0030469	FBgn0033159	FBgn0029771	FBgn0261836	FBgn0259818	FBgn0003510	FBgn0086898	FBgn0029958
FBgn0053503	FBgn0032002	FBgn0030592	FBgn0085352	FBgn0004102	FBgn0000629	FBgn0032221	FBgn0004583
FBgn0028425	FBgn0029123	FBgn0016762	FBgn0261356	FBgn0032858	FBgn0036684	FBgn0036003	FBgn0031319
FBgn0263219	FBgn0002931	FBgn0004108	FBgn0026061	FBgn0038566	FBgn0001099	FBgn0033872	FBgn0000575
FBgn0085424	FBgn0035484	FBgn0004861	FBgn0003117	FBgn0015277	FBgn0038872	FBgn0085408	FBgn0030786

FBgn0264542	FBgn0032693	FBgn0260011	FBgn0034467	FBgn0044028	FBgn0264482	FBgn0031620	FBgn0035981
FBgn0031227	FBgn0021776	FBgn0010389	FBgn0032377	FBgn0259685	FBgn0030766	FBgn0034436	FBgn0003435
FBgn0051217	FBgn0037050	FBgn0061356	FBgn0004607	FBgn0051352	FBgn0039169	FBgn0039157	FBgn0028965
FBgn0082930	FBgn0259173	FBgn0005616	FBgn0005612	FBgn0033686	FBgn0263967	FBgn0031224	FBgn0036516
FBgn0038134	FBgn0000449	FBgn0261538	FBgn0036732	FBgn0004629	FBgn0038811	FBgn0035688	FBgn0020368
FBgn0086057	FBgn0035954	FBgn0050080	FBgn0001090	FBgn0013983	FBgn0052666	FBgn0032744	FBgn0050021
FBgn0026397	FBgn0063391	FBgn0014143	FBgn0052280	FBgn0083123	FBgn0263755	FBgn0016926	FBgn0263603
FBgn0050056	FBgn0032843	FBgn0004512	FBgn0037654	FBgn0034175	FBgn0029095	FBgn0000227	FBgn0031717
FBgn0031488	FBgn0083940	FBgn0001150	FBgn0035526	FBgn0034307	FBgn0035727	FBgn0001291	FBgn0032296
FBgn0034846	FBgn0053493	FBgn0086910	FBgn0019661	FBgn0029853	FBgn0030648	FBgn0026602	FBgn0038582
FBgn0039288	FBgn0031632	FBgn0082582	FBgn0029931	FBgn0040487	FBgn0000565	FBgn0035047	FBgn0025802
FBgn0082928	FBgn0082919	FBgn0261974	FBgn0065064	FBgn0031645	FBgn0050372	FBgn0015618	FBgn0037360
FBgn0035625	FBgn0011653	FBgn0264598	FBgn0082962	FBgn0263468	FBgn0264325	FBgn0037086	FBgn0031356
FBgn0028371	FBgn0001254	FBgn0033067	FBgn0041186	FBgn0033926	FBgn0039101	FBgn0035572	FBgn0040283
FBgn0031646	FBgn0000395	FBgn0010473	FBgn0036150	FBgn0259733	FBgn0019890	FBgn0038532	FBgn0035248
FBgn0030868	FBgn0002945	FBgn0040809	FBgn0031429	FBgn0037552	FBgn0036091	FBgn0010638	FBgn0031540
FBgn0039324	FBgn0259211	FBgn0033987	FBgn0003731	FBgn0034515	FBgn0037261	FBgn0034935	FBgn0022349
FBgn0039286	FBgn0002543	FBgn0003313	FBgn0051314	FBgn0015396	FBgn0040071	FBgn0031434	FBgn0034488
FBgn0033855	FBgn0028789	FBgn0263087	FBgn0261649	FBgn0263022	FBgn0086855	FBgn0034310	FBgn0035295
FBgn0001138	FBgn0003254	FBgn0263470	FBgn0004569	FBgn0034726	FBgn0039266	FBgn0027070	FBgn0011666
FBgn0034606	FBgn0263595	FBgn0000490	FBgn0033389	FBgn0261284	FBgn0004053	FBgn0033210	FBgn0086603
FBgn0010452	FBgn0004364	FBgn0038665	FBgn0032533	FBgn0002905	FBgn0035229	FBgn0028402	FBgn0015371
FBgn0014343	FBgn0053062	FBgn0051721	FBgn0052679	FBgn0261477	FBgn0260238	FBgn0035338	FBgn0263864
FBgn0013953	FBgn0035724	FBgn0034558	FBgn0003866	FBgn0013725	FBgn0005771	FBgn0038578	FBgn0039501
FBgn0082999	FBgn0261563	FBgn0001325	FBgn0032225	FBgn0027621	FBgn0034906	FBgn0023416	FBgn0250876
FBgn0051697	FBgn0033271	FBgn0021874	FBgn0028978	FBgn0011576	FBgn0027795	FBgn0015806	FBgn0067864
FBgn0264273	FBgn0065055	FBgn0034225	FBgn0004959	FBgn0263601	FBgn0259823	FBgn0031494	FBgn0037092
FBgn0015721	FBgn0000014	FBgn0020556	FBgn0086056	FBgn0027330	FBgn0052476	FBgn0261551	FBgn0261882
FBgn0001323	FBgn0031257	FBgn0034514	FBgn0031745	FBgn0038016	FBgn0032864	FBgn0029826	FBgn0036962
FBgn0082929	FBgn0050015	FBgn0032452	FBgn0052100	FBgn0264706	FBgn0035689	FBgn0039928	FBgn0031077
FBgn0040102	FBgn0003463	FBgn0036849	FBgn0040813	FBgn0030360	FBgn0015574	FBgn0050007	FBgn0259238
FBgn0000459	FBgn0038028	FBgn0001258	FBgn0003326	FBgn0250785	FBgn0034602	FBgn0003507	FBgn0028274
FBgn0015777	FBgn0015380	FBgn0034734	FBgn0035833	FBgn0036198	FBgn0004893	FBgn0039273	FBgn0026239
FBgn0035956	FBgn0004456	FBgn0037678	FBgn0000233	FBgn0032117	FBgn0014023	FBgn0031435	FBgn0030004
FBgn0030482	FBgn0010052	FBgn0003041	FBgn0004885	FBgn0052227	FBgn0003444	FBgn0035149	FBgn0263391
FBgn0262624	FBgn0037309	FBgn0026197	FBgn0046301	FBgn0037645	FBgn0042207	FBgn0085193	FBgn0035868
FBgn0083005	FBgn0003285	FBgn0027596	FBgn0000180	FBgn0003720	FBgn0260756	FBgn0033799	FBgn0052856
FBgn0031689	FBgn0030716	FBgn0083015	FBgn0003862	FBgn0039013	FBgn0052486	FBgn0037705	FBgn0039306
FBgn0020299	FBgn0037845	FBgn0020377	FBgn0032336	FBgn0260477	FBgn0036294	FBgn0260482	FBgn0036643
FBgn0004859	FBgn0031805	FBgn0033476	FBgn0036349	FBgn0037742	FBgn0037183	FBgn0050187	FBgn0003209
FBgn0260400	FBgn0020257	FBgn0026398	FBgn0025455	FBgn0038128	FBgn0026179	FBgn0063449	FBgn0011706
FBgn0264344	FBgn0039734	FBgn0039283	FBgn0067905	FBgn0082974	FBgn0034182	FBgn0031740	FBgn0038617
FBgn0032681	FBgn0042111	FBgn0082978	FBgn0000216	FBgn0262203	FBgn0030274	FBgn0035879	FBgn0030271

FBgn0003002	FBgn0004009	FBgn0050115	FBgn0260812	FBgn0035315	FBgn0263380	FBgn0035571	FBgn0011754
FBgn0031775	FBgn0043853	FBgn0016797	FBgn0086671	FBgn0035137	FBgn0023388	FBgn0039067	FBgn0001987
FBgn0014179	FBgn0083000	FBgn0039139	FBgn0000411	FBgn0015772	FBgn0036987	FBgn0040068	FBgn0027889
FBgn0029907	FBgn0033483	FBgn0040984	FBgn0087012	FBgn0031286	FBgn0037637	FBgn0034500	FBgn0261258
FBgn0261973	FBgn0032848	FBgn0034264	FBgn0035656	FBgn0033486	FBgn0031453	FBgn0023172	FBgn0015816
FBgn0065053	FBgn0024250	FBgn0047038	FBgn0026361	FBgn0050062	FBgn0030479	FBgn0028926	FBgn0028931
FBgn0002985	FBgn0032629	FBgn0028956	FBgn0003300	FBgn0026319	FBgn0037017	FBgn0261373	FBgn0038476
FBgn0000439	FBgn0264479	FBgn0023214	FBgn0039154	FBgn0024150	FBgn0031872	FBgn0003044	FBgn0028552
FBgn0028523	FBgn0085253	FBgn0065104	FBgn0045800	FBgn0262112	FBgn0038332	FBgn0264571	FBgn0039339
FBgn0003715	FBgn0038014	FBgn0085432	FBgn0028519	FBgn0086051	FBgn0003486	FBgn0035471	FBgn0037293
FBgn0031879	FBgn0261963	FBgn0000606	FBgn0034468	FBgn0032751	FBgn0031611	FBgn0035541	FBgn0037368
FBgn0004394	FBgn0261930	FBgn0083001	FBgn0037842	FBgn0086785	FBgn0000591	FBgn0027581	FBgn0034859
FBgn0001235	FBgn0082925	FBgn0003448	FBgn0008636	FBgn0030660	FBgn0262887	FBgn0035850	FBgn0052177
FBgn0033093	FBgn0033274	FBgn0034219	FBgn0050421	FBgn0038755	FBgn0037802	FBgn0030251	FBgn0034577
FBgn0051467	FBgn0083946	FBgn0044049	FBgn0035235	FBgn0043362	FBgn0036872	FBgn0259876	FBgn0030960
FBgn0024234	FBgn0259111	FBgn0065073	FBgn0014395	FBgn0031018	FBgn0028894	FBgn0052364	FBgn0036549
FBgn0003892	FBgn0032230	FBgn0041706	FBgn0015513	FBgn0032116	FBgn0037949	FBgn0040763	FBgn0024187
FBgn0035522	FBgn0086068	FBgn0004567	FBgn0032489	FBgn0037992	FBgn0263654	FBgn0035211	FBgn0010379
FBgn0261648	FBgn0001320	FBgn0039170	FBgn0052113	FBgn0038475	FBgn0028382	FBgn0262947	FBgn0259200
FBgn0083919	FBgn0034655	FBgn0083988	FBgn0025739	FBgn0025390	FBgn0044826	FBgn0004860	FBgn0015907
FBgn0000658	FBgn0020616	FBgn0011771	FBgn0033817	FBgn0037083	FBgn0020887	FBgn0051368	FBgn0028538
FBgn0033652	FBgn0001250	FBgn0010105	FBgn0005631	FBgn0038418	FBgn0028426	FBgn0038552	FBgn0039210

Appendix K: Up-regulated genes in *Non-stop* GLC embryos

FBgn0263093	FBgn0026876	FBgn0052549	FBgn0038047	FBgn0036286	FBgn0010905	FBgn0030018	FBgn0010316
FBgn0036302	FBgn0032477	FBgn0014427	FBgn0037021	FBgn0003292	FBgn0036446	FBgn0031194	FBgn0038197
FBgn0002069	FBgn0003139	FBgn0051156	FBgn0029957	FBgn0029979	FBgn0052484	FBgn0014869	FBgn0034897
FBgn0037770	FBgn0020412	FBgn0038772	FBgn0031143	FBgn0086687	FBgn0042134	FBgn0260431	FBgn0037338
FBgn0033653	FBgn0030344	FBgn0260012	FBgn0028343	FBgn0035444	FBgn0033402	FBgn0052103	FBgn0264305
FBgn0262987	FBgn0053087	FBgn0035960	FBgn0015568	FBgn0038686	FBgn0260771	FBgn0010097	FBgn0260946
FBgn0051755	FBgn0027539	FBgn0053193	FBgn0038318	FBgn0033960	FBgn0028406	FBgn0029895	FBgn0035039
FBgn0026418	FBgn0052831	FBgn0032821	FBgn0004655	FBgn0040395	FBgn0010786	FBgn0020513	FBgn0003187
FBgn0027296	FBgn0040233	FBgn0023169	FBgn0033557	FBgn0001233	FBgn0030420	FBgn0039507	FBgn0010611
FBgn0029666	FBgn0031708	FBgn0029531	FBgn0033179	FBgn0038206	FBgn0036772	FBgn0050010	FBgn0004598
FBgn0264481	FBgn0020270	FBgn0040237	FBgn0243513	FBgn0025335	FBgn0031912	FBgn0011740	FBgn0036152
FBgn0010213	FBgn0260941	FBgn0038830	FBgn0033627	FBgn0029858	FBgn0037203	FBgn0032374	FBgn0261938
FBgn0025874	FBgn0000667	FBgn0032079	FBgn0023407	FBgn0013548	FBgn0000376	FBgn0028325	FBgn0053138
FBgn0037031	FBgn0031006	FBgn0027583	FBgn0032704	FBgn0038223	FBgn0053129	FBgn0259834	FBgn0033996
FBgn0264389	FBgn0034858	FBgn0036889	FBgn0010309	FBgn0037620	FBgn0039634	FBgn0015229	FBgn0037602
FBgn0029688	FBgn0261811	FBgn0038916	FBgn0034570	FBgn0036043	FBgn0036685	FBgn0011660	FBgn0029823
FBgn0039304	FBgn0052438	FBgn0086362	FBgn0001404	FBgn0030883	FBgn0030346	FBgn0040294	FBgn0069969
FBgn0039994	FBgn0019948	FBgn0035771	FBgn0086558	FBgn0050055	FBgn0004875	FBgn0015589	FBgn0023515
FBgn0039303	FBgn0050054	FBgn0011774	FBgn0040236	FBgn0030963	FBgn0032135	FBgn0086784	FBgn0026084
FBgn0262684	FBgn0037912	FBgn0032465	FBgn0034854	FBgn0030330	FBgn0031051	FBgn0020626	FBgn0037445
FBgn0030668	FBgn0037913	FBgn0030293	FBgn0039936	FBgn0036331	FBgn0032249	FBgn0017549	FBgn0015571
FBgn0027079	FBgn0051658	FBgn0035589	FBgn0020386	FBgn0004797	FBgn0036689	FBgn0038049	FBgn0024994
FBgn0053969	FBgn0032194	FBgn0034351	FBgn0260934	FBgn0039126	FBgn0038524	FBgn0004183	FBgn0033391
FBgn0034527	FBgn0027287	FBgn0036922	FBgn0035901	FBgn0036622	FBgn0035065	FBgn0014133	FBgn0012034
FBgn0037109	FBgn0026753	FBgn0022724	FBgn0034498	FBgn0042135	FBgn0039959	FBgn0051249	FBgn0040367
FBgn0034410	FBgn0034940	FBgn0033348	FBgn0001330	FBgn0023506	FBgn0262617	FBgn0036008	FBgn0037345
FBgn0030554	FBgn0031992	FBgn0030323	FBgn0030183	FBgn0002948	FBgn0034354	FBgn0036942	FBgn0029504
FBgn0023536	FBgn0263108	FBgn0003345	FBgn0037231	FBgn0001220	FBgn0019982	FBgn0034032	FBgn0034951
FBgn0023526	FBgn0263749	FBgn0085377	FBgn0038569	FBgn0035965	FBgn0022709	FBgn0040347	FBgn0041164
FBgn0021761	FBgn0004167	FBgn0034894	FBgn0085322	FBgn0261445	FBgn0023458	FBgn0030421	FBgn0036893
FBgn0011230	FBgn0259143	FBgn0035060	FBgn0029997	FBgn0032904	FBgn0029704	FBgn0261550	FBgn0026593
FBgn0033052	FBgn0037244	FBgn0020240	FBgn0033899	FBgn0010315	FBgn0260743	FBgn0029092	FBgn0023215
FBgn0005683	FBgn0030743	FBgn0035375	FBgn0037110	FBgn0040298	FBgn0031483	FBgn0052699	FBgn0039451
FBgn0039644	FBgn0031231	FBgn0036988	FBgn0000826	FBgn0028665	FBgn0011661	FBgn0034918	FBgn0038828
FBgn0264493	FBgn0034008	FBgn0263143	FBgn0000719	FBgn0041188	FBgn0037239	FBgn0085370	FBgn0005671
FBgn0050109	FBgn0052296	FBgn0037911	FBgn0260748	FBgn0058191	FBgn0036994	FBgn0022097	FBgn0263112
FBgn0037071	FBgn0031233	FBgn0010303	FBgn0037084	FBgn0086372	FBgn0030850	FBgn0031011	FBgn0036257
FBgn0042092	FBgn0262110	FBgn0015218	FBgn0011703	FBgn0024841	FBgn0052365	FBgn0015553	FBgn0250907
FBgn0031815	FBgn0020647	FBgn0052772	FBgn0036991	FBgn0028974	FBgn0036165	FBgn0000032	FBgn0050377
FBgn0037773	FBgn0261436	FBgn0051224	FBgn0039381	FBgn0010397	FBgn0030502	FBgn0058042	FBgn0259749
FBgn0033259	FBgn0030581	FBgn0023130	FBgn0028499	FBgn0263768	FBgn0039186	FBgn0032705	FBgn0030478

FBgn0029861	FBgn0051092	FBgn0019686	FBgn0036389	FBgn0032620	FBgn0035825	FBgn0024238	FBgn0040321
FBgn0031498	FBgn0034300	FBgn0033918	FBgn0263232	FBgn0030101	FBgn0031703	FBgn0033196	FBgn0263598
FBgn0034965	FBgn0025381	FBgn0011787	FBgn0000588	FBgn0033465	FBgn0053156	FBgn0005632	FBgn0003744
FBgn0030336	FBgn0030481	FBgn0052099	FBgn0039830	FBgn0039924	FBgn0038321	FBgn0015239	FBgn0015522
FBgn0051450	FBgn0038349	FBgn0036843	FBgn0031681	FBgn0050438	FBgn0036099	FBgn0031779	FBgn0262103
FBgn0262527	FBgn0015781	FBgn0001308	FBgn0261560	FBgn0000057	FBgn0000382	FBgn0038401	FBgn0001120
FBgn0032204	FBgn0053054	FBgn0027601	FBgn0033474	FBgn0030966	FBgn0026620	FBgn0263490	FBgn0031998
FBgn0034521	FBgn0031312	FBgn0039296	FBgn0039450	FBgn0041180	FBgn0039226	FBgn0052226	FBgn0035964
FBgn0261619	FBgn0260862	FBgn0039528	FBgn0037960	FBgn0052822	FBgn0033451	FBgn0000808	FBgn0027903
FBgn0001316	FBgn0020272	FBgn0026315	FBgn0025382	FBgn0032485	FBgn0003525	FBgn0000579	FBgn0027342
FBgn0033010	FBgn0031904	FBgn0037777	FBgn0033639	FBgn0027515	FBgn0000166	FBgn0262579	FBgn0037574
FBgn0085810	FBgn0032076	FBgn0041702	FBgn0243516	FBgn0086347	FBgn0027872	FBgn0035807	FBgn0037070
FBgn0038548	FBgn0026056	FBgn0027552	FBgn0024329	FBgn0042180	FBgn0037718	FBgn0250850	FBgn0261553
FBgn0000221	FBgn0015544	FBgn0051935	FBgn0035997	FBgn0029893	FBgn0035473	FBgn0037607	FBgn0032161
FBgn0040513	FBgn0020503	FBgn0038767	FBgn0024182	FBgn0053123	FBgn0035016	FBgn0017551	FBgn0086674
FBgn0031030	FBgn0033808	FBgn0033310	FBgn0024251	FBgn0002787	FBgn0027615	FBgn0053554	FBgn0034804
FBgn0028475	FBgn0015903	FBgn0002413	FBgn0028360	FBgn0024222	FBgn0033413	FBgn0262738	FBgn0034585
FBgn0031170	FBgn0034002	FBgn0031094	FBgn0259824	FBgn0033890	FBgn0037541	FBgn0002524	FBgn0032763
FBgn0000524	FBgn0030854	FBgn0035540	FBgn0038968	FBgn0010053	FBgn0000247	FBgn0013759	FBgn0039156
FBgn0005536	FBgn0036486	FBgn0033155	FBgn0039466	FBgn0031544	FBgn0032397	FBgn0004397	FBgn0030276
FBgn0263975	FBgn0023181	FBgn0032363	FBgn0015799	FBgn0022936	FBgn0261931	FBgn0011656	FBgn0004876
FBgn0033777	FBgn0025726	FBgn0036805	FBgn0029819	FBgn0002909	FBgn0031655	FBgn0032084	FBgn0028670
FBgn0037814	FBgn0033638	FBgn0039831	FBgn0033392	FBgn0259203	FBgn0085248	FBgn0035802	FBgn0259682
FBgn0010173	FBgn0039379	FBgn0030670	FBgn0015279	FBgn0035951	FBgn0028397	FBgn0039209	FBgn0050005
FBgn0028969	FBgn0038816	FBgn0028387	FBgn0052112	FBgn0028703	FBgn0034543	FBgn0026718	FBgn0037248
FBgn0036397	FBgn0026147	FBgn0035206	FBgn0035968	FBgn0029822	FBgn0036053	FBgn0014417	FBgn0026433
FBgn0027088	FBgn0029522	FBgn0031573	FBgn0028734	FBgn0037610	FBgn0025621	FBgn0004187	FBgn0263110
FBgn0010222	FBgn0003483	FBgn0259174	FBgn0261112	FBgn0003204	FBgn0263077	FBgn0039464	FBgn0038316
FBgn0067779	FBgn0033460	FBgn0037734	FBgn0000241	FBgn0029912	FBgn0010438	FBgn0003016	FBgn0033635
FBgn0052195	FBgn0003268	FBgn0039641	FBgn0038662	FBgn0052654	FBgn0262866	FBgn0035113	FBgn0003028
FBgn0038256	FBgn0002031	FBgn0011207	FBgn0020930	FBgn0086359	FBgn0030174	FBgn0033457	FBgn0040309
FBgn0028690	FBgn0029914	FBgn0005777	FBgn0030683	FBgn0261984	FBgn0026313	FBgn0040397	FBgn0026206
FBgn0037645	FBgn0264676	FBgn0037339	FBgn0036746	FBgn0262081	FBgn0004868	FBgn0051807	FBgn0028494
FBgn0001978	FBgn0003076	FBgn0002354	FBgn0036341	FBgn0021750	FBgn0027356	FBgn0030087	FBgn0001092
FBgn0038965	FBgn0029944	FBgn0037018	FBgn0028662	FBgn0037757	FBgn0035769	FBgn0036333	FBgn0040259
FBgn0025352	FBgn0002775	FBgn0030391	FBgn0030735	FBgn0020309	FBgn0015794	FBgn0041150	FBgn0024315
FBgn0011823	FBgn0259221	FBgn0035944	FBgn0086027	FBgn0040056	FBgn0039942	FBgn0038347	FBgn0032474
FBgn0030512	FBgn0039350	FBgn0016031	FBgn0039272	FBgn0027655	FBgn0005427	FBgn0243512	FBgn0010235
FBgn0016053	FBgn0052473	FBgn0034068	FBgn0036144	FBgn0027335	FBgn0264574	FBgn0050403	FBgn0032029
FBgn0033935	FBgn0028427	FBgn0260866	FBgn0051005	FBgn0034271	FBgn0038627	FBgn0027529	FBgn0029155
FBgn0085478	FBgn0032480	FBgn0035989	FBgn0033309	FBgn0037856	FBgn0038515	FBgn0037391	FBgn0023094
FBgn0035109	FBgn0025633	FBgn0035519	FBgn0030791	FBgn0035839	FBgn0037708	FBgn0264090	FBgn0024957
FBgn0030007	FBgn0032340	FBgn0004507	FBgn0030744	FBgn0038360	FBgn0035169	FBgn0037138	FBgn0032791

FBgn0003598	FBgn0000384	FBgn0002781	FBgn0263782	FBgn0003495	FBgn0058006	FBgn0032400	FBgn0038575
FBgn0035111	FBgn0030833	FBgn0024291	FBgn0039212	FBgn0015614	FBgn0036770	FBgn0086358	FBgn0031377
FBgn0038438	FBgn0032341	FBgn0039846	FBgn0039889	FBgn0035842	FBgn0263120	FBgn0262124	FBgn0025628
FBgn0262108	FBgn0038167	FBgn0261049	FBgn0037810	FBgn0262468	FBgn0037142	FBgn0033673	FBgn0036336
FBgn0051120	FBgn0262619	FBgn0015905	FBgn0261845	FBgn0032901	FBgn0260780	FBgn0038763	FBgn0000615
FBgn0039240	FBgn0041203	FBgn0263974	FBgn0040752	FBgn0004913	FBgn0031195	FBgn0030268	FBgn0087040
FBgn0026259	FBgn0051044	FBgn0032646	FBgn0263594	FBgn0032208	FBgn0005694	FBgn0028509	FBgn0003655
FBgn0045823	FBgn0027605	FBgn0024920	FBgn0034976	FBgn0036519	FBgn0004369	FBgn0001226	FBgn0053558
FBgn0260938	FBgn0016693	FBgn0040396	FBgn0036254	FBgn0043458	FBgn0026787	FBgn0050381	FBgn0037838
FBgn0000077	FBgn0032698	FBgn0031848	FBgn0027513	FBgn0033713	FBgn0034628	FBgn0086898	FBgn0023477
FBgn0261988	FBgn0000479	FBgn0029942	FBgn0261397	FBgn0030056	FBgn0045842	FBgn0001612	FBgn0003870
FBgn0036741	FBgn0033900	FBgn0033915	FBgn0263929	FBgn0002044	FBgn0005695	FBgn0052412	FBgn0015924
FBgn0011745	FBgn0259728	FBgn0037117	FBgn0259990	FBgn0032262	FBgn0261954	FBgn0041781	FBgn0010288
FBgn0011297	FBgn0002183	FBgn0031062	FBgn0034535	FBgn0052196	FBgn0033761	FBgn0022772	FBgn0029801
FBgn0034674	FBgn0263847	FBgn0052528	FBgn0037063	FBgn0031018	FBgn0034763	FBgn0028952	FBgn0039153
FBgn0039461	FBgn0037074	FBgn0000018	FBgn0030431	FBgn0041087	FBgn0045862	FBgn0023508	FBgn0030608
FBgn0031450	FBgn0038387	FBgn0037722	FBgn0026083	FBgn0034626	FBgn0036896	FBgn0038325	FBgn0005596
FBgn0015562	FBgn0034455	FBgn0016696	FBgn0263006	FBgn0033812	FBgn0036777	FBgn0035642	FBgn0030737
FBgn0016672	FBgn0034494	FBgn0004370	FBgn0037606	FBgn0039588	FBgn0031119	FBgn0261258	FBgn0010591
FBgn0027087	FBgn0262962	FBgn0023512	FBgn0003480	FBgn0003964	FBgn0041775	FBgn0033989	FBgn0029879
FBgn0042185	FBgn0015582	FBgn0003882	FBgn0052221	FBgn0031589	FBgn0020767	FBgn0050463	FBgn0085216
FBgn0022213	FBgn0051279	FBgn0030026	FBgn0029502	FBgn0000183	FBgn0264331	FBgn0015776	FBgn0035234
FBgn0026428	FBgn0046114	FBgn0052056	FBgn0039876	FBgn0033717	FBgn0029131	FBgn0261983	FBgn0037755
FBgn0030551	FBgn0030800	FBgn0032197	FBgn0085638	FBgn0031535	FBgn0016641	FBgn0031405	FBgn0261987
FBgn0002723	FBgn0038928	FBgn0036837	FBgn0030341	FBgn0036749	FBgn0034269	FBgn0023083	FBgn0259227
FBgn0263260	FBgn0037383	FBgn0262714	FBgn0037980	FBgn0031659	FBgn0031150	FBgn0264439	FBgn0261244
FBgn0024177	FBgn0043796	FBgn0039565	FBgn0031713	FBgn0038549	FBgn0032587	FBgn0030514	FBgn0001225
FBgn0015247	FBgn0034270	FBgn0082831	FBgn0033244	FBgn0016078	FBgn0038769	FBgn0259247	FBgn0050392
FBgn0013773	FBgn0005617	FBgn0031974	FBgn0259735	FBgn0036334	FBgn0039751	FBgn0001137	FBgn0001248
FBgn0029798	FBgn0030991	FBgn0000454	FBgn0026630	FBgn0039932	FBgn0002901	FBgn0260399	FBgn0035040
FBgn0026679	FBgn0036488	FBgn0037931	FBgn0014455	FBgn0025684	FBgn0023441	FBgn0262737	FBgn0051793
FBgn0033092	FBgn0030467	FBgn0010803	FBgn0027359	FBgn0000392	FBgn0037518	FBgn0035936	FBgn0039856
FBgn0031771	FBgn0032956	FBgn0028497	FBgn0039150	FBgn0085339	FBgn0020653	FBgn0026619	FBgn0035083
FBgn0034495	FBgn0032796	FBgn0036142	FBgn0026479	FBgn0031995	FBgn0037242	FBgn0011705	FBgn0262559
FBgn0032790	FBgn0015663	FBgn0014018	FBgn0038252	FBgn0021800	FBgn0039944	FBgn0000052	FBgn0017448
FBgn0034087	FBgn0037671	FBgn0032957	FBgn0052512	FBgn0263199	FBgn0033738	FBgn0261787	FBgn0004611
FBgn0039668	FBgn0033079	FBgn0027620	FBgn0029840	FBgn0030345	FBgn0051072	FBgn0058263	FBgn0260747
FBgn0033339	FBgn0039623	FBgn0034816	FBgn0037843	FBgn0085423	FBgn0038683	FBgn0263706	FBgn0003423
FBgn0025390	FBgn0034529	FBgn0030120	FBgn0051635	FBgn0040366	FBgn0038478	FBgn0053172	FBgn0037944
FBgn0264691	FBgn0036906	FBgn0043070	FBgn0026060	FBgn0261278	FBgn0260789	FBgn0039972	FBgn0003943
FBgn0037926	FBgn0062413	FBgn0260049	FBgn0052446	FBgn0061515	FBgn0037583	FBgn0034989	FBgn0086608
FBgn0033426	FBgn0011211	FBgn0032512	FBgn0040375	FBgn0037747	FBgn0260960	FBgn0260817	FBgn0000346
FBgn0050440	FBgn0026427	FBgn0010328	FBgn0083968	FBgn0034304	FBgn0037716	FBgn0035449	FBgn0031820

FBgn0015286	FBgn0011259	FBgn0003997	FBgn0038220	FBgn0027329	FBgn0035953	FBgn0264307	FBgn0035891
FBgn0038296	FBgn0053230	FBgn0038737	FBgn0037556	FBgn0033224	FBgn0028380	FBgn0022786	FBgn0024991
FBgn0261688	FBgn0033945	FBgn0000084	FBgn0033740	FBgn0030400	FBgn0037144	FBgn0024846	FBgn0003023
FBgn0002921	FBgn0036366	FBgn0023216	FBgn0050491	FBgn0026143	FBgn0028516	FBgn0029905	FBgn0032731
FBgn0032467	FBgn0031117	FBgn0035416	FBgn0261610	FBgn0032699	FBgn0034688	FBgn0031188	FBgn0029831
FBgn0030092	FBgn0037027	FBgn0036374	FBgn0003401	FBgn0019925	FBgn0015036	FBgn0039223	FBgn0052732
FBgn0033544	FBgn0010808	FBgn0030089	FBgn0035627	FBgn0025800	FBgn0010350	FBgn0034583	FBgn0022382
FBgn0039920	FBgn0085437	FBgn0263025	FBgn0025836	FBgn0026252	FBgn0032350	FBgn0002906	FBgn0037779
FBgn0028687	FBgn0041147	FBgn0032444	FBgn0027569	FBgn0261285	FBgn0016070	FBgn0034312	FBgn0030932
FBgn0263237	FBgn0020392	FBgn0001087	FBgn0052350	FBgn0033121	FBgn0039877	FBgn0030286	FBgn0037890
FBgn0039459	FBgn0032259	FBgn0039764	FBgn0034618	FBgn0035892	FBgn0031317	FBgn0032820	FBgn0000008
FBgn0032216	FBgn0038815	FBgn0035630	FBgn0031969	FBgn0035087	FBgn0015268	FBgn0002641	FBgn0032026
FBgn0033032	FBgn0264495	FBgn0030519	FBgn0036815	FBgn0014141	FBgn0263350	FBgn0016970	FBgn0015245
FBgn0026576	FBgn0040372	FBgn0038903	FBgn0032453	FBgn0027558	FBgn0264449	FBgn0038286	FBgn0027512
FBgn0035251	FBgn0033232	FBgn0041210	FBgn0064115	FBgn0051151	FBgn0033273	FBgn0004101	FBgn0029866
FBgn0030343	FBgn0259978	FBgn0039958	FBgn0067102	FBgn0262526	FBgn0086251	FBgn0263005	FBgn0039737
FBgn0025639	FBgn0017414	FBgn0035036	FBgn0011742	FBgn0041582	FBgn0052676	FBgn0259734	FBgn0030432
FBgn0028897	FBgn0087008	FBgn0033101	FBgn0035537	FBgn0039385	FBgn0029911	FBgn0261383	FBgn0035475
FBgn0036621	FBgn0039663	FBgn0039016	FBgn0024889	FBgn0262975	FBgn0045063	FBgn0037379	FBgn0030964
FBgn0264492	FBgn0037636	FBgn0030025	FBgn0261276	FBgn0037482	FBgn0261556	FBgn0031575	FBgn0003178
FBgn0024956	FBgn0027291	FBgn0263602	FBgn0031189	FBgn0061476	FBgn0263555	FBgn0000063	FBgn0031885
FBgn0013799	FBgn0004387	FBgn0011769	FBgn0058045	FBgn0032988	FBgn0034789	FBgn0032805	FBgn0033257
FBgn0035722	FBgn0053169	FBgn0039348	FBgn0028336	FBgn0086697	FBgn0033095	FBgn0263773	FBgn0011274
FBgn0085773	FBgn0038588	FBgn0034246	FBgn0030653	FBgn0262126	FBgn0033757	FBgn0029936	FBgn0002868
FBgn0260003	FBgn0003206	FBgn0261068	FBgn0260972	FBgn0039417	FBgn0004510	FBgn0250848	FBgn0035173
FBgn0037643	FBgn0034177	FBgn0030654	FBgn0000405	FBgn0034113	FBgn0040030	FBgn0033624	FBgn0086355
FBgn0052625	FBgn0260744	FBgn0024509	FBgn0052423	FBgn0025632	FBgn0036199	FBgn0036196	FBgn0030805
FBgn0026370	FBgn0064126	FBgn0025186	FBgn0033783	FBgn0024273	FBgn0030724	FBgn0032018	FBgn0035978
FBgn0034346	FBgn0031682	FBgn0260243	FBgn0030347	FBgn0032943	FBgn0038721	FBgn0040382	FBgn0011761
FBgn0001078	FBgn0008635	FBgn0038268	FBgn0031971	FBgn0027521	FBgn0032873	FBgn0051641	FBgn0032783
FBgn0031107	FBgn0032172	FBgn0046214	FBgn0013770	FBgn0037632	FBgn0034098	FBgn0031213	FBgn0000055
FBgn0032339	FBgn0004654	FBgn0036574	FBgn0046704	FBgn0010551	FBgn0037739	FBgn0263278	FBgn0025693
FBgn0033313	FBgn0033212	FBgn0261461	FBgn0034313	FBgn0050343	FBgn0031263	FBgn0031516	FBgn0035641
FBgn0021873	FBgn0004903	FBgn0011802	FBgn0005654	FBgn0037924	FBgn0001091	FBgn0030740	FBgn0035402
FBgn0037376	FBgn0037728	FBgn0038860	FBgn0031126	FBgn0028916	FBgn0259178	FBgn0022710	FBgn0003015
FBgn0015019	FBgn0035995	FBgn0052485	FBgn0025469	FBgn0003475	FBgn0038344	FBgn0026738	FBgn0001149
FBgn0259709	FBgn0029821	FBgn0031374	FBgn0036237	FBgn0263395	FBgn0030612	FBgn0034629	FBgn0035266
FBgn0039674	FBgn0034371	FBgn0032521	FBgn0001128	FBgn0033984	FBgn0032513	FBgn0002719	FBgn0011826
FBgn0250755	FBgn0036662	FBgn0037026	FBgn0039118	FBgn0052626	FBgn0259711	FBgn0051262	FBgn0086254
FBgn0031091	FBgn0035432	FBgn0030734	FBgn0029157	FBgn0086475	FBgn0001186	FBgn0000351	FBgn0040348
FBgn0036671	FBgn0031395	FBgn0031457	FBgn0042213	FBgn0032889	FBgn0010431	FBgn0000114	
FBgn0028476	FBgn0038400	FBgn0052767	FBgn0037364	FBgn0033195	FBgn0038432	FBgn0039869	
FBgn0036405	FBgn0011692	FBgn0045035	FBgn0037521	FBgn0014906	FBgn0034261	FBgn0037646	

Appendix L: Down-regulated genes in Non-stop GLC embryos

FBgn0003091	FBgn0030684	FBgn0001090	FBgn0010109	FBgn0003944	FBgn0031623	FBgn0036549	FBgn0028982
FBgn0052115	FBgn0051697	FBgn0004456	FBgn0023214	FBgn0085432	FBgn0031717	FBgn0038418	FBgn0001332
FBgn0263219	FBgn0040759	FBgn0083015	FBgn0262531	FBgn0023416	FBgn0038476	FBgn0034817	FBgn0029693
FBgn0038773	FBgn0034515	FBgn0019661	FBgn0025881	FBgn0033210	FBgn0036545	FBgn0039306	FBgn0034611
FBgn0035245	FBgn0261538	FBgn0031257	FBgn0000557	FBgn0003308	FBgn0263967	FBgn0028894	FBgn0035158
FBgn0035246	FBgn0050080	FBgn0051536	FBgn0043841	FBgn0040370	FBgn0028402	FBgn0000629	FBgn0036212
FBgn0038944	FBgn0035956	FBgn0033271	FBgn0002905	FBgn0040071	FBgn0028506	FBgn0083972	FBgn0051922
FBgn0039419	FBgn0024150	FBgn0031620	FBgn0005771	FBgn0013699	FBgn0026666	FBgn0027885	FBgn0023388
FBgn0264273	FBgn0029123	FBgn0262031	FBgn0039167	FBgn0020415	FBgn0040763	FBgn0033744	FBgn0024245
FBgn0004174	FBgn0020299	FBgn0260011	FBgn0034175	FBgn0033785	FBgn0037105	FBgn0035689	FBgn0053052
FBgn0038647	FBgn0035348	FBgn0004108	FBgn0036882	FBgn0031393	FBgn0030004	FBgn0031458	FBgn0051223
FBgn0086671	FBgn0004635	FBgn0011653	FBgn0038894	FBgn0038128	FBgn0001291	FBgn0034447	FBgn0083983
FBgn0085273	FBgn0010389	FBgn0015380	FBgn0033389	FBgn0259745	FBgn0005590	FBgn0024891	FBgn0259113
FBgn0263467	FBgn0063298	FBgn0039098	FBgn0033926	FBgn0013684	FBgn0262947	FBgn0063491	FBgn0035370
FBgn0063391	FBgn0020377	FBgn0034468	FBgn0036338	FBgn0031718	FBgn0003862	FBgn0030659	FBgn0005696
FBgn0031129	FBgn0082926	FBgn0001138	FBgn0263601	FBgn0013694	FBgn0004449	FBgn0003391	FBgn0052038
FBgn0031646	FBgn0034264	FBgn0034013	FBgn0035235	FBgn0037513	FBgn0040823	FBgn0025678	FBgn0036192
FBgn0053503	FBgn0262029	FBgn0087012	FBgn0019650	FBgn0000723	FBgn0052113	FBgn0038166	FBgn0029093
FBgn0051909	FBgn0034462	FBgn0052227	FBgn0036986	FBgn0038755	FBgn0036813	FBgn0039065	FBgn0030028
FBgn0004878	FBgn0020556	FBgn0003300	FBgn0040392	FBgn0259733	FBgn0037368	FBgn0050428	FBgn0039164
FBgn0051217	FBgn0263256	FBgn0033069	FBgn0032002	FBgn0034504	FBgn0039266	FBgn0013674	FBgn0013704
FBgn0050489	FBgn0010452	FBgn0000157	FBgn0261503	FBgn0035137	FBgn0002561	FBgn0052865	FBgn0036000
FBgn0264344	FBgn0033649	FBgn0038909	FBgn0037007	FBgn0011695	FBgn0261477	FBgn0014857	FBgn0001215
FBgn0039324	FBgn0029114	FBgn0031689	FBgn0052829	FBgn0031227	FBgn0263707	FBgn0015816	FBgn0028538
FBgn0004892	FBgn0259173	FBgn0039006	FBgn0053062	FBgn0034822	FBgn0038617	FBgn0052243	FBgn0032452
FBgn0032048	FBgn0000395	FBgn0032533	FBgn0004053	FBgn0051313	FBgn0037265	FBgn0011327	FBgn0033994
FBgn0032693	FBgn0027364	FBgn0262001	FBgn0004867	FBgn0035229	FBgn0082953	FBgn0028382	FBgn0260742
FBgn0038134	FBgn0026061	FBgn0039101	FBgn0259244	FBgn0001965	FBgn0032491	FBgn0013678	FBgn0036927
FBgn0040813	FBgn0037083	FBgn0053653	FBgn0036003	FBgn0037949	FBgn0261393	FBgn0037644	FBgn0003435
FBgn0085424	FBgn0035727	FBgn0040809	FBgn0003517	FBgn0014163	FBgn0035211	FBgn0052486	FBgn0031639
FBgn0052214	FBgn0013953	FBgn0038977	FBgn0027793	FBgn0050421	FBgn0050187	FBgn0263289	FBgn0036734
FBgn0026398	FBgn0039154	FBgn0035954	FBgn0034490	FBgn0264482	FBgn0032535	FBgn0030960	FBgn0027835
FBgn0083919	FBgn0037797	FBgn0015777	FBgn0035725	FBgn0031319	FBgn0025739	FBgn0039638	FBgn0264385
FBgn0033461	FBgn0003892	FBgn0001257	FBgn0020300	FBgn0036648	FBgn0037883	FBgn0250789	FBgn0035372
FBgn0013717	FBgn0031805	FBgn0002633	FBgn0052037	FBgn0036844	FBgn0262109	FBgn0027660	FBgn0052267
FBgn0264467	FBgn0004885	FBgn0038150	FBgn0040532	FBgn0037363	FBgn0032117	FBgn0028926	FBgn0020389
FBgn0083991	FBgn0024250	FBgn0035521	FBgn0035346	FBgn0033528	FBgn0025456	FBgn0083005	FBgn0004587
FBgn0065064	FBgn0001320	FBgn0001234	FBgn0263830	FBgn0019886	FBgn0041627	FBgn0037378	FBgn0035047
FBgn0063386	FBgn0033274	FBgn0003683	FBgn0037974	FBgn0014342	FBgn0003444	FBgn0030572	FBgn0031549
FBgn0015399	FBgn0031592	FBgn0038981	FBgn0026197	FBgn0032493	FBgn0013983	FBgn0264504	FBgn0259676
FBgn0086662	FBgn0039283	FBgn0031417	FBgn0003507	FBgn0038475	FBgn0263485	FBgn0035829	FBgn0250820

FBgn0262605	FBgn0026063	FBgn0051467	FBgn0003430	FBgn0031636	FBgn0050372	FBgn0003353	FBgn0040931
FBgn0011723	FBgn0028523	FBgn0042111	FBgn0031644	FBgn0030660	FBgn0013680	FBgn0000575	FBgn0037293
FBgn0001323	FBgn0035522	FBgn0263873	FBgn0011706	FBgn0014023	FBgn0037816	FBgn0034958	FBgn0033194
FBgn0030482	FBgn0000576	FBgn0085352	FBgn0263316	FBgn0036135	FBgn0038020	FBgn0051032	FBgn0030479
FBgn0034479	FBgn0051004	FBgn0003720	FBgn0033268	FBgn0039937	FBgn0003042	FBgn0031607	FBgn0014879
FBgn0050062	FBgn0004959	FBgn0037678	FBgn0035572	FBgn0037261	FBgn0034083	FBgn0037360	FBgn0003607
FBgn0082930	FBgn0034724	FBgn0004893	FBgn0040038	FBgn0033107	FBgn0005634	FBgn0031459	FBgn0032059
FBgn0034937	FBgn0030868	FBgn0034935	FBgn0003250	FBgn0024194	FBgn0039349	FBgn0031633	FBgn0031764
FBgn0036503	FBgn0029930	FBgn0001250	FBgn0036369	FBgn0083027	FBgn0039172	FBgn0032296	FBgn0035248
FBgn0039585	FBgn0034126	FBgn0026319	FBgn0263477	FBgn0038242	FBgn0263440	FBgn0264721	FBgn0003984
FBgn0035625	FBgn0001077	FBgn0027596	FBgn0039678	FBgn0015543	FBgn0033087	FBgn0038578	FBgn0037696
FBgn0263595	FBgn0032116	FBgn0005631	FBgn0085223	FBgn0030807	FBgn0019936	FBgn0001180	FBgn0003559
FBgn0021776	FBgn0003313	FBgn0036791	FBgn0031907	FBgn0034963	FBgn0030411	FBgn0036271	FBgn0037978
FBgn0037375	FBgn0263087	FBgn0020257	FBgn0021874	FBgn0036872	FBgn0039404	FBgn0034436	FBgn0015600
FBgn0036150	FBgn0035724	FBgn0043853	FBgn0030675	FBgn0052100	FBgn0011225	FBgn0011817	FBgn0001341
FBgn0032682	FBgn0029771	FBgn0032336	FBgn0033481	FBgn0045064	FBgn0032858	FBgn0030786	FBgn0039113
FBgn0041156	FBgn0002528	FBgn0259823	FBgn0046301	FBgn0004054	FBgn0031077	FBgn0034062	FBgn0051368
FBgn0011206	FBgn0004567	FBgn0035608	FBgn0016762	FBgn0035852	FBgn0040234	FBgn0033905	FBgn0034075
FBgn0034225	FBgn0004629	FBgn0003510	FBgn0016926	FBgn0264707	FBgn0024236	FBgn0020496	FBgn0031479
FBgn0010228	FBgn0050296	FBgn0260238	FBgn0037085	FBgn0004861	FBgn0035726	FBgn0015625	FBgn0034335
FBgn0000659	FBgn0261930	FBgn0000233	FBgn0085408	FBgn0010638	FBgn0028956	FBgn0039116	FBgn0020910
FBgn0029907	FBgn0035315	FBgn0261974	FBgn0042207	FBgn0002629	FBgn0262952	FBgn0033372	FBgn0030208
FBgn0030592	FBgn0037309	FBgn0053200	FBgn0082987	FBgn0032213	FBgn0042199	FBgn0024833	FBgn0030870
FBgn0082999	FBgn0001325	FBgn0000658	FBgn0039928	FBgn0041186	FBgn0263233	FBgn0026324	FBgn0031873
FBgn0039286	FBgn0029931	FBgn0065053	FBgn0036461	FBgn0037092	FBgn0015907	FBgn0011305	FBgn0261241
FBgn0004859	FBgn0041160	FBgn0261873	FBgn0263654	FBgn0033241	FBgn0036057	FBgn0016122	FBgn0004915
FBgn0000449	FBgn0034846	FBgn0028978	FBgn0262418	FBgn0000116	FBgn0036056	FBgn0003082	FBgn0035423
FBgn0002985	FBgn0003896	FBgn0036350	FBgn0082958	FBgn0030079	FBgn0029892	FBgn0004367	FBgn0037930
FBgn0000489	FBgn0033652	FBgn0035157	FBgn0050432	FBgn0033486	FBgn0002932	FBgn0027949	FBgn0001280
FBgn0014388	FBgn0051721	FBgn0036351	FBgn0039727	FBgn0039941	FBgn0033871	FBgn0051973	FBgn0004795
FBgn0001123	FBgn0028373	FBgn0004102	FBgn0083971	FBgn0261552	FBgn0027621	FBgn0001297	FBgn0035338
FBgn0033855	FBgn0033987	FBgn0036778	FBgn0031621	FBgn0032633	FBgn0035149	FBgn0261373	FBgn0034644
FBgn0039734	FBgn0053481	FBgn0264270	FBgn0013698	FBgn0032235	FBgn0052816	FBgn0036291	FBgn0263667
FBgn0085243	FBgn0038665	FBgn0085253	FBgn0083039	FBgn0261952	FBgn0001224	FBgn0034726	FBgn0004921
FBgn0260400	FBgn0083000	FBgn0261963	FBgn0043854	FBgn0011829	FBgn0031286	FBgn0263864	FBgn0039743
FBgn0082929	FBgn0033817	FBgn0004956	FBgn0003312	FBgn0038582	FBgn0032050	FBgn0000463	FBgn0037356
FBgn0003002	FBgn0261830	FBgn0016797	FBgn0034219	FBgn0045800	FBgn0086371	FBgn0030053	FBgn0031996
FBgn0264601	FBgn0033159	FBgn0261111	FBgn0029826	FBgn0036551	FBgn0063449	FBgn0261823	FBgn0033751
FBgn0033067	FBgn0263971	FBgn0010651	FBgn0264706	FBgn0027330	FBgn0029958	FBgn0031494	FBgn0035026
FBgn0082941	FBgn0002945	FBgn0014863	FBgn0039013	FBgn0035824	FBgn0003411	FBgn0261380	FBgn0034893
FBgn0034467	FBgn0041706	FBgn0037186	FBgn0086704	FBgn0085295	FBgn0263755	FBgn0086679	FBgn0028504
FBgn0000542	FBgn0261563	FBgn0001174	FBgn0082978	FBgn0036450	FBgn0013697	FBgn0025865	FBgn0010416
FBgn0039673	FBgn0082925	FBgn0034182	FBgn0262577	FBgn0053493	FBgn0037742	FBgn0013685	FBgn0015298

FBgn0262624	FBgn0026320	FBgn0003041	FBgn0261836	FBgn0261269	FBgn0259685	FBgn0032205	FBgn0085192
FBgn0032681	FBgn0026077	FBgn0033093	FBgn0039273	FBgn0261882	FBgn0029959	FBgn0031676	FBgn0038168
FBgn0262112	FBgn0004009	FBgn0030317	FBgn0035571	FBgn0013683	FBgn0010225	FBgn0037844	FBgn0003977
FBgn0003254	FBgn0030469	FBgn0000100	FBgn0038833	FBgn0031435	FBgn0032401	FBgn0025455	FBgn0028399
FBgn0024732	FBgn0261973	FBgn0082582	FBgn0030716	FBgn0040297	FBgn0051040	FBgn0035204	FBgn0015521
FBgn0000459	FBgn0040984	FBgn0036962	FBgn0032691	FBgn0003865	FBgn0037552	FBgn0034705	FBgn0263911
FBgn0034606	FBgn0001150	FBgn0036732	FBgn0086672	FBgn0021875	FBgn0031611	FBgn0260857	FBgn0039543
FBgn0036287	FBgn0053555	FBgn0036349	FBgn0015513	FBgn0037902	FBgn0030648	FBgn0067629	FBgn0024912
FBgn0052679	FBgn0012037	FBgn0001254	FBgn0031488	FBgn0037515	FBgn0030271	FBgn0030289	FBgn0261266
FBgn0039000	FBgn0010052	FBgn0003719	FBgn0050431	FBgn0036771	FBgn0035981	FBgn0039218	FBgn0038491
FBgn0010473	FBgn0032377	FBgn0014143	FBgn0037149	FBgn0025676	FBgn0034614	FBgn0032864	FBgn0034500
FBgn0037845	FBgn0086057	FBgn0033809	FBgn0029095	FBgn0010041	FBgn0036670	FBgn0050499	FBgn0063492
FBgn0259211	FBgn0051144	FBgn0263380	FBgn0038419	FBgn0030361	FBgn0039462	FBgn0033814	FBgn0046322
FBgn0028371	FBgn0264089	FBgn0014179	FBgn0005672	FBgn0031434	FBgn0037017	FBgn0032000	FBgn0022893
FBgn0031632	FBgn0050285	FBgn0001258	FBgn0015949	FBgn0039590	FBgn0037561	FBgn0031540	FBgn0030082
FBgn0260477	FBgn0044049	FBgn0034655	FBgn0004389	FBgn0051352	FBgn0264325	FBgn0031398	FBgn0013762
FBgn0003145	FBgn0083003	FBgn0264542	FBgn0004569	FBgn0024230	FBgn0023172	FBgn0003053	FBgn0039068
FBgn0082919	FBgn0013725	FBgn0086068	FBgn0039204	FBgn0035868	FBgn0037973	FBgn0031260	FBgn0026879
FBgn0025776	FBgn0032428	FBgn0000477	FBgn0061356	FBgn0004646	FBgn0052666	FBgn0013686	FBgn0032329
FBgn0000014	FBgn0260745	FBgn0000565	FBgn0000591	FBgn0028983	FBgn0030799	FBgn0038788	FBgn0030766
FBgn0259111	FBgn0028519	FBgn0032233	FBgn0028552	FBgn0034392	FBgn0036213	FBgn0085261	FBgn0038552
FBgn0005616	FBgn0262719	FBgn0250876	FBgn0259817	FBgn0032382	FBgn0259238	FBgn0052177	FBgn0037573
FBgn0261356	FBgn0044328	FBgn0044028	FBgn0029853	FBgn0086603	FBgn0033240	FBgn0028541	FBgn0033453
FBgn0003328	FBgn0082931	FBgn0031630	FBgn0264469	FBgn0034488	FBgn0037469	FBgn0033842	FBgn0030915
FBgn0039343	FBgn0260482	FBgn0034275	FBgn0015831	FBgn0026179	FBgn0038055	FBgn0031320	FBgn0264507
FBgn0004394	FBgn0003900	FBgn0082954	FBgn0260935	FBgn0262887	FBgn0029868	FBgn0259204	FBgn0011260
FBgn0013272	FBgn0000490	FBgn0036849	FBgn0263468	FBgn0039067	FBgn0036198	FBgn0037670	FBgn0039406
FBgn0063261	FBgn0004364	FBgn0032489	FBgn0035295	FBgn0038016	FBgn0051648	FBgn0035334	FBgn0024285
FBgn0261648	FBgn0000606	FBgn0034906	FBgn0019968	FBgn0053526	FBgn0011704	FBgn0038976	FBgn0040238
FBgn0263610	FBgn0039288	FBgn0010238	FBgn0037086	FBgn0038146	FBgn0035484	FBgn0262517	FBgn0035073
FBgn0000071	FBgn0034514	FBgn0039139	FBgn0067905	FBgn0025790	FBgn0034849	FBgn0032744	FBgn0013981
FBgn0032225	FBgn0010105	FBgn0022160	FBgn0035526	FBgn0001324	FBgn0039169	FBgn0037372	FBgn0024432
FBgn0002931	FBgn0000180	FBgn0034602	FBgn0052476	FBgn0013681	FBgn0035849	FBgn0038760	FBgn0030269
FBgn0024234	FBgn0003448	FBgn0038247	FBgn0035674	FBgn0040068	FBgn0033690	FBgn0259992	FBgn0039930
FBgn0004052	FBgn0027611	FBgn0264571	FBgn0082928	FBgn0031356	FBgn0033590	FBgn0033265	FBgn0014002
FBgn0032230	FBgn0053207	FBgn0015574	FBgn0262166	FBgn0035987	FBgn0033901	FBgn0069923	FBgn0053774
FBgn0001168	FBgn0004595	FBgn0050015	FBgn0035569	FBgn0038332	FBgn0031740	FBgn0036643	FBgn0036847
FBgn0031879	FBgn0031745	FBgn0020616	FBgn0032345	FBgn0030642	FBgn0013675	FBgn0037661	FBgn0040534
FBgn0032335	FBgn0036715	FBgn0003731	FBgn0050383	FBgn0024371	FBgn0051118	FBgn0003567	FBgn0035162
FBgn0038385	FBgn0040296	FBgn0051710	FBgn0052104	FBgn0032751	FBgn0032847	FBgn0011336	FBgn0039713
FBgn0052372	FBgn0261649	FBgn0002732	FBgn0264546	FBgn0038039	FBgn0063497	FBgn0011666	FBgn0035422
FBgn0262867	FBgn0043791	FBgn0263470	FBgn0034964	FBgn0038194	FBgn0259818	FBgn0037719	FBgn0013726
FBgn0050089	FBgn0262203	FBgn0030796	FBgn0034879	FBgn0085443	FBgn0086736	FBgn0025286	FBgn0000617

FBgn0038028	FBgn0030360	FBgn0263022	FBgn0054031	FBgn0037802	FBgn0004583	FBgn0034361	FBgn0033527
FBgn0050056	FBgn0032843	FBgn0083973	FBgn0034464	FBgn0050398	FBgn0033458	FBgn0250837	FBgn0011604
FBgn0082961	FBgn0005636	FBgn0035542	FBgn0022740	FBgn0250788	FBgn0032799	FBgn0014868	FBgn0024332
FBgn0000439	FBgn0035656	FBgn0038071	FBgn0003117	FBgn0051161	FBgn0250814	FBgn0028744	FBgn0037882
FBgn0023001	FBgn0008636	FBgn0032666	FBgn0065104	FBgn0054039	FBgn0262886	FBgn0027259	FBgn0031664
FBgn0031001	FBgn0000411	FBgn0038012	FBgn0001223	FBgn0040283	FBgn0261802	FBgn0034997	FBgn0086711
FBgn0037050	FBgn0020546	FBgn0015277	FBgn0011576	FBgn0000228	FBgn0035436	FBgn0038704	FBgn0037439
FBgn0003067	FBgn0028789	FBgn0040102	FBgn0034501	FBgn0264332	FBgn0052856	FBgn0016984	FBgn0263740
FBgn0050115	FBgn0015773	FBgn0030251	FBgn0086051	FBgn0032244	FBgn0035443	FBgn0025802	FBgn0028411
FBgn0083946	FBgn0026160	FBgn0045761	FBgn0083123	FBgn0014395	FBgn0002873	FBgn0038453	FBgn0051717
FBgn0026397	FBgn0036091	FBgn0086056	FBgn0035546	FBgn0019890	FBgn0032291	FBgn0027617	FBgn0028540
FBgn0003463	FBgn0039738	FBgn0037753	FBgn0033476	FBgn0030974	FBgn0036811	FBgn0040773	FBgn0260750
FBgn0037842	FBgn0264598	FBgn0028491	FBgn0263457	FBgn0036684	FBgn0021847	FBgn0051314	FBgn0030943
FBgn0052982	FBgn0032848	FBgn0026361	FBgn0030274	FBgn0003227	FBgn0086855	FBgn0038395	FBgn0032921
FBgn0037213	FBgn0046253	FBgn0262813	FBgn0037183	FBgn0263619	FBgn0036992	FBgn0037481	FBgn0003396
FBgn0014343	FBgn0024244	FBgn0260812	FBgn0001099	FBgn0085343	FBgn0250785	FBgn0013679	FBgn0033454
FBgn0033483	FBgn0038014	FBgn0003866	FBgn0025712	FBgn0020887	FBgn0001981	FBgn0004227	FBgn0030500
FBgn0264479	FBgn0083940	FBgn0035236	FBgn0037637	FBgn0038431	FBgn0036007	FBgn0038304	FBgn0032248
FBgn0262405	FBgn0261434	FBgn0000216	FBgn0027108	FBgn0033526	FBgn0028426	FBgn0031990	FBgn0039642
FBgn0082974	FBgn0086519	FBgn0083001	FBgn0086785	FBgn0031897	FBgn0053113	FBgn0001104	FBgn0030671
FBgn0083988	FBgn0052595	FBgn0036810	FBgn0261800	FBgn0038191	FBgn0037617	FBgn0039501	FBgn0026373
FBgn0033872	FBgn0082986	FBgn0031645	FBgn0035833	FBgn0038950	FBgn0038363	FBgn0011592	FBgn0034902
FBgn0001235	FBgn0038566	FBgn0031429	FBgn0087007	FBgn0035850	FBgn0263981	FBgn0033450	FBgn0035703
FBgn0085412	FBgn0002631	FBgn0000227	FBgn0013755	FBgn0038811	FBgn0004143	FBgn0031719	FBgn0036667
FBgn0262945	FBgn0086910	FBgn0003486	FBgn0031453	FBgn0026602	FBgn0027795	FBgn0036294	FBgn0050359
FBgn0041184	FBgn0004607	FBgn0082962	FBgn0039859	FBgn0034310	FBgn0260990	FBgn0028965	FBgn0029002
FBgn0002543	FBgn0038172	FBgn0032156	FBgn0034307	FBgn0082979	FBgn0035272	FBgn0033978	FBgn0034982
FBgn0005612	FBgn0003326	FBgn0031775	FBgn0013767	FBgn0031574	FBgn0013676	FBgn0036354	FBgn0038532
FBgn0038804	FBgn0053099	FBgn0065073	FBgn0043362	FBgn0031245	FBgn0004597	FBgn0000022	FBgn0010408
FBgn0004512	FBgn0034558	FBgn0065055	FBgn0040344	FBgn0034734	FBgn0038872	FBgn0032036	FBgn0085364
FBgn0003715	FBgn0032629	FBgn0053267	FBgn0033674	FBgn0035570	FBgn0035879	FBgn0015806	FBgn0037135
FBgn0002645	FBgn0052280	FBgn0037992	FBgn0032891	FBgn0047038	FBgn0033988	FBgn0025830	
FBgn0015721	FBgn0036547	FBgn0040487	FBgn0011771	FBgn0032221	FBgn0022787	FBgn0000394	

Appendix M: Up-regulated genes in *Ada2b* KD embryos

FBgn0261446	FBgn0036501	FBgn0011297	FBgn0263619
FBgn0052816	FBgn0016794	FBgn0261068	FBgn0262886
FBgn0040370	FBgn0031968	FBgn0038974	FBgn0039932
FBgn0034075	FBgn0265525	FBgn0021768	FBgn0010288
FBgn0250907	FBgn0263219	FBgn0028695	FBgn0013681
FBgn0036135	FBgn0004167	FBgn0036493	FBgn0004368
FBgn0031092	FBgn0265533	FBgn0032883	FBgn0265590
FBgn0262108	FBgn0029878	FBgn0264855	FBgn0003654
FBgn0264955	FBgn0264866	FBgn0024920	FBgn0001224
FBgn0027571	FBgn0052485	FBgn0011740	FBgn0033342
FBgn0002868	FBgn0030432	FBgn0022344	FBgn0030174
FBgn0038740	FBgn0031535	FBgn0262902	FBgn0035630
FBgn0011829	FBgn0263110	FBgn0266319	FBgn0016036
FBgn0028743	FBgn0028688	FBgn0029688	FBgn0038742
FBgn0039927	FBgn0266745	FBgn0011745	FBgn0015268
FBgn0042174	FBgn0039357	FBgn0041147	FBgn0036136
FBgn0039114	FBgn0039431	FBgn0038490	FBgn0036772
FBgn0030852	FBgn0063497	FBgn0050159	FBgn0035039
FBgn0261258	FBgn0264841	FBgn0085638	FBgn0031769
FBgn0052625	FBgn0033451	FBgn0014141	FBgn0015036
FBgn0266396	FBgn0032213	FBgn0025800	FBgn0032873
FBgn0034270	FBgn0003997	FBgn0039836	FBgn0052581
FBgn0036368	FBgn0034255	FBgn0034691	FBgn0002354
FBgn0267588	FBgn0029830	FBgn0027085	FBgn0035266
FBgn0032679	FBgn0052772	FBgn0262559	FBgn0029866
FBgn0030294	FBgn0266369	FBgn0030137	
FBgn0031058	FBgn0034245	FBgn0027948	
FBgn0034694	FBgn0052373	FBgn0015282	
FBgn0050460	FBgn0264704	FBgn0003423	
FBgn0063494	FBgn0036896	FBgn0259749	
FBgn0038577	FBgn0033627	FBgn0028692	
FBgn0054001	FBgn0011826	FBgn0039153	
FBgn0265254	FBgn0029504	FBgn0031422	
FBgn0011206	FBgn0261285	FBgn0031894	
FBgn0052364	FBgn0266304	FBgn0266549	
FBgn0040823	FBgn0026206	FBgn0015283	
FBgn0030968	FBgn0031633	FBgn0037602	
FBgn0015299	FBgn0264702	FBgn0029711	
FBgn0262364	FBgn0051145	FBgn0034573	
FBgn0037138	FBgn0032819	FBgn0052594	

Appendix N: Down-regulated genes in *Ada2b* KD embryos

FBgn0053503	FBgn0033067	FBgn0011706	FBgn0029750	FBgn0051217	FBgn0035035	FBgn0051648	FBgn0035570
FBgn0020415	FBgn0063491	FBgn0041721	FBgn0034464	FBgn0000490	FBgn0028491	FBgn0003463	FBgn0015949
FBgn0265203	FBgn0264676	FBgn0032116	FBgn0051658	FBgn0265149	FBgn0004512	FBgn0034467	FBgn0013767
FBgn0038734	FBgn0039938	FBgn0051004	FBgn0038279	FBgn0054031	FBgn0038134	FBgn0037921	FBgn0001323
FBgn0260435	FBgn0035969	FBgn0036330	FBgn0031592	FBgn0263971	FBgn0010109	FBgn0013272	FBgn0038071
FBgn0037555	FBgn0033392	FBgn0038566	FBgn0037372	FBgn0035656	FBgn0020377	FBgn0030807	FBgn0033987
FBgn0020414	FBgn0083991	FBgn0031184	FBgn0266691	FBgn0032645	FBgn0005771	FBgn0267170	FBgn0000228
FBgn0050489	FBgn0039226	FBgn0035264	FBgn0045842	FBgn0001090	FBgn0026361	FBgn0004629	FBgn0038150
FBgn0033875	FBgn0031032	FBgn0266808	FBgn0021776	FBgn0264479	FBgn0044028	FBgn0003002	FBgn0033356
FBgn0027611	FBgn0063923	FBgn0261930	FBgn0034514	FBgn0037085	FBgn0015399	FBgn0004635	FBgn0003300
FBgn0039419	FBgn0030868	FBgn0050359	FBgn0266756	FBgn0051865	FBgn0029907	FBgn0053200	FBgn0266653
FBgn0035189	FBgn0034354	FBgn0036791	FBgn0040984	FBgn0020616	FBgn0031435	FBgn0037007	FBgn0034612
FBgn0036749	FBgn0032889	FBgn0011723	FBgn0037992	FBgn0083039	FBgn0004108	FBgn0035132	FBgn0026197
FBgn0050046	FBgn0031157	FBgn0036857	FBgn0005616	FBgn0266179	FBgn0053207	FBgn0266804	FBgn0035235
FBgn0259710	FBgn0267530	FBgn0264344	FBgn0030251	FBgn0053493	FBgn0010105	FBgn0052829	FBgn0037802
FBgn0039006	FBgn0001987	FBgn0039098	FBgn0263457	FBgn0263745	FBgn0024234	FBgn0025390	FBgn0085732
FBgn0033027	FBgn0038804	FBgn0032335	FBgn0036738	FBgn0029114	FBgn0033817	FBgn0051710	FBgn0042199
FBgn0034756	FBgn0051119	FBgn0085424	FBgn0265985	FBgn0004009	FBgn0001256	FBgn0262945	FBgn0266814
FBgn0267191	FBgn0014143	FBgn0266428	FBgn0250876	FBgn0034614	FBgn0030507	FBgn0053155	FBgn0032489
FBgn0037513	FBgn0029588	FBgn0036778	FBgn0020257	FBgn0037261	FBgn0028789	FBgn0001077	FBgn0259244
FBgn0035246	FBgn0265761	FBgn0004878	FBgn0036350	FBgn0264957	FBgn0041706	FBgn0035956	FBgn0010452
FBgn0039343	FBgn0020300	FBgn0000233	FBgn0032535	FBgn0013755	FBgn0050156	FBgn0034808	FBgn0038385
FBgn0031053	FBgn0250785	FBgn0010228	FBgn0000565	FBgn0031393	FBgn0003892	FBgn0010473	FBgn0000395
FBgn0034126	FBgn0024179	FBgn0003900	FBgn0027793	FBgn0024250	FBgn0050285	FBgn0259936	FBgn0003411
FBgn0038012	FBgn0033926	FBgn0023214	FBgn0004187	FBgn0003719	FBgn0004143	FBgn0024150	FBgn0033590
FBgn0046776	FBgn0004396	FBgn0003720	FBgn0038833	FBgn0262719	FBgn0000180	FBgn0028519	FBgn0033210
FBgn0035642	FBgn0034846	FBgn0266628	FBgn0001325	FBgn0032377	FBgn0264838	FBgn0003865	FBgn0035267
FBgn0051997	FBgn0029881	FBgn0085364	FBgn0043854	FBgn0046253	FBgn0267605	FBgn0033431	FBgn0035348
FBgn0034999	FBgn0000576	FBgn0032230	FBgn0050062	FBgn0262867	FBgn0250824	FBgn0032681	FBgn0031721
FBgn0035641	FBgn0039941	FBgn0004052	FBgn0267728	FBgn0003430	FBgn0000071	FBgn0036461	FBgn0016762
FBgn0035484	FBgn0058053	FBgn0266347	FBgn0031129	FBgn0026570	FBgn0011761	FBgn0031645	FBgn0032244
FBgn0262887	FBgn0003254	FBgn0083973	FBgn0082999	FBgn0002985	FBgn0031086	FBgn0083124	FBgn0264817
FBgn0069969	FBgn0010052	FBgn0036503	FBgn0039266	FBgn0263967	FBgn0031745	FBgn0033978	FBgn0083121
FBgn0066101	FBgn0023197	FBgn0043853	FBgn0019661	FBgn0003731	FBgn0033069	FBgn0039013	FBgn0263595
FBgn0263236	FBgn0013995	FBgn0039288	FBgn0031718	FBgn0035236	FBgn0032235	FBgn0001180	FBgn0058263
FBgn0259224	FBgn0262109	FBgn0015543	FBgn0266686	FBgn0031719	FBgn0012037	FBgn0032336	FBgn0259173
FBgn0030666	FBgn0032431	FBgn0015831	FBgn0035770	FBgn0000606	FBgn0035954	FBgn0265819	FBgn0261648
FBgn0031031	FBgn0040759	FBgn0000542	FBgn0004053	FBgn0085352	FBgn0030716	FBgn0031417	FBgn0265276
FBgn0036369	FBgn0036765	FBgn0266646	FBgn0033855	FBgn0039738	FBgn0052372	FBgn0003308	FBgn0032002
FBgn0001254	FBgn0036821	FBgn0000659	FBgn0000227	FBgn0037050	FBgn0261548	FBgn0036810	FBgn0263707
FBgn0024315	FBgn0026602	FBgn0036786	FBgn0023549	FBgn0037130	FBgn0037753	FBgn0037149	FBgn0034515

FBgn0017448	FBgn0001150	FBgn0015568	FBgn0267635	FBgn0034501	FBgn0085759	FBgn0000244	FBgn0262624
FBgn0034462	FBgn0030360	FBgn0041234	FBgn0005590	FBgn0050115	FBgn0082585	FBgn0036205	FBgn0038191
FBgn0029002	FBgn0032483	FBgn0043791	FBgn0262813	FBgn0034479	FBgn0032848	FBgn0085452	FBgn0082582
FBgn0037515	FBgn0033079	FBgn0039099	FBgn0264270	FBgn0000489	FBgn0039139	FBgn0034606	FBgn0031001
FBgn0037973	FBgn0050410	FBgn0036349	FBgn0051606	FBgn0004364	FBgn0003486	FBgn0039881	FBgn0027070
FBgn0036752	FBgn0001258	FBgn0265274	FBgn0037797	FBgn0045800	FBgn0033051	FBgn0002905	FBgn0002931
FBgn0016715	FBgn0267153	FBgn0259993	FBgn0265984	FBgn0043575	FBgn0262112	FBgn0032682	FBgn0050161
FBgn0267733	FBgn0000411	FBgn0028523	FBgn0004567	FBgn0036150	FBgn0085253	FBgn0013725	FBgn0264482
FBgn0063386	FBgn0001320	FBgn0051999	FBgn0031621	FBgn0031974	FBgn0041184	FBgn0025739	FBgn0004892
FBgn0031227	FBgn0026315	FBgn0032493	FBgn0008636	FBgn0037213	FBgn0030593	FBgn0026398	FBgn0004620
FBgn0051262	FBgn0261434	FBgn0266129	FBgn0001168	FBgn0004956	FBgn0035569	FBgn0260756	FBgn0029958
FBgn0014395	FBgn0003683	FBgn0004959	FBgn0086068	FBgn0035315	FBgn0044049	FBgn0004054	FBgn0033174
FBgn0039430	FBgn0035312	FBgn0039734	FBgn0028978	FBgn0265697	FBgn0003312	FBgn0020493	FBgn0033979
FBgn0038977	FBgn0019650	FBgn0004389	FBgn0001234	FBgn0265887	FBgn0265888	FBgn0033564	
FBgn0265880	FBgn0035521	FBgn0004102	FBgn0041160	FBgn0033483	FBgn0004859	FBgn0000826	
FBgn0000116	FBgn0034225	FBgn0001174	FBgn0011653	FBgn0029931	FBgn0266418	FBgn0262605	
FBgn0030373	FBgn0036992	FBgn0083123	FBgn0003448	FBgn0003145	FBgn0031623	FBgn0031270	
FBgn0082931	FBgn0035852	FBgn0038028	FBgn0259111	FBgn0033304	FBgn0032693	FBgn0000459	

Appendix O: DUB module target genes

FBgn0065032	FBgn0085203	FBgn0263510	FBgn0052262	FBgn0037138	FBgn0039223	FBgn0027342	FBgn0030803
FBgn0033075	FBgn0243513	FBgn0086712	FBgn0035475	FBgn0262951	FBgn0051120	FBgn0029974	FBgn0028974
FBgn0036538	FBgn0031505	FBgn0033638	FBgn0035519	FBgn0058160	FBgn0039250	FBgn0040319	FBgn0030851
FBgn0000575	FBgn0051953	FBgn0004463	FBgn0035537	FBgn0086768	FBgn0039265	FBgn0030007	FBgn0030883
FBgn0034948	FBgn0031549	FBgn0033686	FBgn0035627	FBgn0023023	FBgn0039291	FBgn0020653	FBgn0030946
FBgn0028507	FBgn0031597	FBgn0033748	FBgn0035644	FBgn0037379	FBgn0039465	FBgn0030052	FBgn0031037
FBgn0035568	FBgn0031598	FBgn0033750	FBgn0010406	FBgn0037552	FBgn0004197	FBgn0030063	FBgn0031040
FBgn0030004	FBgn0031601	FBgn0050484	FBgn0035838	FBgn0037608	FBgn0039508	FBgn0052707	FBgn0031041
FBgn0028563	FBgn0031611	FBgn0033962	FBgn0020392	FBgn0037690	FBgn0013972	FBgn0052708	FBgn0031115
FBgn0033614	FBgn0031613	FBgn0034071	FBgn0087039	FBgn0037696	FBgn0042213	FBgn0052706	FBgn0031143
FBgn0264539	FBgn0031628	FBgn0010213	FBgn0035902	FBgn0037722	FBgn0039737	FBgn0040467	FBgn0001565
FBgn0035170	FBgn0031713	FBgn0003091	FBgn0035906	FBgn0037739	FBgn0086355	FBgn0040931	FBgn0020272
FBgn0037012	FBgn0031848	FBgn0085220	FBgn0264307	FBgn0037744	FBgn0039827	FBgn0026206	FBgn0263665
FBgn0030432	FBgn0032005	FBgn0034191	FBgn0035944	FBgn0037781	FBgn0019990	FBgn0030101	FBgn0085787
FBgn0037130	FBgn0032014	FBgn0034223	FBgn0052039	FBgn0037891	FBgn0039850	FBgn0264691	FBgn0035268
FBgn0037698	FBgn0032030	FBgn0034255	FBgn0001224	FBgn0037942	FBgn0039876	FBgn0085437	FBgn0031683
FBgn0036938	FBgn0032032	FBgn0034264	FBgn0036005	FBgn0037998	FBgn0025621	FBgn0030217	FBgn0040384
FBgn0020493	FBgn0051898	FBgn0034313	FBgn0036007	FBgn0038106	FBgn0040346	FBgn0025111	FBgn0039360
FBgn0051973	FBgn0027052	FBgn0034362	FBgn0015321	FBgn0038327	FBgn0052814	FBgn0030263	FBgn0264385
FBgn0039537	FBgn0051719	FBgn0034400	FBgn0036032	FBgn0038369	FBgn0040367	FBgn0030294	FBgn0038438
FBgn0016675	FBgn0032256	FBgn0034402	FBgn0036039	FBgn0040237	FBgn0024365	FBgn0001624	FBgn0030218
FBgn0035998	FBgn0032259	FBgn0034403	FBgn0047038	FBgn0038432	FBgn0023530	FBgn0030306	FBgn0004172
FBgn0250848	FBgn0032429	FBgn0041702	FBgn0262890	FBgn0038455	FBgn0023513	FBgn0030322	FBgn0033566
FBgn0261566	FBgn0025115	FBgn0034432	FBgn0036184	FBgn0038467	FBgn0029594	FBgn0030345	FBgn0032850
FBgn0015524	FBgn0028938	FBgn0050296	FBgn0036237	FBgn0051360	FBgn0023511	FBgn0030351	FBgn0051523
FBgn0033905	FBgn0052971	FBgn0011824	FBgn0036266	FBgn0262562	FBgn0000377	FBgn0030391	FBgn0003373
FBgn0039862	FBgn0001986	FBgn0034688	FBgn0085273	FBgn0038609	FBgn0023525	FBgn0030396	FBgn0000615
FBgn0003116	FBgn0027779	FBgn0034789	FBgn0040296	FBgn0263974	FBgn0011606	FBgn0030420	FBgn0031719
FBgn0031170	FBgn0032746	FBgn0034879	FBgn0036462	FBgn0085312	FBgn0024993	FBgn0030431	FBgn0016036
FBgn0262791	FBgn0032750	FBgn0034931	FBgn0036483	FBgn0260399	FBgn0024996	FBgn0030433	FBgn0039755
FBgn0001091	FBgn0002031	FBgn0034933	FBgn0036519	FBgn0051475	FBgn0000376	FBgn0030456	FBgn0037657
FBgn0263705	FBgn0032763	FBgn0085242	FBgn0036662	FBgn0038772	FBgn0029664	FBgn0040309	FBgn0263544
FBgn0034105	FBgn0032833	FBgn0002791	FBgn0036688	FBgn0261550	FBgn0029676	FBgn0030528	FBgn0263402
FBgn0004397	FBgn0039970	FBgn0035020	FBgn0036691	FBgn0038856	FBgn0260484	FBgn0052626	FBgn0011204
FBgn0001078	FBgn0029131	FBgn0035099	FBgn0036698	FBgn0264357	FBgn0029704	FBgn0030574	FBgn0037659
FBgn0011761	FBgn0033095	FBgn0035102	FBgn0036771	FBgn0038893	FBgn0029718	FBgn0003301	FBgn0030695
FBgn0086901	FBgn0033191	FBgn0035151	FBgn0036773	FBgn0038903	FBgn0029755	FBgn0030584	FBgn0050488
FBgn0003366	FBgn0050379	FBgn0260755	FBgn0036850	FBgn0038953	FBgn0010014	FBgn0030629	
FBgn0031216	FBgn0033316	FBgn0000109	FBgn0260857	FBgn0038979	FBgn0029818	FBgn0030645	
FBgn0051974	FBgn0033354	FBgn0035323	FBgn0052205	FBgn0263143	FBgn0043796	FBgn0027287	
FBgn0010602	FBgn0033377	FBgn0035383	FBgn0036909	FBgn0024509	FBgn0062413	FBgn0030655	

FBgn0260933	FBgn0033389	FBgn0035388	FBgn0036987	FBgn0039126	FBgn0029502	FBgn0052581
FBgn0031321	FBgn0033428	FBgn0035393	FBgn0037020	FBgn0053108	FBgn0029914	FBgn0011742
FBgn0031365	FBgn0013435	FBgn0035444	FBgn0052447	FBgn0020018	FBgn0259204	FBgn0030794

Appendix P: SAGA target genes

FBgn0261617	FBgn0002607	FBgn0013683	FBgn0027081	FBgn0032305	FBgn0036715	FBgn0040297	FBgn0250753
FBgn0001297	FBgn0002626	FBgn0013684	FBgn0027085	FBgn0032335	FBgn0036726	FBgn0040305	FBgn0250786
FBgn0026199	FBgn0002629	FBgn0013685	FBgn0027090	FBgn0032341	FBgn0036728	FBgn0040324	FBgn0250814
FBgn0036516	FBgn0002633	FBgn0013686	FBgn0027101	FBgn0032358	FBgn0036733	FBgn0040372	FBgn0250820
FBgn0262026	FBgn0002638	FBgn0013688	FBgn0027356	FBgn0032363	FBgn0036734	FBgn0040373	FBgn0250830
FBgn0082950	FBgn0002643	FBgn0013689	FBgn0027375	FBgn0032364	FBgn0036745	FBgn0040382	FBgn0250843
FBgn0263510	FBgn0002715	FBgn0013690	FBgn0027493	FBgn0032377	FBgn0036746	FBgn0040394	FBgn0250867
FBgn0002528	FBgn0002732	FBgn0013691	FBgn0027495	FBgn0032444	FBgn0036761	FBgn0040395	FBgn0250906
FBgn0065073	FBgn0002736	FBgn0013692	FBgn0027497	FBgn0032445	FBgn0036762	FBgn0040475	FBgn0259139
FBgn0086533	FBgn0002774	FBgn0013693	FBgn0027499	FBgn0032474	FBgn0036791	FBgn0040487	FBgn0259142
FBgn0263572	FBgn0002780	FBgn0013694	FBgn0027504	FBgn0032475	FBgn0036801	FBgn0040491	FBgn0259168
FBgn0262526	FBgn0002781	FBgn0013695	FBgn0027506	FBgn0032476	FBgn0036838	FBgn0040666	FBgn0259176
FBgn0082987	FBgn0002783	FBgn0013696	FBgn0027507	FBgn0032483	FBgn0036842	FBgn0040705	FBgn0259212
FBgn0034975	FBgn0002873	FBgn0013697	FBgn0027509	FBgn0032485	FBgn0036843	FBgn0040777	FBgn0259214
FBgn0050220	FBgn0002899	FBgn0013698	FBgn0027548	FBgn0032486	FBgn0036900	FBgn0040778	FBgn0259220
FBgn0082973	FBgn0002905	FBgn0013699	FBgn0027561	FBgn0032489	FBgn0036911	FBgn0040809	FBgn0259228
FBgn0039844	FBgn0002921	FBgn0013700	FBgn0027567	FBgn0032533	FBgn0036915	FBgn0040964	FBgn0259234
FBgn0051720	FBgn0002924	FBgn0013701	FBgn0027581	FBgn0032586	FBgn0036918	FBgn0040965	FBgn0259242
FBgn0086070	FBgn0002945	FBgn0013702	FBgn0027598	FBgn0032633	FBgn0036926	FBgn0040984	FBgn0259483
FBgn0086408	FBgn0002968	FBgn0013703	FBgn0027602	FBgn0032656	FBgn0036967	FBgn0040985	FBgn0259685
FBgn0086075	FBgn0002985	FBgn0013704	FBgn0027603	FBgn0032681	FBgn0036980	FBgn0041094	FBgn0259699
FBgn0035317	FBgn0003002	FBgn0013705	FBgn0027616	FBgn0032688	FBgn0037021	FBgn0041111	FBgn0259700
FBgn0086041	FBgn0003041	FBgn0013706	FBgn0027783	FBgn0032698	FBgn0037023	FBgn0041184	FBgn0259785
FBgn0053170	FBgn0003042	FBgn0013707	FBgn0027835	FBgn0032702	FBgn0037024	FBgn0041186	FBgn0259789
FBgn0039180	FBgn0003062	FBgn0013708	FBgn0027865	FBgn0032703	FBgn0037026	FBgn0041188	FBgn0259937
FBgn0082986	FBgn0003067	FBgn0013709	FBgn0027866	FBgn0032705	FBgn0037027	FBgn0041588	FBgn0259978
FBgn0263769	FBgn0003074	FBgn0013710	FBgn0027872	FBgn0032715	FBgn0037044	FBgn0041604	FBgn0259979
FBgn0003922	FBgn0003145	FBgn0013718	FBgn0027885	FBgn0032717	FBgn0037051	FBgn0041720	FBgn0259984
FBgn0031119	FBgn0003169	FBgn0013725	FBgn0027889	FBgn0032720	FBgn0037061	FBgn0042132	FBgn0259985
FBgn0034045	FBgn0003175	FBgn0013732	FBgn0027932	FBgn0032721	FBgn0037065	FBgn0042134	FBgn0259991
FBgn0034464	FBgn0003204	FBgn0013733	FBgn0027948	FBgn0032728	FBgn0037081	FBgn0042185	FBgn0260002
FBgn0082928	FBgn0003205	FBgn0013746	FBgn0027949	FBgn0032812	FBgn0037093	FBgn0042712	FBgn0260008
FBgn0030868	FBgn0003206	FBgn0013749	FBgn0027951	FBgn0032815	FBgn0037120	FBgn0043010	FBgn0260010
FBgn0020305	FBgn0003209	FBgn0013756	FBgn0028327	FBgn0032816	FBgn0037121	FBgn0043021	FBgn0260012
FBgn0259923	FBgn0003256	FBgn0013764	FBgn0028341	FBgn0032821	FBgn0037135	FBgn0043070	FBgn0260233
FBgn0260755	FBgn0003261	FBgn0013765	FBgn0028373	FBgn0032858	FBgn0037137	FBgn0043455	FBgn0260439
FBgn0051223	FBgn0003267	FBgn0013770	FBgn0028377	FBgn0032859	FBgn0037149	FBgn0043456	FBgn0260441
FBgn0263344	FBgn0003268	FBgn0013799	FBgn0028380	FBgn0032883	FBgn0037151	FBgn0043457	FBgn0260455
FBgn0037723	FBgn0003275	FBgn0013981	FBgn0028382	FBgn0032884	FBgn0037153	FBgn0043842	FBgn0260462
FBgn0034786	FBgn0003277	FBgn0013983	FBgn0028399	FBgn0032886	FBgn0037188	FBgn0043884	FBgn0260486
FBgn0003373	FBgn0003300	FBgn0013984	FBgn0028401	FBgn0032919	FBgn0037213	FBgn0043900	FBgn0260635

FBgn0037156	FBgn0003310	FBgn0014002	FBgn0028427	FBgn0032938	FBgn0037220	FBgn0043903	FBgn0260742
FBgn0031092	FBgn0003312	FBgn0014007	FBgn0028434	FBgn0032940	FBgn0037244	FBgn0044020	FBgn0260743
FBgn0261802	FBgn0003326	FBgn0014009	FBgn0028471	FBgn0032943	FBgn0037249	FBgn0044028	FBgn0260747
FBgn0262886	FBgn0003391	FBgn0014010	FBgn0028473	FBgn0032949	FBgn0037250	FBgn0044323	FBgn0260749
FBgn0044508	FBgn0003392	FBgn0014020	FBgn0028480	FBgn0032961	FBgn0037279	FBgn0044510	FBgn0260794
FBgn0038029	FBgn0003410	FBgn0014022	FBgn0028506	FBgn0032974	FBgn0037301	FBgn0044823	FBgn0260795
FBgn0086913	FBgn0003415	FBgn0014023	FBgn0028515	FBgn0032979	FBgn0037315	FBgn0045035	FBgn0260798
FBgn0028974	FBgn0003430	FBgn0014024	FBgn0028554	FBgn0032986	FBgn0037336	FBgn0045073	FBgn0260938
FBgn0263463	FBgn0003444	FBgn0014026	FBgn0028577	FBgn0032987	FBgn0037347	FBgn0045800	FBgn0260939
FBgn0034882	FBgn0003448	FBgn0014037	FBgn0028579	FBgn0032988	FBgn0037350	FBgn0045823	FBgn0260945
FBgn0003731	FBgn0003459	FBgn0014133	FBgn0028662	FBgn0032997	FBgn0037351	FBgn0046114	FBgn0260946
FBgn0005633	FBgn0003510	FBgn0014135	FBgn0028692	FBgn0033000	FBgn0037358	FBgn0046214	FBgn0260970
FBgn0263469	FBgn0003511	FBgn0014163	FBgn0028697	FBgn0033005	FBgn0037359	FBgn0046222	FBgn0260987
FBgn0051485	FBgn0003512	FBgn0014269	FBgn0028717	FBgn0033010	FBgn0037360	FBgn0046692	FBgn0260990
FBgn0038243	FBgn0003517	FBgn0014343	FBgn0028734	FBgn0033017	FBgn0037371	FBgn0046704	FBgn0261014
FBgn0039591	FBgn0003557	FBgn0014366	FBgn0028789	FBgn0033019	FBgn0037374	FBgn0046706	FBgn0261108
FBgn0010548	FBgn0003612	FBgn0014857	FBgn0028953	FBgn0033021	FBgn0037439	FBgn0050015	FBgn0261119
FBgn0010395	FBgn0003683	FBgn0014877	FBgn0028954	FBgn0033028	FBgn0037442	FBgn0050020	FBgn0261239
FBgn0046301	FBgn0003714	FBgn0014879	FBgn0028978	FBgn0033029	FBgn0037443	FBgn0050051	FBgn0261243
FBgn0086042	FBgn0003732	FBgn0015008	FBgn0028980	FBgn0033032	FBgn0037467	FBgn0050055	FBgn0261262
FBgn0032785	FBgn0003862	FBgn0015024	FBgn0029006	FBgn0033081	FBgn0037468	FBgn0050085	FBgn0261269
FBgn0063385	FBgn0003882	FBgn0015218	FBgn0029067	FBgn0033083	FBgn0037521	FBgn0050105	FBgn0261270
FBgn0065053	FBgn0003884	FBgn0015229	FBgn0029079	FBgn0033085	FBgn0037530	FBgn0050118	FBgn0261274
FBgn0086028	FBgn0003887	FBgn0015240	FBgn0029123	FBgn0033086	FBgn0037531	FBgn0050122	FBgn0261283
FBgn0031970	FBgn0003892	FBgn0015247	FBgn0029134	FBgn0033117	FBgn0037554	FBgn0050161	FBgn0261360
FBgn0063391	FBgn0003900	FBgn0015278	FBgn0029148	FBgn0033122	FBgn0037555	FBgn0050163	FBgn0261383
FBgn0030880	FBgn0003916	FBgn0015283	FBgn0029152	FBgn0033159	FBgn0037602	FBgn0050169	FBgn0261385
FBgn0033250	FBgn0003930	FBgn0015288	FBgn0029155	FBgn0033166	FBgn0037623	FBgn0050198	FBgn0261387
FBgn0032682	FBgn0003931	FBgn0015296	FBgn0029157	FBgn0033179	FBgn0037624	FBgn0050199	FBgn0261394
FBgn0086039	FBgn0003935	FBgn0015320	FBgn0029161	FBgn0033195	FBgn0037636	FBgn0050200	FBgn0261403
FBgn0262974	FBgn0003938	FBgn0015324	FBgn0029506	FBgn0033232	FBgn0037644	FBgn0050218	FBgn0261429
FBgn0023081	FBgn0003942	FBgn0015331	FBgn0029507	FBgn0033235	FBgn0037659	FBgn0050227	FBgn0261434
FBgn0034138	FBgn0003969	FBgn0015372	FBgn0029763	FBgn0033241	FBgn0037660	FBgn0050234	FBgn0261444
FBgn0037766	FBgn0003977	FBgn0015379	FBgn0029785	FBgn0033260	FBgn0037661	FBgn0050235	FBgn0261456
FBgn0082926	FBgn0004009	FBgn0015393	FBgn0029798	FBgn0033261	FBgn0037686	FBgn0050289	FBgn0261477
FBgn0029167	FBgn0004052	FBgn0015396	FBgn0029822	FBgn0033264	FBgn0037687	FBgn0050372	FBgn0261479
FBgn0000721	FBgn0004055	FBgn0015509	FBgn0029857	FBgn0033274	FBgn0037702	FBgn0050394	FBgn0261504
FBgn0060292	FBgn0004103	FBgn0015513	FBgn0029867	FBgn0033309	FBgn0037703	FBgn0050428	FBgn0261522
FBgn0260634	FBgn0004106	FBgn0015520	FBgn0029873	FBgn0033310	FBgn0037719	FBgn0050452	FBgn0261535
FBgn0034046	FBgn0004177	FBgn0015543	FBgn0029903	FBgn0033317	FBgn0037720	FBgn0050454	FBgn0261554
FBgn0262407	FBgn0004179	FBgn0015589	FBgn0029905	FBgn0033351	FBgn0037728	FBgn0050476	FBgn0261574
FBgn0039908	FBgn0004183	FBgn0015623	FBgn0029906	FBgn0033352	FBgn0037734	FBgn0050481	FBgn0261592
FBgn0259211	FBgn0004185	FBgn0015625	FBgn0029925	FBgn0033374	FBgn0037746	FBgn0051021	FBgn0261593

FBgn0086071	FBgn0004186	FBgn0015721	FBgn0029931	FBgn0033382	FBgn0037773	FBgn0051064	FBgn0261599
FBgn0038679	FBgn0004187	FBgn0015772	FBgn0029942	FBgn0033392	FBgn0037792	FBgn0051108	FBgn0261602
FBgn0262887	FBgn0004188	FBgn0015778	FBgn0029980	FBgn0033454	FBgn0037808	FBgn0051109	FBgn0261606
FBgn0003950	FBgn0004189	FBgn0015789	FBgn0030048	FBgn0033485	FBgn0037809	FBgn0051122	FBgn0261618
FBgn0262595	FBgn0004190	FBgn0015790	FBgn0030049	FBgn0033486	FBgn0037844	FBgn0051125	FBgn0261641
FBgn0005612	FBgn0004191	FBgn0015791	FBgn0030053	FBgn0033491	FBgn0037845	FBgn0051141	FBgn0261647
FBgn0065055	FBgn0004192	FBgn0015794	FBgn0030054	FBgn0033526	FBgn0037847	FBgn0051158	FBgn0261648
FBgn0084245	FBgn0004227	FBgn0015803	FBgn0030055	FBgn0033527	FBgn0037848	FBgn0051163	FBgn0261649
FBgn0065088	FBgn0004237	FBgn0015805	FBgn0030136	FBgn0033547	FBgn0037855	FBgn0051217	FBgn0261671
FBgn0051438	FBgn0004359	FBgn0015806	FBgn0030141	FBgn0033672	FBgn0037876	FBgn0051282	FBgn0261688
FBgn0037818	FBgn0004362	FBgn0015808	FBgn0030151	FBgn0033673	FBgn0037878	FBgn0051314	FBgn0261786
FBgn0000158	FBgn0004363	FBgn0015816	FBgn0030170	FBgn0033683	FBgn0037884	FBgn0051352	FBgn0261790
FBgn0035667	FBgn0004364	FBgn0015828	FBgn0030178	FBgn0033717	FBgn0037885	FBgn0051363	FBgn0261791
FBgn0262021	FBgn0004373	FBgn0015905	FBgn0030228	FBgn0033718	FBgn0037899	FBgn0051450	FBgn0261792
FBgn0052679	FBgn0004387	FBgn0016070	FBgn0030266	FBgn0033739	FBgn0037900	FBgn0051460	FBgn0261793
FBgn0033429	FBgn0004390	FBgn0016122	FBgn0030274	FBgn0033777	FBgn0037920	FBgn0051472	FBgn0261797
FBgn0032668	FBgn0004391	FBgn0016126	FBgn0030311	FBgn0033784	FBgn0037978	FBgn0051501	FBgn0261811
FBgn0035325	FBgn0004395	FBgn0016685	FBgn0030323	FBgn0033785	FBgn0037979	FBgn0051510	FBgn0261823
FBgn0036663	FBgn0004401	FBgn0016691	FBgn0030327	FBgn0033799	FBgn0038000	FBgn0051536	FBgn0261859
FBgn0261871	FBgn0004403	FBgn0016754	FBgn0030366	FBgn0033844	FBgn0038028	FBgn0051626	FBgn0261885
FBgn0031373	FBgn0004419	FBgn0016756	FBgn0030400	FBgn0033846	FBgn0038039	FBgn0051637	FBgn0261933
FBgn0031644	FBgn0004432	FBgn0016792	FBgn0030474	FBgn0033855	FBgn0038045	FBgn0051694	FBgn0261934
FBgn0036463	FBgn0004435	FBgn0016970	FBgn0030504	FBgn0033859	FBgn0038065	FBgn0051776	FBgn0261938
FBgn0086051	FBgn0004436	FBgn0016977	FBgn0030505	FBgn0033871	FBgn0038069	FBgn0051928	FBgn0261963
FBgn0033738	FBgn0004449	FBgn0016978	FBgn0030520	FBgn0033886	FBgn0038071	FBgn0051943	FBgn0261983
FBgn0083055	FBgn0004462	FBgn0016983	FBgn0030581	FBgn0033906	FBgn0038100	FBgn0051944	FBgn0261984
FBgn0035113	FBgn0004509	FBgn0016984	FBgn0030582	FBgn0033907	FBgn0038107	FBgn0051992	FBgn0261987
FBgn0086672	FBgn0004569	FBgn0017430	FBgn0030599	FBgn0033912	FBgn0038108	FBgn0051998	FBgn0261988
FBgn0037676	FBgn0004574	FBgn0017545	FBgn0030616	FBgn0033929	FBgn0038110	FBgn0052000	FBgn0262109
FBgn0052476	FBgn0004587	FBgn0017549	FBgn0030640	FBgn0033948	FBgn0038195	FBgn0052016	FBgn0262115
FBgn0034476	FBgn0004597	FBgn0017550	FBgn0030641	FBgn0033988	FBgn0038233	FBgn0052133	FBgn0262116
FBgn0015371	FBgn0004603	FBgn0017579	FBgn0030685	FBgn0034013	FBgn0038234	FBgn0052138	FBgn0262117
FBgn0021796	FBgn0004623	FBgn0017581	FBgn0030686	FBgn0034049	FBgn0038271	FBgn0052173	FBgn0262125
FBgn0250785	FBgn0004629	FBgn0019624	FBgn0030693	FBgn0034050	FBgn0038272	FBgn0052177	FBgn0262127
FBgn0259230	FBgn0004635	FBgn0019637	FBgn0030703	FBgn0034054	FBgn0038273	FBgn0052179	FBgn0262166
FBgn0030466	FBgn0004636	FBgn0019661	FBgn0030704	FBgn0034065	FBgn0038286	FBgn0052190	FBgn0262370
FBgn0259185	FBgn0004647	FBgn0019830	FBgn0030710	FBgn0034072	FBgn0038313	FBgn0052196	FBgn0262372
FBgn0033188	FBgn0004650	FBgn0019886	FBgn0030711	FBgn0034073	FBgn0038320	FBgn0052200	FBgn0262373
FBgn0033856	FBgn0004656	FBgn0019890	FBgn0030718	FBgn0034075	FBgn0038363	FBgn0052226	FBgn0262380
FBgn0035669	FBgn0004657	FBgn0019932	FBgn0030719	FBgn0034089	FBgn0038385	FBgn0052230	FBgn0262408
FBgn0030721	FBgn0004828	FBgn0019936	FBgn0030731	FBgn0034139	FBgn0038390	FBgn0052350	FBgn0262410
FBgn0039718	FBgn0004837	FBgn0019968	FBgn0030733	FBgn0034142	FBgn0038400	FBgn0052380	FBgn0262411
FBgn0036423	FBgn0004838	FBgn0020235	FBgn0030744	FBgn0034180	FBgn0038401	FBgn0052409	FBgn0262414

FBgn0000108	FBgn0004860	FBgn0020238	FBgn0030745	FBgn0034237	FBgn0038446	FBgn0052446	FBgn0262418
FBgn0263584	FBgn0004861	FBgn0020255	FBgn0030749	FBgn0034240	FBgn0038452	FBgn0052479	FBgn0262443
FBgn0063392	FBgn0004888	FBgn0020257	FBgn0030757	FBgn0034249	FBgn0038470	FBgn0052486	FBgn0262464
FBgn0053465	FBgn0004893	FBgn0020279	FBgn0030766	FBgn0034258	FBgn0038471	FBgn0052500	FBgn0262515
FBgn0039339	FBgn0004907	FBgn0020304	FBgn0030778	FBgn0034282	FBgn0038473	FBgn0052529	FBgn0262519
FBgn0037470	FBgn0004913	FBgn0020306	FBgn0030786	FBgn0034351	FBgn0038474	FBgn0052672	FBgn0262527
FBgn0029137	FBgn0004915	FBgn0020312	FBgn0030790	FBgn0034447	FBgn0038475	FBgn0052675	FBgn0262604
FBgn0264353	FBgn0005386	FBgn0020368	FBgn0030809	FBgn0034463	FBgn0038476	FBgn0052676	FBgn0262616
FBgn0040507	FBgn0005411	FBgn0020443	FBgn0030869	FBgn0034488	FBgn0038532	FBgn0052758	FBgn0262679
FBgn0034737	FBgn0005533	FBgn0020496	FBgn0030873	FBgn0034503	FBgn0038535	FBgn0052831	FBgn0262716
FBgn0036793	FBgn0005536	FBgn0020497	FBgn0030874	FBgn0034504	FBgn0038536	FBgn0052850	FBgn0262719
FBgn0036799	FBgn0005558	FBgn0020503	FBgn0030941	FBgn0034514	FBgn0038552	FBgn0052856	FBgn0262731
FBgn0082939	FBgn0005585	FBgn0020618	FBgn0030956	FBgn0034564	FBgn0038564	FBgn0052857	FBgn0262733
FBgn0086072	FBgn0005593	FBgn0020620	FBgn0030959	FBgn0034569	FBgn0038566	FBgn0053062	FBgn0262742
FBgn0264331	FBgn0005616	FBgn0020633	FBgn0030970	FBgn0034577	FBgn0038588	FBgn0053087	FBgn0262872
FBgn0000003	FBgn0005617	FBgn0020660	FBgn0030974	FBgn0034592	FBgn0038601	FBgn0053096	FBgn0262952
FBgn0000017	FBgn0005624	FBgn0020887	FBgn0030994	FBgn0034606	FBgn0038662	FBgn0053111	FBgn0263019
FBgn0000022	FBgn0005631	FBgn0020910	FBgn0031006	FBgn0034614	FBgn0038666	FBgn0053113	FBgn0263106
FBgn0000043	FBgn0005634	FBgn0021776	FBgn0031047	FBgn0034631	FBgn0038709	FBgn0053121	FBgn0263120
FBgn0000054	FBgn0005636	FBgn0021795	FBgn0031057	FBgn0034644	FBgn0038737	FBgn0053155	FBgn0263197
FBgn0000083	FBgn0005649	FBgn0021895	FBgn0031066	FBgn0034684	FBgn0038787	FBgn0053169	FBgn0263231
FBgn0000100	FBgn0005655	FBgn0021906	FBgn0031069	FBgn0034742	FBgn0038788	FBgn0053180	FBgn0263289
FBgn0000115	FBgn0005671	FBgn0021967	FBgn0031077	FBgn0034743	FBgn0038805	FBgn0053203	FBgn0263346
FBgn0000117	FBgn0005672	FBgn0022224	FBgn0031078	FBgn0034763	FBgn0038806	FBgn0053217	FBgn0263350
FBgn0000119	FBgn0005683	FBgn0022720	FBgn0031091	FBgn0034802	FBgn0038808	FBgn0053222	FBgn0263380
FBgn0000140	FBgn0005694	FBgn0022764	FBgn0031098	FBgn0034803	FBgn0038829	FBgn0053229	FBgn0263383
FBgn0000163	FBgn0005695	FBgn0022787	FBgn0031106	FBgn0034816	FBgn0038833	FBgn0053494	FBgn0263391
FBgn0000166	FBgn0005696	FBgn0022893	FBgn0031107	FBgn0034817	FBgn0038834	FBgn0053502	FBgn0263395
FBgn0000173	FBgn0005771	FBgn0022960	FBgn0031114	FBgn0034853	FBgn0038853	FBgn0053526	FBgn0263396
FBgn0000180	FBgn0008636	FBgn0023000	FBgn0031118	FBgn0034876	FBgn0038858	FBgn0053554	FBgn0263444
FBgn0000181	FBgn0010051	FBgn0023001	FBgn0031145	FBgn0034877	FBgn0038871	FBgn0053635	FBgn0263447
FBgn0000183	FBgn0010078	FBgn0023143	FBgn0031161	FBgn0034878	FBgn0038872	FBgn0053653	FBgn0263459
FBgn0000212	FBgn0010109	FBgn0023167	FBgn0031174	FBgn0034894	FBgn0038881	FBgn0053963	FBgn0263472
FBgn0000216	FBgn0010198	FBgn0023175	FBgn0031183	FBgn0034915	FBgn0038947	FBgn0053977	FBgn0263536
FBgn0000227	FBgn0010215	FBgn0023177	FBgn0031186	FBgn0034918	FBgn0038976	FBgn0054054	FBgn0263544
FBgn0000228	FBgn0010217	FBgn0023212	FBgn0031187	FBgn0034962	FBgn0038981	FBgn0058002	FBgn0263573
FBgn0000246	FBgn0010228	FBgn0023213	FBgn0031217	FBgn0034965	FBgn0038984	FBgn0058042	FBgn0263594
FBgn0000247	FBgn0010238	FBgn0023388	FBgn0031227	FBgn0034967	FBgn0039002	FBgn0058045	FBgn0263601
FBgn0000250	FBgn0010280	FBgn0023395	FBgn0031229	FBgn0034968	FBgn0039120	FBgn0058178	FBgn0263602
FBgn0000251	FBgn0010292	FBgn0023407	FBgn0031253	FBgn0034970	FBgn0039160	FBgn0058191	FBgn0263603
FBgn0000257	FBgn0010313	FBgn0023423	FBgn0031254	FBgn0034971	FBgn0039172	FBgn0058196	FBgn0263740
FBgn0000259	FBgn0010315	FBgn0023518	FBgn0031286	FBgn0034986	FBgn0039175	FBgn0058263	FBgn0263755
FBgn0000273	FBgn0010328	FBgn0023519	FBgn0031288	FBgn0034987	FBgn0039182	FBgn0058439	FBgn0263832

FBgn0000283	FBgn0010355	FBgn0023528	FBgn0031301	FBgn0035001	FBgn0039183	FBgn0061359	FBgn0263855
FBgn0000289	FBgn0010379	FBgn0024177	FBgn0031345	FBgn0035016	FBgn0039189	FBgn0061360	FBgn0263929
FBgn0000307	FBgn0010408	FBgn0024234	FBgn0031374	FBgn0035032	FBgn0039215	FBgn0061469	FBgn0263933
FBgn0000308	FBgn0010409	FBgn0024236	FBgn0031377	FBgn0035033	FBgn0039254	FBgn0063381	FBgn0263977
FBgn0000370	FBgn0010415	FBgn0024248	FBgn0031378	FBgn0035046	FBgn0039259	FBgn0063389	FBgn0263987
FBgn0000382	FBgn0010417	FBgn0024291	FBgn0031384	FBgn0035059	FBgn0039266	FBgn0063449	FBgn0263993
FBgn0000404	FBgn0010422	FBgn0024320	FBgn0031390	FBgn0035087	FBgn0039271	FBgn0063485	FBgn0264075
FBgn0000405	FBgn0010452	FBgn0024326	FBgn0031391	FBgn0035088	FBgn0039300	FBgn0063670	FBgn0264265
FBgn0000413	FBgn0010473	FBgn0024491	FBgn0031395	FBgn0035106	FBgn0039301	FBgn0064225	FBgn0264270
FBgn0000414	FBgn0010488	FBgn0024555	FBgn0031418	FBgn0035107	FBgn0039303	FBgn0064766	FBgn0264294
FBgn0000416	FBgn0010501	FBgn0024556	FBgn0031419	FBgn0035140	FBgn0039306	FBgn0065046	FBgn0264324
FBgn0000463	FBgn0010520	FBgn0024558	FBgn0031434	FBgn0035157	FBgn0039335	FBgn0065047	FBgn0264332
FBgn0000492	FBgn0010583	FBgn0024698	FBgn0031435	FBgn0035159	FBgn0039338	FBgn0065048	FBgn0264381
FBgn0000524	FBgn0010590	FBgn0024728	FBgn0031436	FBgn0035162	FBgn0039350	FBgn0065076	FBgn0264390
FBgn0000535	FBgn0010620	FBgn0024733	FBgn0031437	FBgn0035204	FBgn0039359	FBgn0065099	FBgn0264426
FBgn0000536	FBgn0010638	FBgn0024734	FBgn0031453	FBgn0035205	FBgn0039381	FBgn0066084	FBgn0264479
FBgn0000541	FBgn0010750	FBgn0024804	FBgn0031454	FBgn0035235	FBgn0039402	FBgn0066303	FBgn0264481
FBgn0000542	FBgn0010762	FBgn0024807	FBgn0031455	FBgn0035236	FBgn0039417	FBgn0066304	FBgn0264491
FBgn0000543	FBgn0010774	FBgn0024811	FBgn0031456	FBgn0035237	FBgn0039449	FBgn0067783	FBgn0264493
FBgn0000547	FBgn0010825	FBgn0024909	FBgn0031457	FBgn0035267	FBgn0039450	FBgn0067903	FBgn0264495
FBgn0000559	FBgn0010830	FBgn0024912	FBgn0031458	FBgn0035285	FBgn0039492	FBgn0069923	FBgn0264546
FBgn0000564	FBgn0010909	FBgn0024947	FBgn0031459	FBgn0035318	FBgn0039505	FBgn0082585	FBgn0264599
FBgn0000565	FBgn0011016	FBgn0024983	FBgn0031474	FBgn0035347	FBgn0039559	FBgn0082924	FBgn0264605
FBgn0000575	FBgn0011202	FBgn0025109	FBgn0031478	FBgn0035397	FBgn0039560	FBgn0082940	FBgn0264718
FBgn0000576	FBgn0011207	FBgn0025286	FBgn0031488	FBgn0035422	FBgn0039562	FBgn0082951	FBgn0039923
FBgn0000577	FBgn0011217	FBgn0025366	FBgn0031540	FBgn0035423	FBgn0039588	FBgn0082953	FBgn0004389
FBgn0000578	FBgn0011225	FBgn0025393	FBgn0031573	FBgn0035424	FBgn0039589	FBgn0082981	FBgn0010433
FBgn0000581	FBgn0011284	FBgn0025394	FBgn0031607	FBgn0035425	FBgn0039590	FBgn0083006	FBgn0083973
FBgn0000591	FBgn0011297	FBgn0025455	FBgn0031620	FBgn0035443	FBgn0039632	FBgn0083015	FBgn0003124
FBgn0000606	FBgn0011305	FBgn0025549	FBgn0031632	FBgn0035488	FBgn0039633	FBgn0083039	FBgn0032135
FBgn0000611	FBgn0011327	FBgn0025574	FBgn0031635	FBgn0035617	FBgn0039634	FBgn0083058	FBgn0082919
FBgn0000662	FBgn0011336	FBgn0025608	FBgn0031636	FBgn0035639	FBgn0039635	FBgn0083123	FBgn0051144
FBgn0000996	FBgn0011592	FBgn0025637	FBgn0031645	FBgn0035640	FBgn0039663	FBgn0083124	FBgn0010044
FBgn0001077	FBgn0011604	FBgn0025638	FBgn0031652	FBgn0035656	FBgn0039664	FBgn0083940	FBgn0043022
FBgn0001084	FBgn0011638	FBgn0025639	FBgn0031659	FBgn0035713	FBgn0039714	FBgn0083946	FBgn0036351
FBgn0001090	FBgn0011655	FBgn0025641	FBgn0031677	FBgn0035714	FBgn0039735	FBgn0083968	FBgn0050016
FBgn0001099	FBgn0011704	FBgn0025674	FBgn0031696	FBgn0035754	FBgn0039738	FBgn0083969	FBgn0031879
FBgn0001104	FBgn0011726	FBgn0025676	FBgn0031736	FBgn0035824	FBgn0039739	FBgn0083983	FBgn0013726
FBgn0001123	FBgn0011737	FBgn0025678	FBgn0031738	FBgn0035831	FBgn0039741	FBgn0085208	FBgn0034590
FBgn0001138	FBgn0011739	FBgn0025700	FBgn0031768	FBgn0035842	FBgn0039766	FBgn0085243	FBgn0028689
FBgn0001139	FBgn0011747	FBgn0025726	FBgn0031779	FBgn0035849	FBgn0039767	FBgn0085260	FBgn0051004
FBgn0001148	FBgn0011754	FBgn0025740	FBgn0031799	FBgn0035850	FBgn0039790	FBgn0085343	FBgn0003525
FBgn0001150	FBgn0011760	FBgn0025741	FBgn0031814	FBgn0035896	FBgn0039802	FBgn0085408	FBgn0022338

FBgn0001168	FBgn0011763	FBgn0025776	FBgn0031815	FBgn0035907	FBgn0039830	FBgn0085430	FBgn0263707
FBgn0001169	FBgn0011785	FBgn0025777	FBgn0031820	FBgn0035953	FBgn0039831	FBgn0085432	FBgn0263620
FBgn0001174	FBgn0011817	FBgn0025865	FBgn0031836	FBgn0035989	FBgn0039846	FBgn0085436	FBgn0040022
FBgn0001197	FBgn0011818	FBgn0025881	FBgn0031882	FBgn0036004	FBgn0039889	FBgn0085451	FBgn0084688
FBgn0001215	FBgn0011823	FBgn0025936	FBgn0031883	FBgn0036052	FBgn0039890	FBgn0085478	FBgn0035315
FBgn0001219	FBgn0011837	FBgn0026015	FBgn0031886	FBgn0036053	FBgn0039902	FBgn0085582	FBgn0262845
FBgn0001234	FBgn0011845	FBgn0026059	FBgn0031896	FBgn0036058	FBgn0039904	FBgn0085814	FBgn0033426
FBgn0001247	FBgn0011848	FBgn0026084	FBgn0031897	FBgn0036059	FBgn0039909	FBgn0086055	FBgn0036714
FBgn0001250	FBgn0011849	FBgn0026149	FBgn0031912	FBgn0036136	FBgn0039920	FBgn0086056	FBgn0040296
FBgn0001280	FBgn0011850	FBgn0026160	FBgn0031950	FBgn0036180	FBgn0039924	FBgn0086078	FBgn0262885
FBgn0001301	FBgn0011868	FBgn0026162	FBgn0031951	FBgn0036211	FBgn0039928	FBgn0086347	FBgn0261974
FBgn0001316	FBgn0011904	FBgn0026170	FBgn0031969	FBgn0036212	FBgn0039929	FBgn0086357	FBgn0035044
FBgn0001332	FBgn0011927	FBgn0026176	FBgn0031971	FBgn0036213	FBgn0039936	FBgn0086359	FBgn0026164
FBgn0001341	FBgn0011928	FBgn0026189	FBgn0031977	FBgn0036302	FBgn0039946	FBgn0086361	FBgn0037533
FBgn0001941	FBgn0011944	FBgn0026196	FBgn0031980	FBgn0036330	FBgn0039955	FBgn0086370	FBgn0026163
FBgn0001942	FBgn0012002	FBgn0026238	FBgn0031981	FBgn0036337	FBgn0039958	FBgn0086378	FBgn0040828
FBgn0001965	FBgn0012051	FBgn0026239	FBgn0032006	FBgn0036340	FBgn0039959	FBgn0086448	FBgn0038527
FBgn0001977	FBgn0012058	FBgn0026252	FBgn0032042	FBgn0036349	FBgn0039969	FBgn0086472	FBgn0261619
FBgn0001981	FBgn0013269	FBgn0026262	FBgn0032050	FBgn0036372	FBgn0039977	FBgn0086532	FBgn0082929
FBgn0001987	FBgn0013272	FBgn0026320	FBgn0032123	FBgn0036373	FBgn0040005	FBgn0086558	FBgn0262455
FBgn0001994	FBgn0013275	FBgn0026361	FBgn0032160	FBgn0036405	FBgn0040007	FBgn0086663	FBgn0050380
FBgn0001995	FBgn0013276	FBgn0026369	FBgn0032189	FBgn0036406	FBgn0040009	FBgn0086667	FBgn0264616
FBgn0002121	FBgn0013303	FBgn0026370	FBgn0032196	FBgn0036414	FBgn0040010	FBgn0086676	FBgn0262458
FBgn0002183	FBgn0013305	FBgn0026371	FBgn0032197	FBgn0036428	FBgn0040011	FBgn0086683	FBgn0085223
FBgn0002283	FBgn0013325	FBgn0026372	FBgn0032198	FBgn0036449	FBgn0040020	FBgn0086710	FBgn0000556
FBgn0002306	FBgn0013343	FBgn0026379	FBgn0032200	FBgn0036450	FBgn0040068	FBgn0086736	FBgn0036350
FBgn0002413	FBgn0013347	FBgn0026400	FBgn0032202	FBgn0036494	FBgn0040079	FBgn0086757	FBgn0033015
FBgn0002441	FBgn0013548	FBgn0026401	FBgn0032216	FBgn0036518	FBgn0040206	FBgn0086779	FBgn0053194
FBgn0002521	FBgn0013672	FBgn0026409	FBgn0032217	FBgn0036536	FBgn0040208	FBgn0086855	FBgn0051909
FBgn0002524	FBgn0013673	FBgn0026417	FBgn0032228	FBgn0036565	FBgn0040227	FBgn0086898	FBgn0041171
FBgn0002526	FBgn0013674	FBgn0026427	FBgn0032229	FBgn0036566	FBgn0040232	FBgn0086902	FBgn0053703
FBgn0002542	FBgn0013675	FBgn0026430	FBgn0032231	FBgn0036580	FBgn0040233	FBgn0086904	FBgn0053002
FBgn0002543	FBgn0013676	FBgn0026533	FBgn0032234	FBgn0036581	FBgn0040234	FBgn0087008	FBgn0262599
FBgn0002552	FBgn0013678	FBgn0026575	FBgn0032236	FBgn0036621	FBgn0040235	FBgn0087021	FBgn0040717
FBgn0002561	FBgn0013679	FBgn0026597	FBgn0032246	FBgn0036622	FBgn0040238	FBgn0087041	FBgn0011742
FBgn0002579	FBgn0013680	FBgn0026777	FBgn0032248	FBgn0036670	FBgn0040271	FBgn0243512	
FBgn0002590	FBgn0013681	FBgn0026778	FBgn0032261	FBgn0036710	FBgn0040286	FBgn0243516	

References

Aihara, H., T. Nakagawa, K. Yasui, T. Ohta, S. Hirose, N. Dhomae, K. Takio, M. Kaneko, Y. Takeshima, M. Muramatsu & T. Ito (2004) Nucleosomal histone kinase-1 phosphorylates H2A Thr 119 during mitosis in the early Drosophila embryo. *Genes Dev,* 18**,** 877-88.

Allard, S., R. T. Utley, J. Savard, A. Clarke, P. Grant, C. J. Brandl, L. Pillus, J. L. Workman & J. Cote (1999) NuA4, an essential transcription adaptor/histone H4 acetyltransferase complex containing Esa1p and the ATM-related cofactor Tra1p. *EMBO J,* 18**,** 5108-19.

Allfrey, V. G. (1966) Structural modifications of histones and their possible role in the regulation of ribonucleic acid synthesis. *Proc Can Cancer Conf,* 6**,** 313-35.

An, W., S. H. Leuba, K. van Holde & J. Zlatanova (1998a) Linker histone protects linker DNA on only one side of the core particle and in a sequence-dependent manner. *Proc Natl Acad Sci U S A,* 95**,** 3396-401.

An, W., K. van Holde & J. Zlatanova (1998b) Linker histone protection of chromatosomes reconstituted on 5S rDNA from Xenopus borealis:a reinvestigation. *Nucleic Acids Res,* 26**,** 4042-6.

Arents, G., R. W. Burlingame, B. C. Wang, W. E. Love & E. N. Moudrianakis (1991) The nucleosomal core histone octamer at 3.1 A resolution: a tripartite protein assembly and a left-handed superhelix. *Proc Natl Acad Sci U S A,* 88**,** 10148-52.

Armstrong, J. A., O. Papoulas, G. Daubresse, A. S. Sperling, J. T. Lis, M. P. Scott & J. W. Tamkun (2002) The Drosophila BRM complex facilitates global transcription by RNA polymerase II. *EMBO J,* 21**,** 5245-54.

Atanassov, B. S., R. D. Mohan, X. Lan, X. Kuang, Y. Lu, K. Lin, E. McIvor, W. Li, Y. Zhang, L. Florens, S. D. Byrum, S. G. Mackintosh, T. Calhoun-Davis, E. Koutelou, L. Wang, D. G. Tang, A. J. Tackett, M. P. Washburn, J. L. Workman & S. Y. Dent (2016) ATXN7L3 and ENY2 Coordinate Activity of Multiple H2B Deubiquitinases Important for Cellular Proliferation and Tumor Growth. *Mol Cell,* 62**,** 558-71.

Ausio, J., F. Dong & K. E. van Holde (1989) Use of selectively trypsinized nucleosome core particles to analyze the role of the histone "tails" in the stabilization of the nucleosome. *J Mol Biol,* 206**,** 451-63.

Avvakumov, N. & J. Cote (2007) The MYST family of histone acetyltransferases and their intimate links to cancer. *Oncogene,* 26**,** 5395-407.

Balasubramanian, R., M. G. Pray-Grant, W. Selleck, P. A. Grant & S. Tan (2002) Role of the Ada2 and Ada3 transcriptional coactivators in histone acetylation. *J Biol Chem,* 277**,** 7989-95.

Bannister, A. J. & T. Kouzarides (2011) Regulation of chromatin by histone modifications. *Cell Res,* 21**,** 381-95.

Bannister, A. J., P. Zegerman, J. F. Partridge, E. A. Miska, J. O. Thomas, R. C. Allshire & T. Kouzarides (2001) Selective recognition of methylated lysine 9 on histone H3 by the HP1 chromo domain. *Nature,* 410**,** 120-4.

Baptista, T., S. Grunberg, N. Minoungou, M. J. E. Koster, H. T. M. Timmers, S. Hahn, D. Devys & L. Tora (2017) SAGA Is a General Cofactor for RNA Polymerase II Transcription. *Mol Cell,* 68**,** 130-143 e5.

Bardot, P., S. D. Vincent, M. Fournier, A. Hubaud, M. Joint, L. Tora & O. Pourquie (2017) The TAF10-containing TFIID and SAGA transcriptional complexes are dispensable for early somitogenesis in the mouse embryo. *Development,* 144**,** 3808-3818.

Barlev, N. A., A. V. Emelyanov, P. Castagnino, P. Zegerman, A. J. Bannister, M. A. Sepulveda, F. Robert, L. Tora, T. Kouzarides, B. K. Birshtein & S. L. Berger (2003) A novel human Ada2 homologue functions with Gcn5 or Brg1 to coactivate transcription. *Mol Cell Biol,* 23**,** 6944-57.

Basehoar, A. D., S. J. Zanton & B. F. Pugh (2004) Identification and distinct regulation of yeast TATA box-containing genes. *Cell,* 116**,** 699-709.

Bastock, R. & D. St Johnston (2008) Drosophila oogenesis. *Curr Biol,* 18**,** R1082-7.

Batta, K., Z. Zhang, K. Yen, D. B. Goffman & B. F. Pugh (2011) Genome-wide function of H2B ubiquitylation in promoter and genic regions. *Genes Dev,* 25**,** 2254-65.

Belmont, A. S., J. W. Sedat & D. A. Agard (1987) A three-dimensional approach to mitotic chromosome structure: evidence for a complex hierarchical organization. *J Cell Biol,* 105**,** 77-92.

Bernstein, B. E., M. Kamal, K. Lindblad-Toh, S. Bekiranov, D. K. Bailey, D. J. Huebert, S. McMahon, E. K. Karlsson, E. J. Kulbokas, 3rd, T. R. Gingeras, S. L. Schreiber & E. S. Lander (2005) Genomic maps and comparative analysis of histone modifications in human and mouse. *Cell,* 120**,** 169-81.

Bhaumik, S. R. & M. R. Green (2001) SAGA is an essential in vivo target of the yeast acidic activator Gal4p. *Genes Dev,* 15**,** 1935-45.

Bhaumik, S. R., T. Raha, D. P. Aiello & M. R. Green (2004) In vivo target of a transcriptional activator revealed by fluorescence resonance energy transfer. *Genes Dev,* 18**,** 333-43.

Bian, C., C. Xu, J. Ruan, K. K. Lee, T. L. Burke, W. Tempel, D. Barsyte, J. Li, M. Wu, B. O. Zhou, B. E. Fleharty, A. Paulson, A. Allali-Hassani, J. Q. Zhou, G. Mer, P. A. Grant, J. L. Workman, J. Zang & J. Min (2011) Sgf29 binds histone H3K4me2/3 and is required for SAGA complex recruitment and histone H3 acetylation. *EMBO J,* 30**,** 2829-42.

Bonnet, J., C. Y. Wang, T. Baptista, S. D. Vincent, W. C. Hsiao, M. Stierle, C. F. Kao, L. Tora & D. Devys (2014) The SAGA coactivator complex acts on the whole transcribed genome and is required for RNA polymerase II transcription. *Genes Dev,* 28**,** 1999-2012.

Bonnet, J., Y. H. Wang, G. Spedale, R. A. Atkinson, C. Romier, A. Hamiche, W. W. Pijnappel, H. T. Timmers, L. Tora, D. Devys & B. Kieffer (2010) The structural plasticity of SCA7 domains defines their differential nucleosome-binding properties. *EMBO Rep,* 11**,** 612-8.

Bownes, M. (1975) A photographic study of development in the living embryo of Drosophila melanogaster. *J Embryol Exp Morphol,* 33**,** 789-801.

Brandt, A., F. Papagiannouli, N. Wagner, M. Wilsch-Brauninger, M. Braun, E. E. Furlong, S. Loserth, C. Wenzl, F. Pilot, N. Vogt, T. Lecuit, G. Krohne & J. Grosshans (2006) Developmental control of nuclear size and shape by Kugelkern and Kurzkern. *Curr Biol,* 16**,** 543-52.

Brendza, R. P., L. R. Serbus, J. B. Duffy & W. M. Saxton (2000) A function for kinesin I in the posterior transport of oskar mRNA and Staufen protein. *Science,* 289**,** 2120-2.

Briggs, S. D., T. Xiao, Z. W. Sun, J. A. Caldwell, J. Shabanowitz, D. F. Hunt, C. D. Allis & B. D. Strahl (2002) Gene silencing: trans-histone regulatory pathway in chromatin. *Nature,* 418**,** 498.

Brown, C. E., L. Howe, K. Sousa, S. C. Alley, M. J. Carrozza, S. Tan & J. L. Workman (2001) Recruitment of HAT complexes by direct activator interactions with the ATM-related Tra1 subunit. *Science,* 292**,** 2333-7.

Brownell, J. E., J. Zhou, T. Ranalli, R. Kobayashi, D. G. Edmondson, S. Y. Roth & C. D. Allis (1996) Tetrahymena histone acetyltransferase A: a homolog to yeast Gcn5p linking histone acetylation to gene activation. *Cell,* 84**,** 843-51.

Bryant, G. O. & M. Ptashne (2003) Independent recruitment in vivo by Gal4 of two complexes required for transcription. *Mol Cell,* 11**,** 1301-9.

Bu, P., Y. A. Evrard, G. Lozano & S. Y. Dent (2007) Loss of Gcn5 acetyltransferase activity leads to neural tube closure defects and exencephaly in mouse embryos. *Mol Cell Biol,* 27**,** 3405-16.

Cairns, B. R., H. Erdjument-Bromage, P. Tempst, F. Winston & R. D. Kornberg (1998) Two actin-related proteins are shared functional components of the chromatin-remodeling complexes RSC and SWI/SNF. *Mol Cell,* 2**,** 639-51.

Cairns, B. R., Y. J. Kim, M. H. Sayre, B. C. Laurent & R. D. Kornberg (1994) A multisubunit complex containing the SWI1/ADR6, SWI2/SNF2, SWI3, SNF5, and SNF6 gene products isolated from yeast. *Proc Natl Acad Sci U S A,* 91**,** 1950-4.

Campos-Ortega, J. A. & V. Hartenstein. 2013. *The embryonic development of Drosophila melanogaster*. Springer Science & Business Media.

Canzonetta, C., S. Vernarecci, M. Iuliani, C. Marracino, C. Belloni, P. Ballario & P. Filetici (2015) SAGA DUB-Ubp8 Deubiquitylates Centromeric Histone Variant Cse4. *G3 (Bethesda),* 6**,** 287-98.

Cao, R., Y. Tsukada & Y. Zhang (2005) Role of Bmi-1 and Ring1A in H2A ubiquitylation and Hox gene silencing. *Mol Cell,* 20**,** 845-54.

Cao, R. & Y. Zhang (2004) SUZ12 is required for both the histone methyltransferase activity and the silencing function of the EED-EZH2 complex. *Mol Cell,* 15**,** 57-67.

Carey, M., B. Li & J. L. Workman (2006) RSC exploits histone acetylation to abrogate the nucleosomal block to RNA polymerase II elongation. *Mol Cell,* 24**,** 481-7.

Carre, C., A. Ciurciu, O. Komonyi, C. Jacquier, D. Fagegaltier, J. Pidoux, H. Tricoire, L. Tora, I. M. Boros & C. Antoniewski (2008) The Drosophila NURF remodelling and the ATAC histone acetylase complexes functionally interact and are required for global chromosome organization. *EMBO Rep,* 9**,** 187-92.

Carre, C., D. Szymczak, J. Pidoux & C. Antoniewski (2005) The histone H3 acetylase dGcn5 is a key player in Drosophila melanogaster metamorphosis. *Mol Cell Biol,* 25**,** 8228-38.

Carrozza, M. J., B. Li, L. Florens, T. Suganuma, S. K. Swanson, K. K. Lee, W. J. Shia, S. Anderson, J. Yates, M. P. Washburn & J. L. Workman (2005) Histone H3 methylation by Set2 directs deacetylation of coding regions by Rpd3S to suppress spurious intragenic transcription. *Cell,* 123**,** 581-92.

Chandrasekharan, M. B., F. Huang & Z. W. Sun (2009) Ubiquitination of histone H2B regulates chromatin dynamics by enhancing nucleosome stability. *Proc Natl Acad Sci U S A,* 106**,** 16686-91.

Chandy, M., J. L. Gutierrez, P. Prochasson & J. L. Workman (2006) SWI/SNF displaces SAGA-acetylated nucleosomes. *Eukaryot Cell,* 5**,** 1738-47.

Chen, K., J. Johnston, W. Shao, S. Meier, C. Staber & J. Zeitlinger (2013) A global change in RNA polymerase II pausing during the Drosophila midblastula transition. *Elife,* 2**,** e00861.

Chen, Y. C., J. R. Gatchel, R. W. Lewis, C. A. Mao, P. A. Grant, H. Y. Zoghbi & S. Y. Dent (2012) Gcn5 loss-of-function accelerates cerebellar and retinal degeneration in a SCA7 mouse model. *Hum Mol Genet,* 21**,** 394-405.

Cheung, P., K. G. Tanner, W. L. Cheung, P. Sassone-Corsi, J. M. Denu & C. D. Allis (2000) Synergistic coupling of histone H3 phosphorylation and acetylation in response to epidermal growth factor stimulation. *Mol Cell,* 5**,** 905-15.

Chou, T. B. & N. Perrimon (1996) The autosomal FLP-DFS technique for generating germline mosaics in Drosophila melanogaster. *Genetics,* 144**,** 1673-9.

Clague, M. J. & S. Urbe (2010) Ubiquitin: same molecule, different degradation pathways. *Cell,* 143**,** 682-5.

Cote, J., J. Quinn, J. L. Workman & C. L. Peterson (1994) Stimulation of GAL4 derivative binding to nucleosomal DNA by the yeast SWI/SNF complex. *Science,* 265**,** 53-60.

Daniel, J. A., M. S. Torok, Z. W. Sun, D. Schieltz, C. D. Allis, J. R. Yates, 3rd & P. A. Grant (2004) Deubiquitination of histone H2B by a yeast acetyltransferase complex regulates transcription. *J Biol Chem,* 279**,** 1867-71.

David, G., N. Abbas, G. Stevanin, A. Durr, G. Yvert, G. Cancel, C. Weber, G. Imbert, F. Saudou, E. Antoniou, H. Drabkin, R. Gemmill, P. Giunti, A. Benomar, N. Wood, M. Ruberg, Y. Agid, J. L. Mandel & A. Brice (1997) Cloning of the SCA7 gene reveals a highly unstable CAG repeat expansion. *Nat Genet,* 17**,** 65-70.

David, G., A. Durr, G. Stevanin, G. Cancel, N. Abbas, A. Benomar, S. Belal, A. S. Lebre, M. Abada-Bendib, D. Grid, M. Holmberg, M. Yahyaoui, F. Hentati, T. Chkili, Y. Agid & A. Brice (1998) Molecular and clinical correlations in autosomal dominant cerebellar ataxia with progressive macular dystrophy (SCA7). *Hum Mol Genet,* 7**,** 165-70.

Davies, N. & G. G. Lindsey (1994) Histone H2B (and H2A) ubiquitination allows normal histone octamer and core particle reconstitution. *Biochim Biophys Acta,* 1218**,** 187-93.

de Jonge, W. J., E. O'Duibhir, P. Lijnzaad, D. van Leenen, M. J. Groot Koerkamp, P. Kemmeren & F. C. Holstege (2017) Molecular mechanisms that distinguish TFIID housekeeping from regulatable SAGA promoters. *EMBO J,* 36**,** 274-290.

de Napoles, M., J. E. Mermoud, R. Wakao, Y. A. Tang, M. Endoh, R. Appanah, T. B. Nesterova, J. Silva, A. P. Otte, M. Vidal, H. Koseki & N. Brockdorff (2004) Polycomb group proteins Ring1A/B link ubiquitylation of histone H2A to heritable gene silencing and X inactivation. *Dev Cell,* 7**,** 663-76.

Dehe, P. M., M. Pamblanco, P. Luciano, R. Lebrun, D. Moinier, R. Sendra, A. Verreault, V. Tordera & V. Geli (2005) Histone H3 lysine 4 mono-methylation does not require ubiquitination of histone H2B. *J Mol Biol,* 353**,** 477-84.

Del-Favero, J., L. Krols, A. Michalik, J. Theuns, A. Lofgren, D. Goossens, A. Wehnert, D. Van den Bossche, K. Van Zand, H. Backhovens, N. van Regenmorter, J. J. Martin & C. Van Broeckhoven (1998) Molecular genetic analysis of autosomal dominant cerebellar ataxia with retinal degeneration (ADCA type II) caused by CAG triplet repeat expansion. *Hum Mol Genet,* 7**,** 177-86.

Demeny, M. A., E. Soutoglou, Z. Nagy, E. Scheer, A. Janoshazi, M. Richardot, M. Argentini, P. Kessler & L. Tora (2007) Identification of a small TAF complex and its role in the assembly of TAF-containing complexes. *PLoS One,* 2**,** e316.

Dingwall, A. K., S. J. Beek, C. M. McCallum, J. W. Tamkun, G. V. Kalpana, S. P. Goff & M. P. Scott (1995) The Drosophila snr1 and brm proteins are related to yeast SWI/SNF proteins and are components of a large protein complex. *Mol Biol Cell,* 6**,** 777-91.

Dou, Y., J. Bowen, Y. Liu & M. A. Gorovsky (2002) Phosphorylation and an ATP-dependent process increase the dynamic exchange of H1 in chromatin. *J Cell Biol,* 158**,** 1161-70.

Dover, J., J. Schneider, M. A. Tawiah-Boateng, A. Wood, K. Dean, M. Johnston & A. Shilatifard (2002) Methylation of histone H3 by COMPASS requires ubiquitination of histone H2B by Rad6. *J Biol Chem,* 277**,** 28368-71.

Doyon, Y. & J. Cote (2004) The highly conserved and multifunctional NuA4 HAT complex. *Curr Opin Genet Dev,* 14**,** 147-54.

Doyon, Y., W. Selleck, W. S. Lane, S. Tan & J. Cote (2004) Structural and functional conservation of the NuA4 histone acetyltransferase complex from yeast to humans. *Mol Cell Biol,* 24**,** 1884-96.

Drobic, B., B. Perez-Cadahia, J. Yu, S. K. Kung & J. R. Davie (2010) Promoter chromatin remodeling of immediate-early genes is mediated through H3 phosphorylation at either serine 28 or 10 by the MSK1 multi-protein complex. *Nucleic Acids Res,* 38**,** 3196-208.

Durant, M. & B. F. Pugh (2007) NuA4-directed chromatin transactions throughout the Saccharomyces cerevisiae genome. *Mol Cell Biol,* 27**,** 5327-35.

Eberharter, A., D. E. Sterner, D. Schieltz, A. Hassan, J. R. Yates, 3rd, S. L. Berger & J. L. Workman (1999) The ADA complex is a distinct histone acetyltransferase complex in Saccharomyces cerevisiae. *Mol Cell Biol,* 19**,** 6621-31.

Fang, J., T. Chen, B. Chadwick, E. Li & Y. Zhang (2004) Ring1b-mediated H2A ubiquitination associates with inactive X chromosomes and is involved in initiation of X inactivation. *J Biol Chem,* 279**,** 52812-5.

Fischle, W., Y. Wang & C. D. Allis (2003a) Binary switches and modification cassettes in histone biology and beyond. *Nature,* 425**,** 475-9.

Fischle, W., Y. Wang, S. A. Jacobs, Y. Kim, C. D. Allis & S. Khorasanizadeh (2003b) Molecular basis for the discrimination of repressive methyl-lysine marks in histone H3 by Polycomb and HP1 chromodomains. *Genes Dev,* 17**,** 1870-81.

Fishburn, J., N. Mohibullah & S. Hahn (2005) Function of a eukaryotic transcription activator during the transcription cycle. *Mol Cell,* 18**,** 369-78.

Fuda, N. J., M. B. Ardehali & J. T. Lis (2009) Defining mechanisms that regulate RNA polymerase II transcription in vivo. *Nature,* 461**,** 186-92.

Galarneau, L., A. Nourani, A. A. Boudreault, Y. Zhang, L. Heliot, S. Allard, J. Savard, W. S. Lane, D. J. Stillman & J. Cote (2000) Multiple links between the NuA4 histone acetyltransferase complex and epigenetic control of transcription. *Mol Cell,* 5**,** 927-37.

Gamper, A. M., J. Kim & R. G. Roeder (2009) The STAGA subunit ADA2b is an important regulator of human GCN5 catalysis. *Mol Cell Biol,* 29**,** 266-80.

Garcia-Ramirez, M., C. Rocchini & J. Ausio (1995) Modulation of chromatin folding by histone acetylation. *J Biol Chem,* 270**,** 17923-8.

Ghannad-Rezaie, M., X. Wang, B. Mishra, C. Collins & N. Chronis (2012) Microfluidic chips for in vivo imaging of cellular responses to neural injury in Drosophila larvae. *PLoS One,* 7**,** e29869.

Glinsky, G. V., O. Berezovska & A. B. Glinskii (2005) Microarray analysis identifies a death-from-cancer signature predicting therapy failure in patients with multiple types of cancer. *J Clin Invest,* 115**,** 1503-21.

Grant, P. A., L. Duggan, J. Cote, S. M. Roberts, J. E. Brownell, R. Candau, R. Ohba, T. Owen-Hughes, C. D. Allis, F. Winston, S. L. Berger & J. L. Workman (1997) Yeast Gcn5 functions in two multisubunit complexes to acetylate nucleosomal histones: characterization of an Ada complex and the SAGA (Spt/Ada) complex. *Genes Dev,* 11**,** 1640-50.

Grant, P. A., A. Eberharter, S. John, R. G. Cook, B. M. Turner & J. L. Workman (1999) Expanded lysine acetylation specificity of Gcn5 in native complexes. *J Biol Chem,* 274**,** 5895-900.

Grant, P. A., D. Schieltz, M. G. Pray-Grant, D. J. Steger, J. C. Reese, J. R. Yates, 3rd & J. L. Workman (1998) A subset of TAF(II)s are integral components of the SAGA complex required for nucleosome acetylation and transcriptional stimulation. *Cell,* 94**,** 45-53.

Green, G. R., H. J. Lee & D. L. Poccia (1993) Phosphorylation weakens DNA binding by peptides containing multiple "SPKK" sequences. *J Biol Chem,* 268**,** 11247-55.

Guelman, S., K. Kozuka, Y. Mao, V. Pham, M. J. Solloway, J. Wang, J. Wu, J. R. Lill & J. Zha (2009) The double-histone-acetyltransferase complex ATAC is essential for mammalian development. *Mol Cell Biol,* 29**,** 1176-88.

Guelman, S., T. Suganuma, L. Florens, S. K. Swanson, C. L. Kiesecker, T. Kusch, S. Anderson, J. R. Yates, 3rd, M. P. Washburn, S. M. Abmayr & J. L. Workman (2006a) Host cell factor and an uncharacterized SANT domain protein are stable components of ATAC, a novel dAda2A/dGcn5-containing histone acetyltransferase complex in Drosophila. *Mol Cell Biol,* 26**,** 871-82.

Guelman, S., T. Suganuma, L. Florens, V. Weake, S. K. Swanson, M. P. Washburn, S. M. Abmayr & J. L. Workman (2006b) The essential gene wda encodes a WD40 repeat subunit of Drosophila SAGA required for histone H3 acetylation. *Mol Cell Biol,* 26**,** 7178-89.

Han, Y., J. Luo, J. Ranish & S. Hahn (2014) Architecture of the Saccharomyces cerevisiae SAGA transcription coactivator complex. *EMBO J,* 33**,** 2534-46.

Happel, N. & D. Doenecke (2009) Histone H1 and its isoforms: contribution to chromatin structure and function. *Gene,* 431**,** 1-12.

Hassan, A. H., S. Awad & P. Prochasson (2006) The Swi2/Snf2 bromodomain is required for the displacement of SAGA and the octamer transfer of SAGA-acetylated nucleosomes. *J Biol Chem,* 281**,** 18126-34.

Hassan, A. H., K. E. Neely & J. L. Workman (2001) Histone acetyltransferase complexes stabilize swi/snf binding to promoter nucleosomes. *Cell,* 104**,** 817-27.

Hassan, A. H., P. Prochasson, K. E. Neely, S. C. Galasinski, M. Chandy, M. J. Carrozza & J. L. Workman (2002) Function and selectivity of bromodomains in anchoring chromatin-modifying complexes to promoter nucleosomes. *Cell,* 111**,** 369-79.

Hayes, J. J., D. Pruss & A. P. Wolffe (1994) Contacts of the globular domain of histone H5 and core histones with DNA in a "chromatosome". *Proc Natl Acad Sci U S A,* 91**,** 7817-21.

Hayes, J. J. & A. P. Wolffe (1993) Preferential and asymmetric interaction of linker histones with 5S DNA in the nucleosome. *Proc Natl Acad Sci U S A,* 90**,** 6415-9.

He, L., X. Wang & D. J. Montell (2011) Shining light on Drosophila oogenesis: live imaging of egg development. *Curr Opin Genet Dev,* 21**,** 612-9.

Helmlinger, D., S. Marguerat, J. Villen, S. P. Gygi, J. Bahler & F. Winston (2008) The S. pombe SAGA complex controls the switch from proliferation to sexual differentiation through the opposing roles of its subunits Gcn5 and Spt8. *Genes Dev,* 22**,** 3184-95.

Helmlinger, D., S. Marguerat, J. Villen, D. L. Swaney, S. P. Gygi, J. Bahler & F. Winston (2011) Tra1 has specific regulatory roles, rather than global functions, within the SAGA co-activator complex. *EMBO J,* 30**,** 2843-52.

Henry, K. W., A. Wyce, W. S. Lo, L. J. Duggan, N. C. Emre, C. F. Kao, L. Pillus, A. Shilatifard, M. A. Osley & S. L. Berger (2003) Transcriptional activation via sequential histone H2B

ubiquitylation and deubiquitylation, mediated by SAGA-associated Ubp8. *Genes Dev,* 17**,** 2648-63.
Hirsch, C. L., Z. Coban Akdemir, L. Wang, G. Jayakumaran, D. Trcka, A. Weiss, J. J. Hernandez, Q. Pan, H. Han, X. Xu, Z. Xia, A. P. Salinger, M. Wilson, F. Vizeacoumar, A. Datti, W. Li, A. J. Cooney, M. C. Barton, B. J. Blencowe, J. L. Wrana & S. Y. Dent (2015) Myc and SAGA rewire an alternative splicing network during early somatic cell reprogramming. *Genes Dev,* 29**,** 803-16.
Horn, P. J., L. M. Carruthers, C. Logie, D. A. Hill, M. J. Solomon, P. A. Wade, A. N. Imbalzano, J. C. Hansen & C. L. Peterson (2002) Phosphorylation of linker histones regulates ATP-dependent chromatin remodeling enzymes. *Nat Struct Biol,* 9**,** 263-7.
Huang, H., B. R. Sabari, B. A. Garcia, C. D. Allis & Y. Zhao (2014) SnapShot: histone modifications. *Cell,* 159**,** 458-458 e1.
Huisinga, K. L. & B. F. Pugh (2004) A genome-wide housekeeping role for TFIID and a highly regulated stress-related role for SAGA in Saccharomyces cerevisiae. *Mol Cell,* 13**,** 573-85.
Ibnsouda, S., F. Schweisguth, G. de Billy & A. Vincent (1993) Relationship between expression of serendipity alpha and cellularisation of the Drosophila embryo as revealed by interspecific transformation. *Development,* 119**,** 471-83.
Ikeda, K., D. J. Steger, A. Eberharter & J. L. Workman (1999) Activation domain-specific and general transcription stimulation by native histone acetyltransferase complexes. *Mol Cell Biol,* 19**,** 855-63.
Ikura, T., V. V. Ogryzko, M. Grigoriev, R. Groisman, J. Wang, M. Horikoshi, R. Scully, J. Qin & Y. Nakatani (2000) Involvement of the TIP60 histone acetylase complex in DNA repair and apoptosis. *Cell,* 102**,** 463-73.
Ingvarsdottir, K., N. J. Krogan, N. C. Emre, A. Wyce, N. J. Thompson, A. Emili, T. R. Hughes, J. F. Greenblatt & S. L. Berger (2005) H2B ubiquitin protease Ubp8 and Sgf11 constitute a discrete functional module within the Saccharomyces cerevisiae SAGA complex. *Mol Cell Biol,* 25**,** 1162-72.
Ito, T., T. Ikehara, T. Nakagawa, W. L. Kraus & M. Muramatsu (2000) p300-mediated acetylation facilitates the transfer of histone H2A-H2B dimers from nucleosomes to a histone chaperone. *Genes Dev,* 14**,** 1899-907.
Jacobs, S. A. & S. Khorasanizadeh (2002) Structure of HP1 chromodomain bound to a lysine 9-methylated histone H3 tail. *Science,* 295**,** 2080-3.
Jason, L. J., R. M. Finn, G. Lindsey & J. Ausio (2005) Histone H2A ubiquitination does not preclude histone H1 binding, but it facilitates its association with the nucleosome. *J Biol Chem,* 280**,** 4975-82.
Johansson, J., L. Forsgren, O. Sandgren, A. Brice, G. Holmgren & M. Holmberg (1998) Expanded CAG repeats in Swedish spinocerebellar ataxia type 7 (SCA7) patients: effect of CAG repeat length on the clinical manifestation. *Hum Mol Genet,* 7**,** 171-6.
Johnstone, O. & P. Lasko (2001) Translational regulation and RNA localization in Drosophila oocytes and embryos. *Annu Rev Genet,* 35**,** 365-406.
Joshi, A. A. & K. Struhl (2005) Eaf3 chromodomain interaction with methylated H3-K36 links histone deacetylation to Pol II elongation. *Mol Cell,* 20**,** 971-8.
Jung, I., S. K. Kim, M. Kim, Y. M. Han, Y. S. Kim, D. Kim & D. Lee (2012) H2B monoubiquitylation is a 5'-enriched active transcription mark and correlates with exon-intron structure in human cells. *Genome Res,* 22**,** 1026-35.

Kasten, M., H. Szerlong, H. Erdjument-Bromage, P. Tempst, M. Werner & B. R. Cairns (2004) Tandem bromodomains in the chromatin remodeler RSC recognize acetylated histone H3 Lys14. *EMBO J,* 23**,** 1348-59.

Keogh, M. C., S. K. Kurdistani, S. A. Morris, S. H. Ahn, V. Podolny, S. R. Collins, M. Schuldiner, K. Chin, T. Punna, N. J. Thompson, C. Boone, A. Emili, J. S. Weissman, T. R. Hughes, B. D. Strahl, M. Grunstein, J. F. Greenblatt, S. Buratowski & N. J. Krogan (2005) Cotranscriptional set2 methylation of histone H3 lysine 36 recruits a repressive Rpd3 complex. *Cell,* 123**,** 593-605.

Kerppola, T. K. (2009) Polycomb group complexes--many combinations, many functions. *Trends Cell Biol,* 19**,** 692-704.

Khorasanizadeh, S. (2004) The nucleosome: from genomic organization to genomic regulation. *Cell,* 116**,** 259-72.

Kim, J. & R. G. Roeder (2009) Direct Bre1-Paf1 complex interactions and RING finger-independent Bre1-Rad6 interactions mediate histone H2B ubiquitylation in yeast. *J Biol Chem,* 284**,** 20582-92.

Kingston, R. E., C. A. Bunker & A. N. Imbalzano (1996) Repression and activation by multiprotein complexes that alter chromatin structure. *Genes Dev,* 10**,** 905-20.

Kingston, R. E. & G. J. Narlikar (1999) ATP-dependent remodeling and acetylation as regulators of chromatin fluidity. *Genes Dev,* 13**,** 2339-52.

Kirilly, D. & T. Xie (2007) The Drosophila ovary: an active stem cell community. *Cell Res,* 17**,** 15-25.

Koehler, C., J. Bonnet, M. Stierle, C. Romier, D. Devys & B. Kieffer (2014) DNA binding by Sgf11 protein affects histone H2B deubiquitination by Spt-Ada-Gcn5-acetyltransferase (SAGA). *J Biol Chem,* 289**,** 8989-99.

Kohler, A., M. Schneider, G. G. Cabal, U. Nehrbass & E. Hurt (2008) Yeast Ataxin-7 links histone deubiquitination with gene gating and mRNA export. *Nat Cell Biol,* 10**,** 707-15.

Kohler, A., E. Zimmerman, M. Schneider, E. Hurt & N. Zheng (2010) Structural basis for assembly and activation of the heterotetrameric SAGA histone H2B deubiquitinase module. *Cell,* 141**,** 606-17.

Kooistra, S. M. & K. Helin (2012) Molecular mechanisms and potential functions of histone demethylases. *Nat Rev Mol Cell Biol,* 13**,** 297-311.

Koop, R., L. Di Croce & M. Beato (2003) Histone H1 enhances synergistic activation of the MMTV promoter in chromatin. *EMBO J,* 22**,** 588-99.

Kosinsky, R. L., F. Wegwitz, N. Hellbach, M. Dobbelstein, A. Mansouri, T. Vogel, Y. Begus-Nahrmann & S. A. Johnsen (2015) Usp22 deficiency impairs intestinal epithelial lineage specification in vivo. *Oncotarget,* 6**,** 37906-18.

Kotadia, S., J. Crest, U. Tram, B. Riggs & W. Sullivan. 2001. Blastoderm Formation and Cellularisation in Drosophila melanogaster. In *eLS*. John Wiley & Sons, Ltd.

Koutelou, E., C. L. Hirsch & S. Y. Dent (2010) Multiple faces of the SAGA complex. *Curr Opin Cell Biol,* 22**,** 374-82.

Kouzarides, T. (2007) Chromatin modifications and their function. *Cell,* 128**,** 693-705.

Krebs, A. R., K. Karmodiya, M. Lindahl-Allen, K. Struhl & L. Tora (2011) SAGA and ATAC histone acetyl transferase complexes regulate distinct sets of genes and ATAC defines a class of p300-independent enhancers. *Mol Cell,* 44**,** 410-23.

Krogan, N. J., J. Dover, S. Khorrami, J. F. Greenblatt, J. Schneider, M. Johnston & A. Shilatifard (2002) COMPASS, a histone H3 (Lysine 4) methyltransferase required for telomeric silencing of gene expression. *J Biol Chem,* 277**,** 10753-5.

Kurabe, N., K. Katagiri, Y. Komiya, R. Ito, A. Sugiyama, Y. Kawasaki & F. Tashiro (2007) Deregulated expression of a novel component of TFTC/STAGA histone acetyltransferase complexes, rat SGF29, in hepatocellular carcinoma: possible implication for the oncogenic potential of c-Myc. *Oncogene,* 26**,** 5626-34.

Kurdistani, S. K., S. Tavazoie & M. Grunstein (2004) Mapping global histone acetylation patterns to gene expression. *Cell,* 117**,** 721-33.

Kurshakova, M. M., A. N. Krasnov, D. V. Kopytova, Y. V. Shidlovskii, J. V. Nikolenko, E. N. Nabirochkina, D. Spehner, P. Schultz, L. Tora & S. G. Georgieva (2007) SAGA and a novel Drosophila export complex anchor efficient transcription and mRNA export to NPC. *EMBO J,* 26**,** 4956-65.

Kusch, T., S. Guelman, S. M. Abmayr & J. L. Workman (2003) Two Drosophila Ada2 homologues function in different multiprotein complexes. *Mol Cell Biol,* 23**,** 3305-19.

Kwon, H., A. N. Imbalzano, P. A. Khavari, R. E. Kingston & M. R. Green (1994) Nucleosome disruption and enhancement of activator binding by a human SW1/SNF complex. *Nature,* 370**,** 477-81.

Lang, G., J. Bonnet, D. Umlauf, K. Karmodiya, J. Koffler, M. Stierle, D. Devys & L. Tora (2011) The tightly controlled deubiquitination activity of the human SAGA complex differentially modifies distinct gene regulatory elements. *Mol Cell Biol,* 31**,** 3734-44.

Laprade, L., D. Rose & F. Winston (2007) Characterization of new Spt3 and TATA-binding protein mutants of Saccharomyces cerevisiae: Spt3 TBP allele-specific interactions and bypass of Spt8. *Genetics,* 177**,** 2007-17.

Larschan, E. & F. Winston (2001) The S. cerevisiae SAGA complex functions in vivo as a coactivator for transcriptional activation by Gal4. *Genes Dev,* 15**,** 1946-56.

Latouche, M., C. Lasbleiz, E. Martin, V. Monnier, T. Debeir, A. Mouatt-Prigent, M. P. Muriel, L. Morel, M. Ruberg, A. Brice, G. Stevanin & H. Tricoire (2007) A conditional pan-neuronal Drosophila model of spinocerebellar ataxia 7 with a reversible adult phenotype suitable for identifying modifier genes. *J Neurosci,* 27**,** 2483-92.

Lee, J. S., A. S. Garrett, K. Yen, Y. H. Takahashi, D. Hu, J. Jackson, C. Seidel, B. F. Pugh & A. Shilatifard (2012) Codependency of H2B monoubiquitination and nucleosome reassembly on Chd1. *Genes Dev,* 26**,** 914-9.

Lee, J. S., A. Shukla, J. Schneider, S. K. Swanson, M. P. Washburn, L. Florens, S. R. Bhaumik & A. Shilatifard (2007) Histone crosstalk between H2B monoubiquitination and H3 methylation mediated by COMPASS. *Cell,* 131**,** 1084-96.

Lee, K. K., L. Florens, S. K. Swanson, M. P. Washburn & J. L. Workman (2005) The deubiquitylation activity of Ubp8 is dependent upon Sgf11 and its association with the SAGA complex. *Mol Cell Biol,* 25**,** 1173-82.

Lee, K. K., M. E. Sardiu, S. K. Swanson, J. M. Gilmore, M. Torok, P. A. Grant, L. Florens, J. L. Workman & M. P. Washburn (2011) Combinatorial depletion analysis to assemble the network architecture of the SAGA and ADA chromatin remodeling complexes. *Mol Syst Biol,* 7**,** 503.

Lee, K. K., S. K. Swanson, L. Florens, M. P. Washburn & J. L. Workman (2009) Yeast Sgf73/Ataxin-7 serves to anchor the deubiquitination module into both SAGA and Slik(SALSA) HAT complexes. *Epigenetics Chromatin,* 2**,** 2.

Lee, K. K. & J. L. Workman (2007) Histone acetyltransferase complexes: one size doesn't fit all. *Nat Rev Mol Cell Biol,* 8**,** 284-95.
Lee, T. I., H. C. Causton, F. C. Holstege, W. C. Shen, N. Hannett, E. G. Jennings, F. Winston, M. R. Green & R. A. Young (2000) Redundant roles for the TFIID and SAGA complexes in global transcription. *Nature,* 405**,** 701-4.
Li, B., M. Carey & J. L. Workman (2007) The role of chromatin during transcription. *Cell,* 128**,** 707-19.
Li, G. & D. Reinberg (2011) Chromatin higher-order structures and gene regulation. *Curr Opin Genet Dev,* 21**,** 175-86.
Li, X., C. W. Seidel, L. T. Szerszen, J. J. Lange, J. L. Workman & S. M. Abmayr (2017) Enzymatic modules of the SAGA chromatin-modifying complex play distinct roles in Drosophila gene expression and development. *Genes Dev,* 31**,** 1588-1600.
Lim, S., J. Kwak, M. Kim & D. Lee (2013) Separation of a functional deubiquitylating module from the SAGA complex by the proteasome regulatory particle. *Nat Commun,* 4**,** 2641.
Lin, Z., H. Yang, Q. Kong, J. Li, S. M. Lee, B. Gao, H. Dong, J. Wei, J. Song, D. D. Zhang & D. Fang (2012) USP22 antagonizes p53 transcriptional activation by deubiquitinating Sirt1 to suppress cell apoptosis and is required for mouse embryonic development. *Mol Cell,* 46**,** 484-94.
Liu, C. L., T. Kaplan, M. Kim, S. Buratowski, S. L. Schreiber, N. Friedman & O. J. Rando (2005) Single-nucleosome mapping of histone modifications in S. cerevisiae. *PLoS Biol,* 3**,** e328.
Liu, X., J. Tesfai, Y. A. Evrard, S. Y. Dent & E. Martinez (2003) c-Myc transformation domain recruits the human STAGA complex and requires TRRAP and GCN5 acetylase activity for transcription activation. *J Biol Chem,* 278**,** 20405-12.
Liu, X., M. Vorontchikhina, Y. L. Wang, F. Faiola & E. Martinez (2008) STAGA recruits Mediator to the MYC oncoprotein to stimulate transcription and cell proliferation. *Mol Cell Biol,* 28**,** 108-21.
Liu, Y. L., S. X. Jiang, Y. M. Yang, H. Xu, J. L. Liu & X. S. Wang (2012) USP22 acts as an oncogene by the activation of BMI-1-mediated INK4a/ARF pathway and Akt pathway. *Cell Biochem Biophys,* 62**,** 229-35.
Liu, Y. L., Y. M. Yang, H. Xu & X. S. Dong (2011) Aberrant expression of USP22 is associated with liver metastasis and poor prognosis of colorectal cancer. *J Surg Oncol,* 103**,** 283-9.
Lo Piccolo, L., R. Bonaccorso & M. C. Onorati (2015) Nuclear and Cytoplasmic Soluble Proteins Extraction from a Small Quantity of Drosophila's Whole Larvae and Tissues. *Int J Mol Sci,* 16**,** 12360-7.
Lo, W. S., R. C. Trievel, J. R. Rojas, L. Duggan, J. Y. Hsu, C. D. Allis, R. Marmorstein & S. L. Berger (2000) Phosphorylation of serine 10 in histone H3 is functionally linked in vitro and in vivo to Gcn5-mediated acetylation at lysine 14. *Mol Cell,* 5**,** 917-26.
Luger, K., A. W. Mader, R. K. Richmond, D. F. Sargent & T. J. Richmond (1997) Crystal structure of the nucleosome core particle at 2.8 A resolution. *Nature,* 389**,** 251-60.
Ma, J., K. J. Brennan, M. R. D'Aloia, P. E. Pascuzzi & V. M. Weake (2016) Transcriptome Profiling Identifies Multiplexin as a Target of SAGA Deubiquitinase Activity in Glia Required for Precise Axon Guidance During Drosophila Visual Development. *G3 (Bethesda),* 6**,** 2435-45.
Macdonald, P. M., P. Ingham & G. Struhl (1986) Isolation, structure, and expression of even-skipped: a second pair-rule gene of Drosophila containing a homeo box. *Cell,* 47**,** 721-34.

Marsden, M. P. & U. K. Laemmli (1979) Metaphase chromosome structure: evidence for a radial loop model. *Cell,* 17**,** 849-58.
Martin, K. A., B. Poeck, H. Roth, A. J. Ebens, L. C. Ballard & S. L. Zipursky (1995) Mutations disrupting neuronal connectivity in the Drosophila visual system. *Neuron,* 14**,** 229-40.
Martinez-Cerdeno, V., J. M. Lemen, V. Chan, A. Wey, W. Lin, S. R. Dent & P. S. Knoepfler (2012) N-Myc and GCN5 regulate significantly overlapping transcriptional programs in neural stem cells. *PLoS One,* 7**,** e39456.
Martinez, E., T. K. Kundu, J. Fu & R. G. Roeder (1998) A human SPT3-TAFII31-GCN5-L acetylase complex distinct from transcription factor IID. *J Biol Chem,* 273**,** 23781-5.
Martinez, E., V. B. Palhan, A. Tjernberg, E. S. Lymar, A. M. Gamper, T. K. Kundu, B. T. Chait & R. G. Roeder (2001) Human STAGA complex is a chromatin-acetylating transcription coactivator that interacts with pre-mRNA splicing and DNA damage-binding factors in vivo. *Mol Cell Biol,* 21**,** 6782-95.
Mazumdar, A. & M. Mazumdar (2002) How one becomes many: blastoderm cellularization in Drosophila melanogaster. *Bioessays,* 24**,** 1012-22.
McMahon, S. B., M. A. Wood & M. D. Cole (2000) The essential cofactor TRRAP recruits the histone acetyltransferase hGCN5 to c-Myc. *Mol Cell Biol,* 20**,** 556-62.
Minsky, N., E. Shema, Y. Field, M. Schuster, E. Segal & M. Oren (2008) Monoubiquitinated H2B is associated with the transcribed region of highly expressed genes in human cells. *Nat Cell Biol,* 10**,** 483-8.
Mohan, R. D., G. Dialynas, V. M. Weake, J. Liu, S. Martin-Brown, L. Florens, M. P. Washburn, J. L. Workman & S. M. Abmayr (2014) Loss of Drosophila Ataxin-7, a SAGA subunit, reduces H2B ubiquitination and leads to neural and retinal degeneration. *Genes Dev,* 28**,** 259-72.
Mohibi, S., C. B. Gurumurthy, A. Nag, J. Wang, S. Mirza, Y. Mian, M. Quinn, B. Katafiasz, J. Eudy, S. Pandey, C. Guda, M. Naramura, H. Band & V. Band (2012) Mammalian alteration/deficiency in activation 3 (Ada3) is essential for embryonic development and cell cycle progression. *J Biol Chem,* 287**,** 29442-56.
Mohibullah, N. & S. Hahn (2008) Site-specific cross-linking of TBP in vivo and in vitro reveals a direct functional interaction with the SAGA subunit Spt3. *Genes Dev,* 22**,** 2994-3006.
Morgan, M. T., M. Haj-Yahya, A. E. Ringel, P. Bandi, A. Brik & C. Wolberger (2016) Structural basis for histone H2B deubiquitination by the SAGA DUB module. *Science,* 351**,** 725-8.
Mosammaparast, N. & Y. Shi (2010) Reversal of histone methylation: biochemical and molecular mechanisms of histone demethylases. *Annu Rev Biochem,* 79**,** 155-79.
Muratoglu, S., S. Georgieva, G. Papai, E. Scheer, I. Enunlu, O. Komonyi, I. Cserpan, L. Lebedeva, E. Nabirochkina, A. Udvardy, L. Tora & I. Boros (2003) Two different Drosophila ADA2 homologues are present in distinct GCN5 histone acetyltransferase-containing complexes. *Mol Cell Biol,* 23**,** 306-21.
Nagy, Z., A. Riss, C. Romier, X. le Guezennec, A. R. Dongre, M. Orpinell, J. Han, H. Stunnenberg & L. Tora (2009) The human SPT20-containing SAGA complex plays a direct role in the regulation of endoplasmic reticulum stress-induced genes. *Mol Cell Biol,* 29**,** 1649-60.
Nakagawa, T., T. Kajitani, S. Togo, N. Masuko, H. Ohdan, Y. Hishikawa, T. Koji, T. Matsuyama, T. Ikura, M. Muramatsu & T. Ito (2008) Deubiquitylation of histone H2A activates transcriptional initiation via trans-histone cross-talk with H3K4 di- and trimethylation. *Genes Dev,* 22**,** 37-49.

Neuwald, A. F. & D. Landsman (1997) GCN5-related histone N-acetyltransferases belong to a diverse superfamily that includes the yeast SPT10 protein. *Trends Biochem Sci,* 22**,** 154-5.

Ng, H. H., R. M. Xu, Y. Zhang & K. Struhl (2002) Ubiquitination of histone H2B by Rad6 is required for efficient Dot1-mediated methylation of histone H3 lysine 79. *J Biol Chem,* 277**,** 34655-7.

Ni, J. Q., R. Zhou, B. Czech, L. P. Liu, L. Holderbaum, D. Yang-Zhou, H. S. Shim, R. Tao, D. Handler, P. Karpowicz, R. Binari, M. Booker, J. Brennecke, L. A. Perkins, G. J. Hannon & N. Perrimon (2011) A genome-scale shRNA resource for transgenic RNAi in Drosophila. *Nat Methods,* 8**,** 405-7.

Noll, M. & R. D. Kornberg (1977) Action of micrococcal nuclease on chromatin and the location of histone H1. *J Mol Biol,* 109**,** 393-404.

Nowak, S. J. & V. G. Corces (2004) Phosphorylation of histone H3: a balancing act between chromosome condensation and transcriptional activation. *Trends Genet,* 20**,** 214-20.

Ogryzko, V. V., T. Kotani, X. Zhang, R. L. Schiltz, T. Howard, X. J. Yang, B. H. Howard, J. Qin & Y. Nakatani (1998) Histone-like TAFs within the PCAF histone acetylase complex. *Cell,* 94**,** 35-44.

Osley, M. A. (2006) Regulation of histone H2A and H2B ubiquitylation. *Brief Funct Genomic Proteomic,* 5**,** 179-89.

Pahi, Z., Z. Kiss, O. Komonyi, B. N. Borsos, L. Tora, I. M. Boros & T. Pankotai (2015) dTAF10- and dTAF10b-Containing Complexes Are Required for Ecdysone-Driven Larval-Pupal Morphogenesis in Drosophila melanogaster. *PLoS One,* 10**,** e0142226.

Pankotai, T., O. Komonyi, L. Bodai, Z. Ujfaludi, S. Muratoglu, A. Ciurciu, L. Tora, J. Szabad & I. Boros (2005) The homologous Drosophila transcriptional adaptors ADA2a and ADA2b are both required for normal development but have different functions. *Mol Cell Biol,* 25**,** 8215-27.

Pankotai, T., N. Zsindely, E. E. Vamos, O. Komonyi, L. Bodai & I. M. Boros (2013) Functional characterization and gene expression profiling of Drosophila melanogaster short dADA2b isoform-containing dSAGA complexes. *BMC Genomics,* 14**,** 44.

Pavri, R., B. Zhu, G. Li, P. Trojer, S. Mandal, A. Shilatifard & D. Reinberg (2006) Histone H2B monoubiquitination functions cooperatively with FACT to regulate elongation by RNA polymerase II. *Cell,* 125**,** 703-17.

Pilot, F., J. M. Philippe, C. Lemmers, J. P. Chauvin & T. Lecuit (2006) Developmental control of nuclear morphogenesis and anchoring by charleston, identified in a functional genomic screen of Drosophila cellularisation. *Development,* 133**,** 711-23.

Poeck, B., S. Fischer, D. Gunning, S. L. Zipursky & I. Salecker (2001) Glial cells mediate target layer selection of retinal axons in the developing visual system of Drosophila. *Neuron,* 29**,** 99-113.

Pokholok, D. K., C. T. Harbison, S. Levine, M. Cole, N. M. Hannett, T. I. Lee, G. W. Bell, K. Walker, P. A. Rolfe, E. Herbolsheimer, J. Zeitlinger, F. Lewitter, D. K. Gifford & R. A. Young (2005) Genome-wide map of nucleosome acetylation and methylation in yeast. *Cell,* 122**,** 517-27.

Powell, D. W., C. M. Weaver, J. L. Jennings, K. J. McAfee, Y. He, P. A. Weil & A. J. Link (2004) Cluster analysis of mass spectrometry data reveals a novel component of SAGA. *Mol Cell Biol,* 24**,** 7249-59.

Pritchard, D. K. & G. Schubiger (1996) Activation of transcription in Drosophila embryos is a gradual process mediated by the nucleocytoplasmic ratio. *Genes Dev,* 10**,** 1131-42.
Qi, D., J. Larsson & M. Mannervik (2004) Drosophila Ada2b is required for viability and normal histone H3 acetylation. *Mol Cell Biol,* 24**,** 8080-9.
Rea, S., F. Eisenhaber, D. O'Carroll, B. D. Strahl, Z. W. Sun, M. Schmid, S. Opravil, K. Mechtler, C. P. Ponting, C. D. Allis & T. Jenuwein (2000) Regulation of chromatin structure by site-specific histone H3 methyltransferases. *Nature,* 406**,** 593-9.
Reeves, W. M. & S. Hahn (2005) Targets of the Gal4 transcription activator in functional transcription complexes. *Mol Cell Biol,* 25**,** 9092-102.
Reid, J. L., V. R. Iyer, P. O. Brown & K. Struhl (2000) Coordinate regulation of yeast ribosomal protein genes is associated with targeted recruitment of Esa1 histone acetylase. *Mol Cell,* 6**,** 1297-307.
Robert, F., D. K. Pokholok, N. M. Hannett, N. J. Rinaldi, M. Chandy, A. Rolfe, J. L. Workman, D. K. Gifford & R. A. Young (2004) Global position and recruitment of HATs and HDACs in the yeast genome. *Mol Cell,* 16**,** 199-209.
Rodriguez-Navarro, S. (2009) Insights into SAGA function during gene expression. *EMBO Rep,* 10**,** 843-50.
Rodriguez-Navarro, S., T. Fischer, M. J. Luo, O. Antunez, S. Brettschneider, J. Lechner, J. E. Perez-Ortin, R. Reed & E. Hurt (2004) Sus1, a functional component of the SAGA histone acetylase complex and the nuclear pore-associated mRNA export machinery. *Cell,* 116**,** 75-86.
Roh, T. Y., S. Cuddapah & K. Zhao (2005) Active chromatin domains are defined by acetylation islands revealed by genome-wide mapping. *Genes Dev,* 19**,** 542-52.
Roth, S. Y., J. M. Denu & C. D. Allis (2001) Histone acetyltransferases. *Annu Rev Biochem,* 70**,** 81-120.
Samara, N. L., A. B. Datta, C. E. Berndsen, X. Zhang, T. Yao, R. E. Cohen & C. Wolberger (2010) Structural insights into the assembly and function of the SAGA deubiquitinating module. *Science,* 328**,** 1025-9.
Sawicka, A. & C. Seiser (2012) Histone H3 phosphorylation - a versatile chromatin modification for different occasions. *Biochimie,* 94**,** 2193-201.
Schejter, E. D. & E. Wieschaus (1993) bottleneck acts as a regulator of the microfilament network governing cellularization of the Drosophila embryo. *Cell,* 75**,** 373-85.
Schneider, J., A. Wood, J. S. Lee, R. Schuster, J. Dueker, C. Maguire, S. K. Swanson, L. Florens, M. P. Washburn & A. Shilatifard (2005) Molecular regulation of histone H3 trimethylation by COMPASS and the regulation of gene expression. *Mol Cell,* 19**,** 849-56.
Sermwittayawong, D. & S. Tan (2006) SAGA binds TBP via its Spt8 subunit in competition with DNA: implications for TBP recruitment. *EMBO J,* 25**,** 3791-800.
Setiaputra, D., J. D. Ross, S. Lu, D. T. Cheng, M. Q. Dong & C. K. Yip (2015) Conformational flexibility and subunit arrangement of the modular yeast Spt-Ada-Gcn5 acetyltransferase complex. *J Biol Chem,* 290**,** 10057-70.
Shahbazian, M. D. & M. Grunstein (2007) Functions of site-specific histone acetylation and deacetylation. *Annu Rev Biochem,* 76**,** 75-100.
Shahbazian, M. D., K. Zhang & M. Grunstein (2005) Histone H2B ubiquitylation controls processive methylation but not monomethylation by Dot1 and Set1. *Mol Cell,* 19**,** 271-7.

Shieh, G. S., C. H. Pan, J. H. Wu, Y. J. Sun, C. C. Wang, W. C. Hsiao, C. Y. Lin, L. Tung, T. H. Chang, A. B. Fleming, C. Hillyer, Y. C. Lo, S. L. Berger, M. A. Osley & C. F. Kao (2011) H2B ubiquitylation is part of chromatin architecture that marks exon-intron structure in budding yeast. *BMC Genomics,* 12**,** 627.

Shilatifard, A. (2012) The COMPASS family of histone H3K4 methylases: mechanisms of regulation in development and disease pathogenesis. *Annu Rev Biochem,* 81**,** 65-95.

Shogren-Knaak, M., H. Ishii, J. M. Sun, M. J. Pazin, J. R. Davie & C. L. Peterson (2006) Histone H4-K16 acetylation controls chromatin structure and protein interactions. *Science,* 311**,** 844-7.

Shukla, A., S. Lahudkar, G. Durairaj & S. R. Bhaumik (2012) Sgf29p facilitates the recruitment of TATA box binding protein but does not alter SAGA's global structural integrity in vivo. *Biochemistry,* 51**,** 706-14.

Simpson, R. T. (1978) Structure of the chromatosome, a chromatin particle containing 160 base pairs of DNA and all the histones. *Biochemistry,* 17**,** 5524-31.

Smith, C. L., R. Horowitz-Scherer, J. F. Flanagan, C. L. Woodcock & C. L. Peterson (2003) Structural analysis of the yeast SWI/SNF chromatin remodeling complex. *Nat Struct Biol,* 10**,** 141-5.

Spedale, G., H. T. Timmers & W. W. Pijnappel (2012) ATAC-king the complexity of SAGA during evolution. *Genes Dev,* 26**,** 527-41.

Stein, J. A., H. T. Broihier, L. A. Moore & R. Lehmann (2002) Slow as molasses is required for polarized membrane growth and germ cell migration in Drosophila. *Development,* 129**,** 3925-34.

Sterner, D. E., P. A. Grant, S. M. Roberts, L. J. Duggan, R. Belotserkovskaya, L. A. Pacella, F. Winston, J. L. Workman & S. L. Berger (1999) Functional organization of the yeast SAGA complex: distinct components involved in structural integrity, nucleosome acetylation, and TATA-binding protein interaction. *Mol Cell Biol,* 19**,** 86-98.

Steunou, A.-L., D. Rossetto & J. Côté. 2014. Regulating Chromatin by Histone Acetylation. In *Fundamentals of Chromatin,* eds. J. L. Workman & S. M. Abmayr, 147-212. New York, NY: Springer New York.

Suganuma, T., J. L. Gutierrez, B. Li, L. Florens, S. K. Swanson, M. P. Washburn, S. M. Abmayr & J. L. Workman (2008) ATAC is a double histone acetyltransferase complex that stimulates nucleosome sliding. *Nat Struct Mol Biol,* 15**,** 364-72.

Sun, Z. W. & C. D. Allis (2002) Ubiquitination of histone H2B regulates H3 methylation and gene silencing in yeast. *Nature,* 418**,** 104-8.

Taatjes, D. J. (2017) The Continuing SAGA of TFIID and RNA Polymerase II Transcription. *Mol Cell,* 68**,** 1-2.

Tadros, W. & H. D. Lipshitz (2009) The maternal-to-zygotic transition: a play in two acts. *Development,* 136**,** 3033-42.

Thisse, B., M. el Messal & F. Perrin-Schmitt (1987) The twist gene: isolation of a Drosophila zygotic gene necessary for the establishment of dorsoventral pattern. *Nucleic Acids Res,* 15**,** 3439-53.

Thoma, F., T. Koller & A. Klug (1979) Involvement of histone H1 in the organization of the nucleosome and of the salt-dependent superstructures of chromatin. *J Cell Biol,* 83**,** 403-27.

Tollervey, J. R. & V. V. Lunyak (2012) Epigenetics: judge, jury and executioner of stem cell fate. *Epigenetics,* 7**,** 823-40.

Utley, R. T., K. Ikeda, P. A. Grant, J. Cote, D. J. Steger, A. Eberharter, S. John & J. L. Workman (1998) Transcriptional activators direct histone acetyltransferase complexes to nucleosomes. *Nature,* 394**,** 498-502.

Vignali, M., D. J. Steger, K. E. Neely & J. L. Workman (2000) Distribution of acetylated histones resulting from Gal4-VP16 recruitment of SAGA and NuA4 complexes. *EMBO J,* 19**,** 2629-40.

Vissers, J. H., F. Nicassio, M. van Lohuizen, P. P. Di Fiore & E. Citterio (2008) The many faces of ubiquitinated histone H2A: insights from the DUBs. *Cell Div,* 3**,** 8.

Vitaliano-Prunier, A., A. Menant, M. Hobeika, V. Geli, C. Gwizdek & C. Dargemont (2008) Ubiquitylation of the COMPASS component Swd2 links H2B ubiquitylation to H3K4 trimethylation. *Nat Cell Biol,* 10**,** 1365-71.

Wang, H., L. Wang, H. Erdjument-Bromage, M. Vidal, P. Tempst, R. S. Jones & Y. Zhang (2004) Role of histone H2A ubiquitination in Polycomb silencing. *Nature,* 431**,** 873-8.

Wang, L., Y. Tang, P. A. Cole & R. Marmorstein (2008a) Structure and chemistry of the p300/CBP and Rtt109 histone acetyltransferases: implications for histone acetyltransferase evolution and function. *Curr Opin Struct Biol,* 18**,** 741-7.

Wang, W., J. Cote, Y. Xue, S. Zhou, P. A. Khavari, S. R. Biggar, C. Muchardt, G. V. Kalpana, S. P. Goff, M. Yaniv, J. L. Workman & G. R. Crabtree (1996a) Purification and biochemical heterogeneity of the mammalian SWI-SNF complex. *EMBO J,* 15**,** 5370-82.

Wang, W., Y. Xue, S. Zhou, A. Kuo, B. R. Cairns & G. R. Crabtree (1996b) Diversity and specialization of mammalian SWI/SNF complexes. *Genes Dev,* 10**,** 2117-30.

Wang, Y. L., F. Faiola, M. Xu, S. Pan & E. Martinez (2008b) Human ATAC Is a GCN5/PCAF-containing acetylase complex with a novel NC2-like histone fold module that interacts with the TATA-binding protein. *J Biol Chem,* 283**,** 33808-15.

Wang, Z., C. Zang, J. A. Rosenfeld, D. E. Schones, A. Barski, S. Cuddapah, K. Cui, T. Y. Roh, W. Peng, M. Q. Zhang & K. Zhao (2008c) Combinatorial patterns of histone acetylations and methylations in the human genome. *Nat Genet,* 40**,** 897-903.

Warfield, L., S. Ramachandran, T. Baptista, D. Devys, L. Tora & S. Hahn (2017) Transcription of Nearly All Yeast RNA Polymerase II-Transcribed Genes Is Dependent on Transcription Factor TFIID. *Mol Cell,* 68**,** 118-129 e5.

Weake, V. M., J. O. Dyer, C. Seidel, A. Box, S. K. Swanson, A. Peak, L. Florens, M. P. Washburn, S. M. Abmayr & J. L. Workman (2011) Post-transcription initiation function of the ubiquitous SAGA complex in tissue-specific gene activation. *Genes Dev,* 25**,** 1499-509.

Weake, V. M., K. K. Lee, S. Guelman, C. H. Lin, C. Seidel, S. M. Abmayr & J. L. Workman (2008) SAGA-mediated H2B deubiquitination controls the development of neuronal connectivity in the Drosophila visual system. *EMBO J,* 27**,** 394-405.

Weake, V. M., S. K. Swanson, A. Mushegian, L. Florens, M. P. Washburn, S. M. Abmayr & J. L. Workman (2009) A novel histone fold domain-containing protein that replaces TAF6 in Drosophila SAGA is required for SAGA-dependent gene expression. *Genes Dev,* 23**,** 2818-23.

Weake, V. M. & J. L. Workman (2008) Histone ubiquitination: triggering gene activity. *Mol Cell,* 29**,** 653-63.

Weissman, A. M., N. Shabek & A. Ciechanover (2011) The predator becomes the prey: regulating the ubiquitin system by ubiquitylation and degradation. *Nat Rev Mol Cell Biol,* 12**,** 605-20.

Wilkie, G. S., K. S. Dickson & N. K. Gray (2003) Regulation of mRNA translation by 5'- and 3'-UTR-binding factors. *Trends Biochem Sci,* 28**,** 182-8.
Winston, F. & M. Carlson (1992) Yeast SNF/SWI transcriptional activators and the SPT/SIN chromatin connection. *Trends Genet,* 8**,** 387-91.
Workman, J. L. (2016) CHROMATIN. It takes teamwork to modify chromatin. *Science,* 351**,** 667.
Wu, P. Y., C. Ruhlmann, F. Winston & P. Schultz (2004) Molecular architecture of the S. cerevisiae SAGA complex. *Mol Cell,* 15**,** 199-208.
Wyce, A., T. Xiao, K. A. Whelan, C. Kosman, W. Walter, D. Eick, T. R. Hughes, N. J. Krogan, B. D. Strahl & S. L. Berger (2007) H2B ubiquitylation acts as a barrier to Ctk1 nucleosomal recruitment prior to removal by Ubp8 within a SAGA-related complex. *Mol Cell,* 27**,** 275-88.
Wysocka, J., T. Swigut, T. A. Milne, Y. Dou, X. Zhang, A. L. Burlingame, R. G. Roeder, A. H. Brivanlou & C. D. Allis (2005) WDR5 associates with histone H3 methylated at K4 and is essential for H3 K4 methylation and vertebrate development. *Cell,* 121**,** 859-72.
Xu, W., D. G. Edmondson, Y. A. Evrard, M. Wakamiya, R. R. Behringer & S. Y. Roth (2000) Loss of Gcn5l2 leads to increased apoptosis and mesodermal defects during mouse development. *Nat Genet,* 26**,** 229-32.
Yoo, S. Y., M. E. Pennesi, E. J. Weeber, B. Xu, R. Atkinson, S. Chen, D. L. Armstrong, S. M. Wu, J. D. Sweatt & H. Y. Zoghbi (2003) SCA7 knockin mice model human SCA7 and reveal gradual accumulation of mutant ataxin-7 in neurons and abnormalities in short-term plasticity. *Neuron,* 37**,** 383-401.
Yudkovsky, N., C. Logie, S. Hahn & C. L. Peterson (1999) Recruitment of the SWI/SNF chromatin remodeling complex by transcriptional activators. *Genes Dev,* 13**,** 2369-74.
Zhang, Y., L. Yao, X. Zhang, H. Ji, L. Wang, S. Sun & D. Pang (2011) Elevated expression of USP22 in correlation with poor prognosis in patients with invasive breast cancer. *J Cancer Res Clin Oncol,* 137**,** 1245-53.
Zhao, K., W. Wang, O. J. Rando, Y. Xue, K. Swiderek, A. Kuo & G. R. Crabtree (1998) Rapid and phosphoinositol-dependent binding of the SWI/SNF-like BAF complex to chromatin after T lymphocyte receptor signaling. *Cell,* 95**,** 625-36.
Zheng, C. & J. J. Hayes (2003) Intra- and inter-nucleosomal protein-DNA interactions of the core histone tail domains in a model system. *J Biol Chem,* 278**,** 24217-24.
Zhou, W., P. Zhu, J. Wang, G. Pascual, K. A. Ohgi, J. Lozach, C. K. Glass & M. G. Rosenfeld (2008) Histone H2A monoubiquitination represses transcription by inhibiting RNA polymerase II transcriptional elongation. *Mol Cell,* 29**,** 69-80.
Zhu, P., W. Zhou, J. Wang, J. Puc, K. A. Ohgi, H. Erdjument-Bromage, P. Tempst, C. K. Glass & M. G. Rosenfeld (2007) A histone H2A deubiquitinase complex coordinating histone acetylation and H1 dissociation in transcriptional regulation. *Mol Cell,* 27**,** 609-21.
Zsindely, N., T. Pankotai, Z. Ujfaludi, D. Lakatos, O. Komonyi, L. Bodai, L. Tora & I. M. Boros (2009) The loss of histone H3 lysine 9 acetylation due to dSAGA-specific dAda2b mutation influences the expression of only a small subset of genes. *Nucleic Acids Res,* 37**,** 6665-80.